A Rabies Model with Distributed Latent Period and Territorial and Diffusing Rabid

Foxes

by

Khalaf Matar Alanazi

A Dissertation Presented in Partial Fulfillment
of the Requirements for the Degree
Doctor of Philosophy

Approved October 2018 by the
Graduate Supervisory Committee:

Horst R. Thieme, Chair
Zdzislaw Jackiewicz
Steven Baer
Carl Gardner
Yang Kuang
Hal Smith

ARIZONA STATE UNIVERSITY

December 2018

ABSTRACT

Rabies is an infectious viral disease. It is usually fatal if a victim reaches the rabid stage, which starts after the appearance of disease symptoms. The disease virus attacks the central nervous system, and then it migrates from peripheral nerves to the spinal cord and brain. At the time when the rabies virus reaches the brain, the incubation period is over and the symptoms of clinical disease appear on the victim. From the brain, the virus travels via nerves to the salivary glands and saliva.

A mathematical model is developed for the spread of rabies in a spatially distributed fox population to model the spread of the rabies epizootic through middle Europe that occurred in the second half of the 20th century. The model considers both territorial and wandering rabid foxes and includes a latent period for the infection. Since the model assumes these two kinds of rabid foxes, it is a system of both partial differential and integral equations (with integration over space and, occasionally, also over time). To study the spreading speeds of the rabies epidemic, the model is reduced to a scalar Volterra-Hammerstein integral equation, and space-time Laplace transform of the integral equation is used to derive implicit formulas for the spreading speed. The spreading speeds are discussed and implicit formulas are given for latent periods of fixed length, exponentially distributed length, Gamma distributed length, and log-normally distributed length. A number of analytic and numerical results are shown pertaining to the spreading speeds.

Further, a numerical algorithm is described for the simulation of the spread of rabies in a spatially distributed fox population on a bounded domain with Dirichlet boundary conditions. I propose the following methods for the numerical approximation of solutions. The partial differential and integral equations are discretized in the space variable by central differences of second order and by the composite trapezoidal rule. Next, the ordinary or delay differential equations that are obtained this way are

discretized in time by explicit continuous Runge-Kutta methods of fourth order for ordinary and delay differential systems. My particular interest is in how the partition of rabid foxes into territorial and diffusing rabid foxes influences the spreading speed, a question that can be answered by purely analytic means only for small basic reproduction numbers. I will restrict the numerical analysis to latent periods of fixed length and to exponentially distributed latent periods.

The results of the numerical calculations are compared for latent periods of fixed and exponentially distributed length and for various proportions of territorial and wandering rabid foxes. The speeds of spread observed in the simulations are compared to spreading speeds obtained by numerically solving the analytic formulas and to observed speeds of epizootic frontlines in the European rabies outbreak 1940 to 1980. For instance, when I assume that all rabid foxes are territorial and the latent period has fixed length, the spreading speed c^* is found to be about 28.3 [km/year], but when all rabid foxes diffuse with exponentially distributed length of the latent period, the spreading speed c^* is about 105.2 [km/year]. These spreading speeds compare quite well with those found in nature and in the literature. In addition, the spreading speeds show that the epidemic model on a bounded domain Ω with Dirichlet boundary conditions shows a less severe epidemic outbreak than the epidemic model on $\mathbb{R}^n$, and the spread of the disease modeled on Ω is not as fast as the spread of the disease modeled on $\mathbb{R}^n$. Furthermore, the numerical results for c^* confirm that the latent period with fixed length always gives the smallest spreading speeds among the latent periods with arbitrary length distribution and same mean length.

DEDICATION

To the memory of my father

ACKNOWLEDGMENTS

TABLE OF CONTENTS

LIST OF TABLES

LIST OF FIGURES

Chapter 1

INTRODUCTION AND BACKGROUND

1.1 Introduction

Rabies was reported in all continents excluding Antarctica (see, e.g., Beyer *et al.* (2011); Childs and Real (2007); Leslie *et al.* (2006); Ruan (2017); Sparkes *et al.* (2016); Vial *et al.* (2006); World Health Organization (WHO), What is rabies (2015); Zhang *et al.* (2012)). In the United States, bats, skunks, foxes, and raccoons are the main wildlife sources of rabies (see (Childs and Real, 2007, Fig.4.2); (Rees *et al.*, 2011, Fig.1)). Bats, skunks, and foxes are the most common infected species in Arizona (see (Arizona Department of Health Services, AZ Rabies Control and Bite Management Manual, 2018, Table 1); Arizona Department of Health Services, Rabies in AZ (2018); Borchering *et al.* (2012); Childs and Real (2007); Hass and Dragoo (2005); Leslie *et al.* (2006)), while raccoons and bats are the most popular reservoirs of rabies in Florida (Florida Department of Health, Rabies (2018)). In Asia and Africa, domestic dogs are consider to be the most common reservoir of rabies (Beyer *et al.* (2011); Ruan (2017); Vial *et al.* (2006); World Health Organization (WHO), What is rabies (2015); Zhang *et al.* (2012)).

In the last century, a rabies epizootic also expanded over parts of Europe. A number of scholars have investigated the epizootic of rabies in the past (Anderson *et al.* (1981); Andral *et al.* (1982); Artois *et al.* (1991); Bögel *et al.* (1976); Bourhy *et al.* (1999); David *et al.* (1982); Källén *et al.* (1985); Lloyd (1980); Macdonald (1980); Moegle *et al.* (1974); Murray *et al.* (1986); Murray (1989); Murray and Seward (1992); Thieme (1980); Toma and Andral (1977); White *et al.* (1995)) and recently (Alanazi

1

et al. (2018a, 2019, 2018b); Holmala and Kauhala (2006); Liu (2013); Ou and Wu (2006); Smith and Wilkinson (2003)). Rabies was mainly carried by foxes (Anderson *et al.* (1981); Murray *et al.* (1986)), started in Poland in 1939 or 1940 and moved westward reaching Denmark in 1964, Belgium, Luxembourg, and Austria in 1966, Switzerland in 1967, France in 1968, and Holland in 1974 (Toma and Andral (1977)). It also moved to the east, to Hungary, the former Czechoslovakia and the former Soviet Union (Toma and Andral (1977)). Its speed ranged from 30 to 60 [km/year] according to (Toma and Andral (1977); van den Bosch *et al.* (1990)) and from 20 to 60 [km/year] according to (Lloyd (1980)). There were important variations where the epidemic front retreated at times in certain areas and moved up to 100 [km] in a given direction in other areas in a single year (Toma and Andral (1977)). A study performed in three areas in the state of Baden-Württemberg (Germany) from January 1963 to March 31, 1971, found that the center of the frontwave moved at about 27 [km/year] (Bögel *et al.* (1976)) while the mean distance of new cases ahead of the frontline within a month was approximately 4.8 [km] (Bögel *et al.* (1976); Moegle *et al.* (1974)).

Rabies is an infectious viral disease. It is usually fatal if a victim reaches the rabid stage, which starts after the appearance of disease symptoms (Arizona Department of Health Services, AZ Rabies Control and Bite Management Manual (2018); Centers for Disease Control and Prevention (CDC), Rabies (2015); World Health Organization (WHO), Rabies (2015)). The disease virus attacks the central nervous system, and then it migrates from peripheral nerves to the spinal cord and brain (Arizona Department of Health Services, AZ Rabies Control and Bite Management Manual (2018); Centers for Disease Control and Prevention (CDC), Rabies (2015)). At the time when the rabies virus reaches the brain, the incubation period is over and the symptoms of clinical disease appear on the victim (Arizona Department of Health Services, AZ Rabies Control and Bite Management Manual (2018); World Health

Organization (WHO), What is rabies (2015)). From the brain, the virus travels via nerves to the salivary glands and saliva (Arizona Department of Health Services, AZ Rabies Control and Bite Management Manual (2018)).

The disease virus is transmitted from an infectious fox to a susceptible fox by bite. Then, the susceptible fox becomes infected and the latent period starts. Since the rabies virus appears in the saliva one or two days before symptoms are evident in the infected fox (Lloyd, 1980, p.247), the latent period is slightly shorter than the incubation period. Fox rabies has a relatively long latent period with highly variable duration (from 12 to 110 days (Anderson *et al.* (1981))) and a relatively short infection period (from 3 to 10 days (Anderson *et al.* (1981))). While the literature seems to agree on the mean length of the infectious period (which is ended by the death of the fox), 5 days, there seems to be disagreement on the mean length of the latent period: 35 days ((van den Bosch *et al.* (1990)) and the references therein) and 28 days Moegle *et al.* (1974) and 28 to 30 days (Anderson *et al.* (1981)), and 25 and 26.5 days and one month according to various sources cited in (Toma and Andral (1977)).

The above-mentioned fox epizootic has motivated quite a few mathematical studies (Liu (2013); Murray (1989); Ou and Wu (2006); Thieme (1980); van den Bosch *et al.* (1990)). Like this one, they all assume that foxes that are susceptible or are in the latent period have home-ranges (unless they are migrating juveniles looking for new home-ranges (Ou and Wu (2006))). Differently from previous studies, our model assumes that some of the rabid foxes essentially behave like susceptible and exposed foxes and keep their home-ranges, while the other rabid foxes loose the attachment to their home-range and disperse by diffusion. We call the first ones *territorial rabid* foxes and the second ones *diffusing (wandering (Toma and Andral (1977))) rabid* foxes. Since our model assumes these two kinds of rabid foxes, it is a system of both

partial differential and integral equations (with integration over space and, occasionally, also over time) (Section 2.2).

Mathematical models have so far assumed that either all rabid foxes are territorial (van den Bosch *et al.* (1990)) or all rabid foxes diffuse (Källén *et al.* (1985); Liu (2013); Murray *et al.* (1986); Murray (1989); Murray and Seward (1992); Ou and Wu (2006)). The radio-tracking in (Andral *et al.* (1982)) supports the existence of territorial rabid foxes, while the distances of new rabies cases in (Bögel *et al.*, 1976, Table 2) seem to support the existence of diffusing foxes.

To study the spreading speeds of the rabies epidemic, we reduce the model to a scalar Volterra Hammerstein integral equation (Section 2.3) and apply the concept of asymptotic speeds of spread (Thieme (1979a); Thieme and Zhao (2003)) (Section 2.5, Section 2.6). This concept had been originally developed by (Aronson (1977); Aronson and Weinberger (1975, 1978)) for partial differential equations in population dynamics and then used by (Aronson and Weinberger (1975)) for certain epidemic models and extended to larger classes of population and epidemic models by (Diekmann (1978, 1979)), (Thieme (1977, 1979a)), and by (Thieme and Zhao (2003)). The spreading speeds are discussed and calculated for latent periods of fixed length, exponentially distributed length, Gamma distributed length, and log-normally distributed length (Chapter 4). For further developments and some applications, see (Beaumont *et al.* (2012); Garnier (2011); Gourley and Kuang (2004); Jones *et al.* (2012, 2013, 2016); Kot (2001); Liang and Zhao (2007); Metz *et al.* (2000); Rass and Radcliffe (2003); Ruan (2007); Smith and Thieme (2011); Thieme (2006); Weinberger *et al.* (2007); Thieme and Zhao (2003); van den Bosch *et al.* (1990); Wang (2011); Wang and Wu (2010); Zhao and Xiao (2006)) and the references therein. For recent progress, we refer the reader to (Fang *et al.* (2017); Garnier and Lewis (2016); Shu *et al.* (2018); Shigesada *et al.* (2015); Tian and Yuan (2017); Wu and Zhao (2018); Xu (2016)).

Numerically, we describe a numerical algorithm for the simulation of the spread of rabies in a spatially distributed fox population on a bounded domain with Dirichlet boundary conditions. We propose the following methods for the numerical approximation of solutions. The partial differential and integral equations are discretized in the space variable by central differences of second order and by the composite trapezoidal rule (Section 5.3 and Section 6.3). Next, the delay or ordinary differential equations that are obtained this way are discretized in time by explicit continuous Runge-Kutta methods of fourth order for delay and ordinary differential systems (Section 5.4 and Section 6.4). The continuous Runge-Kutta method was derived by Owren and Zennaro (Owren and Zennaro (1991, 1992b,a)), and it is discussed in (Bellen and Zennaro (2003)). The continuous Runge-Kutta method was recently applied by (Alanazi *et al.* (2018a, 2019); Bartoszewski *et al.* (2015); Jackiewicz *et al.* (2014)). Our particular interest is in how the partition of rabid foxes into territorial and diffusing rabid foxes influences the spreading speed, a question we cannot answer by purely analytic means. We will restrict the numerical analysis to latent periods of fixed length (Chapter 5) and to exponentially distributed latent periods (Chapter 6). The models in Chapter 5 and Chapter 6 are derived and discussed in Chapter 3. For numerical methods of solving and studying differential equations, we refer the reader to the work by (Bartoszewski and Jackiewicz (2002, 2007, 2008)), (D'Ambrosio and Jackiewicz (2010, 2011)), (Jackiewicz and Zennaro (1992); Jackiewicz and Zubik-Kowal (2006, 2009)), (Recktenwald (2000)), (Schiesser (2013); Schiesser and Griffiths (2009)), (Shampine *et al.* (2003)), and by (Stanoyevitch (2005)).

1.2 Thesis Plan

A mathematical model is developed for the spread of rabies in a spatially distributed fox population to model the spread of the rabies epizootic through middle Europe that occurred in the second half of the 20th century. The model considers both territorial and wandering rabid foxes and includes a latent period for the infection. Since the model assumes these two kinds of rabid foxes, it is a system of both partial differential and integral equations (with integration over space and, occasionally, also over time). To study the spreading speeds of the rabies epidemic, the model is reduced to a scalar Volterra-Hammerstein integral equation, and space-time Laplace transform of the integral equation is used to derive implicit formulas for the spreading speed. The spreading speeds are discussed and implicit formulas are given for latent periods of fixed length, exponentially distributed length, Gamma distributed length, and log-normally distributed length. A number of analytic and numerical results are shown pertaining to the spreading speeds. Our particular interest is in how the partition of rabid foxes into territorial and diffusing rabid foxes influences the spreading speed.

The dissertation is organized as follows. In Chapter 2, a rabies model is derived with both territorial and diffusing rabid foxes. The model is reduced to a scalar Volterra-Hammerstein integral equation, and space-time Laplace transform of the integral equation is used. In Chapter 3, two sub-models are formulated. The first model includes a latent period with fixed length, and the second model includes a latent period with exponentially distributed length. Chapter 4 discusses analytic results and numerical estimations of the asymptotic speeds of spread c^* of fox rabies. Numerical simulations of spread of rabies when the latent period has fixed length and when the latent period has exponentially distributed length with a bounded domain

of $\mathbb{R}$ are discussed in Chapter 5 and Chapter 6, respectively. The work in Chapter 3, Chapter 5, and Chapter 6 was published in Alanazi *et al.* (2018a). The work in Chapter 2 and Chapter 4 has submitted to a journal for publication (Alanazi *et al.* (2018b)).

If someone is interested in numerical simulations of the spread of rabies in two-dimensional space, we refer the reader to the pubished paper in Alanazi *et al.* (2019).

Chapter 2

A RABIES MODEL WITH DISTRIBUTED LATENT PERIOD AND TERRITORIAL AND DIFFUSING RABID FOXES

2.1 Abstract

We build a model that helps to study analytically the spatial spread of rabies on $\mathbb{R}^n$. The model assumes that some of the rabid foxes essentially behave like healthy and susceptible foxes and keep their territories, while the other rabid foxes change their behavior and wander. Since we consider these two kinds of rabid foxes, the model consists of partial and integral equations. In addition, the model considers continuous latent periods with arbitrary length distributions for the infection. We reduce our model to a single scalar Hammerstein Volterra integral equation and use the Laplace transform to find a candidate for the spreading speeds c^*. We use theorems developed by (Thieme (1977, 1979a)), and by (Thieme and Zhao (2003)) to say that c^* is indeed the spreading speed of our solutions. Next, we show a number of analytic results pertaining to the spreading speeds c^*.

2.2 The Model

To study the spread of rabies in a spatially distributed fox population, we consider $\mathbb{R}^n$ which represents the habitat of the foxes.

We consider an epidemic outbreak and assume that it is short enough that the natural turnover of the fox population can be ignored: No foxes are born, and the only deaths are those of rabid foxes dying from rabies.

8

We assume that susceptible and exposed foxes have home-ranges. Home ranges of settled foxes may partly or largely overlap those of other foxes though parts of them may be defended from encroachment by other foxes ((Lloyd, 1980, p.149)). Therefore, it seems to be not only a convenient but also justifiable approximation of reality to model the locations of susceptible and incubating foxes by the centers of their home-ranges in a spatial continuum.

Further, we assume that some of the rabid foxes essentially behave like susceptible and exposed foxes and keep their home-ranges, while the other rabid foxes loose the attachment to their home-range and disperse by diffusion. We call the first territorial rabid foxes and the second diffusing rabid foxes.

Mathematical models have so far assumed that either all rabid foxes are territorial (van den Bosch *et al.* (1990)) or all rabid foxes diffuse (Källén *et al.* (1985); Liu (2013); Murray *et al.* (1986); Murray (1989); Murray and Seward (1992); Ou and Wu (2006)). The radio-tracking in (Andral *et al.* (1982)) supports the existence of territorial rabid foxes, while the distances of new rabies cases in ((Bögel *et al.*, 1976, Table 2)) seems to support the existence of diffusing foxes.

Let $S(x,t)$ denote the density of susceptible foxes (which are all territorial) at time t whose home-ranges center at location $x \in \mathbb{R}^n$. Further $R_1(x,t)$ are the diffusing rabid foxes at location x and time t and $R_2(x,t)$ the territorial rabid foxes at time t whose home-ranges center at location x. Finally, $E(x,t,a)$ is the density of infected foxes in the incubation period (which are also all territorial) at time t that have infection age a and whose home-ranges center at x.

Let $\kappa_1(x,z)$ denote the rate at which a fox with home-range center x visits the location $z \in \mathbb{R}^n$, where κ_1 is assumed to be continuous and $\int_{\mathbb{R}^n} \kappa_1(x,y)dy = 1$. The rate at which a susceptible fox with home-range center x meets a territorial rabid fox

with home-range center z is given by

$$\kappa_2(x,z) = \int_{\mathbb{R}^n} \kappa_1(x,y)\kappa_1(z,y)dy, \tag{2.2.1}$$

which means that it is the rate at which they both visit some common point $y \in \mathbb{R}^n$ (Compare equation (5.1) in (van den Bosch *et al.* (1990))). The model takes the form,

$$
\begin{cases}
\partial_t S(x,t) = -\beta S(x,t) \int_{\mathbb{R}^n} [\kappa_1(x,z)R_1(z,t) + \kappa_2(x,z)R_2(z,t)]dz \\[2mm]
\qquad =: -B(x,t), \\[2mm]
\partial_t R_1(x,t) = D\Delta_x R_1 + p_1 \int_0^\infty \theta(a)E(x,t,a)da - \nu_1 R_1(x,t), \\[2mm]
\partial_t R_2(x,t) = p_2 \int_0^\infty \theta(a)E(x,t,a)da - \nu_2 R_2(x,t),
\end{cases} \tag{2.2.2}
$$

with given initial conditions

$$S(x,0) = S_0(x), \ R_1(x,0) = R_1^\circ(x), \ R_2(x,0) = R_2^\circ(x), \ x \in \mathbb{R}^n. \tag{2.2.3}$$

Here, Δ_x is the Laplace operator such that $\Delta_x R_1 = \sum_{i=1}^n \frac{\partial^2 R_1(x,t)}{\partial x_i^2}$. D is the fixed diffusion rate. $\theta(a)$ is the rate at which infected foxes with infection age a exit the latent period, and ν_1 and ν_2 are the per capita rabies death rate of diffusing and territorial rabid foxes, respectively. p_1 is the chance of a rabid fox to diffuse, and p_2 the chance to be territorial so that $p_1 + p_2 = 1$. β is the chance that a meeting of a susceptible and a rabid fox leads to the infection of the susceptible fox. $B(x,t)$ is the incidence of the disease, i.e., the number of new cases per unit of time. The nonnegative continuous functions S_0, R_1° and R_2° are the initial densities of the susceptible and diffusing and territorial rabid foxes.

The infected foxes in the latent period are described by the system

$$
\begin{cases}
(\partial_t + \partial_a)E(x,t,a) = -\theta(a)E(x,t,a), \\[2mm]
\qquad\qquad E(x,t,0) = B(x,t), \\[2mm]
\qquad\qquad E(x,0,a) = E_0(x,a).
\end{cases} \tag{2.2.4}
$$

10

Here $E(x, t, a)$, and $B(x, t)$ are as above.

Remark 2.2.1. We have modeled the duration of the rabid, infectious, stage in the simplest possible way, namely as exponentially distributed, i.e., by a constant per capita rate of dying from the disease. The duration of the latent period will be modeled by an arbitrary distribution because this will provide very interesting insights (Chapter 4). We could have done something similar for the rabid stage and let the disease-death rate and even the diffusion rate of diffusing rabid foxes depend on the time since becoming infectious (Liu (2013)). We do not do so because this would add a layer of complexity that may obscure the interplay of diffusing and territorial rabid foxes. Instead of separating the latent and the rabid period, we could have looked only at the class of infected foxes and their infection age (Ducrot and Magal (2009); Liu (2013)). We did not do this in order to use the information about the length of the latent period and the rabid period that is available.

Remark 2.2.2. Alternatively to the diffusion equation, the wandering rabid foxes could be modeled by a differential-integral equation

$$
\begin{cases}
\partial_t R_1(x, t) = \int_{\mathbb{R}^n} \kappa_3(x, z) R_1(z, t) dz - R_1(x, t) \int_{\mathbb{R}^n} \kappa_3(x, z) dz \\
\qquad\qquad + \int_0^\infty \theta(a) E(x, t, a) da - \nu_1 R_1(x, t), \\
\kappa_3(x, y) = \kappa_3(y, x).
\end{cases} \tag{2.2.5}
$$

This would make it possible to include studying the effects of fat-tailed kernels κ_3 which should lead to accelerating solutions as in (Bouin *et al.* (2018); Garnier (2011)). While in a few areas rabies has spread with considerable higher speed than in most others (Toma and Andral (1977)), it is not clear whether this is caused by fat kernels (the main example for this seems to be rapid plant migration) or rather by spatial heterogeneities which are not considered in this work. Yet another cause of anomalous

high spreading speeds is the interaction of different species (Weinberger *et al.* (2007)). A mathematical reason for not venturing into the area of fat-tailed kernels is that they do not appear to lead to formulas for the spreading speed that are amenable to a qualitative analysis of how the spreading speed depends on rabies-relevant model parameters.

2.3 Transformation to a Single Volterra Hammerstein Integral Equation

In this section, we are working to reduce the model (2.2.2) to a single nonlinear Volterra-Hammerstein integral equation. We begin by integrating along the characteristics to reduce the system in (2.2.4) to one equation (see, e.g., (Smith and Thieme (1991); Thieme and Zhao (2001, 2003))). Let

$$v(x, r, a) = E(x, r + a, a) \tag{2.3.1}$$

be the foxes in the incubation period that were infected at time $r \geq 0$ with infection age $a \geq 0$. It follows that

$$\partial_a v(x, r, a) = [\partial_t E(x, t, a) + \partial_a E(x, t, a)]_{t=r+a}$$
$$= -\theta(a)E(x, r + a, a) = -\theta(a)v(x, r, a), \tag{2.3.2}$$
$$v(x, r, 0) = E(x, r, 0) = B(x, r).$$

Then, we obtain

$$v(x, r, a) = B(x, r) \exp\left(-\int_0^a \theta(s)ds\right). \tag{2.3.3}$$

Let

$$w(x, t, r) = E(x, t, t + r), \tag{2.3.4}$$

which is the individuals at time t that had been infected before time 0 and had infection age r at time 0. Then

$$\partial_t w(x,t,r) = [\partial_t E(x,t,a) + \partial_a E(x,t,a)]_{a=t+r}$$

$$= -\theta(t+r)E(x,t,t+r) = -\theta(t+r)w(x,t,r), \qquad (2.3.5)$$

$$w(x,0,r) = E(x,0,r) = E_0(x,r).$$

So, we obtain

$$w(x,t,r) = E_0(x,r)\exp\left(-\int_0^t \theta(s+r)ds\right). \qquad (2.3.6)$$

Let $t > a \geq 0$, then

$$E(x,t,a) = v(x,t-a,a) = B(x,t-a)\Upsilon(a),$$

$$\Upsilon(a) = \exp\left(-\int_0^a \theta(s)ds\right), \qquad (2.3.7)$$

where $\Upsilon(a)$ is the probability that infected foxes with infection age a are still in the latent period. Then $\Upsilon : \mathbb{R}_+ \to [0,1]$ is decreasing and $\Upsilon(0) = 1$. We assume that θ: $[0,\infty) \to [0,\infty)$ is a continuous function, and there exist numbers $\sigma_2 > \sigma_1 > 0$ such that for $a \in (\sigma_1, \sigma_2)$,

$$\theta(a) > 0, \quad \int_0^\infty \theta(a)da = \infty. \qquad (2.3.8)$$

For $a > t \geq 0$, we have

$$E(x,t,a) = w(x,t,a-t) = E_0(x,a-t)\mathcal{F}(a,t),$$

$$\mathcal{F}(a,t) = \exp\left(-\int_0^t \theta(s+a-t)ds\right). \qquad (2.3.9)$$

We do a change of variables, we have

$$\mathcal{F}(a,t) = \exp\left(-\int_{a-t}^a \theta(r)dr\right) = \Upsilon(a)/\Upsilon(a-t). \qquad (2.3.10)$$

13

Then we have

$$E(x, t, a) = \begin{cases} E_0(x, a-t)\frac{\Upsilon(a)}{\Upsilon(a-t)}, & a > t \geq 0, \\ B(x, t-a)\Upsilon(a), & t > a \geq 0, \end{cases} \qquad (2.3.11)$$

where $E_0(x, a-t)$ is the number of infected foxes that already were in the latent period and not yet become rabid at time t that have infections age a and whose home ranges center at x. $\frac{\Upsilon(a)}{\Upsilon(a-t)}$ is the conditional probability that the infected foxes at infection age a are still in the latent period with the condition of having been in the latent period already at age $a - t$.

Now, we want now to solve for $R_1(x, t)$, which is the diffusing rabid foxes at location x and time t. From (2.2.2), the density of diffusing rabid foxes satisfies

$$\partial_t R_1(x, t) = D\partial_x^2 R_1(x, t) + p_1 \int_0^\infty \theta(a)E(x, t, a)da - \nu_1 R_1(x, t),$$
$$R_1(x, 0) = R_1^\circ(x). \qquad (2.3.12)$$

Set

$$f(x, t) = \int_0^\infty \theta(a)E(x, t, a)da = f_1(x, t) + f_0(x, t), \qquad (2.3.13)$$

where

$$f_1(x, t) = \int_0^t \theta(a)E(x, t, a)da = \int_0^t \theta(a)B(x, t-a)\Upsilon(a)da, \qquad (2.3.14)$$

and

$$f_0(x, t) = \int_t^\infty \theta(a)E(x, t, a)da = \int_t^\infty \theta(a)E_0(x, a-t)\mathcal{F}(a, t)da. \qquad (2.3.15)$$

Now, the model (2.3.12) shall be

$$\partial_t R_1(x, t) + \nu_1 R_1(x, t) = D\partial_x^2 R_1(x, t) + p_1 f(x, t), \qquad (2.3.16)$$

14

So, the solution for the non-homogeneous PDE is

$$
\begin{aligned}
R_1(x,t) =& p_1 \int_0^t \int_{\mathbb{R}^n} \Gamma_n(D(t-s), x-y) e^{-\nu_1(t-s)} f(s,y) dy ds \\
&+ \int_{\mathbb{R}^n} \Gamma_n(Dt, x-y) R_1^\circ(y) e^{-\nu_1 t} dy.
\end{aligned}
\tag{2.3.17}
$$

By doing a change of variable $s \to t - s$, we have

$$
\begin{aligned}
R_1(x,t) =& p_1 \int_0^t \int_{\mathbb{R}^n} \Gamma_n(Ds, x-y) e^{-\nu_1 s} f(t-s,y) dy ds \\
&+ \int_{\mathbb{R}^n} \Gamma_n(Dt, x-y) R_1^\circ(y) e^{-\nu_1 t} dy.
\end{aligned}
\tag{2.3.18}
$$

Here, Γ_n is the fundamental solutions associated with the differential operator $\partial_t - \Delta_x$ for n space dimensions, and it is given by

$$
\Gamma_n(x,t) = \frac{1}{(\sqrt{4\pi t})^n} e^{\frac{-|x|^2}{4t}}, \qquad x \in \mathbb{R}^n,
\tag{2.3.19}
$$

where $|\cdot|$ is the Euclidean norm on $\mathbb{R}^n$, and it is given by

$$
|x| = \sqrt{\sum_{j=1}^n x_j^2}.
\tag{2.3.20}
$$

Substituting (2.3.13) into (2.3.18), we have

$$
\begin{aligned}
R_1(x,t) =& p_1 \int_0^t \int_{\mathbb{R}^n} \Gamma_n(Ds, x-y) e^{-\nu_1 s} \left(f_1(t-s,y) + f_0(t-s,y) \right) dy ds \\
&+ \int_{\mathbb{R}^n} \Gamma_n(Dt, x-y) R_1^\circ(y) e^{-\nu_1 t} dy.
\end{aligned}
\tag{2.3.21}
$$

That is

$$
R_1(x,t) = R_0^1(x,t) + p_1 \int_0^t \int_{\mathbb{R}^n} \Gamma_n(Ds, x-y) e^{-\nu_1 s} f_1(t-s,y) dy ds,
\tag{2.3.22}
$$

where

$$
\begin{aligned}
R_0^1(x,t) =& p_1 \int_0^t \int_{\mathbb{R}^n} \Gamma_n(Ds, x-y) e^{-\nu_1 s} f_0(t-s,y) dy ds \\
&+ \int_{\mathbb{R}^n} \Gamma_n(Dt, x-y) R_1^\circ(y) e^{-\nu_1 t} dy.
\end{aligned}
\tag{2.3.23}
$$

15

Similarly, we work to find a formula for $R_2(x,t)$, so someone can easily find

$$R_2(x,t) = R_0^2(x,t) + p_2 \int_0^t f_1(t-s,x)e^{-\nu_2 s}ds, \tag{2.3.24}$$

where

$$R_0^2(x,t) = p_2 \int_0^t f_0(t-s,x)e^{-\nu_2 s}ds + R_2^\circ(x)e^{-\nu_2 t}. \tag{2.3.25}$$

Solving for $S(x,t)$, that is in (2.2.2), gives us

$$S(x,t) = S_0(x)e^{-u(x,t)}, \tag{2.3.26}$$

where

$$u(x,t) = \beta \int_0^t \int_{\mathbb{R}^n} [\kappa_1(x,z)R_1(z,s) + \kappa_2(x,z)R_2(z,s)]dzds \tag{2.3.27}$$

is the cumulative rate of rabid foxes meet the susceptible foxes. Let us first divide (2.3.27) into two parts $U_1(x,t)$ and $U_2(x,t)$ such that

$$u(x,t) = U_1(x,t) + U_2(x,t), \tag{2.3.28}$$

where

$$U_1(x,t) = \beta \int_0^t \int_{\mathbb{R}^n} \kappa_1(x,z)R_1(z,s)dzds,$$

and

$$U_2(x,t) = \beta \int_0^t \int_{\mathbb{R}^n} \kappa_2(x,z)R_2(z,s)dzds.$$

Also, for the foxes that already were infected at the beginning, we set

$$u_0(x,t) = U_{10}(x,t) + U_{20}(x,t), \tag{2.3.29}$$

where

$$U_{10}(x,t) = \beta \int_0^t \int_{\mathbb{R}^n} \kappa_1(x,z)R_0^1(z,s)dzds,$$

16

and

$$U_{20}(x,t) = \beta \int_0^t \int_{\mathbb{R}^n} \kappa_2(x,z) R_0^2(z,s) dz ds.$$

The following result will be used a couple of times.

Lemma 2.3.1. *Let* $\phi_2 : \mathbb{R}_+ \to \mathbb{R}$ *be continuous and*

$$\phi_1(t) = \int_0^t \kappa(r)\phi_2(t-r) dr,$$

for $t \geqslant 0$, *and* $\Phi_j(t) = \int_0^t \phi_j(s) ds$ *the anti-derivative of* ϕ_j. *Then*

$$\Phi_1(t) = \int_0^t \kappa(s)\Phi_2(t-s) ds,$$

for $t \geqslant 0$.

Proof. We substitute the formula for ϕ_1 into Φ_1, so we get

$$\Phi_1(t) = \int_0^t \left(\int_0^t \kappa(r)\phi_2(s-r) dr \right) ds, \quad t \geqslant 0.$$

By changing the order of integration, we obtain

$$\Phi_1(t) = \int_0^t \kappa(r) \left(\int_r^t \phi_2(s-r) ds \right) dr.$$

That is

$$\Phi_1(t) = \int_0^t \kappa(r)\Phi_2(t-r) dr.$$

Let $r \to s$, then

$$\Phi_1(t) = \int_0^t \kappa(s)\Phi_2(t-s) ds, \quad \text{for} \quad t \geqslant 0.$$

$\square$

From (2.3.23), $U_{10}(x,t)$ shall be

$$U_{10}(x,t) = \beta \int_0^t \int_{\mathbb{R}^n} \kappa_1(x,z) \Big(p_1 \int_0^t \int_{\mathbb{R}^n} \Gamma_n(Ds, z-y) e^{-\nu_1 s} f_0(s-r,y)$$

$$dy dr + \int_{\mathbb{R}^n} \Gamma_n(Ds, z-y) R_1^\circ(y) e^{-\nu_1 s} dy \Big) dz ds.$$

(2.3.30)

We interchange the order of integration and use Lemma 2.3.1,

$$U_{10}(x,t) = \beta \int_0^t \int_{\mathbb{R}^n} \kappa_1(x,z) \Big(p_1 \int_{\mathbb{R}^n} \Gamma_n(Ds, z-y) e^{-\nu_1 s} \Big(\int_0^{t-s} f_0(r,y) dr \Big) dy$$

$$+ \int_{\mathbb{R}^n} \Gamma_n(Ds, z-y) R_1^\circ(y) e^{-\nu_1 s} dy \Big) dz ds.$$

(2.3.31)

That is

$$U_{10}(x,t) = \beta p_1 \int_0^t \int_{\mathbb{R}^n} \int_{\mathbb{R}^n} \kappa_1(x,z) \Gamma_n(Ds, z-y) e^{-\nu_1 s} \Big(\int_0^{t-s} f_0(r,y) dr \Big) dy dz ds$$

$$+ \beta \int_0^t \int_{\mathbb{R}^n} \int_{\mathbb{R}^n} \kappa_1(x,z) \Gamma_n(Ds, z-y) R_1^\circ(y) e^{-\nu_1 s} dy dz ds.$$

(2.3.32)

From (2.3.15), we have

$$\int_0^t f_0(y,s) = \int_0^t \int_0^\infty \theta(a+s) E_0(y,a) \mathcal{F}(a+s,s) da ds.$$

(2.3.33)

We substitute (2.3.33) into (2.3.32)

$$U_{10}(x,t) = \beta p_1 \int_0^t \int_{\mathbb{R}^n} \int_{\mathbb{R}^n} \kappa_1(x,z) \Gamma_n(Ds, z-y) e^{-\nu_1 s}$$

$$\Big(\int_0^{t-s} \int_0^\infty \theta(a+r) E_0(y,a) \mathcal{F}(a+r,r) da dr \Big) dy dz ds$$

(2.3.34)

$$+ \beta \int_0^t \int_{\mathbb{R}^n} \int_{\mathbb{R}^n} \kappa_1(x,z) \Gamma_n(Ds, z-y) R_1^\circ(y) e^{-\nu_1 s} dy dz ds.$$

From (2.3.25), $U_{20}(x,t)$ shall be

$$U_{20}(x,t) = p_2 \beta \int_0^t \int_{\mathbb{R}^n} \kappa_2(x,z) e^{-\nu_2 s} \Big(\int_0^{t-s} f_0(r,z) dr \Big) dz ds$$

$$+ \beta \int_0^t \int_{\mathbb{R}^n} \kappa_2(x,z) R_2^\circ(z) e^{-\nu_2 s} dz ds.$$

(2.3.35)

We substitute (2.3.33) into (2.3.35)

$$U_{20}(x,t) = p_2\beta \int_0^t \int_{\mathbb{R}^n} \kappa_2(x,z) e^{-\nu_2 s}$$

$$\left(\int_0^{t-s} \int_0^\infty \theta(a+r) E_0(z,a) \mathcal{F}(a+r,r) da dr \right) dz ds \qquad (2.3.36)$$

$$+ \beta \int_0^t \int_{\mathbb{R}^n} \kappa_2(x,z) R_2^\circ(z) e^{-\nu_2 s} dz ds.$$

From (2.3.34) and (2.3.36), $u_0(x,t)$ shall be

$$u_0(x,t) = \beta p_1 \int_0^t \int_{\mathbb{R}^n} \int_{\mathbb{R}^n} \kappa_1(x,z) \Gamma_n(Ds, z-y) e^{-\nu_1 s}$$

$$\left(\int_0^{t-s} \int_0^\infty \theta(a+r) E_0(y,a) \mathcal{F}(a+r,r) da dr \right) dy dz ds$$

$$+ \beta \int_0^t \int_{\mathbb{R}^n} \int_{\mathbb{R}^n} \kappa_1(x,z) \Gamma_n(Ds, z-y) R_1^\circ(y) e^{-\nu_1 s} dy dz ds$$

$$+ p_2\beta \int_0^t \int_{\mathbb{R}^n} \kappa_2(x,z) e^{-\nu_2 s} \qquad (2.3.37)$$

$$\left(\int_0^{t-s} \int_0^\infty \theta(a+r) E_0(z,a) \mathcal{F}(a+r,r) da dr \right) dz ds$$

$$+ \beta \int_0^t \int_{\mathbb{R}^n} \kappa_2(x,z) R_2^\circ(z) e^{-\nu_2 s} dz ds.$$

Now, from (2.3.22), we have

$$R_1(x,t) - R_0^1(x,t) = p_1 \int_0^t \int_{\mathbb{R}^n} \Gamma_n(Ds, x-y) e^{-\nu_1 s} f_1(t-s,y) dy ds. \qquad (2.3.38)$$

Also, we have

$$U_1(x,t) - U_{10}(x,t) = \beta \int_0^t \int_{\mathbb{R}^n} \kappa_1(x,z) \left(R_1(z,s) - R_0^1(z,s) \right) dz ds. \qquad (2.3.39)$$

So, after changing the order of integration and use Lemma 2.3.1, we obtain

$$U_1(x,t) - U_{10}(x,t) =$$

$$\beta \int_0^t \int_{\mathbb{R}^n} \kappa_1(x,z) \left(p_1 \int_{\mathbb{R}^n} \Gamma_n(Ds, z-y) e^{-\nu_1 s} \left(\int_0^{t-s} f_1(r,y) dr \right) dy \right) dz ds \qquad (2.3.40)$$

$$= p_1\beta \int_0^t \int_{\mathbb{R}^n} \int_{\mathbb{R}^n} \kappa_1(x,z) \Gamma_n(Ds, z-y) e^{-\nu_1 s} \left(\int_0^{t-s} f_1(r,y) dr \right) dy dz ds.$$

19

By (2.3.14),

$$\int_0^t f_1(y, s)ds = \int_0^t \int_0^s \theta(a)\Upsilon(a)B(y, s-a)dads$$

$$= \int_0^t \theta(a)\Upsilon(a) \int_a^t B(y, s-a)dsda$$

$$= \int_0^t \theta(a)\Upsilon(a) \int_0^{t-a} B(y, s)dsda$$

$$= \int_0^t \theta(a)\Upsilon(a) \int_0^{t-a} B(y, r)drda.$$

(2.3.41)

From the fundamental theorem of calculus and (2.2.2), we have

$$\int_0^{t-a} B(y, r)dr = -\int_0^{t-a} \partial_r S(y, r)dr$$

$$= -[S(y, t-a) - S(y, 0)] = S_0(y) - S(y, t-a).$$

(2.3.42)

From (2.3.26),

$$\int_0^{t-a} B(y, r)dr = S_0(y)[1 - e^{-u(y, t-a)}] = S_0(y)F(u(y, t-a)),$$

(2.3.43)

where

$$F(u) = 1 - e^{-u}, \qquad u \geq 0.$$

(2.3.44)

Substituting (2.3.43) into (2.3.41), we have

$$\int_0^t f_1(y, s)ds = \int_0^t \theta(a)\Upsilon(a)S_0(y)F(u(y, t-a))da.$$

(2.3.45)

Substituting (2.3.45) into (2.3.40), we have

$$U_1(x, t) - U_{10}(x, t) = p_1\beta \int_0^t \int_{\mathbb{R}^n} \int_{\mathbb{R}^n} \kappa_1(x, z)\Gamma_n(Ds, z-y)e^{-\nu_1 s}$$

$$\left(\int_0^{t-s} \theta(a)\Upsilon(a)S_0(y)F(u(y, t-s-a))da \right) dydzds.$$

(2.3.46)

We change the order of integration and use the substitution $a = r - s$ in the interior integral, so we obtain

$$U_1(x, t) - U_{10}(x, t) = p_1\beta \int_0^t e^{-\nu_1 s}ds \int_s^t \int_{\mathbb{R}^n} \int_{\mathbb{R}^n} \theta(r-s)\Upsilon(r-s)S_0(y)$$

$$F(u(y, t-r))\kappa_1(x, z)\Gamma_n(Ds, z-y)dydzdr.$$

(2.3.47)

After another change of variables, we have

$$U_1(x,t) - U_{10}(x,t) = p_1\beta \int_0^t \int_0^r \int_{\mathbb{R}^n} \int_{\mathbb{R}^n} \theta(r-s)\Upsilon(r-s)S_0(y)$$

$$F(u(y,t-r))e^{-\nu_1 s}\kappa_1(x,z)\Gamma_n(Ds, z-y)dydzdsdr,$$

(2.3.48)

which can be written as

$$U_1(x,t) - U_{10}(x,t) = \int_0^t \int_{\mathbb{R}^n} \xi_1(x,y,r)F(u(y,t-r))dydr, \qquad (2.3.49)$$

where

$$\xi_1(x,y,r) = \int_{\mathbb{R}^n} \eta_1(r,z,y)\kappa_1(x,z)dz, \qquad (2.3.50)$$

and

$$\eta_1(r,z,y) = p_1\beta \int_0^r \theta(r-s)\Upsilon(r-s)S_0(y)e^{-\nu_1 s}\Gamma_n(Ds, z-y))ds. \qquad (2.3.51)$$

We also have that

$$U_2(x,t) - U_{20}(x,t) = \beta \int_0^t \int_{\mathbb{R}^n} \kappa_2(x,z)[R_2(z,s) - R_0^2(z,s)]dzds. \qquad (2.3.52)$$

Substituting (2.3.24) into (2.3.52) and using Lemma 2.3.1, we have

$$U_2(x,t) - U_{20}(x,t) = p_2\beta \int_0^t \int_{\mathbb{R}^n} \kappa_2(x,z)e^{-\nu_1 s}\left(\int_0^{t-s} f_1(r,z)dr\right)dzds. \qquad (2.3.53)$$

Substituting (2.3.45) into (2.3.53), we have

$$U_2(x,t) - U_{20}(x,t) = p_2\beta \int_0^t \int_{\mathbb{R}^n} \kappa_2(x,z)e^{-\nu_1 s}$$

$$\left(\int_0^{t-s} \theta(a)\Upsilon(a)S_0(z)F(u(z,t-s-a))da\right)dzds.$$

(2.3.54)

We change the order of integration and use the substitution $a = r - s$ in the interior integral,

$$U_2(x,t) - U_{20}(x,t) = p_2\beta \int_0^t e^{-\nu_1 s}$$

$$\int_s^t \int_{\mathbb{R}^n} \theta(r-s)\Upsilon(r-s)S_0(z)F(u(z,t-r))\kappa_1(x,z)dzdrds.$$

(2.3.55)

21

After another change of variables, we have

$$U_2(x,t) - U_{20}(x,t) =$$

$$p_2\beta \int_0^t \int_0^r \int_{\mathbb{R}^n} \theta(r-s)\Upsilon(r-s)S_0(z)F(u(z,t-r))e^{-\nu_1 s}\kappa_2(x,z)dzdsdr, \qquad (2.3.56)$$

which can be written as

$$U_2(x,t) - U_{20}(x,t) = \int_0^t \int_{\mathbb{R}^n} \xi_2(x,z,r)F(u(z,t-r))dzdr, \qquad (2.3.57)$$

where

$$\xi_2(x,z,r) = \eta_2(r,z)\kappa_2(x,z), \qquad (2.3.58)$$

and

$$\eta_2(r,z) = p_2\beta \int_0^r \theta(r-s)\Upsilon(r-s)S_0(z)e^{-\nu_2 s}ds. \qquad (2.3.59)$$

We have from (2.3.28) and (2.3.29) that

$$u(x,t) - u_0(x,t) = \big(U_1(x,t) - U_{10}(x,t)\big) + \big(U_2(x,t) - U_{20}(x,t)\big). \qquad (2.3.60)$$

Substituting (2.3.49) and (2.3.57) into (2.3.60), we obtain

$$u(x,t) - u_0(x,t)$$

$$= \int_0^t \int_{\mathbb{R}^n} \Big[\xi_1(x,z,r)F(u(z,t-r)) + \xi_2(x,z,r)F(u(z,t-r))\Big]dzdr \qquad (2.3.61)$$

$$= \int_0^t \int_{\mathbb{R}^n} \xi(x,z,r)F(u(z,t-r))dzdr,$$

where

$$\xi(x,z,r) = \xi_1(x,z,r) + \xi_2(x,z,r). \qquad (2.3.62)$$

We need to assume that S_0 is a constant and $\kappa_1(x,z)$ must be replaced by $\kappa_1(x-z)$. So, from (2.2.1), we have

$$\kappa_2(x,z) = \int_{\mathbb{R}^n} \kappa_1(x-y)\kappa_1(z-y)dy = \tilde{\kappa}_2(x-z), \qquad (2.3.63)$$

22

with

$$\tilde{\kappa}_2(z) = \int_{\mathbb{R}^n} \kappa_1(y+z)\kappa_1(y)dy. \tag{2.3.64}$$

Therefore, (2.3.50) and (2.3.51) shall be

$$\xi_1(y,r) = \int_{\mathbb{R}^n} \eta_1(r, y-z)\kappa_1(z)dz, \tag{2.3.65}$$

and

$$\eta_1(r,y) = p_1\beta \int_0^r \theta(r-s)\Upsilon(r-s)S_0 e^{-\nu_1 s}\Gamma_n(Ds, y-z))ds. \tag{2.3.66}$$

After we drop the tilde, (2.3.58) and (2.3.59) shall be

$$\xi_2(y,r) = \eta_2(r)\kappa_2(y), \tag{2.3.67}$$

and

$$\eta_2(r) = p_2\beta \int_0^r \theta(r-s)\Upsilon(r-s)S_0 e^{-\nu_2 s}ds. \tag{2.3.68}$$

Also, we rewrite (2.3.61) as

$$\begin{aligned}
u(x,t) =& u_0(x,t) + \int_0^t \int_{\mathbb{R}^n} \xi(x-z,r)F(u(z,t-r))dzdr, \\
=& u_0(x,t) + \int_0^t \int_{\mathbb{R}^n} \xi(z,r)F(u(x-z,t-r))dzdr.
\end{aligned} \tag{2.3.69}$$

Thus, $u(x,t)$ satisfies

$$u(x,t) = u_0(x,t) + \int_0^t \int_{\mathbb{R}^n} G(u(x-z,t-r),z,r)dzdr, \tag{2.3.70}$$

where

$$G(u,x,r) = \xi(x,r)F(u), \tag{2.3.71}$$

$$F(u) = 1 - e^{-u}, \quad u \geq 0,$$

23

$$\xi(x, r) = \xi_1(x, r) + \xi_2(x, r),$$

$$\xi_1(x, r) = \int_{\mathbb{R}^n} \eta_1(x, r)\kappa_1(z)dz,$$

$$\eta_1(x, r) = p_1\beta \int_0^r \theta(r - s)\Upsilon(r - s)S_0 e^{-\nu_1 s}\Gamma_n(Ds, x))ds,$$

$$\xi_2(x, r) = \eta_2(r)\kappa_2(x),$$

$$\eta_2(r) = p_2\beta \int_0^r \theta(r - s)\Upsilon(r - s)S_0 e^{-\nu_2 s}ds.$$

The Volterra-Hammerstein integral equation (2.3.70) describes the development of the population (Thieme (1979b)). So, u is the cumulative rate of rabid foxes meet the susceptible foxes. η_1 and η_2 are the densities of diffusing and territorial rabid foxes, respectively. ξ_1 and ξ_2 are the contribution of diffusing and territorial rabid foxes, respectively, to the infection rate. u_0 combines the various initial conditions, and it is given in (2.3.37).

2.4 Properties of κ_1 and κ_2

We assume $\kappa_1(x, z) = \tilde{\kappa}_1(x - z) \geq 0$. By (2.2.1)

$$\kappa_2(x, z) = \int_{\mathbb{R}^n} \tilde{\kappa}_1(x - y)\tilde{\kappa}_1(z - y)dy = \tilde{\kappa}_2(x - z). \qquad (2.4.1)$$

After a substitution

$$\tilde{\kappa}_2(z) = \int_{\mathbb{R}^n} \tilde{\kappa}_1(y + z)\tilde{\kappa}_1(y)dy. \qquad (2.4.2)$$

For simplicity, we are dropping the tildes from κ_1 and κ_2. We also assume κ_1 is isotropic and

$$\int_{\mathbb{R}^n} \kappa_1(y)dy = 1, \qquad \int_{\mathbb{R}^n} e^{-\lambda y_1}\kappa_1(y)dy < \infty, \quad \lambda > 0. \qquad (2.4.3)$$

Definition 2.4.1. (Thieme and Zhao, 2003, p.434) A function $\psi : \mathbb{R}^n \to \mathbb{R}$ is said to be isotropic if $\psi(x) = \psi(y)$ whenever $|x| = |y|$.

Definition 2.4.2. (Thieme and Zhao, 2003, p.434) A function $\xi : [0, \infty) \times \mathbb{R}^n \to \mathbb{R}$ is said to be isotropic if $\xi(s, \cdot)$ is isotropic for almost all $s > 0$.

Lemma 2.4.3. *Assume κ_1 is isotropic, and $\|x\| = 1$. Let $\kappa_2(x)$ be defined as $\kappa_2(x) = \int_{\mathbb{R}^n} \kappa_1(y + x)\kappa_1(y)dy$, then κ_2 is isotropic.*

Proof. Assume $\|x\| = \|u\| = \|e_1\|$, where e_1 is the first column of the standard basis for $\mathbb{R}^n$. Then, there exists an orthogonal matrix A such that $x_1 = x = Ae_1$, and there exists an orthogonal matrix B such that $u_1 = u = Be_1$. The orthogonal matrices A and B can be constructed using Gram-Schmidt process. Since B is an orthogonal matrix, $B^T = B^{-1}$. So, we have that $e_1 = B^T u$, and then $x = AB^T u$, where AB^T is an orthogonal matrix. Thus,

$$\kappa_2(x) = \kappa_2(AB^T u) = \int_{\mathbb{R}^n} \kappa_1(y + AB^T u)\kappa_1(y)dy.$$

We make a substitution $y = AB^T z$, then

$$\kappa_2(x) = \kappa_2(AB^T u) = \int_{\mathbb{R}^n} \kappa_1(AB^T z + AB^T u)\kappa_1(AB^T z)|det AB^T|dz.$$

Since AB^T is an orthogonal matrix,

$$\kappa_2(x) = \int_{\mathbb{R}^n} \kappa_1(AB^T(z + u))\kappa_1(AB^T z)dz.$$

Since κ_1 is isotropic,

$$\kappa_2(x) = \int_{\mathbb{R}^n} \kappa_1(z + u)\kappa_1(z)dz = \kappa_2(u). \tag{2.4.4}$$

So, whenever $\|x\| = \|u\|$, we have $\kappa_2(x) = \kappa_2(u)$. Therefore, κ_2 is isotropic. $\quad\square$

Lemma 2.4.4. *Assume κ is isotropic, and $\|u\| = 1$. Then, $\int_{\mathbb{R}^n} \kappa(z)e^{\lambda(u \cdot z)}dz = \int_{\mathbb{R}^n} \kappa(z)e^{\lambda z_1}dz$.*

Proof. Assume $\|u\| = \|e_1\|$, where e_1 is the first column of the standard basis for $\mathbb{R}^n$. Then, there exists an orthogonal matrix A such that $u_1 = u = Ae_1$. After we make a substitution $z = Ay$, then we get

$$\int_{\mathbb{R}^n} \kappa(z)e^{\lambda(u \cdot z)}dz = \int_{\mathbb{R}^n} \kappa(Ay)e^{\lambda(Ae_1 \cdot Ay)}|det A|dy.$$

Since A is an orthogonal matrix,

$$\int_{\mathbb{R}^n} \kappa(z)e^{\lambda(u \cdot z)}dz = \int_{\mathbb{R}^n} \kappa(Ay)e^{\lambda(e_1 \cdot y)}dy.$$

Since κ is isotropic,

$$\int_{\mathbb{R}^n} \kappa(z)e^{\lambda(u \cdot z)}dz = \int_{\mathbb{R}^n} \kappa(y)e^{\lambda(e_1 \cdot y)}dy = \int_{\mathbb{R}^n} \kappa(y)e^{\lambda y_1}dy = \int_{\mathbb{R}^n} \kappa(z)e^{\lambda z_1}dz.$$

$\square$

Proposition 2.4.5. *Assume κ_1 is isotropic. Let $\kappa_2(x)$ be defined as $\kappa_2(x) = \int_{\mathbb{R}^n} \kappa_1(y + x)\kappa_1(y)dy$, then*

1. $\int_{\mathbb{R}^n} \kappa_2(x)dx = \left(\int_{\mathbb{R}^n} \kappa_1(y)dy\right)^2.$

2. $\int_{\mathbb{R}^n} e^{-\lambda x_1}\kappa_2(x)dx = \left(\int_{\mathbb{R}^n} e^{-\lambda y_1}\kappa_1(y)dy\right)^2.$

Proof.   1.
$$\int_{\mathbb{R}^n} \kappa_2(x)dx = \int_{\mathbb{R}^n}\left(\int_{\mathbb{R}^n} \kappa_1(y + x)\kappa_1(y)dy\right)dx.$$

We change the order of integration,

$$\int_{\mathbb{R}^n} \kappa_2(x)dx = \int_{\mathbb{R}^n} \kappa_1(y)\left(\int_{\mathbb{R}^n} \kappa_1(y + x)dx\right)dy.$$

The result follows after a change of variables in the interior integral. Therefore,

$$\int_{\mathbb{R}^n} \kappa_2(x)dx = \left(\int_{\mathbb{R}^n} \kappa_1(y)dy\right)^2.$$

2. For this part we have,

$$\int_{\mathbb{R}^n} e^{-\lambda x_1} \kappa_2(x) dx = \int_{\mathbb{R}^n} e^{-\lambda x_1} \left(\int_{\mathbb{R}^n} \kappa_1(y+x)\kappa_1(y) dy \right) dx.$$

That is,

$$\int_{\mathbb{R}^n} e^{-\lambda x_1} \kappa_2(x) dx = \int_{\mathbb{R}^n} e^{-\lambda(x_1+y_1)} \left(\int_{\mathbb{R}^n} e^{\lambda y_1} \kappa_1(y+x)\kappa_1(y) dy \right) dx.$$

We change the order of integration,

$$\int_{\mathbb{R}^n} e^{-\lambda x_1} \kappa_2(x) dx = \int_{\mathbb{R}^n} e^{\lambda y_1} \kappa_1(y) \left(\int_{\mathbb{R}^n} e^{-\lambda(x_1+y_1)} \kappa_1(y+x) dx \right) dy.$$

By a change of variables $x \to u - y$,

$$\int_{\mathbb{R}^n} e^{-\lambda x_1} \kappa_2(x) dx = \int_{\mathbb{R}^n} e^{\lambda y_1} \kappa_1(y) \left(\int_{\mathbb{R}^n} e^{-\lambda u_1} \kappa_1(u) du \right) dy.$$

The claim now follows Since κ_1 is isotropic. So,

$$\int_{\mathbb{R}^n} e^{-\lambda x_1} \kappa_2(x) dx = \left(\int_{\mathbb{R}^n} e^{-\lambda y_1} \kappa_1(y) dy \right)^2.$$

$\square$

2.5   Spreading Speeds

A number $c^* > 0$ is called the asymptotic speed of spread for a function $u :$ $\mathbb{R}_+ \times \mathbb{R}^n \to \mathbb{R}_+$ if $\lim_{t \to \infty, |x| \geq ct} u(t, x) = 0$ for every $c > c^*$, and if there exists some $\epsilon > 0$ such that $\liminf_{t \to \infty, |x| \leq ct} u(t, x) \geq \epsilon$ for every $c \in (0, c^*)$ (Aronson and Weinberger (1975, 1978); Diekmann (1978); Thieme and Zhao (2003)). With that being said, if we move in any direction with speed c that is not exceeding c^*, then we will not be able to out run the spreading virus. In the other hand, if we travel with speed $c > c^*$, then we are going to escape from the spreading virus. In this section, we are going to analyze (2.3.70) for spreading speeds based on theories developed on (Thieme (1979a); Thieme and Zhao (2003)).

27

2.5.1   Space-Time Laplace Transform

We use the space-time Laplace transform $\Xi(c, \lambda)$ to study of the asymptotic behavior of solutions of Eq. (2.3.70) (see, e.g., (Thieme and Zhao (2003); Thieme (1979a))). $\Xi(c, \lambda)$ is defined as

$$\Xi(c, \lambda) = \int_0^\infty \int_{\mathbb{R}^n} e^{-\lambda(cr+y_1)} \xi(y, r) dy dr \tag{2.5.1}$$

where y_1 is the first coordinate of y (Thieme and Zhao (2003)). We have

$$\begin{aligned}
\Xi(c, \lambda) &= \int_0^\infty \int_{\mathbb{R}^n} e^{-\lambda(cr+y_1)} \xi(y, r) dy dr \\
&= \int_0^\infty \int_{\mathbb{R}^n} e^{-\lambda(cr+y_1)} \left(\xi_1(y, r) + \xi_2(y, r) \right) dy dr \\
&= \int_0^\infty \int_{\mathbb{R}^n} e^{-\lambda(cr+y_1)} \xi_1(y, r) dy dr \\
&\quad + \int_0^\infty \int_{\mathbb{R}^n} e^{-\lambda(cr+y_1)} \xi_2(y, r) dy dr = \Xi_1(c, \lambda) + \Xi_2(c, \lambda),
\end{aligned} \tag{2.5.2}$$

where

$$\Xi_1(c, \lambda) = \int_0^\infty \int_{\mathbb{R}^n} e^{-\lambda(cr+y_1)} \xi_1(y, r) dy dr, \tag{2.5.3}$$

and

$$\Xi_2(c, \lambda) = \int_0^\infty \int_{\mathbb{R}^n} e^{-\lambda(cr+y_1)} \xi_2(y, r) dy dr. \tag{2.5.4}$$

For $\Xi_1(c, \lambda)$, we have

$$\Xi_1(c, \lambda) = \int_0^\infty \int_{\mathbb{R}^n} e^{-\lambda(cr+y_1)} \xi_1(y, r) dy dr. \tag{2.5.5}$$

Substituting (2.3.65) and (2.3.66) into (2.5.5), we obtain

$$\begin{aligned}
\Xi_1(c, \lambda) = \int_0^\infty \int_{\mathbb{R}^n} e^{-\lambda(cr+y_1)} \\
\left(p_1 \beta \int_{\mathbb{R}^n} \int_0^r \theta(r-s) \Upsilon(r-s) S_0 e^{-\nu_1 s} \Gamma_n(Ds, y-z)) \kappa_1(z) ds dz \right) dy dr.
\end{aligned} \tag{2.5.6}$$

We change the order of integration,

$$
\Xi_1(c, \lambda) = p_1 \beta S_0 \int_0^\infty e^{-\lambda cr}
$$
$$
\int_{\mathbb{R}^n} \int_0^r \theta(r-s) \Upsilon(r-s) e^{-\nu_1 s} \left(\int_{\mathbb{R}^n} e^{-\lambda y_1} \Gamma_n(Ds, y-z)) dy \right) \quad (2.5.7)
$$
$$
\kappa_1(z) ds dz dr.
$$

We change the order of integration another time,

$$
\Xi_1(c, \lambda) = p_1 \beta S_0 \int_0^\infty e^{-\lambda cr}
$$
$$
\int_0^r \theta(r-s) \Upsilon(r-s) e^{-\nu_1 s} \int_{\mathbb{R}^n} \left(\int_{\mathbb{R}^n} e^{-\lambda y_1} \Gamma_n(Ds, y-z)) dy \right) \quad (2.5.8)
$$
$$
\kappa_1(z) dz ds dr.
$$

Now, we make a change of variables $y \to z + y$,

$$
\Xi_1(c, \lambda) = p_1 \beta S_0 \int_0^\infty e^{-\lambda cr}
$$
$$
\int_0^r \theta(r-s) \Upsilon(r-s) e^{-\nu_1 s} \int_{\mathbb{R}^n} \left(\int_{\mathbb{R}^n} e^{-\lambda(z_1+y_1)} \Gamma_n(Ds, y) dy \right) \quad (2.5.9)
$$
$$
\kappa_1(z) dz ds dr.
$$

That is,

$$
\Xi_1(c, \lambda) = p_1 \beta S_0 \int_0^\infty \int_0^r \theta(r-s) \Upsilon(r-s) e^{-\nu_1 s} e^{-\lambda cr} \left(\int_{\mathbb{R}^n} e^{-\lambda y_1} \Gamma_n(Ds, y) dy \right)
$$
$$
ds dr \int_{\mathbb{R}^n} e^{-\lambda z_1} \kappa_1(z) dz.
$$
$$
(2.5.10)
$$

Proposition 2.5.1. *(Proposition 4.2 in Thieme and Zhao(2003)). Let $\Gamma(t, x)$ be the fundamental solution associated with the partial differential operator $\partial_t - \Delta_x$. Then*

$$
\int_{\mathbb{R}^n} e^{\lambda x_1} \Gamma(x, t) dx = e^{\lambda^2 t}, \quad t \geq 0.
$$

By Proposition (2.5.1), (2.5.10) shall be

$$
\Xi_1(c, \lambda) = p_1 \beta S_0 \int_0^\infty \left(\int_0^r \theta(r-s) \Upsilon(r-s) e^{-\nu_1 s} e^{-\lambda cr} e^{\lambda^2 Ds} ds \right) dr
$$
$$
\int_{\mathbb{R}^n} e^{-\lambda z_1} \kappa_1(z) dz.
$$
$$
(2.5.11)
$$

We change the order of integration and do another change of variables, so we get

$$
\begin{aligned}
\Xi_1(c,\lambda) =& p_1\beta S_0 \int_0^\infty e^{(\lambda^2 D - \lambda c - \nu_1)s} ds \int_0^\infty \theta(r)\Upsilon(r)e^{-\lambda cr} dr \\
& \int_{\mathbb{R}^n} e^{-\lambda z_1}\kappa_1(z)dz.
\end{aligned}
\tag{2.5.12}
$$

Since $\Upsilon(r) = \exp\left(-\int_0^r \theta(s)ds\right), \Upsilon'(r) = -\theta(r)\Upsilon(r)$. So, (2.5.12) shall be

$$
\begin{aligned}
\Xi_1(c,\lambda) =& p_1\beta S_0 \int_0^\infty e^{(\lambda^2 D - \lambda c - \nu_1)s} ds \left(\int_0^\infty -\Upsilon'(r)e^{-\lambda cr} dr\right) \\
& \int_{\mathbb{R}^n} e^{-\lambda z_1}\kappa_1(z)dz.
\end{aligned}
\tag{2.5.13}
$$

Evaluating the integral, we obtain

$$
\Xi_1(c,\lambda) = \frac{p_1\beta S_0}{\nu_1 + \lambda c - \lambda^2 D}\left(\int_0^\infty -\Upsilon'(r)e^{-\lambda cr} dr\right)\int_{\mathbb{R}^n} e^{-\lambda z_1}\kappa_1(z)dz.
\tag{2.5.14}
$$

if $\nu_1 + \lambda c - \lambda^2 D > 0$, and $\Xi_1(c,\lambda) = \infty$ otherwise.

For $\Xi_2(c,\lambda)$, we have

$$
\Xi_2(c,\lambda) = \int_0^\infty \int_{\mathbb{R}^n} e^{-\lambda(cr+y_1)}\xi_2(y,r)dydr.
\tag{2.5.15}
$$

Form (2.3.67) and (2.3.68), we have

$$
\Xi_2(c,\lambda) = \int_0^\infty \int_{\mathbb{R}^n} e^{-\lambda(cr+y_1)}\left(p_2\beta \int_0^r \theta(r-s)\Upsilon(r-s)S_0 e^{-\nu_2 s}ds\kappa_2(y)\right)dydr.
\tag{2.5.16}
$$

We change the order of integration,

$$
\Xi_2(c,\lambda) = p_2\beta S_0 \int_0^\infty e^{-\lambda cr}\left(\int_0^r \theta(r-s)\Upsilon(r-s)e^{-\nu_2 s}ds\right)dr \int_{\mathbb{R}^n} e^{-\lambda y_1}\kappa_2(y)dy.
\tag{2.5.17}
$$

That is

$$
\Xi_2(c,\lambda) = p_2\beta S_0 \int_0^\infty \left(\int_0^r \theta(r-s)\Upsilon(r-s)e^{-\nu_2 s}e^{-\lambda cr}ds\right)dr \int_{\mathbb{R}^n} e^{-\lambda y_1}\kappa_2(y)dy.
\tag{2.5.18}
$$

30

By changing the order of integration and doing a change of variables, we shall have

$$
\begin{aligned}
\Xi_2(c,\lambda) &= p_2\beta S_0 \int_0^\infty e^{(-\nu_2-\lambda c)s}ds \int_0^\infty \theta(r)\Upsilon(r)e^{-\lambda cr}dr \int_{\mathbb{R}^n} e^{-\lambda y_1}\kappa_2(y)dy \\
&= p_2\beta S_0 \int_0^\infty e^{(-\nu_2-\lambda c)s}ds \left(\int_0^\infty -\Upsilon'(r)e^{-\lambda cr}dr\right) \int_{\mathbb{R}^n} e^{-\lambda y_1}\kappa_2(y)dy.
\end{aligned}
\tag{2.5.19}
$$

Evaluating the integral, we get

$$
\Xi_2(c,\lambda) = \frac{p_2\beta S_0}{\nu_2 + \lambda c}\left(\int_0^\infty -\Upsilon'(r)e^{-\lambda cr}dr\right)\int_{\mathbb{R}^n} e^{-\lambda y_1}\kappa_2(y)dy.
\tag{2.5.20}
$$

By Proposition (2.4.5), we have

$$
\Xi_2(c,\lambda) = \frac{p_2\beta S_0}{\nu_2 + \lambda c}\left(\int_0^\infty -\Upsilon'(r)e^{-\lambda cr}dr\right)\left(\int_{\mathbb{R}^n} e^{-\lambda z_1}\kappa_1(z)dz\right)^2.
\tag{2.5.21}
$$

Let

$$
\hat{\kappa}_1(\lambda) = \int_{\mathbb{R}^n} e^{-\lambda z_1}\kappa_1(z)dz,
$$

then from (2.5.14) and (2.5.21) we conclude that

$$
\Xi(c,\lambda) = \left(\frac{p_1\hat{\kappa}_1(\lambda)}{\nu_1 + \lambda c - \lambda^2 D} + \frac{p_2(\hat{\kappa}_1(\lambda))^2}{\nu_2 + \lambda c}\right)\beta S_0\left(\int_0^\infty -\Upsilon'(r)e^{-\lambda cr}dr\right)
\tag{2.5.22}
$$

if $\nu_1 + \lambda c - \lambda^2 D > 0$, otherwise $\Xi(c,\lambda) = \infty$.

2.5.2   Generalization of Space-Time Laplace Transform

Since Υ is decreasing, it is of bounded variation (Thieme, 2003, Sec.B.1). So, we use the Stieltjes integral to generalize space-time Laplace transform such that $\Upsilon'(r) = d\Upsilon(r)$. Therefore,

$$
\Xi(c,\lambda) = \left(-\frac{p_1\hat{\kappa}_1(\lambda)}{\nu_1 + \lambda c - \lambda^2 D} - \frac{p_2(\hat{\kappa}_1(\lambda))^2}{\nu_2 + \lambda c}\right)\beta S_0 \int_0^\infty e^{-\lambda cr}d\Upsilon(r)
\tag{2.5.23}
$$

if $\nu_1 + \lambda c - \lambda^2 D > 0$, otherwise $\Xi(c,\lambda) = \infty$, where

$$
\hat{\kappa}_1(\lambda) = \int_{\mathbb{R}^n} e^{-\lambda z_1}\kappa_1(z)dz.
$$

31

2.5.3 The Basic Reproduction Number of Rabies $\mathcal{R}_0$

The *basic reproduction number of rabies* is given by

$$\mathcal{R}_0 = \Xi(0,0) = \left(\frac{p_1}{\nu_1} + \frac{p_2}{\nu_2}\right)\beta S_0. \tag{2.5.24}$$

Here, $1/\nu_j$ is the average time a rabid fox has available for infecting others before disease-inflicted death if it is territorial or diffusing, respectively. The weighted average of these, $\left(p_1/\nu_1 + p_2/\nu_2\right)$ is the time available for a typical rabid fox. S_0 is the density of susceptible foxes available to be infected, and β is the transmission rate.

2.5.4 Assumptions on G, ξ, and F

We start by stating the assumptions that (Thieme and Zhao (2003)) have imposed on G, ξ, and F. These function are given in (2.3.70).

(A) There exists a function $\xi : \mathbb{R}_+ \times \mathbb{R}^n \to \mathbb{R}_+$ such that

(A1) $\xi^* := \int_0^\infty \int_{\mathbb{R}^n} \xi(y,r)dydr < \infty$.

(A2) $0 \leq G(u,x,r) \leq u\xi(x,r)$, $\forall\ u,r \geq 0$, $x \in \mathbb{R}^n$.

(A3) For every compact interval I in $(0,\infty)$, there exists some $\epsilon > 0$ such that
$$G(u,x,r) \geqslant \epsilon\xi(x,r),\ \forall\ u \in I,\ r \geqslant 0,\ x \in \mathbb{R}^n.$$

(A4) for every $\epsilon > 0$, there exists some $\delta > 0$ such that
$$G(u,x,r) \geqslant (1-\epsilon)u\xi(x,r),\ \forall\ u \in [0,\delta],\ r \geqslant 0,\ x \in \mathbb{R}^n.$$

(A5) for every $w > 0$, there exists some $\Lambda > 0$ such that
$$|G(u,x,r) - G(v,x,r)| \leqslant \Lambda|u-v|\xi(x,r),\ \forall\ u \in [0,w],\ r \geqslant 0,\ x \in \mathbb{R}^n.$$

The assumptions on ξ are:

(B) The function $\xi : \mathbb{R}_+ \times \mathbb{R}^n \to \mathbb{R}_+$ is borel measurable such that

(B1) $\xi^* := \int_0^\infty \int_{\mathbb{R}^n} \xi(y, r) dy dr \in (1, \infty)$.

(B2) There exists some $\lambda_0 > 0$ such that

$$\int_0^\infty \int_{\mathbb{R}^n} e^{\lambda_0 y} \xi(y, r) dy dr < \infty$$

(B3) There exist numbers $\delta_2 > \delta_1 > 0$, $p > 0$ such that

$$\xi(y, r) > 0, \ \forall \ r \in (\delta_1, \delta_2), \ |y| \in [0, p).$$

(B4) ξ is isotropic.

The following assumptions are about $F(u)$,

(C) The function $F : \mathbb{R}_+ \to \mathbb{R}_+$ is a Lipschitz continuous function such that

(C1) $F(0) = 0$ and $F(u) > 0$, $\forall \ u > 0$.

(C2) F is differentiable at $u = 0$, $F'(0) = 1$ and $F(u) \leqslant u, \forall u > 0$.

(C3) $\lim_{u \to \infty} \frac{F(u)}{u} = 0$.

(C4) There exists a positive solution u^* of $u = \xi^* F(u)$ such that $\xi^* F(u) > u$,

$\forall u \in (0, u^*)$, and $\xi^* F(u) < u$, $\forall u > u^*$.

We start by verifying the assumptions (A).

(A1) See (B1).

(A2) From (2.3.43), we have that $F(u) = 1 - e^{-u}$, and so $F(0) = 0$. So, $F(u)$ is differentiable, and thus it is continuous. Since $F : [0, \infty) \to \mathbb{R}_+$ is differenetiable and continuous on $[0, \infty)$, we can use the mean value theorem. So, there exists some $\omega \in [0, \infty)$, such that

$$F(u) - F(0) = F'(\omega)(u - 0) = uF'(\omega) \leq u.$$

Therefore, $0 \leq G(u, x, r) = F(u)\xi(x, r) \leq u\xi(y, r)$, $\forall \ u, r \geq 0$, $x \in \mathbb{R}^n$.

(A3) For every compact interval $I \in (0, \infty)$, $F(u)$ has a minimum. That is there

exists some $\epsilon > 0$, such that $F(u) \geq \epsilon$. Therefore, $G(u, x, r) = F(u)\xi(x, r) \geqslant \epsilon\xi(x, r)$, $\forall\, u \in I$, $r \geqslant 0$, $x \in \mathbb{R}^n$.

(A4) From (A2), we have $F(u) = uF'(\omega)$, where $\omega, u \in [0, \delta]$, and $F'(\omega) = e^{-\omega}$. We can choose $\delta > 0$ such that $\delta < -\ln(1 - \epsilon)$ such that

$$F'(\omega) = e^{-\omega} \geqslant e^{-\delta} > e^{\ln(1-\epsilon)} = 1 - \epsilon.$$

Hence, for every $\epsilon > 0$, there exists some $\delta > 0$ such that

$G(u, x, r) = F(u)\xi(x, r) = uF'(\omega)\xi(x, r) \geqslant (1-\epsilon)u\xi(x, r)$, $\forall\, u \in [0, \delta]$, $r \geqslant 0$, $x \in \mathbb{R}^n$.

(A5) By the mean value theorem, there exists $p \in [0, \omega]$, where $\omega > 0$, such that

$$|F(u) - F(v)| = |F'(p)(u - v)|.$$

But $F'(p) = e^{-p} \leq 1 = \Lambda$, hence

$$|F(u) - F(v)| = |F'(p)(u - v)| \leqslant \Lambda|u - v|.$$

From that we get,

$$
\begin{aligned}
|G(u, x, r) - G(v, x, r)| &= |F(u)\xi(x, r) - F(v)\xi(x, r)| \\
&= |F'(p)(u - v)\xi(x, r)| \\
&\leq |F'(p)||(u - v)|\xi(x, r) \\
&\leq \Lambda|(u - v)|\xi(x, r).
\end{aligned}
$$

Therefore, for every $w > 0$, there exists some $\Lambda > 0$ such that

$|G(u, x, r) - G(v, x, r)| \leqslant \Lambda|u - v|\xi(x, r)$, $\forall\, u \in [0, w]$, $r \geqslant 0$, $x \in \mathbb{R}^n$.

In the following lines, we verify the assumptions on (B).

(B1) We assume $\nu_1, \nu_2 > 0$, then from (2.5.23)

$$\xi^* = \Xi(0, 0) = \left(\frac{p_1}{\nu_1} + \frac{p_2}{\nu_2}\right)\beta S_0 < \infty. \tag{2.5.25}$$

34

Choosing $\nu_1 = \nu_2 = \beta$ and $S_0 > 1$, we can achieve that $\xi^* > 1$.

(B2) Assume $\nu_1 - \lambda^2 D > 0$. Notice that

$$\int_0^\infty \int_{\mathbb{R}^n} e^{\lambda_0 y_1} \xi(y, r) dy dr = \Xi(0, \lambda).$$

Then by (2.5.23), we have

$$\Xi(0, \lambda) = \left(\frac{p_1 \hat{\kappa}_1(\lambda)}{\nu_1 - \lambda^2 D} + \frac{p_2 (\hat{\kappa}_1(\lambda))^2}{\nu_2} \right) \beta S_0 \left(\int_0^\infty -\Upsilon'(r) dr \right), \qquad (2.5.26)$$

where

$$\hat{\kappa}_1(\lambda) = \int_{\mathbb{R}^n} e^{-\lambda z_1} \kappa_1(z) dz.$$

$\Upsilon(a)$ is the probability that an infected fox is still in the latent stage a time units after infection. Then Υ is decreasing and $\Upsilon(0) = 1$. Also, as $a \to \infty$, we assume $\Upsilon(a) \to 0$. So, we have

$$\int_0^\infty -\Upsilon'(r) dr = -(\Upsilon(\infty) - \Upsilon(0)) = 1.$$

By (2.4.3), we have

$$\Xi(0, \lambda) = \left(\frac{p_1 \hat{\kappa}_1(\lambda)}{\nu_1 - \lambda^2 D} + \frac{p_2 (\hat{\kappa}_1(\lambda))^2}{\nu_2} \right) \beta S_0 < \infty. \qquad (2.5.27)$$

(B3) Let $\delta_2 > \delta_1 > 0$, $p > 0$, $r \in (\delta_1, \delta_2)$, and $r > s > 0$. From (2.3.65), (2.3.66), (2.3.67), and (2.3.68), we have

$$\xi(y, r) = p_1 \beta \int_{\mathbb{R}^n} \int_0^r S_0 \theta(r - s) \Upsilon(r - s) e^{-\nu_1 s} \Gamma_n(Ds, y - z) \kappa_1(z) ds dz$$

$$+ p_2 \beta S_0 \int_0^r \theta(r - s) \Upsilon(r - s) e^{-\nu_2 s} ds \kappa_2(y).$$

Assume there is some $\rho \in (0, \infty)$ such that $\kappa(r) > 0$ for all $r \in [0, \rho)$. Then, by (2.3.8) and (2.4.3), we conclude that $\xi(y, r) > 0$, $\forall\, r \in (\delta_1, \delta_2)$, and $|y| \in [0, p)$.

(B4) Assume κ_1 is isotropic, then κ_2 is isotropic by Lemma 2.4.3. Since Γ_n is isotropic, we conclude that ξ is isotropic.

35

In the following lines, we verify the assumptions on (C).

(C1) We have $F(u) = 1 - e^{-u}$, and clearly $e^{-u} < 1$, for all $u > 0$. Therefore, $F(0) = 0$, and $F(u) > 0$, $\forall u > 0$.

(C2) See (A2) for details.

(C3) Clearly, we have $\lim_{u \to \infty} \frac{1 - e^{-u}}{u} = 0$.

(C4) From (B1), we have $\xi^* \in (1, \infty)$. Set, $E(u) = \xi^*(1 - e^{-u}) - u$. Then, clearly, if $u^* = \ln(\xi^*)$, then $\xi^* e^{-u^*} - 1 = 0$. That is, for $\forall u \in (0, u^*)$, $\xi^* e^{-u^*} > 1$ and $E(u)$ is increasing on $(0, u^*)$. Therefore, $\xi^* F(u) > u$, $\forall u \in (0, u^*)$. In the other hand, $\forall u > u^*$, $\xi^* e^{-u^*} < 1$, and $E(u)$ is decreasing $\forall u > u^*$. Therefore, $\xi^* F(u) < u$, $\forall u > u^*$.

2.6   Results

Since we have verified the assumptions on A, B, C, and D, Theorem 2.2 and Lemma 2.1 in (Thieme and Zhao (2003)) hold and so Proposition 2.3 in (Thieme and Zhao (2003)) holds. We can say that the *spreading speed* (aka asymptotic speed of spread) is defined by

$$c^* := \inf\{c \geq 0; \; \exists \lambda > 0 : \; \Xi(c, \lambda) < 1\}, \tag{2.6.1}$$

(Diekmann (1978, 1979); Thieme (1979a)), where $\Xi(c, \lambda)$ is given by (2.5.1).

2.6.1   General Results

Lemma 2.6.1. *Let $\Upsilon(r)$ be defined as in (2.3.7), which is the probability that infected foxes with infection age r are still in the latent period. Then $\int_0^\infty -\Upsilon'(r)e^{-\lambda cr}dr$ is non-negative.*

Proof. Since $\Upsilon(0) = 1 > \Upsilon(t)$ for sufficiently large $t > 0$, then we have

$$\int_0^\infty -\Upsilon'(r)e^{-\lambda cr}dr \geq \int_0^t -\Upsilon'(r)dre^{-\lambda ct} = \left(\Upsilon(0) - \Upsilon(t)\right)e^{-\lambda ct} > 0. \tag{2.6.2}$$

36

$\square$

Lemma 2.6.2. *Given that $c, \lambda > 0$, with $\Xi_1(c, \lambda) < 1$ and $\Xi_2(c, \lambda) < 1$, then we have the following holds:*

1. $\int_{\mathbb{R}^n} \kappa_1(z) e^{-\lambda z_1} dz < \frac{\nu_1 + \lambda c - \lambda^2 D}{p_1 \beta S_0} \frac{1}{\int_0^\infty -\Upsilon'(r) e^{-\lambda cr} dr}.$

   with $\nu_1 + \lambda c - \lambda^2 D > 0.$

2. $\int_{\mathbb{R}^n} \kappa_2(z) e^{-\lambda z_1} dz < \frac{\nu_2 + \lambda c}{p_2 \beta S_0} \frac{1}{\int_0^\infty -\Upsilon'(r) e^{-\lambda cr} dr}.$

Proof. 1. For all $c, \lambda > 0$, we have that

$$\Xi_1(c, \lambda) < 1$$

where $\Xi_1(c, \lambda)$ is defined in (2.5.5), so by (2.5.14),

$$\frac{p_1 \beta S_0}{\nu_1 + \lambda c - \lambda^2 D} \left(\int_0^\infty -\Upsilon'(r) e^{-\lambda cr} dr \right) \int_{\mathbb{R}^n} e^{-\lambda z_1} \kappa_1(z) dz < 1.$$

Therefore,

$$\int_{\mathbb{R}^n} \kappa_1(z) e^{-\lambda z_1} dz < \frac{\nu_1 + \lambda c - \lambda^2 D}{p_1 \beta S_0} \frac{1}{\int_0^\infty -\Upsilon'(r) e^{-\lambda cr} dr}$$

with $\nu_1 + \lambda c - \lambda^2 D > 0.$

2. For all $c, \lambda > 0$, we have that

$$\Xi_2(c, \lambda) < 1$$

where $\Xi_2(c, \lambda)$ is defined in (2.5.15). So, by (2.5.20),

$$\frac{p_2 \beta S_0}{\nu_2 + \lambda c} \left(\int_0^\infty -\Upsilon'(r) e^{-\lambda cr} dr \right) \int_{\mathbb{R}^n} e^{-\lambda y_1} \kappa_2(y) dy < 1.$$

Therefore,

$$\int_{\mathbb{R}^n} \kappa_2(z) e^{-\lambda z_1} dz < \frac{\nu_2 + \lambda c}{p_2 \beta S_0} \frac{1}{\int_0^\infty -\Upsilon'(r) e^{-\lambda cr} dr}.$$

$\square$

37

2.6.2   Admissible u_0

We have found that

$$u_0(x,t) = u_{01}(x,t) + u_{02}(x,t) + u_{03}(x,t) + u_{04}(x,t), \tag{2.6.3}$$

where

$$
\begin{cases}
u_{01}(x,t) = \beta p_1 \int_0^t \int_{\mathbb{R}^n} \int_{\mathbb{R}^n} \kappa_1(x-z) \Gamma_n(Ds, z-y) e^{-\nu_1 s} \\[2mm]
\left(\int_0^{t-s} \int_0^\infty \theta(a+r) E_0(y,a) \mathcal{F}(a+r,r) \, da \, dr \right) dy \, dz \, ds, \\[3mm]
u_{02}(x,t) = \beta \int_0^t \int_{\mathbb{R}^n} \int_{\mathbb{R}^n} \kappa_1(x-z) \Gamma_n(Ds, z-y) R_1^\circ(y) e^{-\nu_1 s} dy \, dz \, ds \\[3mm]
u_{03}(x,t) = p_2 \beta \int_0^t \int_{\mathbb{R}^n} \kappa_2(x-z) e^{-\nu_2 s} \\[2mm]
\left(\int_0^{t-s} \int_0^\infty \theta(a+r) E_0(z,a) \mathcal{F}(a+r,r) \, da \, dr \right) dz \, ds, \\[3mm]
u_{04}(x,t) = \beta \int_0^t \int_{\mathbb{R}^n} \kappa_2(x-z) R_2^\circ(z) e^{-\nu_2 s} dz \, ds.
\end{cases}
$$

Definition 2.6.3. (Thieme and Zhao, 2003, p.436) We say that u_0 is admissible if for every $c, \lambda > 0$ with $\Xi(c,\lambda) < 1$, there is some $\gamma > 0$ such that $u_0(t,x) \leqslant \gamma e^{\lambda(ct-|x|)}$, $\forall\, t \geqslant 0$, $x \in \mathbb{R}^n$.

In the next theorem, we want to show u_0 is admissible.

Theorem 2.6.4. *Let (B), and (C) hold, and κ_1 is isotropic. Assume that $E_0 : \mathbb{R}_+ \times \mathbb{R}^n \to \mathbb{R}_+$ is a continuous function with the property that for every $\lambda > 0$, there exists some $\gamma > 0$ such that $\int_0^\infty E_0(y,a) da \leq \gamma e^{-\lambda|y|}$, $\forall\, y \in \mathbb{R}^n$. Also, for any $\lambda > 0$, we assume $R_1^\circ, R_2^\circ : \mathbb{R}^n \to \mathbb{R}_+$ are continuous functions with the property that $R_1^\circ(y) \leq \gamma e^{-\lambda|y|}$ and $R_2^\circ(y) \leq \gamma e^{-\lambda|y|}$, $\forall\, y \in \mathbb{R}^n$. Then the following holds:*

1. *u_0 is admissible.*

2. *The unique solution $u(t,x)$ of (2.3.70) satisfies $\lim_{t\to\infty, |x|\geqslant ct} u(t,x) = 0$ for every $c > c^*$.*

Proof.   1. we have

$$u_{01}(x,t) = \beta p_1 \int_0^t \int_{\mathbb{R}^n} \int_{\mathbb{R}^n} \kappa_1(x-z)\Gamma_n(Ds, z-y)e^{-\nu_1 s}$$
$$\left(\int_0^{t-s} \int_0^\infty \theta(a+r)E_0(y,a)\mathcal{F}(a+r,r)dadr \right) dydzds. \tag{2.6.4}$$

From (2.3.10), we have $\mathcal{F}(a,t) = \Upsilon(a)/\Upsilon(a-t)$. Then,

$$u_{01}(x,t) = \beta p_1 \int_0^t \int_{\mathbb{R}^n} \int_{\mathbb{R}^n} \kappa_1(x-z)\Gamma_n(Ds, z-y)e^{-\nu_1 s}$$
$$\left(\int_0^{t-s} \int_0^\infty \theta(a+r)E_0(y,a)\frac{\Upsilon(a+r)}{\Upsilon(a)}dadr \right) dydzds. \tag{2.6.5}$$

Note that

$$\int_0^{t-s} \int_0^\infty \theta(a+r)E_0(y,a)\frac{\Upsilon(a+r)}{\Upsilon(a)}dadr$$
$$= \int_0^\infty \left(\int_0^{t-s} \theta(a+r)\Upsilon(a+r)dr \right) \frac{E_0(y,a)}{\Upsilon(a)}da$$
$$= \int_0^\infty \left(\int_0^{t-s} -\Upsilon'(a+r)dr \right) \frac{E_0(y,a)}{\Upsilon(a)}da \tag{2.6.6}$$
$$= \int_0^\infty \left(\Upsilon(a) - \Upsilon(a+t-s) \right) \frac{E_0(y,a)}{\Upsilon(a)}da$$
$$\leq \int_0^\infty \Upsilon(a)\frac{E_0(y,a)}{\Upsilon(a)}da = \int_0^\infty E_0(y,a)da.$$

Thus, (2.6.5) shall be

$$u_{01}(x,t) \leq \beta p_1 \int_0^t \int_{\mathbb{R}^n} \int_{\mathbb{R}^n} \kappa_1(x-z)\Gamma_n(Ds, z-y)e^{-\nu_1 s}$$
$$\left(\int_0^\infty E_0(y,a)da \right) dydzds. \tag{2.6.7}$$

By the assumption on $E_0(y,a)$, there exists some $\gamma > 0$ such that

$$\int_0^\infty E_0(y,a)da \leq \gamma e^{-\lambda|y|}, \text{ for all } a \geq 0, y \in \mathbb{R}^n.$$

Then, it follows that

$$u_{01}(x,t) \leq \gamma \beta p_1 \int_0^t \int_{\mathbb{R}^n} \int_{\mathbb{R}^n} \kappa_1(x-z)\Gamma_n(Ds, z-y)e^{-\nu_1 s}e^{-\lambda|y|}dydzds. \tag{2.6.8}$$

39

Note that for every $u \in \mathbb{R}^n$ with $\mid u \mid = 1$, there holds $- \mid y \mid \leq u \cdot y \leq \mid y \mid$ (Thieme and Zhao (2003)). So,

$$u_{01}(x,t) \leq \gamma \beta p_1 \int_0^t \int_{\mathbb{R}^n} \int_{\mathbb{R}^n} \kappa_1(x-z) \Gamma_n(Ds, z-y) e^{-\nu_1 s} e^{\lambda u \cdot y} dy dz ds. \quad (2.6.9)$$

We change the order of integration, then let $z \to x - z$,

$$u_{01}(x,t) \leq \gamma \beta p_1 \int_0^t \int_{\mathbb{R}^n} \int_{\mathbb{R}^n} \kappa_1(z) \Gamma_n(Ds, x-z-y) e^{-\nu_1 s} e^{\lambda u \cdot y} dy dz ds. \quad (2.6.10)$$

We change the order of integration another time, and do another change of variables,

$$u_{01}(x,t) \leq \gamma \beta p_1 e^{-\lambda u \cdot x} \int_0^t \int_{\mathbb{R}^n} \int_{\mathbb{R}^n} \kappa_1(z) \Gamma_n(Ds, y) e^{-\nu_1 s} e^{\lambda u \cdot (z-y)} dy dz ds. \quad (2.6.11)$$

By Lemma(2.4.4), we have that

$$\begin{aligned} u_{01}(x,t) \leq \gamma \beta p_1 e^{-\lambda u \cdot x} \int_0^t e^{-\nu_1 s} \left(\int_{\mathbb{R}^n} \Gamma_n(Ds, y) e^{\lambda y_1} dy \right) ds \\ \int_{\mathbb{R}^n} \kappa_1(z) e^{\lambda z_1} dz. \end{aligned} \quad (2.6.12)$$

Multiply both sides by $e^{-\lambda ct}$, we have

$$\begin{aligned} e^{-\lambda ct} u_{01}(x,t) &\leq \gamma \beta p_1 e^{-\lambda u \cdot x} e^{-\lambda ct} \int_0^t e^{-\nu_1 s} \left(\int_{\mathbb{R}^n} \Gamma_n(Ds, y) e^{\lambda y_1} dy \right) ds \\ &\int_{\mathbb{R}^n} \kappa_1(z) e^{\lambda z_1} dz \\ &\leq \gamma \beta p_1 e^{-\lambda u \cdot x} \int_0^t e^{(-\nu_1 - \lambda c)s} \left(\int_{\mathbb{R}^n} \Gamma_n(Ds, y) e^{\lambda y_1} dy \right) ds \\ &\int_{\mathbb{R}^n} \kappa_1(z) e^{\lambda z_1} dz \\ &= \gamma \beta p_1 e^{-\lambda u \cdot x} \int_0^t e^{(-\nu_1 - \lambda c + \lambda^2 D)s} ds \int_{\mathbb{R}^n} \kappa_1(z) e^{\lambda z_1} dz \\ &\leq \gamma \beta p_1 e^{-\lambda u \cdot x} \int_0^\infty e^{(-\nu_1 - \lambda c + \lambda^2 D)s} ds \int_{\mathbb{R}^n} \kappa_1(z) e^{\lambda z_1} dz \\ &= \frac{\gamma \beta p_1}{\nu_1 + \lambda c - \lambda^2 D} e^{-\lambda u \cdot x} \int_{\mathbb{R}^n} \kappa_1(z) e^{\lambda z_1} dz. \end{aligned} \quad (2.6.13)$$

40

That is

$$u_{01}(x,t) \leq \frac{\gamma \beta p_1}{\nu_1 + \lambda c - \lambda^2 D} e^{\lambda(ct - u \cdot x)} \int_{\mathbb{R}^n} \kappa_1(z) e^{\lambda z_1} dz. \tag{2.6.14}$$

By using Lemma(2.6.2), we obtain

$$u_{01}(x,t) \leq \frac{\gamma}{S_0} \frac{1}{\int_0^\infty -\Upsilon'(r) e^{-\lambda cr} dr} e^{\lambda(ct - u \cdot x)}. \tag{2.6.15}$$

Letting $u = \frac{x}{|x|}$, then we obtain

$$u_{01}(x,t) \leq \frac{\gamma}{S_0} \frac{1}{\int_0^\infty -\Upsilon'(r) e^{-\lambda cr} dr} e^{\lambda(ct - |x|)}, \text{ for all } t \geq 0, x \in \mathbb{R}^n. \tag{2.6.16}$$

Now, we work on $u_{02}(x,t)$,

$$u_{02}(x,t) = \beta \int_0^t \int_{\mathbb{R}^n} \int_{\mathbb{R}^n} \kappa_1(x-z) \Gamma_n(Ds, z-y) R_1^\circ(y) e^{-\nu_1 s} dy dz ds. \tag{2.6.17}$$

By the assumption on $R_1^\circ(y)$, there exists some $\gamma > 0$ such that

$$R_1^\circ(y) \leq \gamma e^{-\lambda|y|}, \text{ for all } y \in \mathbb{R}^n.$$

Then, it follows that

$$u_{02}(x,t) \leq \gamma \beta \int_0^t \int_{\mathbb{R}^n} \int_{\mathbb{R}^n} \kappa_1(x-z) \Gamma_n(Ds, z-y) e^{-\lambda|y|} e^{-\nu_1 s} dy dz ds. \tag{2.6.18}$$

That is

$$u_{02}(x,t) \leq \gamma \beta \int_0^t \int_{\mathbb{R}^n} \int_{\mathbb{R}^n} \kappa_1(x-z) \Gamma_n(Ds, z-y) e^{\lambda u \cdot y} e^{-\nu_1 s} dy dz ds. \tag{2.6.19}$$

We change the order of integration, then do a change of variables $z \to x - z$, then

$$u_{02}(x,t) \leq \gamma \beta \int_0^t \int_{\mathbb{R}^n} \int_{\mathbb{R}^n} \kappa_1(z) \Gamma_n(Ds, x - z - y) e^{\lambda u \cdot y} e^{-\nu_1 s} dz dy ds. \tag{2.6.20}$$

41

We change the order of integration, then do another change of variables

$$u_{02}(x,t) \leq \gamma\beta \int_0^t \int_{\mathbb{R}^n} \int_{\mathbb{R}^n} \kappa_1(z)\Gamma_n(Ds, y)e^{\lambda u \cdot (z-x-y)}e^{-\nu_1 s}dydzds$$

$$= \gamma\beta e^{-\lambda u \cdot x} \int_0^t \left(\int_{\mathbb{R}^n} \Gamma_n(Ds, y)e^{-\lambda u \cdot y}dy \right) e^{-\nu_1 s}ds \qquad (2.6.21)$$

$$\int_{\mathbb{R}^n} \kappa_1(z)e^{\lambda u \cdot z}dz.$$

By Lemma(2.4.4),

$$u_{02}(x,t) \leq \gamma\beta e^{-\lambda u \cdot x} \int_0^t \left(\int_{\mathbb{R}^n} \Gamma_n(Ds, y)e^{-\lambda y_1}dy \right) e^{-\nu_1 s}ds$$

$$\int_{\mathbb{R}^n} \kappa_1(z)e^{\lambda z_1}dz \qquad (2.6.22)$$

$$= \gamma\beta e^{-\lambda u \cdot x} \int_0^t e^{(\lambda^2 D - \nu_1)s}ds \int_{\mathbb{R}^n} \kappa_1(z)e^{\lambda z_1}dz.$$

Multiply both sides by $e^{-\lambda ct}$,

$$e^{-\lambda ct}u_{02}(x,t) \leq \gamma\beta e^{-\lambda u \cdot x}e^{-\lambda ct} \int_0^t e^{(\lambda^2 D - \nu_1)s}ds \int_{\mathbb{R}^n} \kappa_1(z)e^{\lambda z_1}dz$$

$$\leq \gamma\beta e^{-\lambda u \cdot x} \int_0^t e^{(\lambda^2 D - \nu_1 - \lambda c)s}ds \int_{\mathbb{R}^n} \kappa_1(z)e^{\lambda z_1}dz$$

$$\leq \gamma\beta e^{-\lambda u \cdot x} \int_0^\infty e^{(\lambda^2 D - \nu_1 - \lambda c)s}ds \int_{\mathbb{R}^n} \kappa_1(z)e^{\lambda z_1}dz \qquad (2.6.23)$$

$$= \frac{\gamma\beta}{\nu_1 + \lambda c - \lambda^2 D}e^{-\lambda u \cdot x} \int_{\mathbb{R}^n} \kappa_1(z)e^{\lambda z_1}dz.$$

That is

$$u_{02}(x,t) \leq \frac{\gamma\beta}{\nu_1 + \lambda c - \lambda^2 D}e^{\lambda(ct - u \cdot x)} \int_{\mathbb{R}^n} \kappa_1(z)e^{\lambda z_1}dz. \qquad (2.6.24)$$

Using Lemma(2.6.2), we have

$$u_{02}(x,t) \leq \frac{\gamma}{p_1 S_0} \frac{1}{\int_0^\infty -\Upsilon'(r)e^{-\lambda cr}dr}e^{\lambda(ct - u \cdot x)}. \qquad (2.6.25)$$

Letting $u = \frac{x}{|x|}$, then we get

$$u_{02}(x,t) \leq \frac{\gamma}{p_1 S_0} \frac{1}{\int_0^\infty -\Upsilon'(r)e^{-\lambda cr}dr}e^{\lambda(ct - |x|)}, \text{ for all } t \geq 0, x \in \mathbb{R}^n. \qquad (2.6.26)$$

42

For $u_{03}(x, t)$, we have

$$
\begin{aligned}
u_{03}(x, t) = & p_2 \beta \int_0^t \int_{\mathbb{R}^n} \kappa_2(x - z) e^{-\nu_2 s} \\
& \left(\int_0^{t-s} \int_0^\infty \theta(a + r) E_0(z, a) \mathcal{F}(a + r, r) \, da \, dr \right) dz \, ds.
\end{aligned}
\tag{2.6.27}
$$

By (2.3.10), we have

$$
\begin{aligned}
u_{03}(x, t) = & p_2 \beta \int_0^t \int_{\mathbb{R}^n} \kappa_2(x - z) e^{-\nu_2 s} \\
& \left(\int_0^{t-s} \int_0^\infty \theta(a + r) E_0(z, a) \frac{\Upsilon(a + r)}{\Upsilon(a)} \, da \, dr \right) dz \, ds.
\end{aligned}
\tag{2.6.28}
$$

By (2.6.6), we have

$$
u_{03}(x, t) = p_2 \beta \int_0^t \int_{\mathbb{R}^n} \kappa_2(x - z) e^{-\nu_2 s} \left(\int_0^\infty E_0(z, a) \, da \right) dz \, ds.
\tag{2.6.29}
$$

By the assumption on $E_0(z, a)$, there exists some $\gamma > 0$ such that

$$
\int_0^\infty E_0(z, a) \, da \le \gamma e^{-\lambda |z|}, \text{ for all } a \ge 0, z \in \mathbb{R}^n.
$$

Then, we obtain

$$
u_{03}(x, t) \le \gamma p_2 \beta \int_0^t \int_{\mathbb{R}^n} \kappa_2(x - z) e^{-\nu_2 s} e^{-\lambda |z|} \, dz \, ds.
\tag{2.6.30}
$$

That is

$$
u_{03}(x, t) \le \gamma p_2 \beta \int_0^t \int_{\mathbb{R}^n} \kappa_2(x - z) e^{-\nu_2 s} e^{\lambda u \cdot z} \, dz \, ds.
\tag{2.6.31}
$$

We do a change of variables, we then have

$$
\begin{aligned}
u_{03}(x, t) \le & \gamma p_2 \beta \int_0^t \int_{\mathbb{R}^n} \kappa_2(z) e^{-\nu_2 s} e^{\lambda u \cdot (x - z)} \, dz \, ds \\
= & \gamma p_2 \beta e^{\lambda u \cdot x} \int_0^t e^{-\nu_2 s} \, ds \int_{\mathbb{R}^n} \kappa_2(z) e^{-\lambda u \cdot z} \, dz.
\end{aligned}
\tag{2.6.32}
$$

By Lemma(2.4.4),

$$
u_{03}(x, t) \le \gamma p_2 \beta e^{\lambda u \cdot x} \int_0^t e^{-\nu_2 s} \, ds \int_{\mathbb{R}^n} \kappa_2(z) e^{-\lambda z_1} \, dz.
\tag{2.6.33}
$$

43

Multiply both sides by $e^{-\lambda ct}$,

$$
\begin{aligned}
e^{-\lambda ct} u_{03}(x,t) &\leq \gamma p_2 \beta e^{\lambda u \cdot x} e^{-\lambda ct} \int_0^t e^{-\nu_2 s} ds \int_{\mathbb{R}^n} \kappa_2(z) e^{-\lambda z_1} dz \\
&\leq \gamma p_2 \beta e^{\lambda u \cdot x} \int_0^t e^{-(\nu_2 + \lambda c)s} ds \int_{\mathbb{R}^n} \kappa_2(z) e^{-\lambda z_1} dz \\
&\leq \gamma p_2 \beta e^{\lambda u \cdot x} \int_0^\infty e^{-(\nu_2 + \lambda c)s} ds \int_{\mathbb{R}^n} \kappa_2(z) e^{-\lambda z_1} dz \\
&= \frac{\gamma p_2 \beta}{\nu_2 + \lambda c} e^{\lambda u \cdot x} \int_{\mathbb{R}^n} \kappa_2(z) e^{-\lambda z_1} dz.
\end{aligned}
\tag{2.6.34}
$$

That is

$$
u_{03}(x,t) \leq \frac{\gamma p_2 \beta}{\nu_2 + \lambda c} e^{\lambda(ct - u \cdot x)} \int_{\mathbb{R}^n} \kappa_2(z) e^{-\lambda z_1} dz.
\tag{2.6.35}
$$

Using Lemma(2.6.2) and letting $u = \frac{-x}{|x|}$, then we obtain

$$
u_{03}(x,t) \leq \frac{\gamma}{S_0} \frac{1}{\int_0^\infty -\Upsilon'(r) e^{-\lambda cr} dr} e^{\lambda(ct - |x|)}, \text{ for all } t \geq 0, x \in \mathbb{R}^n.
\tag{2.6.36}
$$

Lastly, we want to verify $u_{04}(x,t)$ is admissible, so we have

$$
u_{04}(x,t) = \beta \int_0^t \int_{\mathbb{R}^n} \kappa_2(x-z) R_2^\circ(z) e^{-\nu_2 s} dz ds.
\tag{2.6.37}
$$

By the assumption on $R_2^\circ(z)$, there exists some $\gamma > 0$ such that

$$
R_1^\circ(z) \leq \gamma e^{-\lambda |z|}, \text{ for all } z \in \mathbb{R}^n.
$$

Then, it follows that

$$
\begin{aligned}
u_{04}(x,t) &\leq \gamma \beta \int_0^t \int_{\mathbb{R}^n} \kappa_2(x-z) e^{-\lambda |z|} e^{-\nu_2 s} dz ds \\
&\leq \gamma \beta \int_0^t \int_{\mathbb{R}^n} \kappa_2(x-z) e^{\lambda u \cdot z} e^{-\nu_2 s} dz ds.
\end{aligned}
\tag{2.6.38}
$$

Let $z \to x - z$,

$$
u_{04}(x,t) \leq \gamma \beta \int_0^t \int_{\mathbb{R}^n} \kappa_2(z) e^{\lambda u \cdot (x-z)} e^{-\nu_2 s} dz ds.
\tag{2.6.39}
$$

By Lemma(2.4.4),

$$u_{04}(x,t) \leq \gamma\beta e^{\lambda u \cdot x} \int_0^t \int_{\mathbb{R}^n} \kappa_2(z) e^{-\lambda z_1} e^{-\nu_2 s} dz ds. \qquad (2.6.40)$$

Multiply both sides by $e^{-\lambda ct}$,

$$
\begin{aligned}
e^{-\lambda ct} u_{04}(x,t) &\leq \gamma\beta e^{\lambda u \cdot x} e^{-\lambda ct} \int_0^t e^{-\nu_2 s} ds \int_{\mathbb{R}^n} \kappa_2(z) e^{-\lambda z_1} dz \\
&\leq \gamma\beta e^{\lambda u \cdot x} \int_0^t e^{-(\nu_2 + \lambda c)s} ds \int_{\mathbb{R}^n} \kappa_2(z) e^{-\lambda z_1} dz \\
&\leq \gamma\beta e^{\lambda u \cdot x} \int_0^\infty e^{-(\nu_2 + \lambda c)s} ds \int_{\mathbb{R}^n} \kappa_2(z) e^{-\lambda z_1} dz \\
&= \frac{\gamma\beta}{\nu_2 + \lambda c} e^{\lambda u \cdot x} \int_{\mathbb{R}^n} \kappa_2(z) e^{-\lambda z_1} dz.
\end{aligned}
\qquad (2.6.41)
$$

That is

$$u_{04}(x,t) \leq \frac{\gamma\beta}{\nu_2 + \lambda c} e^{\lambda(ct + u \cdot x)} \int_{\mathbb{R}^n} \kappa_2(z) e^{-\lambda z_1} dz. \qquad (2.6.42)$$

Using Lemma(2.6.2) and letting $u = \frac{-x}{|x|}$ in the last inequality, we obtain

$$u_{04}(x,t) \leq \frac{\gamma}{p_2 S_0} \frac{1}{\int_0^\infty -\Upsilon'(r) e^{-\lambda cr} dr} e^{\lambda(ct - |x|)} \text{ for all } t \geq 0, x \in \mathbb{R}^n. \qquad (2.6.43)$$

By (2.6.16), (2.6.26), (2.6.39) and (2.6.43), it follows that $u_0(t,x)$ is admissible.

2. By ((Thieme and Zhao, 2003, Theorem. 2.1)), the statement holds.

$\square$

2.6.3   Results for Spreading Speeds

Let Ξ_1 be Ξ with $p_1 = 1$ and $p_2 = 0$ and Ξ_2 be Ξ with $p_1 = 0$ and $p_2 = 1$ and c_j^* be the spreading speed associated with Ξ_j by (2.6.1) with Ξ_j replacing Ξ. Then $\Xi = p_1 \Xi_1 + p_2 \Xi_2$. So, we have the following theorem.

Theorem 2.6.5. $c^* \geq \min\{c_1^*, c_2^*\}$.

Proof. We can assume that $c_j^* > 0$ for $j = 1, 2$. Set $c_\bullet = \min\{c_1^*, c_2^*\}$. Let $c \in (0, c_\bullet)$. By (2.6.1) $\Xi_j(c, \lambda) \geq 1$ for all $\lambda \geq 0$. So $\Xi(c, \lambda) \geq 1$ for all $\lambda \geq 0$. By (2.6.1), $c^* \geq c$. Since $c \in (0, c_\bullet)$ has been arbitrary, $c^* \geq c_\bullet$. $\square$

Remark 2.6.6. It is an open problem whether $c^* \leq \max\{c_1^*, c_2^*\}$.

Theorem 2.6.7. *Let $\xi_1, \xi_2 :\to \mathbb{R}_+ \times \mathbb{R} \to \mathbb{R}_+$ be integral kernels, and Ξ_i be the associated space-time Laplace transforms and c_i^* the associated spreading speeds. If $\Xi_1(c, \lambda) \geq \Xi_2(c, \lambda)$ for all $c > 0$ and $\lambda \geq 0$, then $c_1^* \geq c_2^*$.*

Proof. Let $\Xi_1(c, \lambda) \geq \Xi_2(c, \lambda)$. Let's define Ξ_1^* and Ξ_2^* to be $\Xi_1^* = \{c \geq 0 : \Xi_1(c, \lambda) < 1 \text{ for some } \lambda > 0\}$ and $\Xi_2^* = \{c \geq 0 : \Xi_2(c, \lambda) < 1 \text{ for some } \lambda > 0\}$. Let's choose $\tilde{c}_1 > 0$ and $\lambda_1 \geq 0$ such that $\Xi_1(\tilde{c}_1, \lambda_1) < 1$. Since $\Xi_1(c, \lambda) \geq \Xi_2(c, \lambda)$ holds for all $c > 0$ and $\lambda \geq 0$, we have $\Xi_2(\tilde{c}_1, \lambda_1) \leqslant \Xi_1(\tilde{c}_1, \lambda_1) < 1$. So, clearly we conclude that $\Xi_1^* \subseteq \Xi_2^*$. It follows that

$$\inf(\Xi_1^*) \geqslant \inf(\Xi_2^*). \tag{2.6.44}$$

Therefore, $c_1^* \geq c_2^*$ for all $c > 0$ and $\lambda \geq 0$. $\square$

Theorem 2.6.8. *The spreading speed c^* is monotone increasing function of β, S_0, b, and D.*

Proof. Clearly if we increase β, S_0, b, or D, then $\Xi(c, \lambda)$ in (2.5.23) will increase. By Theorem (2.6.7), the spreading speed c^* is a monotone increasing function of β, S_0, b, and D. $\square$

Theorem 2.6.9. *The spreading speed c^* is monotone decreasing function of ν_1, and ν_2.*

Proof. Clearly if we increase ν_1 or ν_2, then $\Xi(c, \lambda)$ in (2.5.23) will decrease. By Theorem (2.6.7), the spreading speed c^* is a monotone decreasing function of ν_1, and ν_2. $\square$

Theorem 2.6.10. *The spreading speed c^* is monotone decreasing function of Υ.*

Proof. After integration by parts, (2.5.23) shall be

$$\Xi(c,\lambda) = \left(\frac{p_1\hat{\kappa}_1(\lambda)}{\nu_1 + \lambda c - \lambda^2 D} + \frac{p_2(\hat{\kappa}_1(\lambda))^2}{\nu_2 + \lambda c}\right)\beta S_0 \left(1 - \lambda c \int_0^\infty \Upsilon(r)e^{-\lambda cr}dr\right), \quad (2.6.45)$$

where

$$\hat{\kappa}_1(\lambda) = \int_{\mathbb{R}^n} e^{-\lambda z_1}\kappa_1(z)dz.$$

So, clearly if we increase Υ, then $\Xi(c,\lambda)$ will decrease. By Theorem (2.6.7), the spreading speed c^* is a monotone decreasing function of Υ. $\square$

2.7 Discussion and Conclusions

We reduce (2.2.2) to a scalar Volterra-Hammerstein integral equation

$$u(x,t) = u_0(x,t) + \int_0^t \int_{\mathbb{R}^n} \xi(r,|x-z|)F(u(z,t-s))dzdr. \quad (2.7.1)$$

The integral kernel ξ essentially consists of convolutions of κ_1 and of the fundamental solution of the partial differential operator $\partial_t - D\Delta_x$ and of Υ, and $F(u) = 1 - e^{-u}$. u_0 combines the various initial conditions such that

$$u_0(x,t) = u_{01}(x,t) + u_{02}(x,t) + u_{03}(x,t) + u_{04}(x,t),$$

where

$$\begin{cases} u_{01}(x,t) = \beta p_1 \int_0^t \int_{\mathbb{R}^n} \int_{\mathbb{R}^n} \kappa_1(x-z)\Gamma_n(Ds,z-y)e^{-\nu_1 s} \\[2mm] \left(\int_0^{t-s}\int_0^\infty \theta(a+r)E_0(y,a)\mathcal{F}(a+r,r)dadr\right)dydzds, \\[2mm] u_{02}(x,t) = \beta \int_0^t \int_{\mathbb{R}^n} \int_{\mathbb{R}^n} \kappa_1(x-z)\Gamma_n(Ds,z-y)R_1^\circ(y)e^{-\nu_1 s}dydzds \\[2mm] u_{03}(x,t) = p_2\beta \int_0^t \int_{\mathbb{R}^n} \kappa_2(x-z)e^{-\nu_2 s} \\[2mm] \left(\int_0^{t-s}\int_0^\infty \theta(a+r)E_0(z,a)\mathcal{F}(a+r,r)dadr\right)dzds, \\[2mm] u_{04}(x,t) = \beta \int_0^t \int_{\mathbb{R}^n} \kappa_2(x-z)R_2^\circ(z)e^{-\nu_2 s}dzds. \end{cases}$$

Here, u is the cumulative rate of rabid foxes meet the susceptible foxes. ξ is the contribution of diffusion and territorial rabid foxes to the infection rate. The space-time Laplace transform is found to be

$$\Xi(c, \lambda) = \left(-\frac{p_1 \hat{\kappa}_1(\lambda)}{\nu_1 + \lambda c - \lambda^2 D} - \frac{p_2(\hat{\kappa}_1(\lambda))^2}{\nu_2 + \lambda c} \right) \beta S_0 \int_0^\infty e^{-\lambda c r} d\Upsilon(r)$$

if $\nu_1 + \lambda c - \lambda^2 D > 0$, otherwise $\Xi(c, \lambda) = \infty$, where

$$\hat{\kappa}_1(\lambda) = \int_{\mathbb{R}^n} e^{-\lambda z_1} \kappa_1(z) dz.$$

The *basic reproduction number of rabies* is given by

$$\mathcal{R}_0 = \Xi(0, 0) = \left(\frac{p_1}{\nu_1} + \frac{p_2}{\nu_2} \right) \beta S_0.$$

We show that u_0 is admissible if E_0 and R_j° for $j = 1, 2$ are continuous on $\mathbb{R}^n$, and if there exists some $\gamma > 0$ such that $\int_0^\infty E_0(y, a) da \leq \gamma e^{-\lambda |y|}$, $R_1^\circ(y) \leq \gamma e^{-\lambda |y|}$, and $R_2^\circ(y) \leq \gamma e^{-\lambda |y|}$ for every $\lambda > 0$ and $y \in \mathbb{R}^n$. Also, we show that for every $c > c^*$,

$$\lim_{t \to \infty, \, |x| \geq ct} u(x, t) \to 0,$$

and for every $c \in (0, c^*)$,

$$\lim_{t \to \infty} \inf_{|x| \leq ct} u(x, t) \geq u^*,$$

where $u^* > 0$ is the unique solution of $\mathcal{R}_0(1 - e^{-u^*}) = u^*$. Therefore, c^* is the spreading speed of our solution u. With that being said, if we move in any direction with speed c that is not exceeding c^*, then we will not be able to out run the spreading virus. In the other hand, if we travel with speed $c > c^*$, then we are going to escape from the spreading virus.

If $\mathcal{R}_0 > 1$, the spreading speed $c^* > 0$ is uniquely determined as the solution of the system

$$\Xi(c^*, \lambda) = 1, \quad \frac{d}{d\lambda} \Xi(c^*, \lambda) = 0.$$

48

Otherwise, if $\mathcal{R}_0 \leq 1$, we define $c^* := 0$.

In addition, we have proved analytically that the spreading speed of rabies c^* is a monotone increasing function of β, S_0, b, and D, and c^* is a monotone decreasing function of Υ, ν_1, and ν_2. At this moment, we are not able to confirm whether c^* is a monotone decreasing or increasing function of the proportion of wandering rabid foxes p_1.

Chapter 3

DERIVATION OF MODELS WITH LATENT PERIODS OF FIXED AND EXPONENTIALLY DISTRIBUTED LENGTH

3.1 Abstract

We derive two different sub-models based on two different choices of the latent period. For the first model, we assume the latent period has a fixed length. For the second model, we assume the latent period has exponentially distributed length. We show that the latent period with arbitrary distributed length can be used to derive these two models. Existence and uniqueness of solutions are also discussed.

3.2 The Model

In order to include and study more cases especially when the latent period has fixed duration and when the latent period is exponentially distributed, the model in (2.2.2) must reformulate. We consider an open subset Ω of $\mathbb{R}^n$ to represent the habitat of the foxes. We also consider an epidemic outbreak and assume that it is short enough that the natural turnover of the fox population can be ignored: No foxes are born, and the only deaths are those of rabid foxes dying from rabies.

Let $S(x,t)$ denote the density of susceptible foxes (which are all territorial) at time t whose home-ranges center at location $x \in \Omega$. Further $R_1(x,t)$ are the diffusing rabid foxes at location x and time t and $R_2(x,t)$ the territorial rabid foxes at time t whose home-ranges center at location x. Finally, $L(x,t)$ are the foxes with home-range center at x at time t that are in the latent period (they are all territorial), and $I(x,t)$ is the transition rate at which foxes in the latent period become infectious.

Let $\kappa_1(x,z)$ denote the rate at which a fox with home-range center x visits the location $z \in \Omega$. The rate at which a susceptible fox with home-range center x meets a territorial rabid fox with home-range center z is given by

$$\kappa_2(x,z) = \int_\Omega \kappa_1(x,y)\kappa_1(z,y)dy, \tag{3.2.1}$$

which means that it is the rate at which they both visit some common point $y \in \Omega$ (Compare equation (5.1) in (van den Bosch *et al.* (1990))). The model takes the form,

$$\begin{cases} \partial_t S(x,t) = -\beta S(x,t) \int_\Omega \big[\kappa_1(x,z)R_1(z,t) + \kappa_2(x,z)R_2(z,t)\big]dz \\[2mm] \qquad =: -B(x,t), \\[2mm] \partial_t R_1(x,t) = D\nabla_x^2 R_1(x,t) + p_1 I(x,t) - \nu_1 R_1(x,t), \\[2mm] \partial_t R_2(x,t) = p_2 I(x,t) - \nu_2 R_2(x,t), \end{cases} \tag{3.2.2}$$

with given initial conditions

$$S(x,0) = S_0(x), \ R_1(x,0) = R_1^\circ(x), \ R_2(x,0) = R_2^\circ(x), \ x \in \Omega. \tag{3.2.3}$$

If $\Omega \neq \mathbb{R}^n$, the partial differential equation for R_1 is accompanied by boundary conditions.

The parameters $\nu_1 > 0$ and $\nu_2 > 0$ are the per capita rabies death rates of diffusing and territorial rabid foxes, respectively. p_1 is the chance of a rabid fox to diffuse, and p_2 the chance to be territorial, $p_j \geq 0$ and $p_1 + p_2 = 1$. $\beta > 0$ is the rate at which the meeting of a susceptible and rabid fox leads to the infection of the susceptible fox. $B(x,t)$ is the incidence of the disease, i.e., the number of new cases per unit of time. $D > 0$ is the diffusion constant and $\nabla_x^2 = \sum_{i=1}^n \partial_{x_i}^2$ the Laplace operator. The nonnegative continuous functions S_0, R_1° and R_2° are the initial densities of the susceptible and diffusing and territorial rabid foxes.

3.3 Latent Period of Fixed Length

If $\tau > 0$ is the fixed length of the latent period, then the individuals transiting from the latent to the infectious state at time $t > \tau$ are exactly those that were infected τ time units ago, at time $t - \tau$,

$$I(x,t) = B(x, t - \tau) = -\partial_t S(x, t - \tau), \qquad t > \tau. \tag{3.3.1}$$

For simplicity of exposition and numerical calculation, we assume that the epizootic is started at time 0 by rabid foxes with no foxes being in the latent stage, i.e.,

$$I(x,t) = 0, \qquad 0 \le t < \tau. \tag{3.3.2}$$

Therefore, for $0 \le t < \tau$, we obtain a model of ordinary differential equations

$$
\begin{cases}
\partial_t S(x,t) = -\beta S(x,t) \int_\Omega \big[\kappa_1(x,z) R_1(z,t) + \kappa_2(x,z) R_2(z,t) \big] dz \\
\qquad =: -B(x,t), \\
\partial_t R_1(x,t) = D \nabla_x^2 R_1(x,t) - \nu_1 R_1(x,t), \qquad 0 \le t < \tau \\
\partial_t R_2(x,t) = -\nu_2 R_2(x,t),
\end{cases}
\tag{3.3.3}
$$

By combining (3.3.1) and (3.3.2) with (3.2.2), we obtain a model delay differential equations for $t > \tau$

$$
\begin{cases}
\partial_t S(x,t) = -\beta S(x,t) \int_\Omega \big[\kappa_1(x,z) R_1(z,t) + \kappa_2(x,z) R_2(z,t) \big] dz \\
\qquad =: -B(x,t), \\
\partial_t R_1(x,t) = D \nabla_x^2 R_1(x,t) + p_1 B(x, t - \tau) - \nu_1 R_1(x,t), \qquad t > \tau \\
\partial_t R_2(x,t) = p_2 B(x, t - \tau) - \nu_2 R_2(x,t),
\end{cases}
\tag{3.3.4}
$$

with given initial conditions

$$S(x,0) = S_0(x), \ R_1(x,0) = R_1^\circ(x), \ R_2(x,0) = R_2^\circ(x),$$

$x \in \Omega$. We will use the system of ordinary differential equations in (3.3.3) and the system of delay differential equations (3.3.3) with the given initial conditions to do the numerical experiment in chapter 5.

3.4   Latent Period with Exponentially Distributed Length

Let $\theta > 0$ be the constant per capita rate at which infected foxes transit from the latent to the rabid (infectious) stage. In this case, we formulate a submodel for the infected foxes in the latent stage the number of which, at location x and time t, is denoted by $L(x,t)$. Since foxes are infected at rate $B(x,t)$ and do not die during the latent period, we have

$$\partial_t L(x,t) = B(x,t) - \theta L(x,t) = -\partial_t S(x,t) - \theta L(x,t). \tag{3.4.1}$$

As before, we assume that there are no foxes in the latent period at time 0, i.e.,

$$L(x,0) = 0. \tag{3.4.2}$$

Since the rate of change of $L(x,t)$ in time is the difference of the entry and exit rates of the latent stage and $B(x,t)$ is the entry rate, we obtain

$$I(x,t) = \theta L(x,t). \tag{3.4.3}$$

By (3.4.1), I satisfies the differential equation,

$$\partial_t I(x,t) = \theta B(x,t) - \theta I(x,t) = -\theta \partial_t S(x,t) - \theta I(x,t), \tag{3.4.4}$$

with the initial condition $I(x,0) = 0$. We combine (3.4.4) and $I(x,0) = 0$ with (3.2.2), which lead to the model

$$
\begin{cases}
\partial_t S(x,t) = -\beta S(x,t) \int_\Omega \big[\kappa_1(x,z)R_1(z,t) + \kappa_2(x,z)R_2(z,t)\big] dz \\
\qquad =: -B(x,t), \\
\partial_t R_1(x,t) = D\nabla_x^2 R_1(x,t) + p_1 I(x,t) - \nu_1 R_1(x,t), \\
\partial_t R_2(x,t) = p_2 I(x,t) - \nu_2 R_2(x,t), \\
\partial_t I(x,t) = \theta B(x,t) - \theta I(x,t),
\end{cases}
\tag{3.4.5}
$$

with given initial conditions

$$
S(x,0) = S_0(x), \ R_1(x,0) = R_1^\circ(x), \ R_2(x,0) = R_2^\circ(x), \ I(x,0) = I_0(x), \ x \in \Omega.
$$

We will use the system of ordinary differential equations in (3.4.5) with the given initial conditions to do the numerical experiment in chapter 6.

3.5   Latent Periods with General Length Distribution

Let $L(x,t)$ be again the number of foxes in the latent stage. Since foxes are infected at rate $B(x,t)$ and, by assumption, do not die during the latent period,

$$
\partial_t L(x,t) = B(x,t) - I(x,t),
\tag{3.5.1}
$$

where $I(x,t)$ is the transition rate of foxes from the latent period to the rabid period appearing in (3.2.2).

Let $\Upsilon(a)$ be the probability that an infected fox is still in the latent stage a time units after infection. Then Υ is decreasing and $\Upsilon(0) = 1$.

We again assume that there are no foxes in the latent stage at time 0; so all foxes in the latent stage at time $t > 0$ have been infected at some $t - a$ with $0 \le a \le t$, and

$$
L(x,t) = \int_0^t B(x,t-a)\Upsilon(a)da.
\tag{3.5.2}
$$

54

After a substitution,

$$L(x, t) = \int_0^t B(x, s)\Upsilon(t - s)ds. \tag{3.5.3}$$

Assume for a moment that Υ is continuously differentiable. By Leibnitz differentiation rule, L has partial derivatives with respect to time and we have

$$\partial_t L(x, t) = B(x, t) + \int_0^t B(x, s)\Upsilon'(t - s)ds = B(x, t) + \int_0^t B(x, t - a)\Upsilon'(a)da.$$

If Υ is not continuously differentiable, one can show that $L(x, t)$ is absolutely continuous with respect to t and

$$\partial_t L(x, t) = B(x, t) + \int_0^t B(x, t - a)d\Upsilon(a),$$

for almost all $t > 0$, where the integral is a Stieltjes integral ((Thieme, 2003, Lem.B.29)). By (3.5.1),

$$I(x, t) = -\int_0^t B(x, t - a)d\Upsilon(a). \tag{3.5.4}$$

This formula needs to be added to (2.2.2), if a latent period with general length distribution is considered.

If the latent period has a fixed length τ,

$$\Upsilon(a) = \begin{cases} 1, & 0 \leq a < \tau, \\ 0, & a > \tau, \end{cases} \tag{3.5.5}$$

and $\Upsilon(\tau)$ can be any number in $[0, 1]$. By (3.5.3),

$$\begin{aligned} L(t, x) &= \int_0^t B(x, s)ds, && 0 \leq t \leq \tau, \\ L(t, x) &= \int_{t-\tau}^t B(x, s)ds, && t > \tau. \end{aligned} \tag{3.5.6}$$

L is differentiable for $0 \leq t \neq \tau$, and

$$\begin{aligned} \partial_t L(x, t) &= B(x, t), && 0 \leq t < \tau, \\ \partial_t L(x, t) &= B(x, t) - B(x, t - \tau), && t > \tau. \end{aligned} \tag{3.5.7}$$

55

By (3.5.1),

$$I(x,t) = 0, \qquad 0 \le t < \tau,$$

$$I(x,t) = B(x, t - \tau), \qquad t > \tau, \tag{3.5.8}$$

the same equations as (3.3.1) and (3.3.2).

If the latent period has exponentially distributed length with constant exit rate θ, then

$$\Upsilon(a) = e^{-\theta a}, \tag{3.5.9}$$

and (3.5.3) is the solution to (3.4.1).

3.6 Comparison to Spatial Spread on a Bounded Domain

If one wants to see how solutions of (3.2.2) look like, one cannot solve it on $\mathbb{R}^n$ but rather solves it on a bounded domain Ω of $\mathbb{R}^n$ with sufficiently smooth boundary and Dirichlet boundary conditions. A Dirichlet condition represents a hostile absorbing boundary, alternatively a Neumann boundary conditions would represent a non-hostile reflecting boundary. It is not quite clear to us whether a seashore is a hostile or reflecting boundary for foxes. We choose Dirichlet boundary conditions for mathematical reasons because we can prove that the solutions on a bounded domain with Dirichlet boundary condition are dominated by the solutions of the homogeneous solutions on $\mathbb{R}^n$ while we have no good idea of how the solutions are related if the Dirichlet condition is replaced by a Neumann boundary condition.

The auxiliary variable $u(x,t) = \ln(S_0/S(x,t)) \ge 0$ still satisfies a Volterra-Hammerstein integral equation, but now of the form

$$u(x,t) = \int_0^t \int_\Omega \xi(x, y, s) F(u(y, t - s)) ds dy + u_0(x,t). \tag{3.6.1}$$

Here ξ incorporates the Green's function associated with $\partial_t - D\Delta_x$ and Dirichlet boundary conditions (Garroni and Menaldi (1992)) rather than the fundamental so-

lution. Again, this equation has a unique nonnegative solution u by the contraction mapping theorem ((Thieme, 1979a, Theorem 2.2)) which implies that (3.2.2) with Dirichlet boundary conditions has a unique solution.

By the maximum principle, the Green's function lies below the fundamental solution on its domain of definition. This implies that the integral kernel ξ associated with the Green's function lies below the integral kernel associated with the fundamental solution. Since $F(u) = 1 - e^{-u}$ is an increasing function of u, monotone iteration shows that the solution u of (3.6.1) lies below the solution u of (2.7.1). So the epidemic model on a bounded domain Ω with Dirichlet boundary conditions shows a less severe epidemic outbreak than the epidemic model on $\mathbb{R}^n$, and the spread of the disease modeled on Ω is not as fast as the spread of the disease modeled on $\mathbb{R}^n$ (Alanazi *et al.* (2018a)).

3.7   Discussion and Conclusions

We derived sub-models of delay and ordinary differential equations. When we assume the latent period of fixed length, we have a model of delay differential equations (see (3.3.3) and (3.3.4)). When the latent period has exponentially distributed length, we come up with a system of ordinary differential equations (see (3.4.5)).

To find the solution numerically, one does not use (3.6.1), but discretizes (3.3.3), (3.3.4), and (3.4.5), first in space and then in time. So, the numerical simulations of (3.3.3), (3.3.4) and (3.4.5) with Dirichlet boundary conditions are in Chapter 5 and Chapter 6. Since we will work on bounded domains for the numerical experiments in Chapter 5 and Chapter 6, we will have a less severe epidemic outbreak. That is the speeds of rabies will not be as fast as the speeds we have in Chapter 4.

Chapter 4

SPREADING SPEEDS

4.1 Abstract

This chapter is devoted to a study of spreading speeds c^* of rabies. It also addresses the effects of the model parameters on the spreading spreads c^*. We show a number of analytic and numerical results regarding the spreading spreads c^*. For numerical computations of the spreading speeds c^*, we assume that the movements of territorial foxes about the center of their home-range are normally distributed. We do our analytic and numerical analysis of c^* to latent periods of fixed length, exponentially distributed length, Gamma distributed length, and log-normally distributed length.

4.2 Overview

If $\mathcal{R}_0 > 1$, the *spreading speed* (aka asymptotic speed of spread) is defined by

$$c^* := \inf\{c \geq 0; \ \exists \lambda > 0 : \ \Xi(c, \lambda) < 1\}, \tag{4.2.1}$$

(Diekmann (1978, 1979); Thieme (1979a)) where, in general,

$$\Xi(c, \lambda) = \int_0^\infty \int_{\mathbb{R}^n} e^{-\lambda(cs+y_1)} \xi(s, |y|) ds dy. \tag{4.2.2}$$

$\Xi(c, \lambda)$ is found to be

$$\Xi(c, \lambda) = \left(-\frac{p_1 \hat{\kappa}_1(\lambda)}{\nu_1 + \lambda c - \lambda^2 D} - \frac{p_2 (\hat{\kappa}_1(\lambda))^2}{\nu_2 + \lambda c} \right) \beta S_0 \int_0^\infty e^{-\lambda cr} d\Upsilon(r) \tag{4.2.3}$$

if $\nu_1 + \lambda c - \lambda^2 D > 0$, otherwise $\Xi(c, \lambda) = \infty$, where

$$\hat{\kappa}_1(\lambda) = \int_{\mathbb{R}^n} e^{-\lambda z_1} \kappa_1(z) dz$$

(see Section 2.5.2). If $\mathcal{R}_0 \leq 1$, we define $c^* := 0$.

4.3 κ_1 is Normally Distributed

For the numerical computation of c^*, we assume that the movements of territorial foxes about the center of their home-range are normally distributed, i.e.,

$$\kappa_1(z) = \Gamma_n(z, b) = (4\pi b)^{-n/2} e^{-|z|^2/(4b)}, \qquad z \in \mathbb{R}^n, \tag{4.3.1}$$

where $|\cdot|$ is the Euclidean norm on $\mathbb{R}^n$, $b > 0$, and Γ_n is the fundamental solutions associated with the differential operator $\partial_t - \Delta_x$ for n space dimensions. Then $\hat{\kappa}_1(\lambda) = e^{b\lambda^2}$ in (4.2.3), (see, Proposition 2.5.1), and

$$\Xi(c, \lambda) = -\left(\frac{p_1 e^{b\lambda^2}}{\nu_1 + \lambda c - \lambda^2 D} + \frac{p_2 e^{2b\lambda^2}}{\nu_2 + \lambda c}\right) \beta S_0 \int_0^\infty e^{-\lambda c r} d\Upsilon(r). \tag{4.3.2}$$

Notice that Ξ does not depend on the space dimension! This observation is important because our numerical simulations will be in one space dimension while the foxes live in two dimensional space and the parameters b and D need to be estimated from two-dimensional data (Alanazi et $al.$ (2018a)).

4.4 Latent Period of Fixed Length

By assuming that the movements of territorial foxes about the center of their home-range are normally distributed, $\Xi(c, \lambda)$ takes the form

$$\Xi(c, \lambda) = -\left(\frac{p_1 e^{b\lambda^2}}{\nu_1 + \lambda c - \lambda^2 D} + \frac{p_2 e^{2b\lambda^2}}{\nu_2 + \lambda c}\right) \beta S_0 \int_0^\infty e^{-\lambda c r} d\Upsilon(r) \tag{4.4.1}$$

with arbitrarily distributed length of the latent stage, as discussed in Section 2.5.2 and Section 4.3. If the latent period has a fixed length τ,

$$\Upsilon(r) = \begin{cases} 1, & 0 \leq r < \tau, \\ 0, & r > \tau, \end{cases} \tag{4.4.2}$$

then

$$-\int_0^\infty e^{-\lambda c r} d\Upsilon(r) = e^{-\lambda c \tau}. \tag{4.4.3}$$

Therefore,

$$\Xi(c, \lambda) = \left(\frac{p_1 e^{b\lambda^2}}{\nu_1 + \lambda c - \lambda^2 D} + \frac{p_2 e^{2b\lambda^2}}{\nu_2 + \lambda c} \right) \beta S_0 e^{-\lambda c \tau}, \qquad (4.4.4)$$

if $\nu_1 + \lambda c - \lambda^2 D > 0$, otherwise $\Xi(c, \lambda) = \infty$. A plot of $\Xi(c, \lambda)$ versus λ for various values of c is given in Fig. 4.4.1. So, Fig. 4.4.1 depicts some of the properties of $\Xi(c, \lambda)$ such that $\Xi(c, \lambda)$ is a convex function of λ, $\Xi(c, \lambda)$ is a decreasing convex function of c, and $\Xi(c, \lambda) < \Xi(c, 0) = \mathcal{R}_0$ for some $\lambda > 0$, (see (Thieme and Zhao, 2003, Lemma. 2.1)).
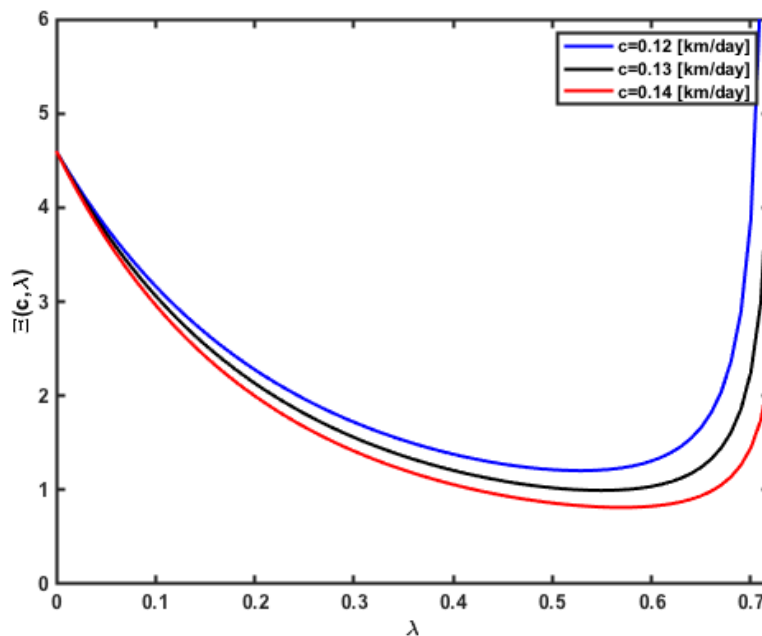
Figure 4.4.1: Graph of $\Xi(c, \lambda)$ versus λ for various values of c with $p_1 = p_2 = 0.5$ and fixed length of the latent period. The numerical values of the parameters are in 4.1.

4.4.1 The Importance of Latent Periods with Fixed Length

Among all arbitrary length distributions with mean length τ, the distribution with fixed length τ is associated with the smallest spreading speed. This follows

60

from (4.2.1) and the fact that $\Xi(c, \lambda)$ in (4.2.2) is a decreasing function of c and from Jensen's inequality (Rudin, 1966, Thm.3.3) (Thieme, 2003, Thm.B.35). Since the exponential function is convex, by Jensen's inequality,

$$-\int_0^\infty e^{-\lambda ca} d\Upsilon(a) \geq \exp\left(\int_0^\infty \lambda ca \, d\Upsilon(a)\right) = e^{-\lambda c\tau}, \tag{4.4.5}$$

where

$$\tau = -\int_0^\infty a d\Upsilon(a) = \int_0^\infty \Upsilon(a) da \tag{4.4.6}$$

is the mean length of the latent stage (Thieme, 2003, Sec.12.2). (Compare with equation (4.4.3)). We assumed $a \times 0 \to 0$ as $a \to \infty$.

This means that the spatial spread is sped up if the length of the latent period has some variation rather than no variation at all. Whether the spreading speed is an increasing function of the variation of the length of the latent period seems an open problem. As we will see in the next sections, this is the case for Gamma distributed lengths, but we could neither prove it in general nor find a counterexample.

4.4.2 Numerical Estimation of c^*

We can determine the solution (c^*, λ) uniquely by solving the system,

$$\Xi(c^*, \lambda) = 1, \quad \frac{d}{d\lambda}\Xi(c^*, \lambda) = 0 \tag{4.4.7}$$

(van den Bosch *et al.* (1990); Thieme and Zhao (2003)), where $\Xi(c^*, \lambda)$ is given in (4.4.4) with $c = c^*$. Therefore, by (4.4.4) and (4.4.7),

$$\frac{p_1 \beta S_0}{\nu_1 + \lambda c^* - \lambda^2 D} e^{\lambda^2 b} e^{-\lambda c^* \tau} + \frac{p_2 \beta S_0}{\nu_2 + \lambda c^*} e^{2\lambda^2 b} e^{-\lambda c^* \tau} = 1, \tag{4.4.8}$$

and

$$\frac{d}{d\lambda}\left[\frac{p_1 \beta S_0}{\nu_1 + \lambda c^* - \lambda^2 D} e^{\lambda^2 b} e^{-\lambda c^* \tau} + \frac{p_2 \beta S_0}{\nu_2 + \lambda c^*} e^{2\lambda^2 b} e^{-\lambda c^* \tau}\right] = 0. \tag{4.4.9}$$

The equation in (4.4.8) can be written as

$$p_1 \beta S_0 e^{\lambda^2 b} e^{-\lambda c^* \tau} (\nu_2 + \lambda c^*) + p_2 \beta S_0 e^{2\lambda^2 b} e^{-\lambda c^* \tau} (\nu_1 + \lambda c^* - \lambda^2 D)$$
$$= (\nu_2 + \lambda c^*)(\nu_1 + \lambda c^* - \lambda^2 D), \tag{4.4.10}$$

and the derivative in (4.4.9) is

$$-\frac{p_1 \beta S_0 (c^* - 2\lambda D) e^{-\lambda c^* \tau + \lambda^2 b}}{(\nu_1 + \lambda c^* - \lambda^2 D)^2} - \frac{p_2 \beta S_0 c^* e^{-\lambda c^* \tau + 2\lambda^2 b}}{(\nu_2 + \lambda c^*)^2}$$
$$+ \frac{p_1 \beta S_0 (2\lambda b - c^* \tau) e^{-\lambda c^* \tau + \lambda^2 b}}{(\nu_1 + \lambda c^* - \lambda^2 D)} + \frac{p_2 \beta S_0 (4\lambda b - c^* \tau) e^{-\lambda c^* \tau + 2\lambda^2 b}}{(\nu_2 + \lambda c^*)} = 0. \tag{4.4.11}$$

Therefore, (c^*, λ) is the unique solution of the equations (4.4.10) and (4.4.11). The numerical values of the parameters are given in Table 4.1.

Parameter	Brief description	Values	Units	References
S_0	The initial number of susceptible foxes	4.6	[fox/km^2]	(Murray *et al.* (1986); Murray (1989); Murray and Seward (1992))
β	Disease transmission coefficient	73	[km^2/year]	Estimated, see Section 5.6
D	diffusion coefficient of R_1	200	[km^2/year]	(Murray *et al.* (1986); Murray (1989); Murray and Seward (1992))
b	The constant of κ_1 and κ_2	$5/\pi^2$	[km^2]	Estimated, see Section 5.6
τ	Latent period fixed length	28	[day]	(Anderson *et al.* (1981); Källén *et al.* (1985); Murray (1989))
$1/\nu_1$	The mean length of infectious period of diffusing rabid foxes	5	[day]	(Anderson *et al.* (1981); Murray *et al.* (1986))
$1/\nu_2$	The mean length of infectious period of territorial rabid foxes	5	[day]	(Anderson *et al.* (1981); Murray *et al.* (1986))

Table 4.1: Numerical values of the model parameters.

We use Mathematica to solve the equations (4.4.10) and (4.4.11), so the unique solutions of the equations (4.4.10) and (4.4.11) are

$$(c^*, \lambda) \approx (0.0774794\,[\text{km/day}], 1.20104) \approx (28.28\,[\text{km/year}], 1.20104)$$

when $p_1 = 0$,

$$(c^*, \lambda) \approx (0.121047\,[\text{km/day}], 0.566099) \approx (44.1821\,[\text{km/year}], 0.566099)$$

when $p_1 = 0.3$,

$$(c^*, \lambda) \approx (0.129782\,[\text{km/day}], 0.548928) \approx (47.3705\,[\text{km/year}], 0.548928)$$

when $p_1 = 0.5$,

$$(c^*, \lambda) \approx (0.136702 \, [\text{km/day}], 0.538601) \approx (49.8961 \, [\text{km/year}], 0.538601)$$

when $p_1 = 0.7$, and

$$(c^*, \lambda) \approx (0.145169 \, [\text{km/day}], 0.529397) \approx (52.9868 \, [\text{km/year}], 0.529397)$$

when $p_1 = 1$. A plot of c^* versus p_1 when the latent period has a fixed length is presented on Fig. 4.10.1.

4.4.3   Results

Theorem 4.4.1. *The spreading speed c^* is monotone decreasing function of τ.*

Proof. Clearly if we increase τ, then $\Xi(c, \lambda)$ in (4.4.4) will decrease. By Theorem (2.6.7), the speed of spread c^* is a monotone decreasing function of τ. $\qquad \square$

4.5   Latent Period of Exponentially Distributed Length

We learn form Section 2.5.2 and Section 4.3 that $\Xi(c, \lambda)$ takes the form

$$\Xi(c, \lambda) = -\left(\frac{p_1 e^{b\lambda^2}}{\nu_1 + \lambda c - \lambda^2 D} + \frac{p_2 e^{2b\lambda^2}}{\nu_2 + \lambda c} \right) \beta S_0 \int_0^\infty e^{-\lambda c r} d\Upsilon(r) \qquad (4.5.1)$$

with arbitrarily distributed length of the latent stage. If the latent period has exponentially distributed length with constant exit rate θ, then

$$\Upsilon(r) = e^{-\theta r}, \qquad (4.5.2)$$

and

$$-\int_0^\infty e^{-\lambda c r} d\Upsilon(r) = \int_0^\infty e^{-\lambda c r} \theta e^{-\theta r} dr = \frac{\theta}{\theta + \lambda c}. \qquad (4.5.3)$$

Since the mean length of the latent period is $\tau = 1/\theta$, we conclude

$$\Xi(c, \lambda) = \left(\frac{p_1 e^{b\lambda^2}}{\nu_1 + \lambda c - \lambda^2 D} + \frac{p_2 e^{2b\lambda^2}}{\nu_2 + \lambda c} \right) \frac{\beta S_0}{1 + \tau \lambda c} \qquad (4.5.4)$$

63

if $\nu_1 + \lambda c - \lambda^2 D > 0$, otherwise $\Xi(c, \lambda) = \infty$. A plot of $\Xi(c, \lambda)$ versus λ for various values of c is given in Fig. 4.5.1. Fig. 4.5.1 illustrates some of the properties of $\Xi(c, \lambda)$ which are given in (Thieme and Zhao, 2003, Lemma. 2.1) such that $\Xi(c, \lambda)$ is a convex function of λ, $\Xi(c, \lambda)$ is a decreasing convex function of c, and $\Xi(c, \lambda) < \Xi(c, 0) = \mathcal{R}_0$ for some $\lambda > 0$.
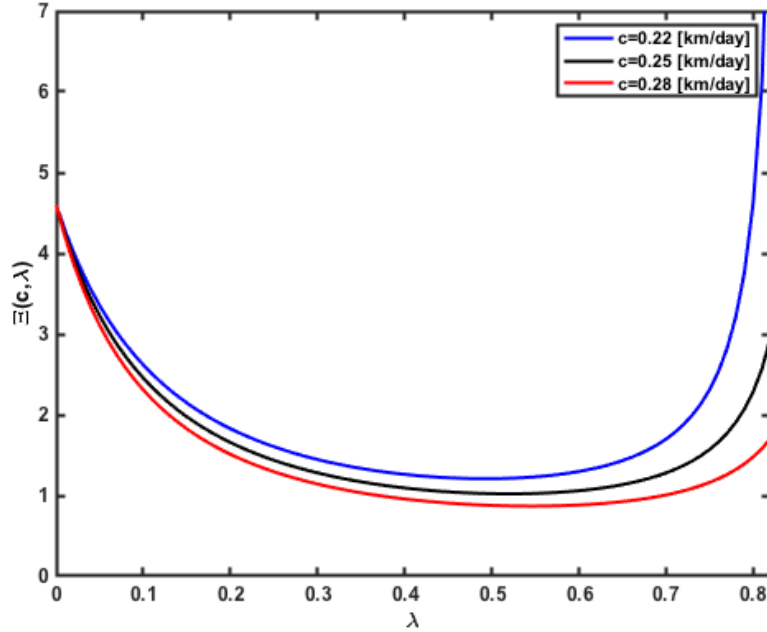
Figure 4.5.1: Graph of $\Xi(c, \lambda)$ versus λ for various values of c with $p_1 = p_2 = 0.5$ and exponentially distributed length of the latent period. The numerical values of the parameters are in Table 4.1.

4.5.1   Numerical Estimation of c^*

We can determine the solution (c^*, λ) uniquely by solving the system,

$$\Xi(c^*, \lambda) = 1, \quad \frac{d}{d\lambda}\Xi(c^*, \lambda) = 0 \tag{4.5.5}$$

64

(van den Bosch *et al.* (1990); Thieme and Zhao (2003)), where $\Xi(c^*, \lambda)$ is given in (4.5.4) with $c = c^*$. Therefore, by (4.5.4) and (4.5.5),

$$\frac{p_1\beta S_0}{\nu_1 + \lambda c^* - \lambda^2 D}\frac{\theta}{\theta + \lambda c^*}e^{\lambda^2 b} + \frac{p_2\beta S_0}{\nu_2 + \lambda c^*}\frac{\theta}{\theta + \lambda c^*}e^{2\lambda^2 b} = 1, \qquad (4.5.6)$$

and

$$\frac{d}{d\lambda}\left[\frac{p_1\beta S_0}{\nu_1 + \lambda c^* - \lambda^2 D}\frac{\theta}{\theta + \lambda c^*}e^{\lambda^2 b} + \frac{p_2\beta S_0}{\nu_2 + \lambda c^*}\frac{\theta}{\theta + \lambda c^*}e^{2\lambda^2 b}\right] = 0. \qquad (4.5.7)$$

The equation in (4.5.6) can be written as

$$p_1\beta S_0 e^{\lambda^2 b}\theta(\nu_2 + \lambda c^*) + p_2\beta S_0 e^{2\lambda^2 b}\theta(\nu_1 + \lambda c^* - \lambda^2 D)$$
$$= (\nu_2 + \lambda c^*)(\nu_1 + \lambda c^* - \lambda^2 D)(\theta + \lambda c^*), \qquad (4.5.8)$$

and the derivative for (4.5.7) is

$$-\frac{p_1\beta c^* S_0\theta e^{\lambda^2 b}}{(\nu_1 + \lambda c^* - \lambda^2 D)(\theta + c^*\lambda)^2} - \frac{p_2\beta c^* S_0\theta e^{2\lambda^2 b}}{(\nu_2 + \lambda c^*)(\theta + c^*\lambda)^2}$$
$$-\frac{p_1\beta S_0\theta(c^* - 2\lambda D)e^{\lambda^2 b}}{(\nu_1 + \lambda c^* - \lambda^2 D)^2(\theta + \lambda c^*)} + \frac{2p_1 b\beta S_0\theta\lambda e^{\lambda^2 b}}{(\nu_1 + \lambda c^* - \lambda^2 D)(\theta + \lambda c^*)} \qquad (4.5.9)$$
$$-\frac{p_2\beta S_0\theta c^* e^{2\lambda^2 b}}{(\nu_2 + \lambda c^*)^2(\theta + \lambda c^*)} + \frac{4p_2 b\lambda\beta S_0\theta e^{2\lambda^2 b}}{(\nu_2 + \lambda c^*)(\theta + \lambda c^*)} = 0.$$

Therefore, (c^*, λ) is the unique solution of the equations (4.5.8) and (4.5.9). The values of the parameters $\tau, \beta, S_0, p_1, p_2, \nu_1$, and ν_2 are given in Table 4.1. We use Mathematica to solve the equations (4.5.8) and (4.5.9), so the unique solutions of the system of equations are

$$(c^*, \lambda) \approx (0.182245\,[\text{km/day}], 0.773071) \approx (66.5195\,[\text{km/year}], 0.773071)$$

when $p_1 = 0$,

$$(c^*, \lambda) \approx (0.235233\,[\text{km/day}], 0.550237) \approx (85.86\,[\text{km/year}], 0.550237)$$

when $p_1 = 0.3$,

$$(c^*, \lambda) \approx (0.253677\,[\text{km/day}], 0.522531) \approx (92.592\,[\text{km/year}], 0.522531)$$

65

when $p_1 = 0.5$,

$$(c^*, \lambda) \approx (0.268893\,[\text{km/day}], 0.504089) \approx (98.146\,[\text{km/year}], 0.504089)$$

when $p_1 = 0.7$, and

$$(c^*, \lambda) \approx (0.288236\,[\text{km/day}], 0.484747) \approx (105.206\,[\text{km/year}], 0.484747)$$

when $p_1 = 1$. A plot of c^* versus p_1 when the length of the latent period is exponentially distributed is given in Fig. 4.10.1.

4.5.2 Results

Theorem 4.5.1. *The spreading speed c^* is monotone decreasing function of τ.*

Proof. Clearly if we increase τ, then $\Xi(c, \lambda)$ in (4.5.4) will decrease. By Theorem (2.6.7), the spreading speed c^* is a monotone decreasing function of τ. $\qquad\square$

4.6 Latent Period of Gamma Distributed Length

We know form Section 2.5.2 and Section 4.3 that $\Xi(c, \lambda)$ takes the form

$$\Xi(c, \lambda) = -\left(\frac{p_1 e^{b\lambda^2}}{\nu_1 + \lambda c - \lambda^2 D} + \frac{p_2 e^{2b\lambda^2}}{\nu_2 + \lambda c}\right)\beta S_0 \int_0^\infty e^{-\lambda c r} d\Upsilon(r). \qquad (4.6.1)$$

If we assume the length of the latent period is Gamma distributed, then

$$\Upsilon(r) = \int_r^\infty \hat{\gamma}(x; q, h) dx, \quad \hat{\gamma}(x; q, h) = \frac{q(qx)^{h-1}}{\hat{\Gamma}(h)} e^{-qx}, \quad x \geq 0, \qquad (4.6.2)$$

where q is the scale parameter, and h is the shape parameter with $q, h > 0$. $\hat{\Gamma}(h)$ is the Gamma function, and it is defined by $\hat{\Gamma}(h) = \int_0^\infty e^{-t}t^{h-1}dt$ (Bhattacharya and Burman (2016)). The mean of the Gamma distribution is $\tau = h/q$, which represents the average length of the latent period. In addition, the variance of the Gamma distribution is $\sigma^2 = \tau/q$, which represents the variance of the latent period

66

(Bhattacharya and Burman (2016); Jones *et al.* (2016); Smith and Thieme (2012)).
Clearly,we have that $h = \tau^2/\sigma^2$. Note that when $h = 1$, the length of the latent period
is exponentially distributed. We have

$$-\int_0^\infty e^{-\lambda cr} d\Upsilon(r) = \int_0^\infty \frac{q^h r^{h-1}}{\hat{\Gamma}(h)} e^{-r(q+\lambda c)} dr = \left(\frac{h}{h + \tau\lambda c}\right)^h, \qquad (4.6.3)$$

(see (Thieme, 2003, p.235)). Therefore,

$$\Xi(c, \lambda) = \left(\frac{p_1 e^{b\lambda^2}}{\nu_1 + \lambda c - \lambda^2 D} + \frac{p_2 e^{2b\lambda^2}}{\nu_2 + \lambda c}\right) \beta S_0 \left(\frac{h}{h + \tau\lambda c}\right)^h \qquad (4.6.4)$$

if $\nu_1 + \lambda c - \lambda^2 D > 0$, otherwise $\Xi(c, \lambda) = \infty$. Fig. 4.6.1 demonstrates some of the
properties of $\Xi(c, \lambda)$ for $h = 2$ and $h = 5$. $\Xi(c, \lambda)$ is a convex function of λ, $\Xi(c, \lambda)$ is
a decreasing convex function of c, and $\Xi(c, \lambda) < \Xi(c, 0) = \mathcal{R}_0$ for some $\lambda > 0$, (see
(Thieme and Zhao, 2003, Lemma. 2.1)).
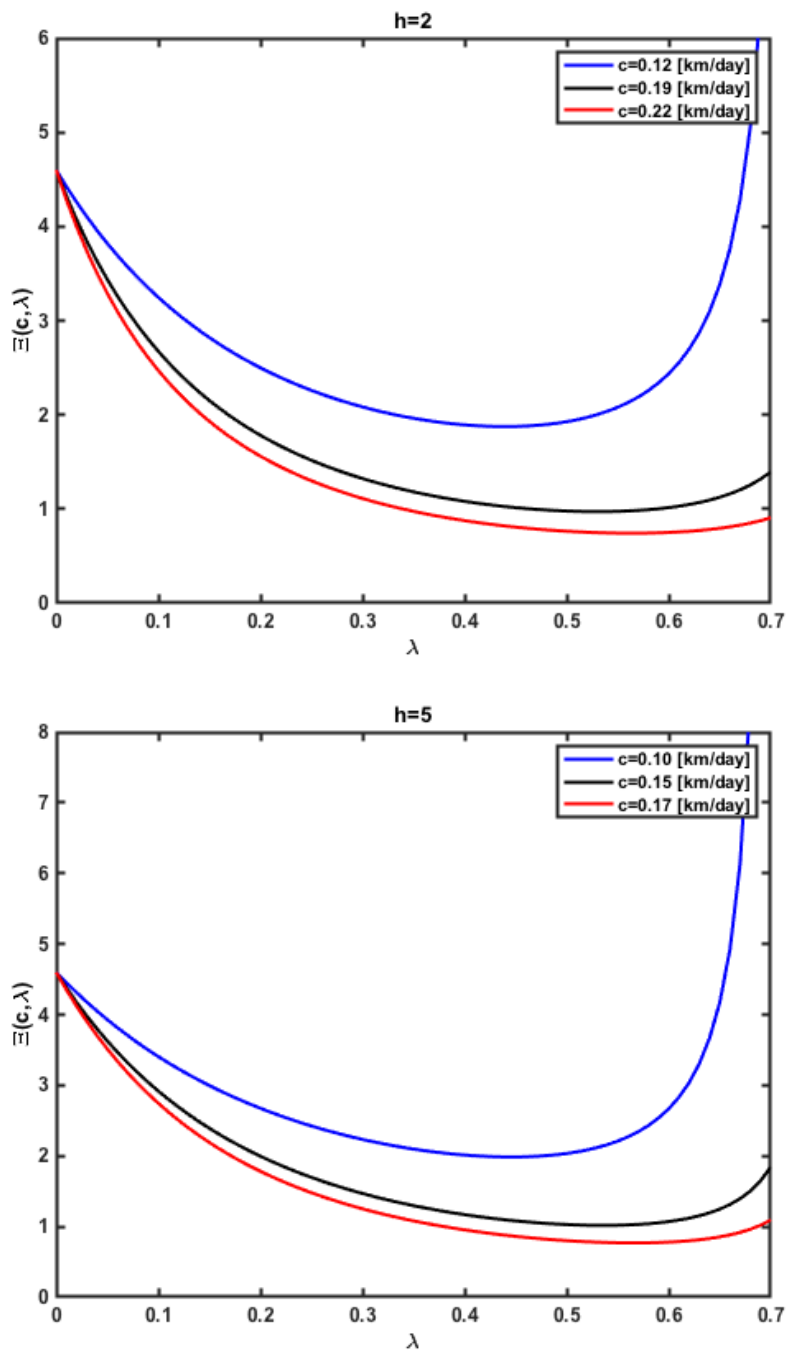
Figure 4.6.1: Graph of $\Xi(c, \lambda)$ versus λ for various values of c and h with $p_1 = p_2 = 0.5$ and Gamma distributed length of the latent period. The numerical values of the parameters are in Table 4.1.

4.6.1 Numerical Estimation of c^*

We can determine the solution (c^*, λ) uniquely by solving the system,

$$\Xi(c^*, \lambda) = 1, \quad \frac{d}{d\lambda}\Xi(c^*, \lambda) = 0, \tag{4.6.5}$$

where $\Xi(c^*, \lambda)$ is given in (4.6.4) with $c = c^*$. When $h = 1$, the latent period is exponentially distributed, and the speeds of spread c^* are given in Section 4.5.1. We use Mathematica to solve the system of equations (4.6.5) for $h = 2$ and $h = 5$ where the values of the parameters $\tau, \beta, S_0, p_1, p_2, \nu_1$, and ν_2 are given in Table 4.1. So, the unique solutions of the system of equations (4.6.5) when $h = 2$ are

$$(c^*, \lambda) \approx (0.125647\,[\text{km/day}], 0.880659) \approx (45.8612\,[\text{km/year}], 0.880659)$$

when $p_1 = 0$,

$$(c^*, \lambda) \approx (0.17323\,[\text{km/day}], 0.551591) \approx (63.2288\,[\text{km/year}], 0.551591)$$

when $p_1 = 0.3$,

$$(c^*, \lambda) \approx (0.186926\,[\text{km/day}], 0.526517) \approx (68.2278\,[\text{km/year}], 0.526517)$$

when $p_1 = 0.5$,

$$(c^*, \lambda) \approx (0.198078\,[\text{km/day}], 0.509931) \approx (72.2984\,[\text{km/year}], 0.509931)$$

when $p_1 = 0.7$, and

$$(c^*, \lambda) \approx (0.212109\,[\text{km/day}], 0.492723) \approx (77.4196\,[\text{km/year}], 0.492723)$$

when $p_1 = 1$. A plot of c^* versus p_1 when the length of the latent period is Gamma distributed and $h = 2$ is given in Fig. 4.10.1.

When $h = 5$, the system (4.6.5) has the following solutions

$$(c^*, \lambda) \approx (0.0958041\,[\text{km/day}], 1.01582) \approx (34.9685\,[\text{km/year}], 1.015829)$$

69

when $p_1 = 0$,

$$(c^*, \lambda) \approx (0.140481\,[\text{km/day}], 0.558589) \approx (51.2754\,[\text{km/year}], 0.558589)$$

when $p_1 = 0.3$,

$$(c^*, \lambda) \approx (0.151185\,[\text{km/day}], 0.537392) \approx (55.1824\,[\text{km/year}], 0.537392)$$

when $p_1 = 0.5$,

$$(c^*, \lambda) \approx (0.159787\,[\text{km/day}], 0.523766) \approx (58.3222\,[\text{km/year}], 0.523766)$$

when $p_1 = 0.7$, and

$$(c^*, \lambda) \approx (0.170476\,[\text{km/day}], 0.510225) \approx (62.2238\,[\text{km/year}], 0.510225)$$

when $p_1 = 1$.

4.6.2   Results

Theorem 4.6.1. *The spreading speed c^* is monotone decreasing function of τ.*

Proof. Clearly if we increase τ, then $\Xi(c, \lambda)$ in (4.6.4) will decrease. By Theorem (2.6.7), the spreading speed c^* is a monotone decreasing function of τ. $\qquad\square$

Theorem 4.6.2. *The spreading speed c^* is monotone decreasing function of h if the mean length of the latent period τ is fixed.*

Proof. Assume the mean length of the latent period τ is fixed. From (4.6.4), we set

$$\omega(x) = \left(\frac{h}{h + \tau x} \right)^h.$$

Similarly as in (Jones *et al.*, 2013, Sec. 6), we have

$$\frac{\partial}{\partial h} \log \omega(x) = \frac{r}{1 + r} - \log(1 + r) < 0,$$

where $r = x\tau/h$. Therefore, $\Xi(c, \lambda)$ in (4.6.4) is a decreasing function of h. By Theorem (2.6.7), the speed of spread c^* is a monotone decreasing function of h. $\qquad\square$

70

Theorem 4.6.3. *The spreading speed c^* is monotone increasing function of the variance of the latent period $v = \sigma^2$ if the mean length of the latent period τ is fixed.*

Proof. Assume the mean length of the latent period τ is fixed. Since the shape parameter of Gamma distribution $h = \tau^2/v$, we have that

$$\omega(x) = \left(\frac{h}{h + \tau x}\right)^h = \left(\frac{\tau}{\tau + xv}\right)^{\tau^2/v}.$$

By (Jones *et al.*, 2013, Sec. 6),

$$\frac{\partial}{\partial v} \log \omega(x) = \frac{\tau^2}{v^2}\left(\log(1 + r) - \frac{r}{1 + r}\right) > 0,$$

where $r = xv/\tau$. Therefore, $\Xi(c, \lambda)$ in (4.6.4) is an increasing function of the variance $v = \sigma^2$. By Theorem (2.6.7), the speed of spread c^* is a monotone increasing function of the variance $v = \sigma^2$. $\square$

Theorem 4.6.4. *The spreading speed c^* is monotone decreasing function of the mean length of the latent period τ if the variance of the latent period $v = \sigma^2$ is fixed.*

Proof. Assume the variance of the latent period $v = \sigma^2$ is fixed. We have

$$\omega(x) = \left(\frac{h}{h + \tau x}\right)^h = \left(\frac{\tau}{\tau + xv}\right)^{\tau^2/v}.$$

By (Jones *et al.*, 2013, Sec. 6),

$$\frac{\partial}{\partial \tau} \log \omega(x) = \frac{\tau}{v}\left(-\log(1 + r) - \left(\log(1 + r) - \frac{r}{1 + r}\right)\right) < 0,$$

where $r = xv/\tau$. Therefore, $\Xi(c, \lambda)$ in (4.6.4) is a decreasing function of τ. By Theorem (2.6.7), the spreading speed c^* is a monotone decreasing function of τ. $\square$

4.7 Latent Period of Log-normally Distributed Length

$\Xi(c, \lambda)$ takes the form

$$\Xi(c, \lambda) = -\left(\frac{p_1 e^{b\lambda^2}}{\nu_1 + \lambda c - \lambda^2 D} + \frac{p_2 e^{2b\lambda^2}}{\nu_2 + \lambda c}\right)\beta S_0 \int_0^\infty e^{-\lambda c r} d\Upsilon(r), \tag{4.7.1}$$

71

(see Section 2.5.2 and Section 4.3). Following Sartwell (Sartwell (1950, 1966)), we assume the length of the latent period is log-normally distributed such that

$$\Upsilon(r) = \int_{\ln(r)}^{\infty} \exp\left(\frac{-1}{2}\left[\frac{x - \ln(m)}{\sigma}\right]^2\right) \frac{1}{\sigma\sqrt{2\pi}} dx. \tag{4.7.2}$$

So, the mean length of the latent period is $\tau = me^{\sigma^2/2}$, and the variance is $m^2 e^{\sigma^2}(e^{\sigma^2} - 1)$ (Thieme, 2003, p.204). Therefore,

$$-\int_0^{\infty} e^{-\lambda cr} d\Upsilon(r) = \int_0^{\infty} \frac{1}{r\sigma\sqrt{2\pi}} \exp\left(\frac{-1}{2}\left[\frac{\ln(\frac{r}{m})}{\sigma}\right]^2\right) e^{-\lambda cr} dr$$

$$= \frac{1}{\sigma\sqrt{2\pi}} \int_0^{\infty} \frac{1}{t} \exp\left(\frac{-1}{2}\left[\frac{\ln(t)}{\sigma}\right]^2\right) e^{-\lambda cmt} dt$$

$$= \frac{1}{\sigma\sqrt{2\pi}} \int_{-\infty}^{\infty} \exp\left(\frac{-1}{2}\left[\frac{s}{\sigma}\right]^2\right) e^{-\lambda cme^s} ds$$

$$= \frac{1}{\sqrt{2\pi}} \int_{-\infty}^{\infty} \exp\left(\frac{-1}{2}t^2\right) e^{-\lambda cme^{\sigma t}} dt \tag{4.7.3}$$

$$= \frac{1}{\sqrt{2\pi}} \int_{-\infty}^{0} \exp\left(\frac{-1}{2}t^2\right) e^{-\lambda cme^{\sigma t}} dt + \frac{1}{\sqrt{2\pi}} \int_0^{\infty} \exp\left(\frac{-1}{2}t^2\right) e^{-\lambda cme^{\sigma t}} dt$$

$$= \frac{-1}{\sqrt{2\pi}} \int_{\infty}^{0} \exp\left(\frac{-1}{2}t^2\right) e^{-\lambda cme^{-\sigma t}} dt + \frac{1}{\sqrt{2\pi}} \int_0^{\infty} \exp\left(\frac{-1}{2}t^2\right) e^{-\lambda cme^{\sigma t}} dt$$

$$= \frac{1}{\sqrt{2\pi}} \int_0^{\infty} \exp\left(\frac{-1}{2}t^2\right) e^{-\lambda cme^{-\sigma t}} dt + \frac{1}{\sqrt{2\pi}} \int_0^{\infty} \exp\left(\frac{-1}{2}t^2\right) e^{-\lambda cme^{\sigma t}} dt$$

$$= \frac{1}{\sqrt{2\pi}} \int_0^{\infty} \exp\left(\frac{-1}{2}t^2\right) \left(e^{-\lambda cme^{-\sigma t}} + e^{-\lambda cme^{\sigma t}}\right) dt.$$

So, the space-time Laplace transform is now of the form,

$$\Xi(c, \lambda) = \left(\frac{p_1 e^{\lambda^2 b}}{\nu_1 + \lambda c - \lambda^2 D} + \frac{p_2 e^{2\lambda^2 b}}{\nu_2 + \lambda c}\right) \beta S_0$$

$$\left(\frac{1}{\sqrt{2\pi}} \int_0^{\infty} \exp\left(\frac{-1}{2}t^2\right) \left(e^{-\lambda cme^{-\sigma t}} + e^{-\lambda cme^{\sigma t}}\right) dt\right) \tag{4.7.4}$$

if $\nu_1 + \lambda c - \lambda^2 D > 0$, otherwise $\Xi(c, \lambda) = \infty$.

4.7.1   Results

Theorem 4.7.1. *The spreading speed c^* is monotone decreasing function of m.*

Proof. If we increase m, $\Xi(c, \lambda)$ will decrease. So, by Theorem (2.6.7), the speed of spread c^* is a monotone decreasing function of m. □

4.8   Monotone Dependence on the Proportion of Diffusing Rabid Foxes

We assume that diffusing and territorial rabid foxes die from rabies at the same rate $\nu_1 = \nu_2 =: \nu$. In Section 4.3, we assume that the movements of territorial foxes about the center of their home-range are normally distributed, i.e.,

$$\kappa_1(z) = \Gamma_n(z, b) = (4\pi b)^{-n/2} e^{-|z|^2/(4b)}, \qquad z \in \mathbb{R}^n, \tag{4.8.1}$$

where $|\cdot|$ is the Euclidean norm on $\mathbb{R}^n$, $b > 0$. In Section 5.6, we find that $b = r_0^2/\pi$, where r_0 is the mean maximum distance of a territorial fox from the center of its home-range. Then, we have the following result.

Theorem 4.8.1 (Alanazi *et al.* (2018b)). *If $b\nu > D$, the spreading speed decreases as a function of the proportion of p_1 of diffusing rabid foxes provided that $\mathcal{R}_0 > 1$ is sufficiently close to* 1.

if $b\nu < D$, the spreading speed increases as a function of the proportion of p_1 of diffusing rabid foxes provided that $\mathcal{R}_0 > 1$ is sufficiently close to 1.

Let assume, for instance, that the length of the latent period has a fixed length. If $\nu_1 = \nu_2 =: \nu$, then from (2.5.24) $\mathcal{R}_0 = \frac{\beta S_0}{\nu}$, and

$$\Xi(c, \lambda) = \left(\frac{p_1 e^{b\lambda^2}}{\nu + \lambda c - \lambda^2 D} + \frac{p_2 e^{2b\lambda^2}}{\nu + \lambda c} \right) \nu \mathcal{R}_0 e^{-\lambda c \tau}. \tag{4.8.2}$$

A plot of $\Xi(c, \lambda)$ versus p_1 for $b\nu > D$ and $b\nu < D$ is given in Fig. 4.8.1. The numerical results in Fig. 4.8.1 suggest that $\mathcal{R}_0$ may not need to be very close to 1 for the results in Theorem 4.8.1 to hold.
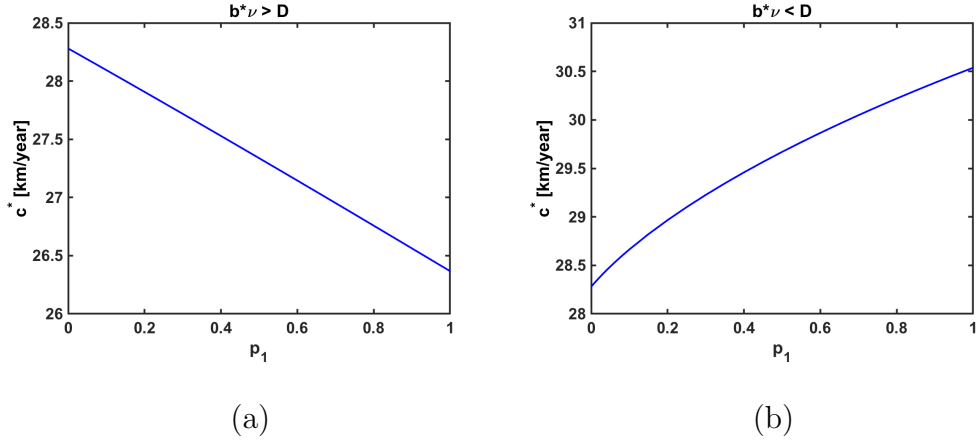
Figure 4.8.1: Different monotonicity in the dependence of the spreading speed c^* on p_1. We use (4.8.2) to solve (4.4.7). Here, $1/\nu = 5\,[\text{day}]$, $\tau = 28\,[\text{day}]$, $\mathcal{R}_0 = 4.6$, $b\nu = 36.98\,[\text{km}^2/\text{year}]$, (a) $D = 30\,[\text{km}^2/\text{year}]$ and (b) $D = 50\,[\text{km}^2/\text{year}]$.

4.9 Numerical comparison to a model with diffusing foxes only but with population turnover

The rabies model in (Murray, 1989, Sec.20.4) Murray *et al.* (1986); Murray and Seward (1992) incorporates the turnover of the fox population into an epidemic model with diffusing rabid foxes and exponentially distributed length of the latent period. Newborn foxes enter the population at a fixed per capita rate and all foxes are subject to a natural density-dependent per capita death rate. We have not included this turnover in order to be able to analyze a model that includes territorial rabid foxes.

In reality, fox reproduction is seasonal. In Britain, e.g., most cubs are born between mid-March and mid-April (Lloyd, 1980, p.115) as it seems to be the case in continental Europe (Toma and Andral, 1977, III.A.2).

In order to have an educated guess about the impact of population turnover, we look at the special case of our model with the same assumptions, including that

susceptible and incubating foxes stay at the center of their home-ranges all the time. For $p_1 = 1$, (4.5.4) takes the form

$$\Xi(c, \lambda) = \left(\frac{1}{\nu_1 + \lambda c - \lambda^2 D}\right)\frac{\beta S_0}{1 + \tau \lambda c} \tag{4.9.1}$$

if $\nu_1 + \lambda c - \lambda^2 D > 0$, otherwise $\Xi(c, \lambda) = \infty$. In Table 4.2, we compare spreading speeds that have been determined by numerically solving system (4.5.5) with the minimum wave speeds calculated in (Murray, 1989, Sec.20.4) Murray *et al.* (1986); Murray and Seward (1992). The results agree qualitatively and are not too different quantitatively.

This encourages us to believe that the qualitative behavior of the spreading speed is not affected by the omission of population turnover and that the quantitative results contain useful information as long as they are seen as approximations.

S_0 [fox/km^2]	c^* [km/year]	The speeds as in (Murray *et al.*, 1986, Table 3) and (Murray and Seward, 1992, Table 2)
1.5	36	35
2.0	52	50
2.5	65	70
3	76	80
4.6	103	103

Table 4.2: Spreading speed c^* dependence on S_0 when the latent period has exponentially distributed length, $p_1 = 1$, and $\beta = 80$ [km^2/year]. The initial fox density S_0 is equal to the fox carrying capacity K in Murray (1989); Murray *et al.* (1986); Murray and Seward (1992). The other parameters are chosen as therein though the symbols may be different, and they are given in Table 4.1.

4.10 Discussion and Conclusions

By assuming that the movements of territorial foxes about the center of their home-range are normally distributed, $\Xi(c, \lambda)$ takes the form

$$\Xi(c, \lambda) = -\left(\frac{p_1 e^{b\lambda^2}}{\nu_1 + \lambda c - \lambda^2 D} + \frac{p_2 e^{2b\lambda^2}}{\nu_2 + \lambda c}\right)\beta S_0 \int_0^\infty e^{-\lambda c r} d\Upsilon(r) \qquad (4.10.1)$$

with arbitrarily distributed length of the latent stage, as discussed in Section 2.5.2 and Section 4.3. When the latent period has a fixed length τ, we show that the space-time Laplace transform is given by

$$\Xi(c, \lambda) = \left(\frac{p_1 e^{b\lambda^2}}{\nu_1 + \lambda c - \lambda^2 D} + \frac{p_2 e^{2b\lambda^2}}{\nu_2 + \lambda c}\right)\beta S_0 e^{-\lambda c \tau}. \qquad (4.10.2)$$

In this case, rabies spreads with speeds c^* ranging from $28.28\,[\text{km/year}]$ when $p_1 = 0$ up to $52.9868\,[\text{km/year}]$ when $p_1 = 1$.

When we assume the length of the latent periods is Gamma distributed, we obtain

$$\Xi(c, \lambda) = \left(\frac{p_1 e^{b\lambda^2}}{\nu_1 + \lambda c - \lambda^2 D} + \frac{p_2 e^{2b\lambda^2}}{\nu_2 + \lambda c}\right)\beta S_0 \left(\frac{h}{h + \tau \lambda c}\right)^h. \qquad (4.10.3)$$

If $h = 1$, the length of the latent period is exponentially distributed (see (4.5.4)), and we find that rabies propagates with asymptotic speeds $c^* = 66.5195\,[\text{km/year}]$ for $p_1 = 0$ and $c^* = 105.206\,[\text{km/year}]$ for $p_1 = 1$. Also, rabies spreads with speed ranging from $c^* = 45.8612\,[\text{km/year}]$ to $c^* = 77.4196\,[\text{km/year}]$ when $h = 2$, while the speed's range decreases to be from $c^* = 34.9685\,[\text{km/year}]$ to $c^* = 62.2238\,[\text{km/year}]$ when $h = 5$. In addition, $\left(\frac{h}{h+\tau\lambda c}\right)^h \to e^{-\lambda c \tau}$ as $h \to \infty$. Therefore, as $h \to \infty$ in (4.10.3), the length of the latent period converges to a distribution of fixed length τ.

When we assume the latent period is log-normally distributed, we obtain

$$
\Xi(c, \lambda) = \left(\frac{p_1 e^{\lambda^2 b}}{\nu_1 + \lambda c - \lambda^2 D} + \frac{p_2 e^{2\lambda^2 b}}{\nu_2 + \lambda c} \right) \beta S_0
$$
$$
\left(\frac{1}{\sqrt{2\pi}} \int_0^\infty \exp\left(\frac{-1}{2} t^2 \right) \left(e^{-\lambda c m e^{-\sigma t}} + e^{-\lambda c m e^{\sigma t}} \right) dt \right).
$$

(4.10.4)

Therefore, as $\sigma \to 0$, we have

$$
\Xi(c, \lambda) \to \left(\frac{p_1 e^{\lambda^2 b}}{\nu_1 + \lambda c - \lambda^2 D} + \frac{p_2 e^{2\lambda^2 b}}{\nu_2 + \lambda c} \right) \beta S_0 e^{-\lambda c m}.
$$

(4.10.5)

So, as $\sigma \to 0$ in (4.10.4), the length of the latent period converges to a distribution of fixed length m. In this case, it is so complicated to find an estimate for the asymptotic spreading speeds of rabies c^*.

The numerical results of c^* confirm that the latent period with fixed length gives the smallest spreading speeds (see Section 4.4.1). In addition, the numerical computations of c^* confirm that Theorem 2.6.5 in Section 2.6.3 holds.

Furthermore, it has been proved analytically that the spreading speed of rabies c^* is a monotone increasing function of β, S_0, b, and D, and c^* is a monotone decreasing function of Υ, ν_1, and ν_2. When the length of the latent period is fixed, c^* is a monotone decreasing function of the mean length of the latent period τ. For the case where the latent period has Gamma distributed length, c^* is monotone decreasing function of the mean length of the latent period τ and of h if the mean length of the latent period τ is fixed, and c^* is monotone increasing function of the variance of the latent period σ^2 if the mean length of the latent period τ is fixed. When the length of the latent period is log-normally distributed, we find that c^* is monotone decreasing function of m.

Also, c^* increases as we increase the proportion of wandering rabid foxes p_1 when the latent period has fixed length, exponentially distributed length, and Gamma distributed length, as demonstrated by the numerical simulations shown in Fig. 4.10.1.

77

The last happens for what we believe is a realistic choice of parameters b and D. In general, the monotone behavior of c^* as a function of p_1 depends on the relation between b and D, as depicted in Fig. 4.8.1. In addition, the numerical results in Fig. 4.8.1 suggest that $\mathcal{R}_0$ may not need to be very close to 1 for the results in Theorem 4.8.1 to hold.
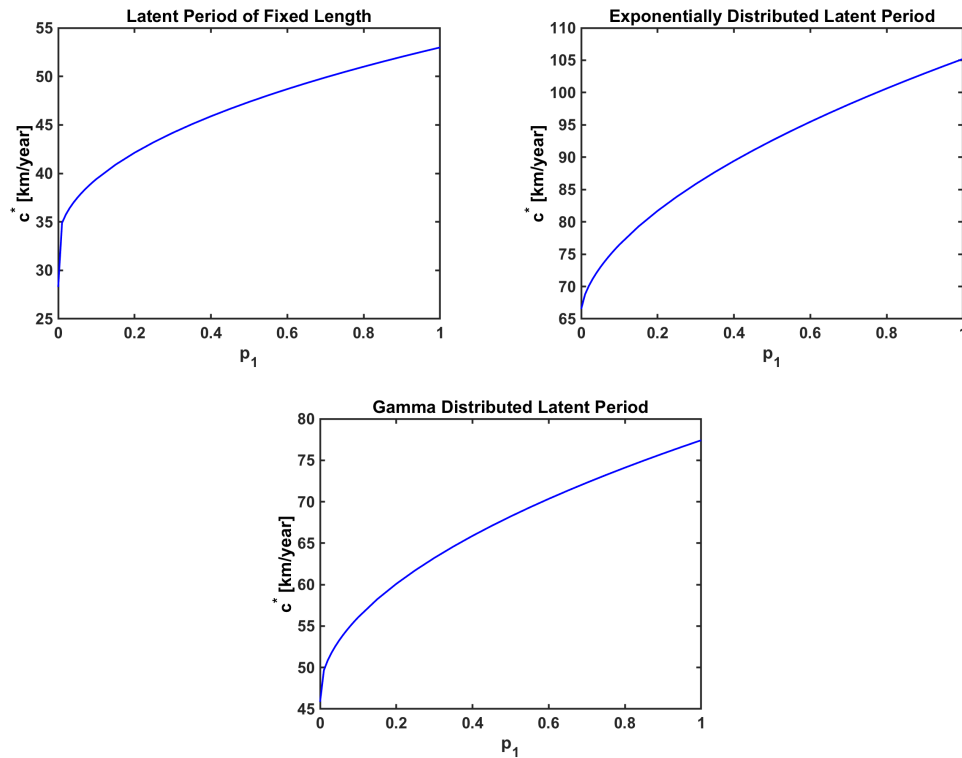
Figure 4.10.1: Spreading speed c^* dependence on p_1. We solve (4.4.7) for latent periods of fixed length, exponentially distributed length, and Gamma distributed length. Here, $h = 2$ and the values of the other parameters are in Table 4.1.

Chapter 5

NUMERICAL SIMULATIONS OF SPREAD OF RABIES: LATENT PERIOD
WITH FIXED LENGTH

5.1 Abstract

We describe a numerical algorithm for the simulation of the spread of rabies
in a spatially distributed fox population. As we know, the model considers both
territorial and wandering rabid foxes and includes a latent period for the infection.
The resulting systems are mixtures of partial differential and integral equations. They
are discretized in the space variable by central differences of second order and by
the composite trapezoidal rule. In a second step, the ordinary or delay differential
equations obtained this way are discretized in time by explicit continuous Runge-
Kutta methods of fourth order for ordinary and delay differential systems. The results
of the numerical calculations are compared for latent periods of fixed distributed
length and for various proportions of territorial and wandering rabid foxes. The speeds
of spread observed in the simulations are compared to spreading speeds obtained by
analytic methods and to observed speeds of epizootic frontlines in the European rabies
outbreak 1940 to 1980.

5.2 The Model

We consider the models in (3.3.3) and (3.3.4) with Ω to be a bounded domain on
$\mathbb{R}$, which represents the habitat of the foxes. So, when $0 \leq t < \tau$, the spread of rabies

is described by

$$
\begin{cases}
\partial_t S(x,t) = -\beta S(x,t) \int_\Omega \big[\kappa_1(x,z)R_1(z,t) + \kappa_2(x,z)R_2(z,t)\big]dz \\[2mm]
\qquad =: -B(x,t), \\[2mm]
\partial_t R_1(x,t) = D\partial_x^2 R_1(x,t) - \nu_1 R_1(x,t), \qquad 0 \le t < \tau \\[2mm]
\partial_t R_2(x,t) = -\nu_2 R_2(x,t),
\end{cases}
\tag{5.2.1}
$$

By combining (3.3.1) and (3.3.2) with (2.2.2), we obtain a model delay differential equations for $t > \tau$

$$
\begin{cases}
\partial_t S(x,t) = -\beta S(x,t) \int_\Omega \big[\kappa_1(x,z)R_1(z,t) + \kappa_2(x,z)R_2(z,t)\big]dz \\[2mm]
\qquad =: -B(x,t), \\[2mm]
\partial_t R_1(x,t) = D\partial_x^2 R_1(x,t) + p_1 B(x,t-\tau) - \nu_1 R_1(x,t), \qquad t > \tau \\[2mm]
\partial_t R_2(x,t) = p_2 B(x,t-\tau) - \nu_2 R_2(x,t),
\end{cases}
\tag{5.2.2}
$$

with given initial conditions

$$
S(x,0) = S_0(x), \ \ R_1(x,0) = R_1^\circ(x), \ \ R_2(x,0) = R_2^\circ(x),
$$

$x \in \Omega$. We assume the following boundary conditions

$$
R_1(x,t) = w(x,t), \quad x \in \partial\Omega, \quad t > 0.
\tag{5.2.3}
$$

$S(x,t)$ denote the density of susceptible foxes at time t whose home-ranges center at location $x \in \mathbb{R}$. Further, $R_1(x,t)$ are the diffusing rabid foxes at location x and time t, $R_2(x,t)$ are the territorial rabid foxes at time t whose home-ranges center at location x. The parameters $\nu_1 > 0$ and $\nu_2 > 0$ are the per capita rabies death rates of diffusing and territorial rabid foxes, respectively. p_1 is the chance of a rabid fox to diffuse, and p_2 the chance to be territorial, $p_j \ge 0$ and $p_1 + p_2 = 1$. $\beta > 0$ is the rate at which

80

the meeting of a susceptible and rabid fox leads to the infection of the susceptible fox. $B(x,t)$ is the incidence of the disease, i.e., the number of new cases per unit of time. $D > 0$ is the diffusion constant. $\kappa_1(x,z)$ denotes the rate at which a fox with home-range center x visits the location $z \in \Omega$. The rate at which a susceptible fox with home-range center x meets a territorial rabid fox with home-range center z is given by

$$\kappa_2(x,z) = \int_\Omega \kappa_1(x,y)\kappa_1(z,y)dy, \tag{5.2.4}$$

which means that it is the rate at which they both visit some common point $y \in \Omega$. The nonnegative continuous functions S_0, R_1° and R_2° are the initial densities of the susceptible and diffusing and territorial rabid foxes.

5.3   Discretization in Space

We use the method of lines to come up with algebraic approximations that we could use to replace all the spatial derivatives only with finite differences (see, e.g., Schiesser (2013); Schiesser and Griffiths (2009)). So, we discretize the partial differential equation PDE by using central in space second order scheme. The integrals in (5.2.1) and (5.2.2) are approximated using composite trapezoid rule. Then, we use the continuous explicit Runge-Kutta methods of order four and three to solve the systems of nonlinear ordinary and delay differential equations as in the next section. The continuous Runge-Kutta method was derived by Owren and Zennaro (Owren and Zennaro (1991, 1992b,a)), and it is discussed in (Bellen and Zennaro (2003)). The continuous Runge-Kutta method was recently applied by (Alanazi *et al.* (2018a, 2019); Bartoszewski *et al.* (2015); Jackiewicz *et al.* (2014)).

Henceforth, we use the notations $R_{1,i}(t)$, $R_{2,i}(t)$, and $S_i(t)$, and $Q_i(t)$, for the approximations of $R_1(x_i,t)$, $R_2(x_i,t)$, $S(x_i,t)$, and $Q(x_i,t)$, respectively.

We consider $\Omega = [-a, a]$ to be a bounded domain on $\mathbb{R}$ to represent the habitat of foxes. Let x_i to be a sequence of uniformly spaced points on $[-a, a]$, such that $x_i = -a + ih$, where $h = \frac{2a}{N+1}$ is the spacing stepsize and $i = 0, ..., N+1$. In addition, we define z_k be a sequence of uniformly spaced points on $[-a, a]$, such that $z_k = -a + kh, k = 0, ..., N+1$, and $h = \frac{2a}{N+1}$. We replace x with x_i for $i = 1, ..., N$, and set

$$Q_i(t) = \int_{\mathbb{R}} [\kappa_1(x_i - z)R_1(z, t) + \kappa_2(x_i - z)R_2(z, t)]dz. \tag{5.3.1}$$

To find an approximation for $Q_i(t)$, we use composite trapezoid rule on $[-a, a] \subset \mathbb{R}$, where $a > 0$ is sufficiently large. $Q_i(t)$ shall be

$$
\begin{aligned}
Q_i(t) &= \int_{\mathbb{R}} [\kappa_1(x_i - z)R_1(z, t) + \kappa_2(x_i - z)R_2(z, t)]dz \\
&\simeq \int_{-a}^{a} [\kappa_1(x_i - z)R_1(z, t) + \kappa_2(x_i - z)R_2(z, t)]dz + O(h^2) \\
&= h[\frac{1}{2}\kappa_1(x_i - z_0)R_1(z_0, t) + \sum_{k=1}^{N} \kappa_1(x_i - z_k)R_1(z_k, t) \\
&\quad + \frac{1}{2}\kappa_1(x_i - z_{N+1})R_1(z_{N+1}, t)] \\
&\quad + h[\frac{1}{2}\kappa_2(x_i - z_0)R_2(z_0, t) + \sum_{k=1}^{N} \kappa_2(x_i - z_k)R_2(z_k, t) \\
&\quad + \frac{1}{2}\kappa_2(x_i - z_{N+1})R_2(z_{N+1}, t)] + O(h^2) \\
&= Q_{1,i}(t) + Q_{2,i}(t) + O(h^2),
\end{aligned}
\tag{5.3.2}
$$

where

$$
\begin{aligned}
Q_{1,i}(t) &= h\left[\frac{1}{2}\kappa_1(x_i - z_0)R_1(z_0, t) + \sum_{k=1}^{N} \kappa_1(x_i - z_k)R_1(z_k, t) \right.\\
&\quad \left. + \frac{1}{2}\kappa_1(x_i - z_{N+1})R_1(z_{N+1}, t)\right], \\
Q_{2,i}(t) &= h\left[\frac{1}{2}\kappa_2(x_i - z_0)R_2(z_0, t) + \sum_{k=1}^{N} \kappa_2(x_i - z_k)R_2(z_k, t) \right.\\
&\quad \left. + \frac{1}{2}\kappa_2(x_i - z_{N+1})R_2(z_{N+1}, t)\right],
\end{aligned}
\tag{5.3.3}
$$

82

(see, e.g., (Recktenwald, 2000, p.605-612)). Another approach to approximate (5.3.1) is by using Gauss-Hermite quadrature rule (see, e.g., Jackiewicz *et al.* (2006)). We discretize the PDE in (5.2.1) and (5.2.2) using second-order central approximation such that

$$\frac{\partial^2 R_{1,i}(t)}{\partial x_i^2} \approx \frac{R_{1,i+1}(t) - 2R_{1,i}(t) + R_{1,i-1}(t)}{h^2}. \tag{5.3.4}$$

Therefore, when $0 \leq t \leq \tau$, we obtain

$$
\begin{aligned}
S_i'(t) =& - \beta S_i(t) Q_i(t), \\
R_{1,i}'(t) =& D \frac{R_{1,i+1}(t) - 2R_{1,i}(t) + R_{1,i-1}(t)}{h^2} - \nu_1 R_{1,i}(t), \\
R_{2,i}'(t) =& - \nu_2 R_{2,i}(t).
\end{aligned}
\tag{5.3.5}
$$

where $Q_i(t) = Q_{1,i}(t) + Q_{2,i}(t)$, $i = 1, ..., N$. When foxes exit the latent period and become rabid such that $t > \tau$, the system in (5.2.2) start to contribute to the dynamics of the fox population. Therefore, when $i = 1, ..., N$ and $t > \tau$, we have the following numerical schemes for the model in (5.2.2)

$$
\begin{aligned}
S_i'(t) =& - \beta S_i(t) Q_i(t), \\
R_{1,i}'(t) =& D \frac{R_{1,i+1}(t) - 2R_{1,i}(t) + R_{1,i-1}(t)}{h^2} + p_1 \beta S_i(t - \tau) Q_i(t - \tau) \\
& - \nu_1 R_{1,i}(t), \\
R_{2,i}'(t) =& p_2 \beta S_i(t - \tau) Q_i(t - \tau) - \nu_2 R_{2,i}(t).
\end{aligned}
\tag{5.3.6}
$$

We assume that (5.3.5) and (5.3.6) satisfy the following boundary conditions

$$R_1(-a, t) = w_1(t), \quad R_1(a, t) = w_2(t), \quad t \geq 0,$$

where $w_1(t)$ and $w_2(t)$ are given functions.

For $0 \leq t \leq \tau$ and when $i = 1$, $R_{1,0}(t) = w_1(t)$ and the scheme for R_1 shall be

$$R_{1,1}'(t) = D \frac{R_{1,2}(t) - 2R_{1,1}(t)}{h^2} + \frac{D}{h^2} w_1(t) - \nu_1 R_{1,1}(t), \tag{5.3.7}$$

83

and when $i = N$, $R_{1,N+1}(t) = w_2(t)$ and the scheme for R_1 shall be

$$R'_{1,N}(t) = D\frac{R_{1,N-1}(t) - 2R_{1,N}(t)}{h^2} + \frac{D}{h^2}w_2(t) - \nu_1 R_{1,N}(t). \qquad (5.3.8)$$

For $t > \tau$, when $i = 1$, R_1 scheme shall be after we use the boundary conditions

$$\begin{aligned} R'_{1,1}(t) = &D\frac{R_{1,2}(t) - 2R_{1,1}(t)}{h^2} + \frac{D}{h^2}w_1(t) + p_1\beta S_1(t-\tau)Q_1(t-\tau) \\ &- \nu_1 R_{1,1}(t). \end{aligned} \qquad (5.3.9)$$

and at $i = N$, R_1 scheme shall be

$$\begin{aligned} R'_{1,N}(t) = &D\frac{R_{1,N-1}(t) - 2R_{1,N}(t)}{h^2} + \frac{D}{h^2}w_2(t) + p_1\beta S_N(t-\tau)Q_N(t-\tau) \\ &- \nu_1 R_{1,N}(t). \end{aligned} \qquad (5.3.10)$$

The initial conditions are

$$\begin{aligned} S_i(0) &= S_0(x_i), \\ R_{1,i}(0) &= R_1^\circ(x_i), \qquad\qquad (5.3.11) \\ R_{2,i}(0) &= R_2^\circ(x_i), \end{aligned}$$

for $i = 1, ..., N$.

5.4   Discretization in Time

We use the following matrix forms for our notations,

$$S(t) = \begin{bmatrix} S_1(t) \\ \vdots \\ S_N(t) \end{bmatrix}, \quad R_1(t) = \begin{bmatrix} R_{1,1}(t) \\ \vdots \\ R_{1,N}(t) \end{bmatrix}, \quad R_2(t) = \begin{bmatrix} R_{2,1}(t) \\ \vdots \\ R_{2,N}(t) \end{bmatrix},$$

then we let

$$y(t) = \begin{bmatrix} S(t) \\ R_1(t) \\ R_2(t) \end{bmatrix}, \quad y_0 = \begin{bmatrix} S(0) \\ R_1(0) \\ R_2(0) \end{bmatrix}.$$

84

In addition, for $0 \leq t \leq \tau$, we define $f(y(t))$ to be the right hand side of the system in (5.3.5). For $t > \tau$, we let the right hand side of (5.3.6) to be $g(y(t), y(t - \tau))$. Therefore, we rewrite the systems in (5.3.5) and (5.3.6) with the initial conditions in (5.3.11) as the following

$$
\begin{aligned}
y'(t) &= f(y(t)), & 0 \leq t \leq \tau, \\
y'(t) &= g(y(t), y(t - \tau)), & t > \tau, \\
y(0) &= y_0 \in \mathbb{R}^{3N},
\end{aligned}
\tag{5.4.1}
$$

where $f : \mathbb{R}^{3N} \to \mathbb{R}^{3N}$, and $g : \mathbb{R}^{3N} \times \mathbb{R}^{3N} \to \mathbb{R}^{3N}$.

We solve the system in (5.4.1) by using the continuous explicit Runge-Kutta method of order $p = 4$ with $s = 6$ stages, and the embedded discrete Runge-Kutta method of order $p = 3$(see, Owren and Zennaro (1991, 1992b,a)). We use the embedded discrete Runge-Kutta method to estimate the local discretization error of the method with order $p = 4$. The coefficients of the continuous and discrete Runge-Kutta method of order p with s stages are given by the following Butcher table (Table 5.1),

In Table 5.1, $c_i = \Sigma_{j=1}^{s} a_{ij}$, for $i = 1, \cdots, s$. $b_i(\theta)$ are called the continuous weights, and A is strictly lower triangular matrix such that $A = \left[a_{ij} \right]_{i,j=1}^{s}$. $\hat{y}_{n+1}$ is the discrete Runge-Kutta method of order $p - 1$, and $\hat{b}_i$ are the weight vector of $\hat{y}_{n+1}$.

Table 5.2 gives us the coefficients of the continuous explicit Runge-Kutta method of order $p = 4$ with $s = 6$ stages and the coefficients of the embedded discrete Runge-Kutta method of order $p = 3$.

$$
\begin{array}{c|c}
\mathbf{c} & \mathbf{A} \\
\hline
\mathbf{y}_h & \mathbf{b}(\theta) \\
\hat{\mathbf{y}}_{n+1} & \hat{\mathbf{b}}
\end{array}
=
\begin{array}{c|cccccc}
c_1 = 0 & & & & & & \\
c_2 & a_{2,1} & & & & & \\
c_3 & a_{3,1} & a_{3,2} & & & & \\
c_4 & a_{4,1} & a_{4,2} & a_{4,3} & & & \\
\vdots & \vdots & \vdots & \vdots & \ddots & & \\
c_s & a_{s,1} & a_{s,2} & a_{s,3} & \cdots & a_{s,s-1} & \\
\hline
y_h(t_n + \theta h_n) & b_1(\theta) & b_2(\theta) & b_3(\theta) & b_4(\theta) & \cdots & b_s(\theta) \\
\hat{y}_{n+1} & \hat{b}_1 & \hat{b}_2 & \hat{b}_3 & \hat{b}_4 & \cdots & \hat{b}_s
\end{array}
$$

Table 5.1: The coefficients of continuous and discrete Runge-Kutta method of order p with s stages.

$$
\begin{array}{c|c}
\mathbf{c} & \mathbf{A} \\
\hline
\mathbf{y}_h & \mathbf{b}(\theta) \\
\hat{\mathbf{y}}_{n+1} & \hat{\mathbf{b}}
\end{array}
=
\begin{array}{c|cccccc}
0 & & & & & & \\[4pt]
\frac{1}{6} & \frac{1}{6} & & & & & \\[4pt]
\frac{11}{37} & \frac{44}{1369} & \frac{369}{1369} & & & & \\[4pt]
\frac{11}{17} & \frac{3388}{4913} & -\frac{8349}{4913} & \frac{8140}{4913} & & & \\[4pt]
\frac{13}{15} & -\frac{36764}{408375} & \frac{767}{1125} & -\frac{32708}{136125} & \frac{210392}{408375} & & \\[4pt]
1 & \frac{1697}{18876} & 0 & \frac{50653}{116160} & \frac{299693}{1626240} & \frac{3375}{11648} & \\[4pt]
\hline
y_h(t_n + \theta h_n) & b_1(\theta) & b_2(\theta) & b_3(\theta) & b_4(\theta) & b_5(\theta) & b_6(\theta) \\[4pt]
\hat{y}_{n+1} & \frac{101}{363} & 0 & -\frac{1369}{14520} & \frac{11849}{14520} & 0 & 0
\end{array}
$$

Table 5.2: The coefficients of the optimal pair of continuous and discrete Runge-Kutta method of order $p = 4$ with $s = 6$ stages.

The continuous weights $b_i(\theta)$ are given by

$$
\begin{cases}
b_1(\theta) = -\frac{866577}{824252}\,\theta^4 + \frac{1806901}{618189}\,\theta^3 - \frac{104217}{37466}\,\theta^2 + \theta, \\[2ex]
b_2(\theta) = 0, \\[2ex]
b_3(\theta) = \frac{12308679}{5072320}\,\theta^4 - \frac{2178079}{380424}\,\theta^3 + \frac{861101}{230560}\,\theta^2, \\[2ex]
b_4(\theta) = -\frac{7816583}{10144640}\,\theta^4 + \frac{6244423}{5325936}\,\theta^3 - \frac{63869}{293440}\,\theta^2, \\[2ex]
b_5(\theta) = -\frac{624375}{217984}\,\theta^4 + \frac{982125}{190736}\,\theta^3 - \frac{1522125}{762944}\,\theta^2, \\[2ex]
b_6(\theta) = \frac{296}{131}\,\theta^4 - \frac{461}{131}\,\theta^3 + \frac{165}{131}\,\theta^2.
\end{cases}
\tag{5.4.2}
$$

To implement this pair for delay differential equations we have to compute the approximate solution $y_h(t_n - \tau)$, where $t_n - \tau$ is not, in general, a grid point. To compute this approximate solution we search for the index q such that $t_n - \tau \in (t_q, t_{q+1}]$, and compute $y_h(t_n - \tau)$ from the formula

$$
y_h(t_n - \tau) = b_1(\theta)F_{1,q} + b_2(\theta)F_{2,q} + b_3(\theta)F_{3,q} + b_4(\theta)F_{4,q} + b_5(\theta)F_{5,q} + b_6(\theta)F_{6,q}
$$

if $0 \leq t_n - \tau \leq \tau$, or

$$
y_h(t_n - \tau) = b_1(\theta)G_{1,q} + b_2(\theta)G_{2,q} + b_3(\theta)G_{3,q} + b_4(\theta)G_{4,q} + b_5(\theta)G_{5,q} + b_6(\theta)G_{6,q}
$$

if $t_n - \tau > \tau$. Here, $b_i(\theta)$ are given by (5.4.2),

$$
\theta = \frac{t_n - \tau - t_q}{t_{q+1} - t_q} \in (0, 1],
$$

$$
F_{k,q} = f\big(y_h(t_q + c_k h_q)\big),
$$

$$
G_{k,q} = g\big(y_h(t_q + c_k h_q), y_h(t_q + c_k h_q - \tau)\big),
$$

$k = 1, 2, 3, 4, 5, 6$, $h_q = t_{q+1} - t_q$, and $\mathbf{c} = [c_1, c_2, c_3, c_4, c_5, c_6]^T$.

The embedded pair of Runge-Kutta methods was implemented in a variable stepsize environment with the estimates of the local discretization errors computed according to the formula

$$
\mathrm{EST}(t_{n+1}) = \big\| \hat{y}_{n+1} - y_h(t_{n+1}) \big\|_2.
$$

Following (Gladwell *et al.* (1987); Shampine and Gordon (1975)) the initial stepsize h_0 was computed from the formula

$$h_0 = \min \left\{ 0.01 \, \tau, \frac{\text{TOL}^{1/5}}{\|f(0, y_0)\|_2} \right\},$$

where TOL is the accuracy tolerance prescribed by the user of the code. Then for $n = 0, 1, \ldots$, the stepsize h_n from t_n to $t_{n+1} = t_n + h_n$ is accepted if

$$\text{EST}(t_{n+1}) \leq \text{TOL},$$

and a new stepsize h_{n+1} from t_{n+1} to $t_{n+2} = t_{n+1} + h_{n+1}$ is computed from the formula

$$h_{n+1} = \eta \, h_n \left(\frac{\text{TOL}}{\text{EST}(t_{n+1})} \right)^{1/5},$$

where η is a safety coefficient to avoid too many rejected steps. In our implementation of the code we have chosen $\eta = 0.8$. If

$$\text{EST}(t_{n+1}) > \text{TOL},$$

the stepsize is rejected, and the computations are repeated with a halved stepsize $h_n/2$.

The construction of embedded pairs of continuous and discrete Runge-Kutta methods employed in this section, and their convergence and order properties, are discussed in (Owren and Zennaro (1991, 1992b,a)) and in the monographs (Bellen and Zennaro (2003); Hairer *et al.* (1993)).

5.5 Units Check

Before we go further, we need to check units throughout the equations in (5.2.1) and (5.2.2) for consistency (Schiesser (2013)).The units of the dependent and independent variables of the equations in (5.2.1) and (5.2.2) are in Table 5.3. In addition,

Variable	Units
S	[fox/km]
R_1	[fox/km]
R_2	[fox/km]
t	[day]
x	[km]

Table 5.3: Units of the model dependent and independent variables.

Parameters	Units
b	[km^2]
β	[fox/day]
ν_1	[1/day]
ν_2	[1/day]
D	[km^2/day]

Table 5.4: Units of the model parameters.

the units of the parameters in (5.2.1) and (5.2.2) are in Table 5.4.

Form the Table 5.3 and Table 5.4, the units of the equation of susceptible foxes in (5.2.1) and (5.2.2) are

$$\frac{fox/km}{day} = \frac{km}{day}\left(fox/km\right)\left[\left(fox/km\right) + \left(fox/km\right)\right] \tag{5.5.1}$$

Therefore, the consistency of the units is hold throughout the equation (5.5.1), $(\frac{fox/km}{day})$. The units of $R_1(x,t)$ in (5.2.1) are

$$\frac{fox/km}{day} = \frac{km^2}{day}\frac{fox/km}{km^2} + \frac{fox/km}{day} - \frac{1}{day}(fox/km). \tag{5.5.2}$$

So, the units are consistent for $R_1(x, t)$. From Table 5.3 and Table 5.4, the units of $R_2(x, t)$ in (5.2.1) are

$$\frac{fox/km}{day} = \frac{fox/km}{day} - \frac{1}{day}(fox/km). \tag{5.5.3}$$

The equation (5.5.3) shows the units are consistent for territorial rabid foxes. We now check the units of $R_1(x, t)$ in (5.2.2); so we have

$$\begin{aligned}\frac{fox/km}{day} = &\frac{km^2}{day}\frac{fox/km}{km^2} + \frac{km}{day}\left(fox/km\right)\left[\left(fox/km\right) + \left(fox/km\right)\right]\\ &- \frac{1}{day}(fox/km).\end{aligned} \tag{5.5.4}$$

Units are consistent for $R_1(x, t)$ in (5.2.2) as it is clear from the equation (5.5.4). Lastly, we check the units for $R_2(x, t)$ in (5.2.2). So, we get

$$\begin{aligned}\frac{fox/km}{day} = &\frac{km}{day}\left(fox/km\right)\left[\left(fox/km\right) + \left(fox/km\right)\right]\\ &- \frac{1}{day}(fox/km).\end{aligned} \tag{5.5.5}$$

That clearly shows the net units of both sides of equation (5.5.5) are $(\frac{fox/km}{day})$.

5.6 Numerical Experiments and Simulations

We compute approximations to the systems (5.3.5) and (5.3.6) for $x \in [-a, a]$, $a = 50\,[\text{km}]$, and $t \in [t_0, t_{end}]$, $t_0 = 0\,[\text{day}]$, $t_{end} = 180\,[\text{day}]$. We choose $N = 199$ unless otherwise specified. We choose the homogeneous Dirichlet boundary conditions such that

$$R_1(-a, t) = w_1(t) = 0\,[\text{fox/km}], \quad R_1(a, t) = w_2(t) = 0\,[\text{fox/km}], \ t \in [0, 180], \tag{5.6.1}$$

and initial conditions

$$R_{1,i}(0) = R_1^\circ(x_i), \ R_{2,i}(0) = R_2^\circ(x_i),$$

90

$i = 1, 2, \ldots, N$, where the functions $R_1^\circ(x)$ and $R_2^\circ(x)$ are defined by

$$R_1^\circ(x) = \begin{cases} 0.2 \ [\text{fox/km}], & -5 \leq x \leq 5, \\ 0 \ \ [\text{fox/km}], & \text{otherwise}, \end{cases}$$

$$R_2^\circ(x) = 0 \ [\text{fox/km}], \quad x \in [-a, a].$$

Murray et al let $S_0 = 4.6 \ [\text{fox/km}^2]$, as in (Murray *et al.*, 1986, Fig.2). So, since we are working on $\mathbb{R}$, $S_0 = 4.6 \ [\text{fox/km}]$ will be used. The rabid foxes have a long incubation period and a short life expectancy (Anderson *et al.* (1981); Murray (1989); van den Bosch *et al.* (1990)). The average duration of the latent period for the diffusing and territorial rabid foxes is about $\tau = 28 \ [\text{day}]$ (Anderson *et al.* (1981); Källén *et al.* (1985); Murray (1989)). The mean length of the infectious periods of diffusing rabid foxes $1/\nu_1$ and territorial rabid foxes $1/\nu_2$ are $5 \ [\text{day}]$ (Anderson *et al.* (1981); Murray *et al.* (1986)). The diffusion coefficient D, which measures the distance rabid foxes can cross after the onset of clinical disease, is chosen to be $D = 200 \ [\text{km}^2/\text{year}]$ (Murray *et al.* (1986); Murray (1989); Murray and Seward (1992)).

The chance that a meeting of a susceptible and a rabid fox leads to the infection of the susceptible fox β is hard to estimate (Murray (1989)). Anderson et al.(1981) has estimated β by using indirect expression to be about $79.69 \ [\text{km}^2/\text{year}]$ (Anderson *et al.* (1981)). From the formula of the basic reproduction number, S_T is defined by

$$S_T = \frac{1}{\beta} \left(\frac{\nu_1 \nu_2}{\nu_2 p_1 + \nu_1 p_2} \right) = \frac{\nu_1}{\beta}. \tag{5.6.2}$$

Following (Anderson *et al.* (1981)), we will use the formula of S_T with $S_T = 1 \ [\text{fox/km}^2]$ (Anderson *et al.* (1981); Murray *et al.* (1986)) and the parameters values above to find an estimate of the disease transmission parameter β. That gives $\beta = 73 \ [\text{km}^2/\text{year}]$. Again since we are working on $\mathbb{R}$, $\beta = 73 \ [\text{km/year}]$ will be used. We also assume

$$\kappa_1(z) = \Gamma_1(z, b) = \frac{1}{\sqrt{4\pi b}} e^{-z^2/4b}, \tag{5.6.3}$$

91

(see Section 4.3). After dropping the tilde from (2.3.64), κ_2 shall be

$$\kappa_2(z) = \int_{\mathbb{R}} \kappa_1(y+z)\kappa_1(y)dy = \int_{\mathbb{R}} \Gamma_1(y+z,b)\Gamma_1(y,b)dy. \qquad (5.6.4)$$

By the Chapman-Kolmogorov equation,

$$\kappa_2(z) = \Gamma_1(z,2b). \qquad (5.6.5)$$

Now, we are working to find an estimate to b. We assume that foxes are circling around the center of their home-ranges. So, the areas of these circles are equal the average territory size A. We let $\Gamma_2(t,x)$ to be the fundamental solution of $\partial_t - \Delta_x$ in two space dimensions. Then the mean maximum distance of a territorial fox from the center of its home-range (the mean radius of its home-range) is given by

$$r_0 = \int_{\mathbb{R}^2} |z|\Gamma_2(z,b)dz = \int_{\mathbb{R}^2} |z|(4b\pi)^{-1}e^{-|z|^2/(4b)}dz,$$

where $|\cdot|$ being the Euclidean norm in $\mathbb{R}^2$. We translate the integral into polar coordinates $(z_1,z_2) = (r\cos\theta, r\sin\theta)$, where $0 \le r \le \infty$ and $\theta \in [0,2\pi)$, so we shall have

$$r_0 = \frac{1}{4\pi b} \int_0^{2\pi} \int_0^\infty r^2 e^{-r^2/(4b)}drd\theta = \frac{1}{2b} \int_0^\infty r^2 e^{-r^2/4b}dr.$$

We substitute $r = s\sqrt{4b}$,

$$r_0 = 4\sqrt{b} \int_0^\infty s^2 e^{-s^2}ds.$$

By integration by parts and Fubini's theorem,

$$\int_0^\infty s^2 e^{-s^2}ds = -(1/2) \int_0^\infty s\frac{d}{ds}e^{-s^2}ds = (1/2) \int_0^\infty e^{-s^2}ds = (1/4) \int_{\mathbb{R}} e^{-s^2}ds$$
$$=(1/4)\left(\int_{\mathbb{R}^2} e^{-|x|^2}dx \right)^{1/2} = (1/4)\left(2\pi \int_0^\infty re^{-r^2}dr \right)^{1/2} = (1/4)\pi^{1/2}.$$

So

$$r_0 = b^{1/2}\pi^{1/2}.$$

So the mean area of the home range is

$$A = \pi r_0^2 = b\pi^2.$$

So $b = A\pi^{-2}\,[\text{km}^2]$. A is between 2 and 8 $[\text{km}^2]$ according to (Toma and Andral (1977)), the average area is taken as 5 $[\text{km}^2]$ by (Källén *et al.* (1985)) and (Murray *et al.* (1986)). Then b is $5\pi^{-2}\,[\text{km}^2] \approx 0.506605918\,[\text{km}^2]$. A summary of numerical values of the model parameters are in Table 4.1.

In the coming cases, we study the spread of rabies for various proportions of territorial and wandering rabid foxes. For the first case, we assume that the chance for a rabid fox to diffuse or to be territorial is equal, i.e., $p_1 = p_2 = 0.5$. In the second case, we assume that the chance for a rabid fox to diffuse is $p_1 = 0.3$, and the chance for a rabid fox to be territorial is $p_2 = 0.7$. In the third case, we assume that the chance for a rabid fox to diffuse is $p_1 = .7$, and the chance for a rabid fox to be territorial is $p_2 = 0.3$. In the fourth case, we assume that all rabid foxes diffuse, i.e., $p_1 = 1$. In the fifth case, we assume that all rabid foxes are territorial, i.e., $p_2 = 1$.

5.6.1   I. $p_1 = p_2 = 0.5$

In the first case, we assume that the chance for a rabid fox to diffuse is equal the chance for a rabid fox to be territorial such that $p_1 = p_2 = 0.5$. To ensure the spread of rabies, the basic reproduction number of rabies $\mathcal{R}_0$ shall be larger than one. With this choice of parameters (see Table 4.1),

$$\mathcal{R}_0 = \left(\frac{p_1}{\nu_1} + \frac{p_2}{\nu_2}\right)\beta S_0 = 4.6 > 1,$$

so rabies is going to spread among the fox population.

The results of numerical simulations on the model (5.3.5) and (5.3.6) are presented on Fig. 5.6.1–5.6.5. Fig. 5.6.1 and Fig. 5.6.2 show the dynamics of susceptible foxes,

diffusing rabid foxes, and territorial rabid foxes at specific times. Surface plots of approximations $S_h(x,t)$, $R_{1,h}(x,t)$, and $R_{2,h}(x,t)$ to $S(x,t)$, $R_1(x,t)$, and $R_2(x,t)$ are presented on Fig. 5.6.3. Fig. 5.6.4 depicts contour plots of susceptible foxes, diffusing rabid foxes, and territorial rabid foxes. The contour plots in Fig. 5.6.4 demonstrate that rabies spreads with asymptotic speed

$$c^\diamond \approx 43\,[\text{km/year}].$$

We also present in Fig. 5.6.5 the stepsize pattern for the algorithm described in Section 5.4 for the accuracy tolerances $\text{TOL} = 10^{-3}$, 10^{-6}, 10^{-9}, and 10^{-12}. On these figures the rejected steps are denoted by '$\times$'.
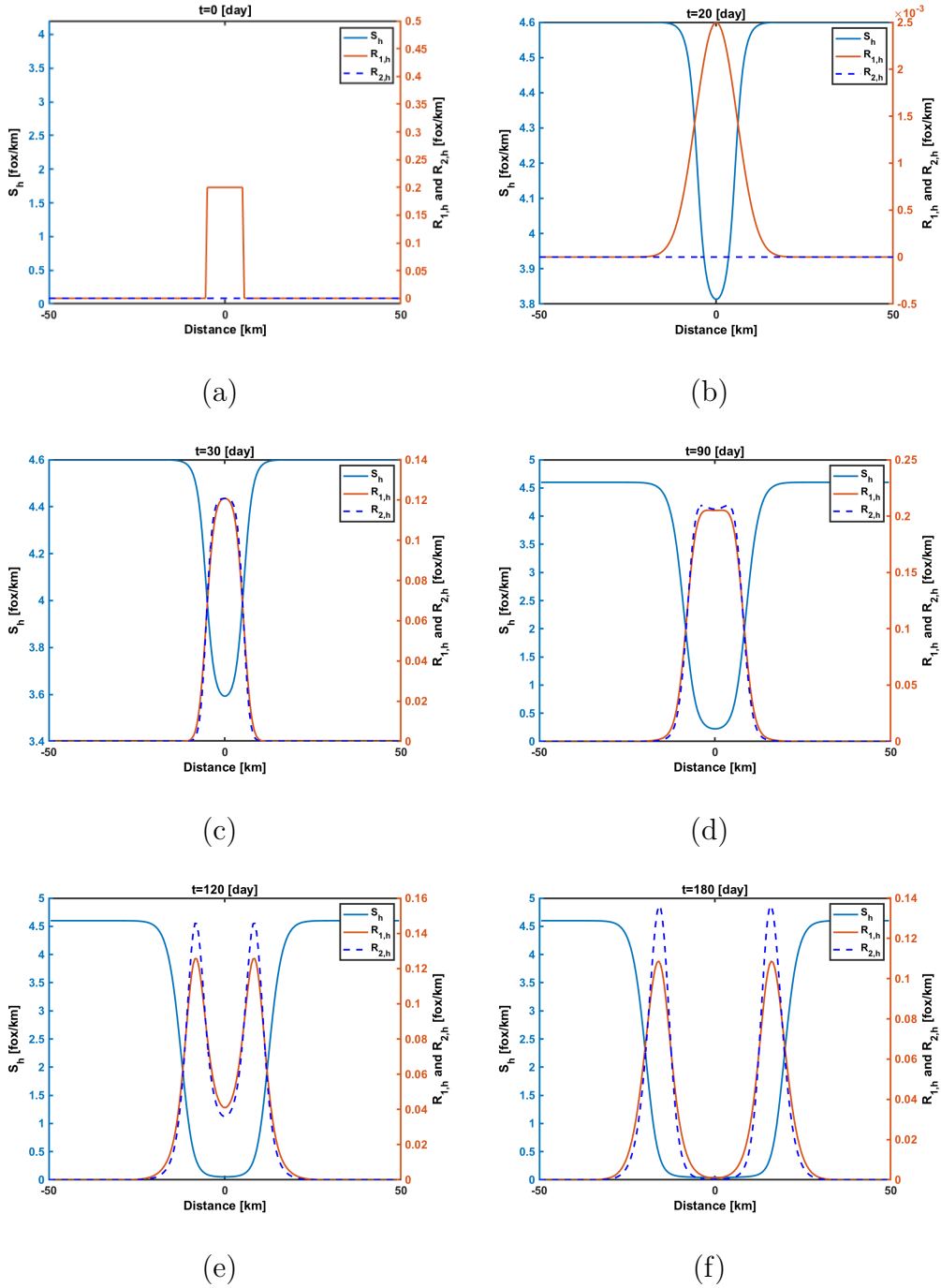
Figure 5.6.1: Approximations $S_h(x,t)$, $R_{1,h}(x,t)$, and $R_{2,h}(x,t)$ to $S(x,t)$, $R_1(x,t)$, and $R_2(x,t)$ at t=0, 20, 30, 90, 120, 180 when $p_1 = p_2 = 0.5$.
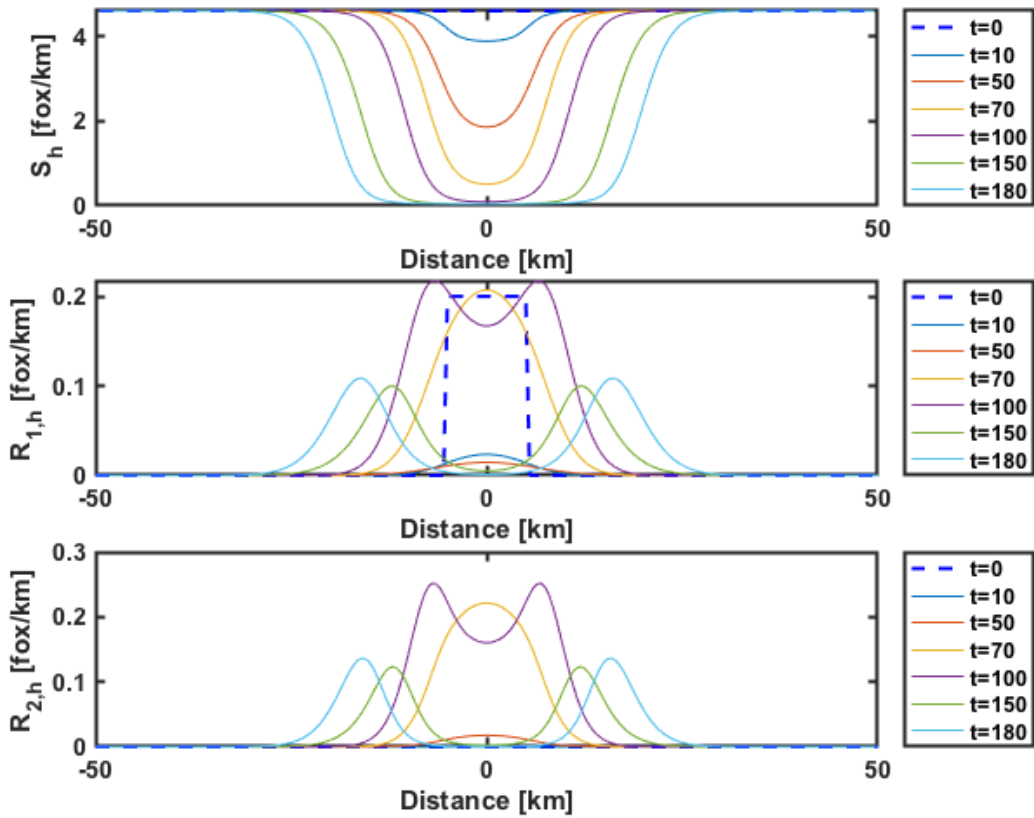
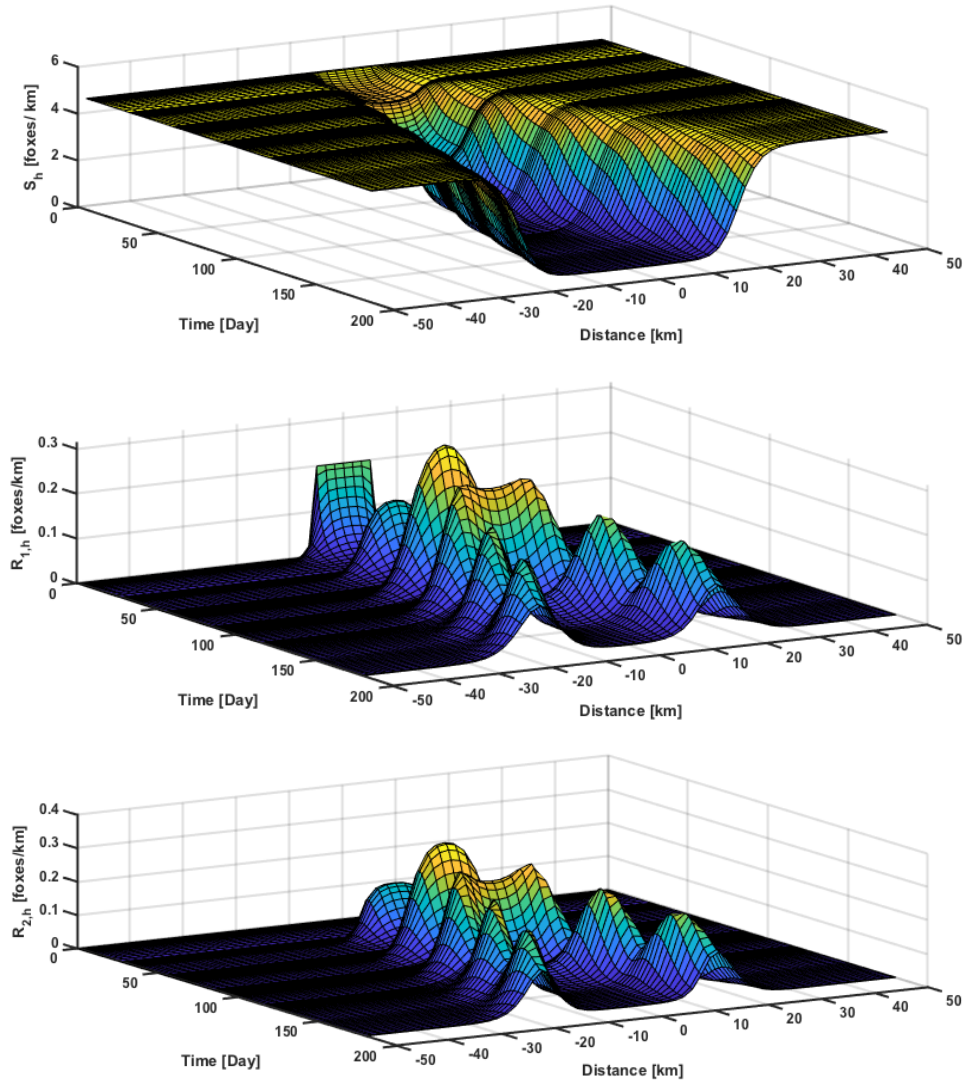Figure 5.6.2: Approximations of fox population densities at different times when $p_1 = p_2 = 0.5$.

Figure 5.6.3: Surface plots of approximations $S_h(x,t)$, $R_{1,h}(x,t)$, and $R_{2,h}(x,t)$ to $S(x,t)$, $R_1(x,t)$, and $R_2(x,t)$ when $p_1 = p_2 = 0.5$ and $N = 59$.
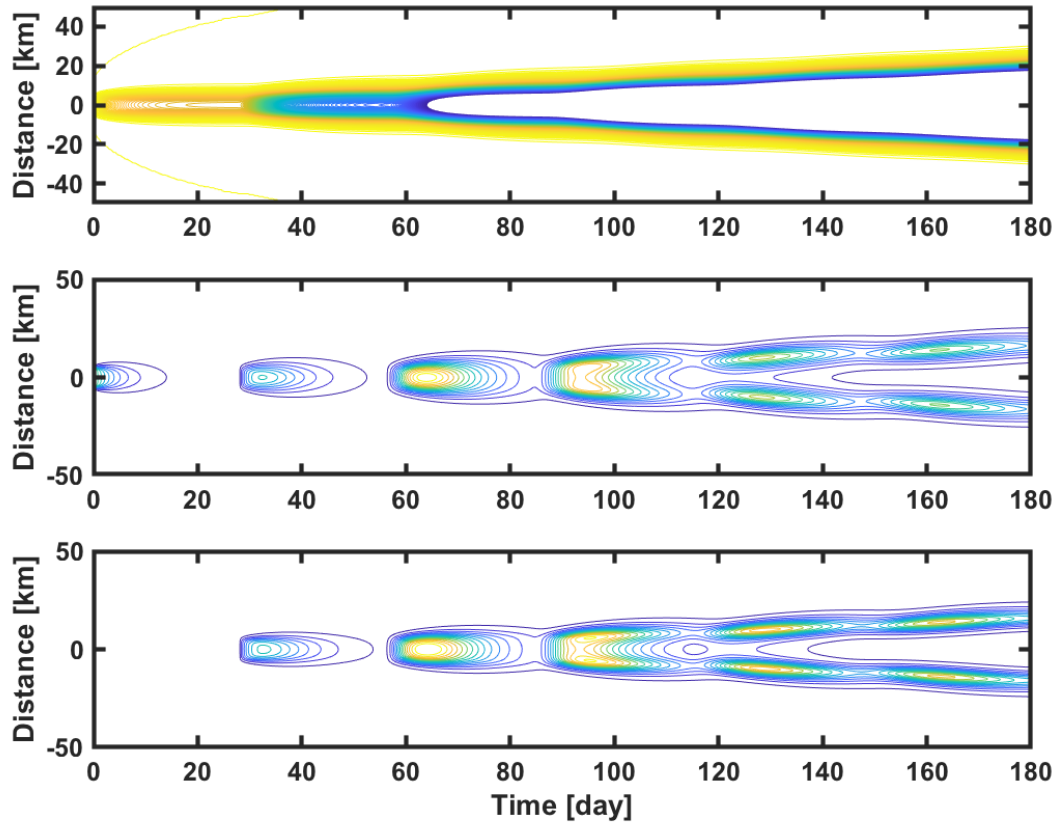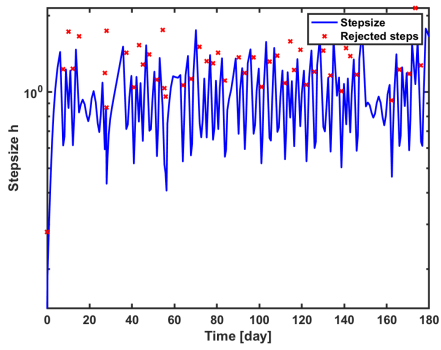
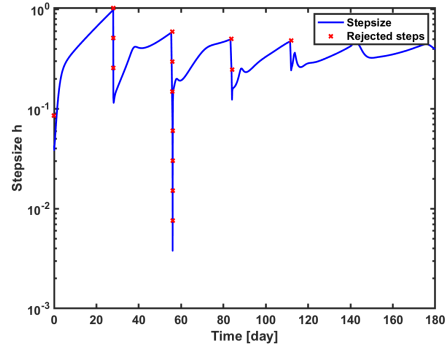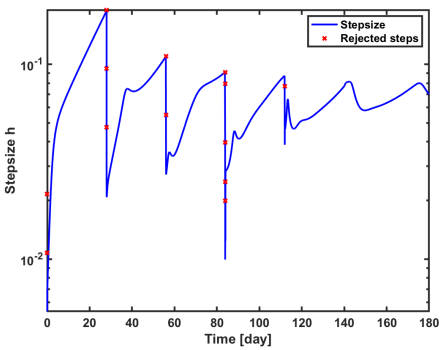Figure 5.6.4: Contour plots of approximations $S_h(x,t)$ (top), $R_{1,h}(x,t)$ (middle), and $R_{2,h}(x,t)$ (bottom) to $S(x,t)$, $R_1(x,t)$, and $R_2(x,t)$ when $p_1 = p_2 = 0.5$.
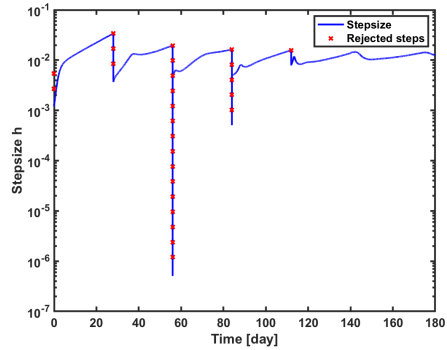
Figure 5.6.5: Variable stepsize pattern for the algorithm based on continuous Runge-Kutta method of fourth order with $N = 119$, $p_1 = p_2$, and Tol $= 10^{-3}(a)$, $10^{-6}(b), 10^{-9}(c), 10^{-12}(d)$. Rejected steps are denoted by '$\times$'.

5.6.2 II. $p_1 = 0.3$, $p_2 = 0.7$

In the second case, we assume that the chance for a rabid fox to be territorial is higher than the chance for the rabid foxes to diffuse such that $p_1 = 0.3$, and $p_2 = 0.7$. The basic reproduction number of rabies is

$$\mathcal{R}_0 = \left(\frac{p_1}{\nu_1} + \frac{p_2}{\nu_2}\right)\beta S_0 = 4.6 > 1.$$

The results of numerical simulations on the model (5.3.5) and (5.3.6) are presented on Fig. 5.6.6–5.6.9. Fig. 5.6.6 and Fig. 5.6.7 show the dynamics of susceptible foxes, diffusing rabid foxes, and territorial rabid foxes at specific times. Surface plots of approximations $S_h(x,t)$, $R_{1,h}(x,t)$, and $R_{2,h}(x,t)$ to $S(x,t)$, $R_1(x,t)$, and $R_2(x,t)$ are presented on Fig. 5.6.8. Fig. 5.6.9 depicts contour plots of susceptible foxes, diffusing rabid foxes, the territorial rabid foxes. The contour plots in Fig. 5.6.9 demonstrate that rabies spreads with asymptotic speed
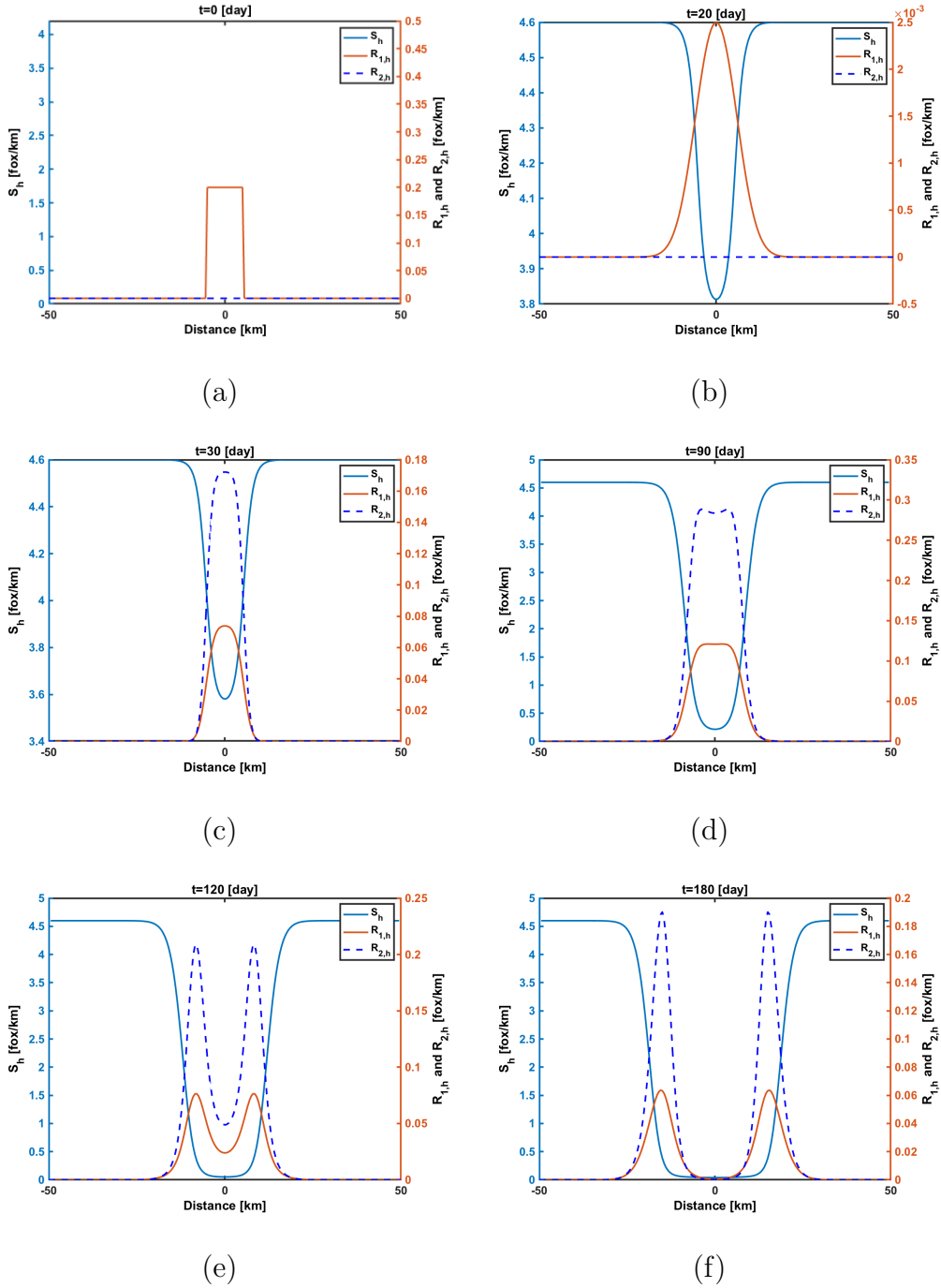
$$c^\diamond \approx 37\,[\text{km/year}].$$

Figure 5.6.6: Approximations $S_h(x,t)$, $R_{1,h}(x,t)$, and $R_{2,h}(x,t)$ to $S(x,t)$, $R_1(x,t)$, and $R_2(x,t)$ at t=0, 20, 30, 90, 120, 180 when $p_1 = 0.3$ and $p_2 = 0.7$.
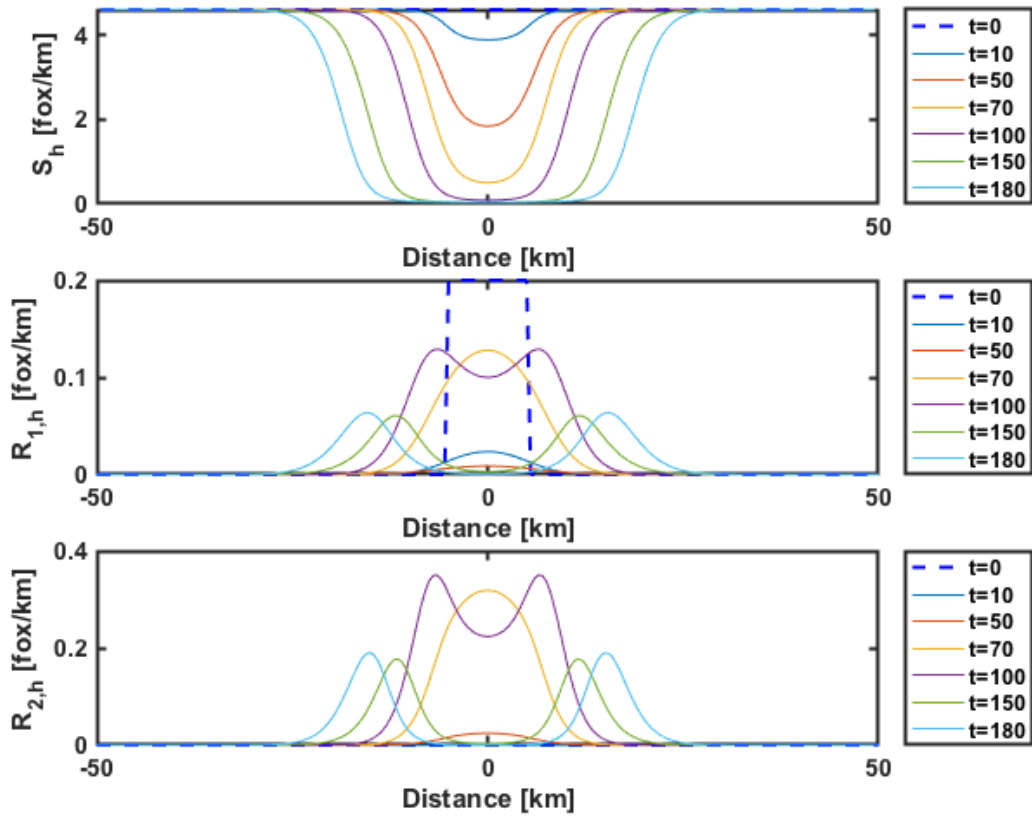
Figure 5.6.7: Approximations of fox population densities at different times when $p_1 = 0.3$ and $p_2 = 0.7$.
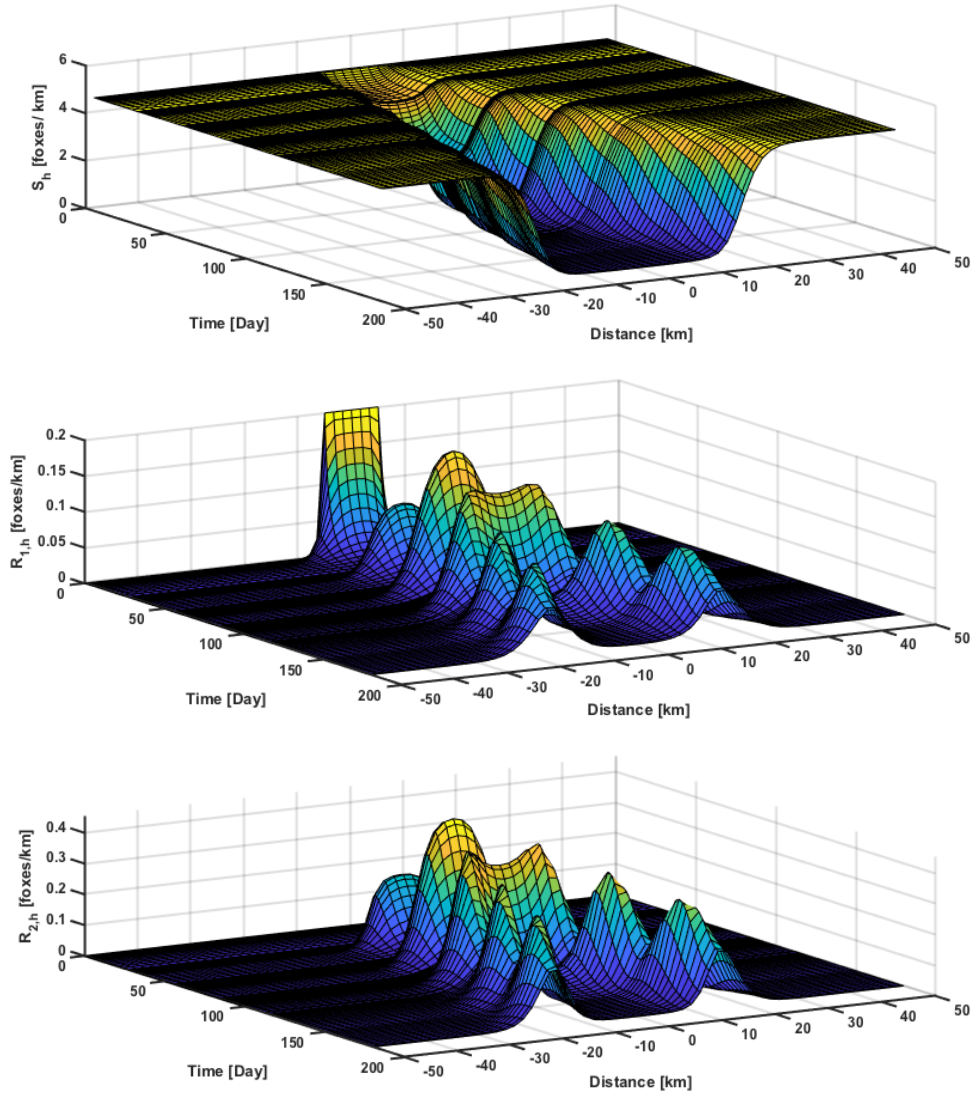
Figure 5.6.8: Surface plots of approximations $S_h(x, t)$, $R_{1,h}(x, t)$, and $R_{2,h}(x, t)$ to $S(x, t)$, $R_1(x, t)$, and $R_2(x, t)$ when $p_1 = 0.3$, $p_2 = 0.7$, and $N = 59$.
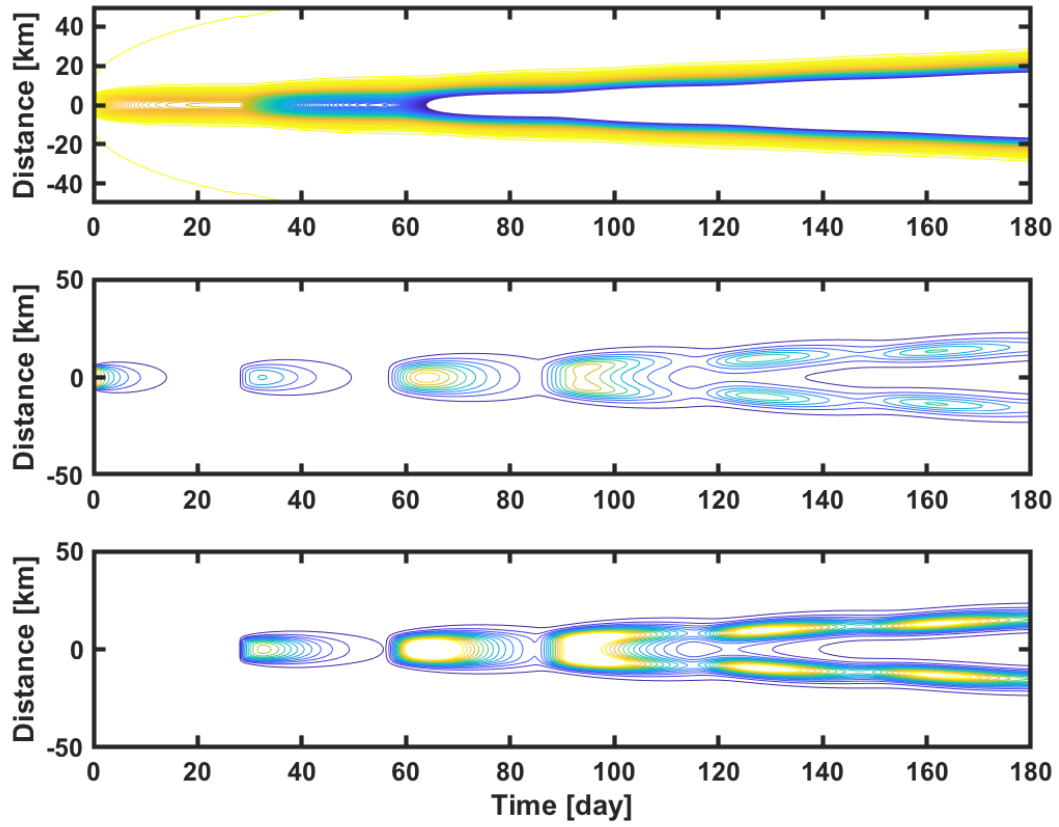
Figure 5.6.9: Contour plots of approximations $S_h(x,t)$ (top), $R_{1,h}(x,t)$ (middle), and $R_{2,h}(x,t)$ (bottom) to $S(x,t)$, $R_1(x,t)$, and $R_2(x,t)$ when $p_1 = 0.3$ and $p_2 = 0.7$.

5.6.3   III. $p_1 = 0.7$, $p_2 = 0.3$

In this case, we assume that the chance for a rabid fox to diffuse is higher than the chance for the rabid foxes to be territorial such that $p_1 = 0.7$, and $p_2 = 0.3$. To ensure the spread of rabies, the basic reproduction number of rabies $\mathcal{R}_0$ shall be larger than one. We have

$$\mathcal{R}_0 = \left(\frac{p_1}{\nu_1} + \frac{p_2}{\nu_2}\right)\beta S_0 = 4.6 > 1.$$

The results of numerical simulations on the model (5.3.5) and (5.3.6) are presented on Fig. 5.6.10–5.6.13. Fig. 5.6.6 and Fig. 5.6.11 show the dynamics of susceptible foxes, diffusing rabid foxes, and territorial rabid foxes at specific times. Surface plots of approximations $S_h(x,t)$, $R_{1,h}(x,t)$, and $R_{2,h}(x,t)$ to $S(x,t)$, $R_1(x,t)$, and $R_2(x,t)$ are presented on Fig. 5.6.12. Fig. 5.6.13 depicts contour plots of susceptible foxes, diffusing rabid foxes, the territorial rabid foxes. The contour plots in Fig. 5.6.13 demonstrate that rabies spreads with asymptotic speed

$$c^\diamond \approx 45 \, [\text{km/year}].$$

Figure 5.6.10: Approximations $S_h(x,t)$, $R_{1,h}(x,t)$, and $R_{2,h}(x,t)$ to $S(x,t)$, $R_1(x,t)$, and $R_2(x,t)$ at t=0, 20, 30, 90, 120, 180 when $p_1 = 0.7$ and $p_2 = 0.3$.

Figure 5.6.11: Approximations of fox population densities at different times when $p_1 = 0.7$ and $p_2 = 0.3$.
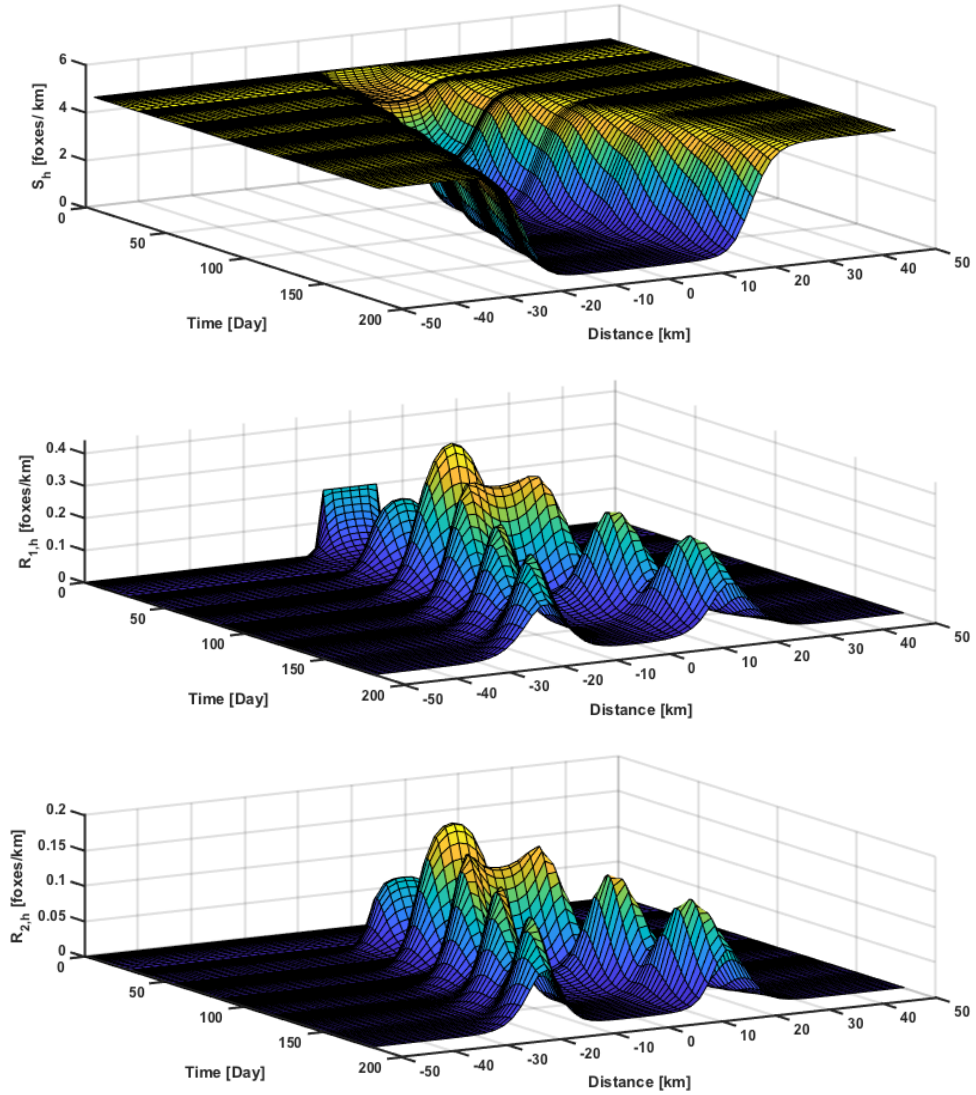
Figure 5.6.12: Surface plots of approximations $S_h(x,t)$, $R_{1,h}(x,t)$, and $R_{2,h}(x,t)$ to $S(x,t)$, $R_1(x,t)$, and $R_2(x,t)$ when $p_1 = 0.7$, $p_2 = 0.3$, and $N = 59$.

Figure 5.6.13: Contour plots of approximations $S_h(x,t)$ (top), $R_{1,h}(x,t)$ (middle), and $R_{2,h}(x,t)$ (bottom) to $S(x,t)$, $R_1(x,t)$, and $R_2(x,t)$ when $p_1 = 0.7$ and $p_2 = 0.3$.

5.6.4   IV. $p_1 = 1$, $p_2 = 0$

We assume that all rabid foxes diffuse. The basic reproduction number of rabies $\mathcal{R}_0$ is

$$\mathcal{R}_0 = \left(\frac{p_1}{\nu_1} + \frac{p_2}{\nu_2}\right)\beta S_0 = 4.6 > 1.$$

The results of numerical simulations on the model (5.3.5) and (5.3.6) are presented on Fig. 5.6.14–5.6.17. Fig. 5.6.14 and Fig. 5.6.15 show the dynamics of susceptible foxes, diffusing rabid foxes, and territorial rabid foxes at specific times. Surface plots of approximations $S_h(x,t)$, $R_{1,h}(x,t)$, and $R_{2,h}(x,t)$ to $S(x,t)$, $R_1(x,t)$, and $R_2(x,t)$ are presented on Fig. 5.6.16. Fig. 5.6.17 depicts contour plots of susceptible foxes, diffusing rabid foxes, the territorial rabid foxes. The contour plots in Fig. 5.6.17 demonstrate that rabies spreads with asymptotic speed
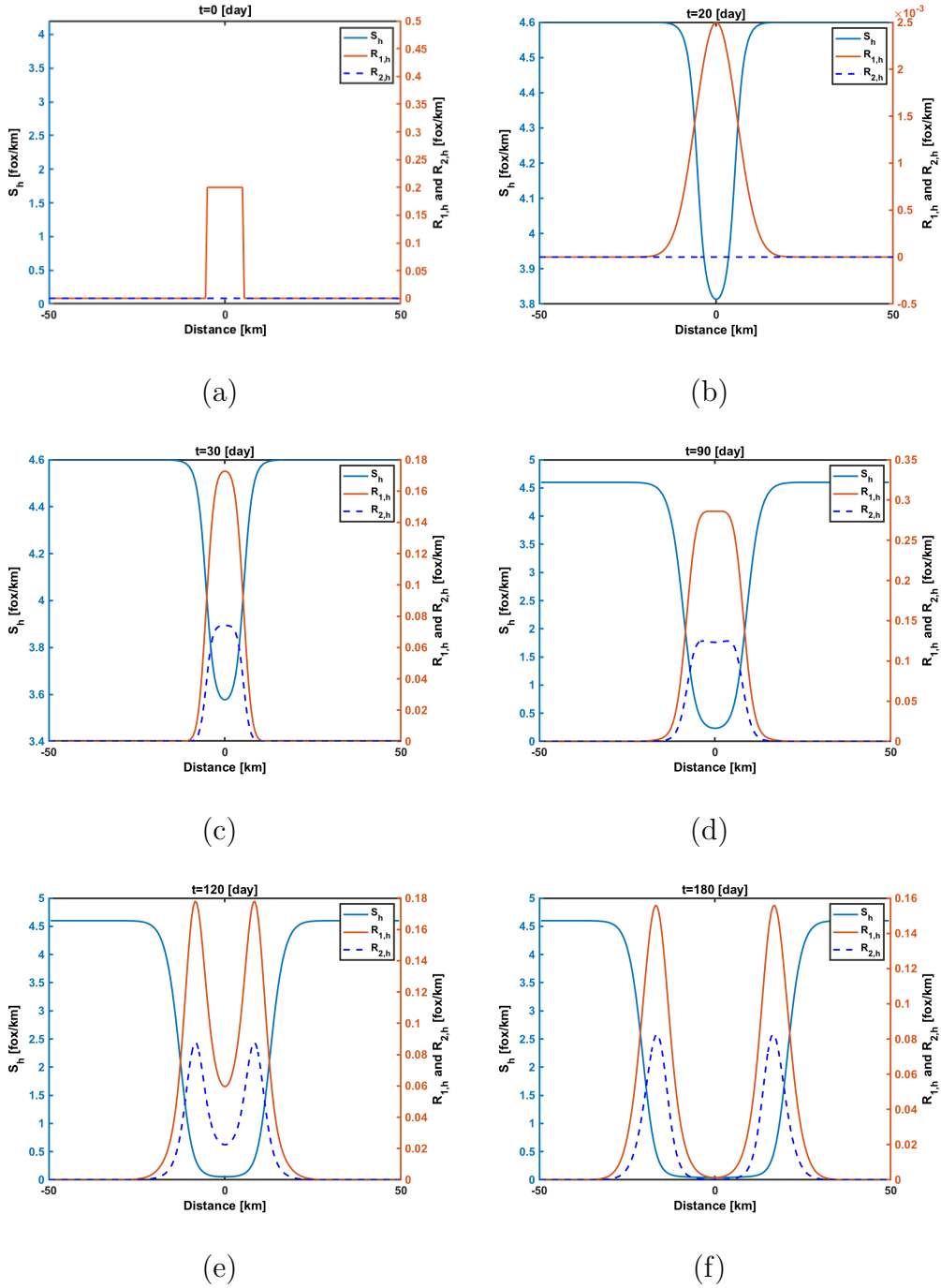
$$c^\diamond \approx 47\,[\text{km/year}].$$

Figure 5.6.14: Approximations $S_h(x,t)$, $R_{1,h}(x,t)$, and $R_{2,h}(x,t)$ to $S(x,t)$, $R_1(x,t)$, and $R_2(x,t)$ at t=0, 20, 30, 90, 120, 180 when $p_1 = 1$ and $p_2 = 0$.
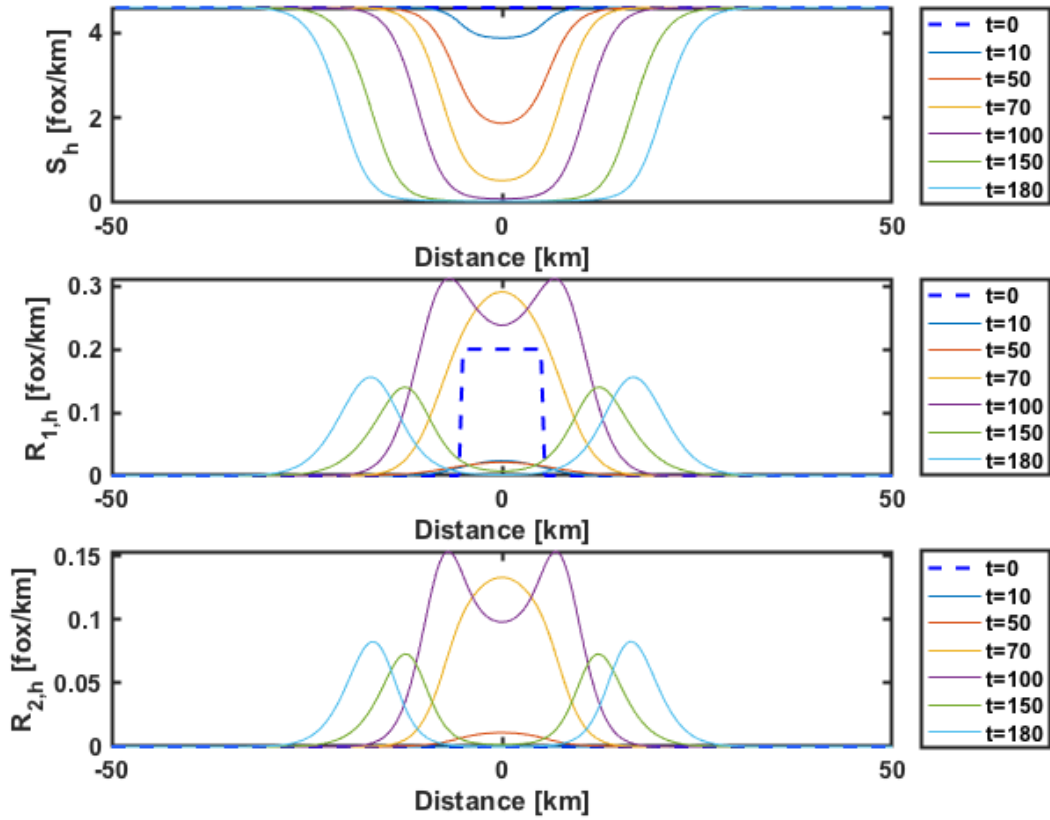
Figure 5.6.15: Approximations of fox population densities at different times when $p_1 = 1$ and $p_2 = 0$.
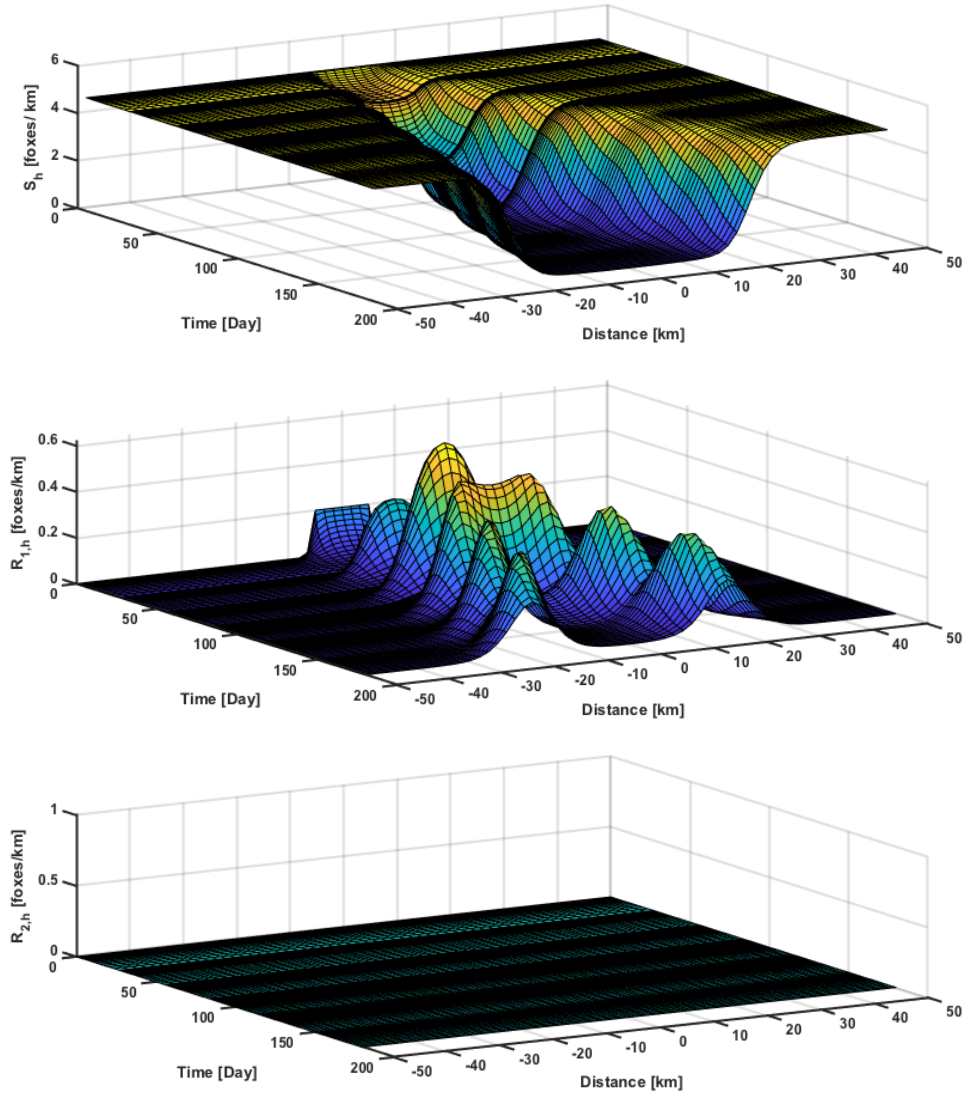
Figure 5.6.16: Surface plots of approximations $S_h(x,t)$, $R_{1,h}(x,t)$, and $R_{2,h}(x,t)$ to $S(x,t)$, $R_1(x,t)$, and $R_2(x,t)$ when $p_1 = 1$, $p_2 = 0$, and $N = 59$.

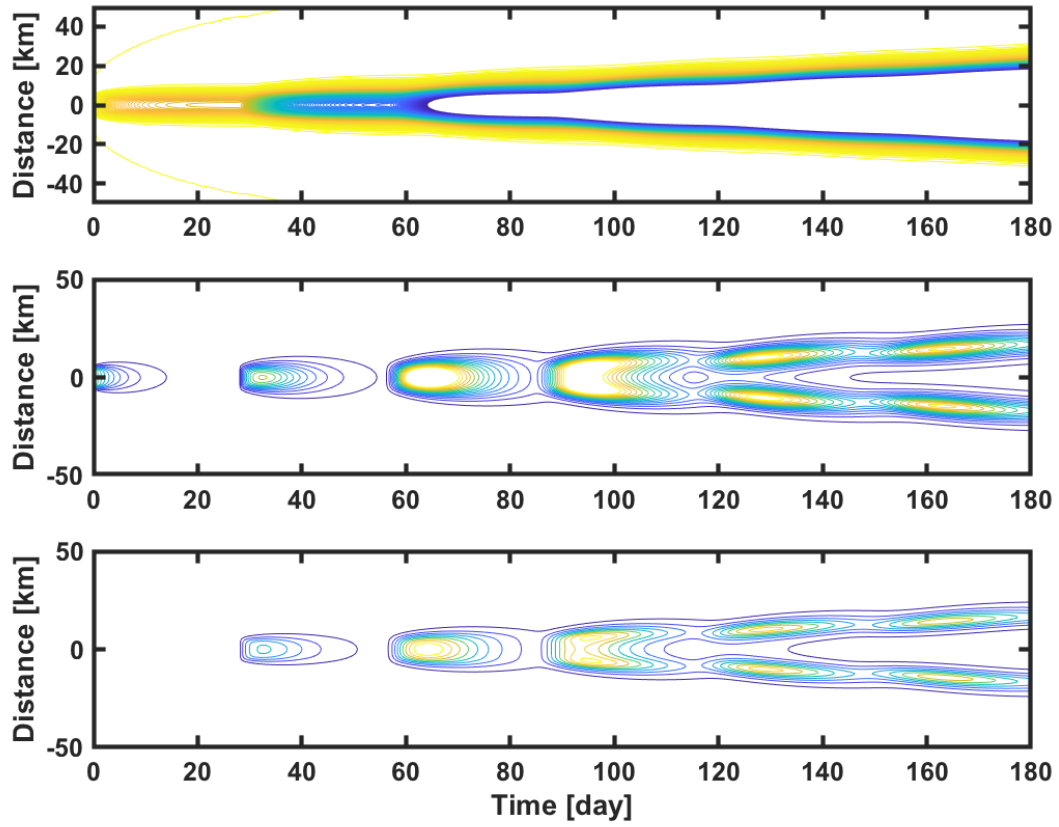Figure 5.6.17: Contour plots of approximations $S_h(x,t)$ (top) and $R_{1,h}(x,t)$ (bottom) to $S(x,t)$ and $R_1(x,t)$ when $p_1 = 1$ and $p_2 = 0$.

5.6.5   V. $p_1 = 0$, $p_2 = 1$

In the fifth case, we assume all infectious foxes are residential. Also for this case, the basic reproduction number of rabies is

$$\mathcal{R}_0 = \left(\frac{p_1}{\nu_1} + \frac{p_2}{\nu_2}\right)\beta S_0 = 4.6 > 1.$$

The results of numerical simulations on the model (5.3.5) and (5.3.6) are presented on Fig. 5.6.18–5.6.21. Fig. 5.6.18 and Fig. 5.6.19 show the dynamics of susceptible foxes, diffusing rabid foxes, and territorial rabid foxes at specific times. Surface plots of approximations $S_h(x,t)$, $R_{1,h}(x,t)$, and $R_{2,h}(x,t)$ to $S(x,t)$, $R_1(x,t)$, and $R_2(x,t)$ are presented on Fig. 5.6.20. Fig. 5.6.21 depicts contour plots of susceptible foxes, diffusing rabid foxes, the territorial rabid foxes. The contour plots in Fig. 5.6.21 demonstrate that rabies spreads with asymptotic speed
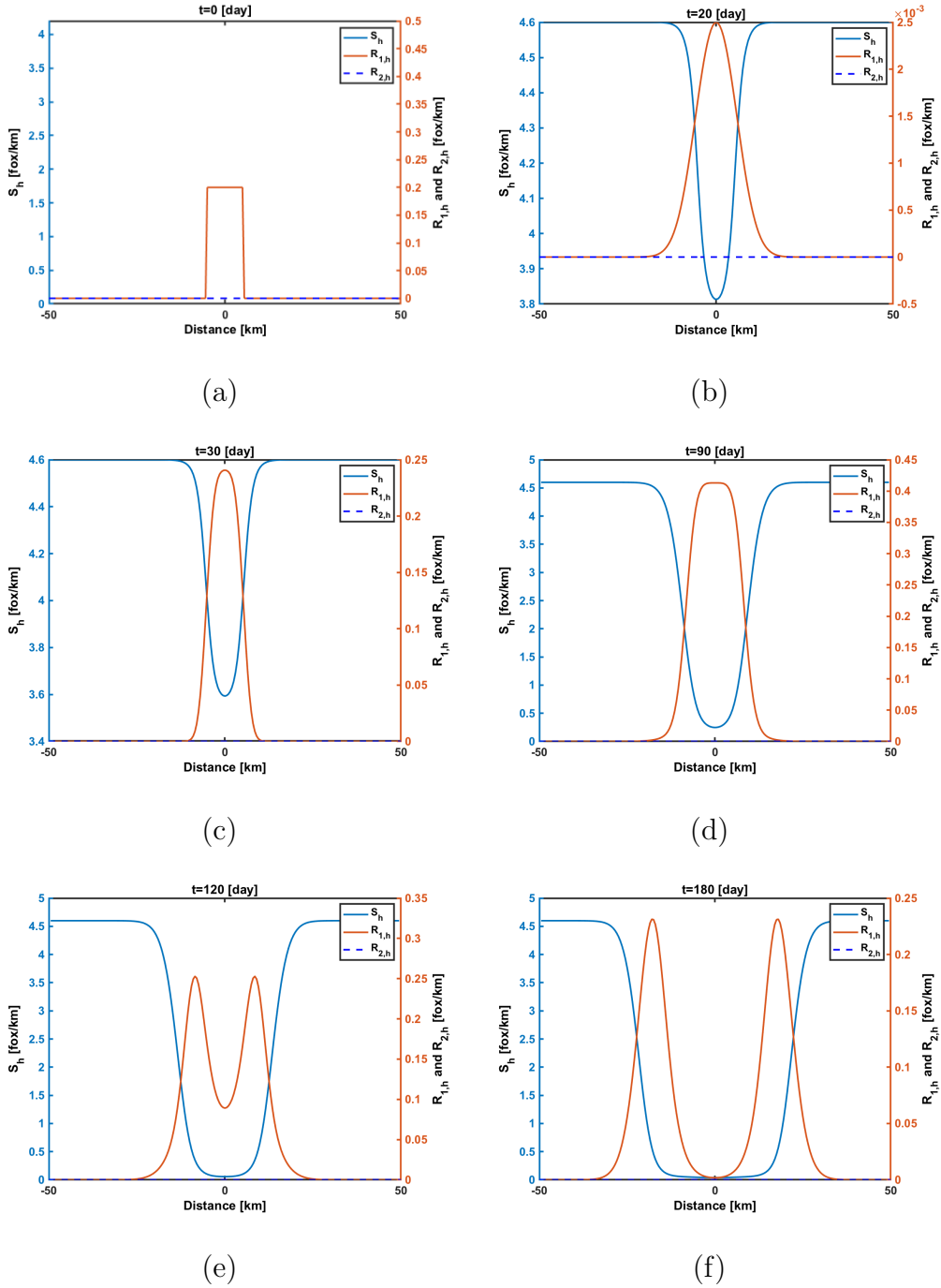
$$c^\diamond \approx 26\,[\text{km/year}].$$
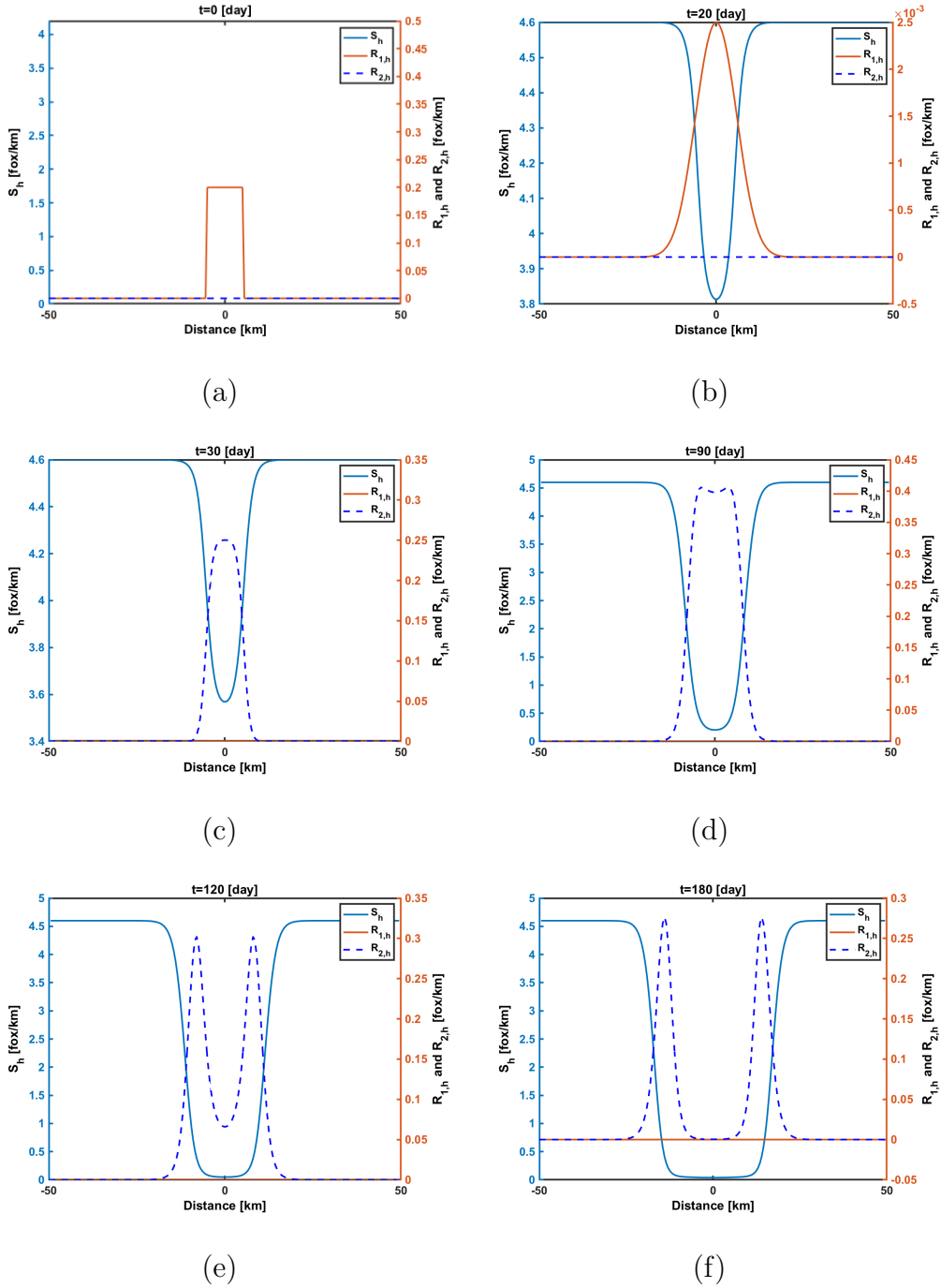
Figure 5.6.18: Approximations $S_h(x,t)$, $R_{1,h}(x,t)$, and $R_{2,h}(x,t)$ to $S(x,t)$, $R_1(x,t)$, and $R_2(x,t)$ at t=0, 20, 30, 90, 120, 180 when $p_1 = 0$ and $p_2 = 1$.
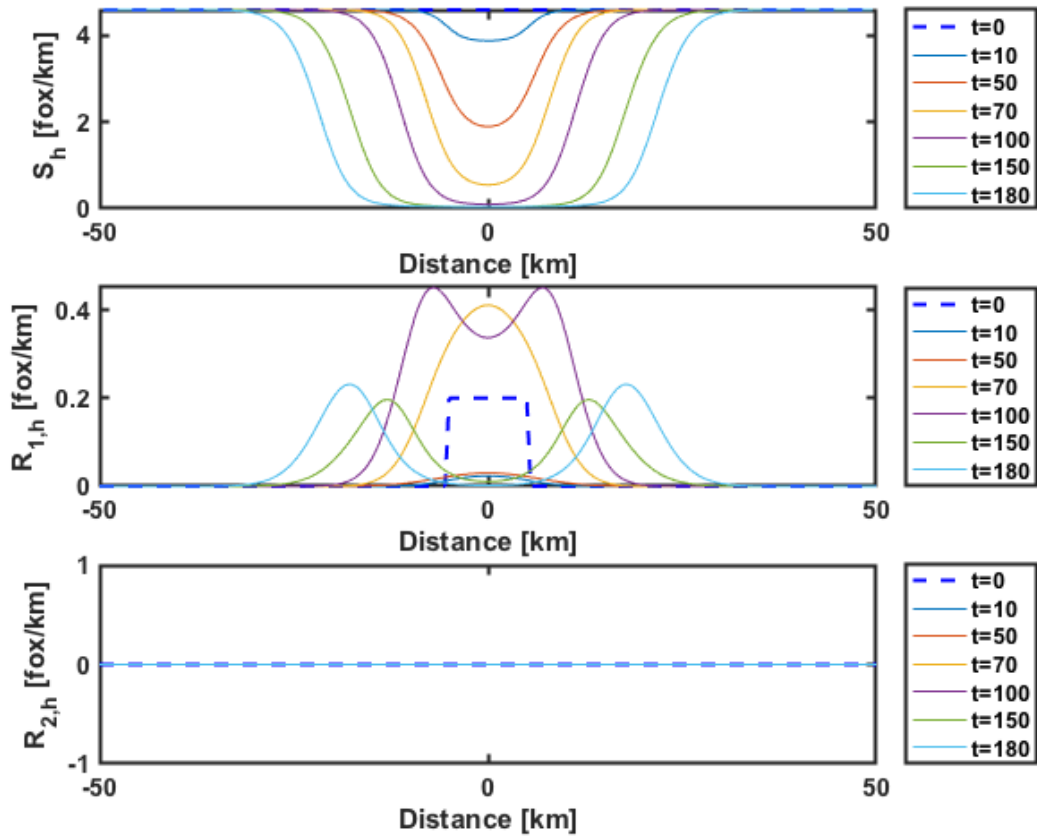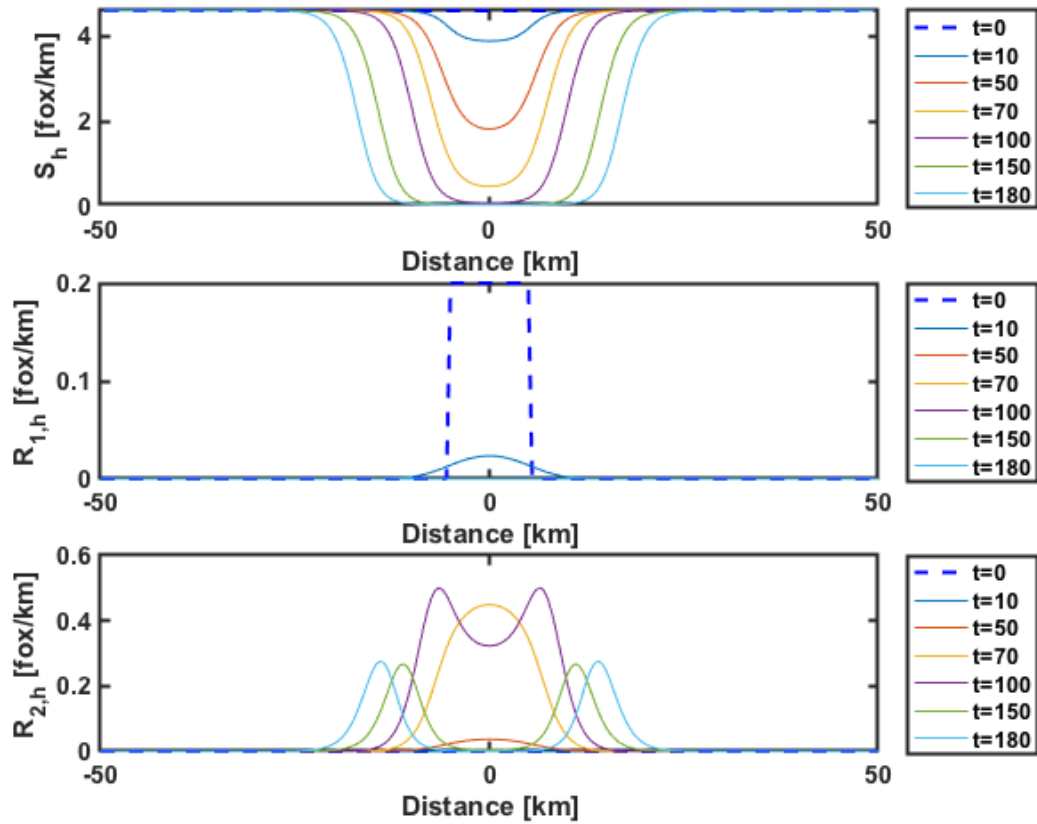
Figure 5.6.19: Approximations of fox population densities at different times when $p_1 = 0$ and $p_2 = 1$.
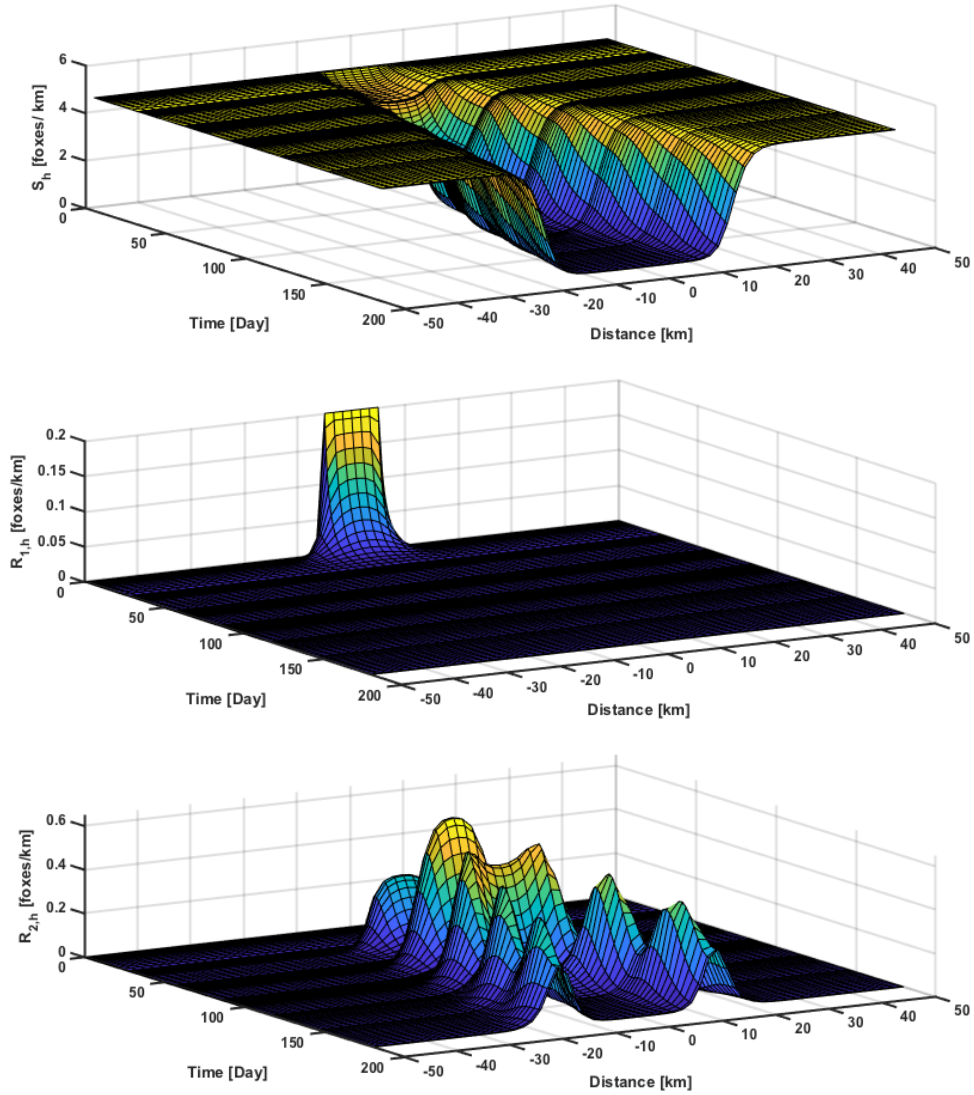
Figure 5.6.20: Surface plots of approximations $S_h(x,t)$, $R_{1,h}(x,t)$, and $R_{2,h}(x,t)$ to $S(x,t)$, $R_1(x,t)$, and $R_2(x,t)$ when $p_1 = 0$, $p_2 = 1$, and $N = 59$.
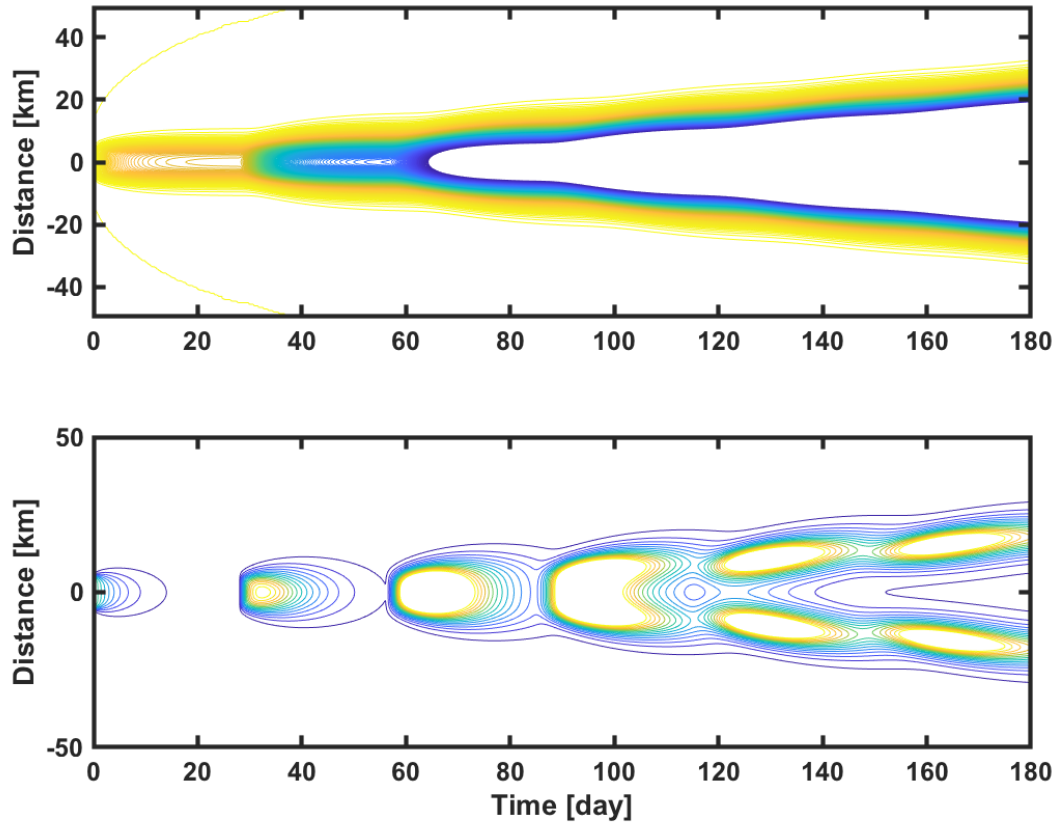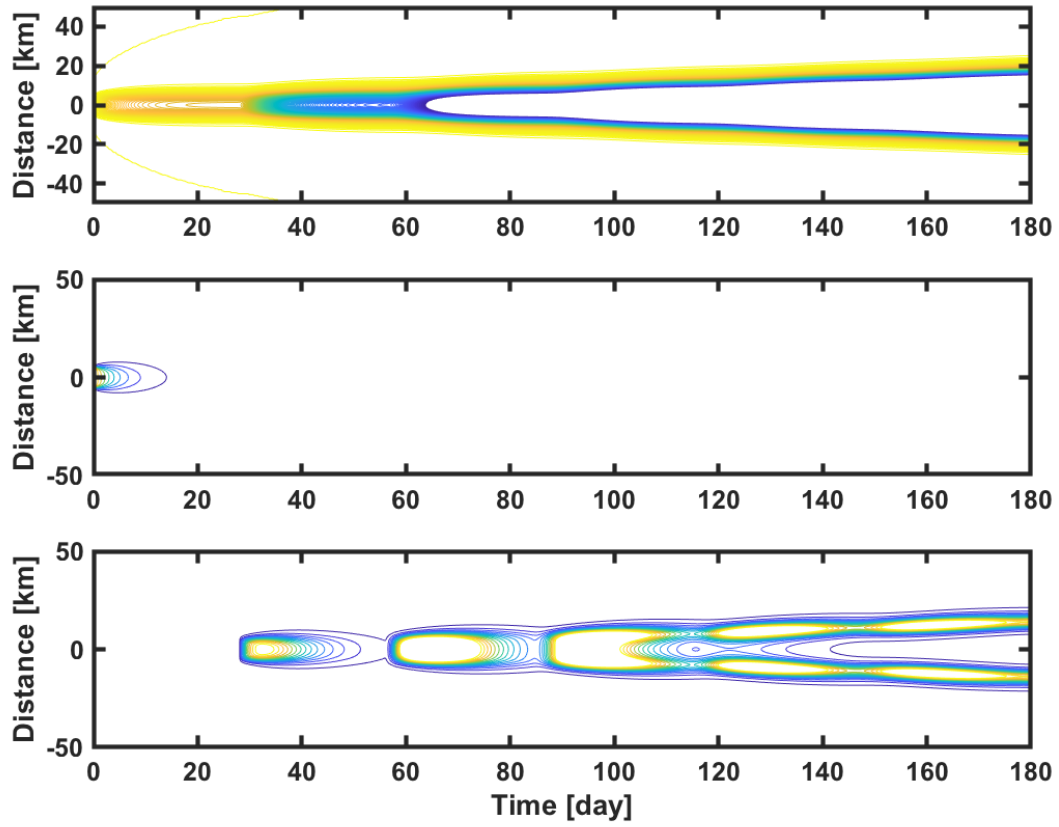
Figure 5.6.21: Contour plots of approximations $S_h(x,t)$ (top), $R_{1,h}(x,t)$ (middle), and $R_{2,h}(x,t)$ (bottom) to $S(x,t)$, $R_1(x,t)$, and $R_2(x,t)$ when $p_1 = 0$ and $p_2 = 1$.

5.7 Discussion and Conclusions

When the latent has a fixed length, the unique solutions of the system (4.4.7) are

$$(c^*, \lambda) \approx (0.0774794 \,[\text{km/day}], 1.20104) \approx (28.28 \,[\text{km/year}], 1.20104)$$

when $p_1 = 0$,

$$(c^*, \lambda) \approx (0.121047 \,[\text{km/day}], 0.566099) \approx (44.1821 \,[\text{km/year}], 0.566099)$$

when $p_1 = 0.3$,

$$(c^*, \lambda) \approx (0.129782 \,[\text{km/day}], 0.548928) \approx (47.3705 \,[\text{km/year}], 0.548928)$$

when $p_1 = 0.5$,

$$(c^*, \lambda) \approx (0.136702 \,[\text{km/day}], 0.538601) \approx (49.8961 \,[\text{km/year}], 0.538601)$$

when $p_1 = 0.7$, and

$$(c^*, \lambda) \approx (0.145169 \,[\text{km/day}], 0.529397) \approx (52.9868 \,[\text{km/year}], 0.529397)$$

when $p_1 = 1$. The contour plots in Fig. 5.6.21, Fig. 5.6.9,Fig. 5.6.4,Fig. 5.6.13, and Fig. 5.6.17 demonstrate that

$$c^\diamond \approx 26 \,[\text{km/year}] \quad \text{when} \quad p_1 = 0,$$

$$c^\diamond \approx 37 \,[\text{km/year}] \quad \text{when} \quad p_1 = 0.3,$$

$$c^\diamond \approx 43 \,[\text{km/year}] \quad \text{when} \quad p_1 = 0.5,$$

$$c^\diamond \approx 45 \,[\text{km/year}] \quad \text{when} \quad p_1 = 0.7,$$

and

$$c^\diamond \approx 47 \,[\text{km/year}] \quad \text{when} \quad p_1 = 1.$$

Therefore, the asymptotic speeds c^*, which we get by solving the system (4.4.7), are quite close to asymptotic speeds $c^\diamond$, which we get from the contour plots. In addition, the asymptotic speeds c^* and $c^\diamond$ confirm that the epidemic model on a bounded domain Ω with Dirichlet boundary conditions shows a less severe epidemic outbreak than the epidemic model on $\mathbb{R}^n$, and the spread of the disease modeled on Ω is not as fast as the spread of the disease modeled on $\mathbb{R}^n$, as discussed in Section 3.6. Also, The numerical results confirm for the spreading speeds c^* and $c^\diamond$ that the latent period with fixed length gives the smallest spreading speeds, as discussed in Section 4.4.1. In addition, the numerical simulations confirm that Theorem 2.6.5 in Section 2.6.3 holds.

When $p_1 = 0$, all rabid foxes are territorial, and the asymptotic speeds of spread c^* that we obtain by solving the system (4.4.7) for a latent period of fixed length can be compared with the asymptotic speeds in (van den Bosch *et al.* (1990)). There are differences in some assumptions and in the determination of parameters, though; for instance, it is assumed in (van den Bosch *et al.* (1990)) that the sizes of the home-ranges decrease with fox density while we assume them to be independent. For a fox population density S_0 of 4.6 [fox/km], we obtain an asymptotic speed of rabies spread $c^* \approx 28.3$ [km/year], while (van den Bosch *et al.*, 1990, Fig.7) shows an asymptotic speed of about 33 [km/year] when $S_0 = 4.6$ [fox/km^2]. Furthermore, for this case, the asymptotic speed of rabies spread c^* compares quite well with the observed speeds about 27 [km/year] in (Bögel *et al.* (1976)) and from 20 to 60 [km/year] according to (Lloyd (1980)).

The numerical simulations depict that the density of diffusing rabid foxes R_1 decays when $t \leq \tau$, then it increases for a period of time when the infected foxes leave the latent period at $t > \tau$, as shown in Fig. 5.6.1, Fig. 5.6.2, Fig. 5.6.3, Fig. 5.6.6, Fig. 5.6.7, Fig. 5.6.8, Fig. 5.6.10, Fig. 5.6.11, Fig. 5.6.12, Fig. 5.6.14, Fig. 5.6.15,

Fig. 5.6.16, Fig. 5.6.18, Fig. 5.6.19, and Fig. 5.6.20. The decrease in the density of diffusing rabid foxes is because the death from rabies ν_1, which gives the rabid foxes as few as five days on average to live (Anderson *et al.* (1981); Murray *et al.* (1986); Murray (1989); Murray and Seward (1992)).

The density of territorial rabid foxes R_2, on the other hand, remains zero when $t \leq \tau$ because we assume there are no territorial rabid foxes initially at time zero. When $t > \tau$, we see R_2 grows again before it loses some of its members with rate ν_2, as demonstrated in Fig. 5.6.1, Fig. 5.6.2, Fig. 5.6.3, Fig. 5.6.6, Fig. 5.6.7, Fig. 5.6.8, Fig. 5.6.10, Fig. 5.6.11, Fig. 5.6.12, Fig. 5.6.14, Fig. 5.6.15, Fig. 5.6.16, Fig. 5.6.18, Fig. 5.6.19, and Fig. 5.6.20.

Since, by assumptions, no foxes are born and infected foxes cannot recover and become susceptible again, the densities of susceptible foxes continue to decrease, as shown in Fig. 5.6.1, Fig. 5.6.2, Fig. 5.6.3, Fig. 5.6.6, Fig. 5.6.7, Fig. 5.6.8, Fig. 5.6.10, Fig. 5.6.11, Fig. 5.6.12, Fig. 5.6.14, Fig. 5.6.15, Fig. 5.6.16, Fig. 5.6.18, Fig. 5.6.19, and Fig. 5.6.20.

The embedded pair of Runge-Kutta methods was implemented in a variable stepsize environment with the estimates of the local discretization errors computed according to the formula

$$\text{EST}(t_{n+1}) = \left\| \hat{y}_{n+1} - y_h(t_{n+1}) \right\|_2,$$

(see Section 5.4). The stepsize h_n from t_n to $t_{n+1} = t_n + h_n$ for $n = 0, 1, \ldots,$ is accepted if

$$\text{EST}(t_{n+1}) \leq \text{TOL},$$

but if

$$\text{EST}(t_{n+1}) > \text{TOL},$$

the stepsize is rejected, and the computations are repeated with a halved stepsize $h_n/2$. Fig. 5.6.5 demonstrates that most of rejected steps occur for Tol $= 10^{-3}$.

Chapter 6

NUMERICAL SIMULATIONS OF SPREAD OF RABIES: LATENT PERIOD
WITH EXPONENTIALLY DISTRIBUTED LENGTH

6.1   Abstract

We describe a numerical algorithm for the simulation of the spread of rabies in a spatially distributed fox population. As we already know, the model considers both territorial and wandering rabid foxes and includes a latent period for the infection. The resulting systems are mixtures of partial differential and integral equations. They are discretized in the space variable by central differences of second order and by the composite trapezoidal rule. In a second step, the ordinary differential equations we obtained are discretized in time by explicit continuous Runge-Kutta methods of fourth order for ordinary and delay differential systems. The results of the numerical calculations are compared for latent periods of exponentially distributed length and for various proportions of territorial and wandering rabid foxes. The speeds of spread observed in the simulations are compared to spreading speeds obtained by analytic methods and to observed speeds of epizootic frontlines in the European rabies outbreak 1940 to 1980.

6.2   The Model

We consider the system in (3.4.5) with Ω to be a bounded domain on $\mathbb{R}$, which represents the habitat of foxes. So, when the latent period is exponentially distributed,

124

the spread of rabies is described by

$$
\begin{cases}
\partial_t S(x,t) = -\beta S(x,t) \int_\Omega \big[\kappa_1(x,z)R_1(z,t) + \kappa_2(x,z)R_2(z,t)\big]dz \\[2mm]
\qquad =: -B(x,t), \\[2mm]
\partial_t R_1(x,t) = D\nabla_x^2 R_1(x,t) + p_1 I(x,t) - \nu_1 R_1(x,t), \\[2mm]
\partial_t R_2(x,t) = p_2 I(x,t) - \nu_2 R_2(x,t), \\[2mm]
\partial_t I(x,t) = \theta B(x,t) - \theta I(x,t),
\end{cases}
\tag{6.2.1}
$$

with given initial conditions

$$
S(x,0) = S_0(x), \ R_1(x,0) = R_1^\circ(x), \ R_2(x,0) = R_2^\circ(x), \ I(x,0) = I_0(x), \ x \in \Omega.
$$

The boundary conditions are given by

$$
R_1(x,t) = w(x,t), \quad x \in \partial\Omega, \quad t > 0.
\tag{6.2.2}
$$

As before, $S(x,t)$ denote the density of susceptible foxes at time t whose home-ranges center at location $x \in \mathbb{R}$. Further, $R_1(x,t)$ are the diffusing rabid foxes at location x and time t, $R_2(x,t)$ are the territorial rabid foxes at time t whose home-ranges center at location x, and $I(x,t)$ is the rate at which foxes in the latent period become infectious. The parameters $\nu_1 > 0$ and $\nu_2 > 0$ are the per capita rabies death rates of diffusing and territorial rabid foxes, respectively. p_1 is the chance of a rabid fox to diffuse, and p_2 the chance to be territorial, $p_j \geq 0$ and $p_1 + p_2 = 1$. $\beta > 0$ is the rate at which the meeting of a susceptible and rabid fox leads to the infection of the susceptible fox. $B(x,t)$ is the incidence of the disease, i.e., the number of new cases per unit of time. $D > 0$ is the diffusion constant. $\kappa_1(x,z)$ denotes the rate at which a fox with home-range center x visits the location $z \in \Omega$. The rate at which a susceptible fox with home-range center x meets a territorial rabid fox with

home-range center z is given by

$$\kappa_2(x, z) = \int_\Omega \kappa_1(x, y)\kappa_1(z, y)dy, \qquad (6.2.3)$$

which means that it is the rate at which they both visit some common point $y \in \Omega$. The nonnegative continuous functions S_0, R_1°, R_2° and I_0 are the initial densities of the susceptible foxes, diffusing rabid foxes, territorial rabid foxes, and transition rate, respectively.

6.3 Discretization in Space

We use the method of lines to find finite difference approximations for the spatial derivatives (see, e.g., Schiesser (2013); Schiesser and Griffiths (2009)), then we use the continuous explicit Runge Kutta methods of order four and three to solve the systems of nonlinear ordinary differential equations. The continuous Runge-Kutta method was derived by Owren and Zennaro (Owren and Zennaro (1991, 1992b,a)), and it is discussed in (Bellen and Zennaro (2003)). The continuous Runge-Kutta method was recently applied by (Alanazi *et al.* (2018a, 2019); Bartoszewski *et al.* (2015); Jackiewicz *et al.* (2014)).

We discretize the partial differential equation PDE by using central in space second order scheme. The integrals in (6.2.1) are approximated using composite trapezoid rule. Another approach to approximate integrals in (6.2.1) is by using Gauss-Hermite quadrature rule (see, e.g., Jackiewicz *et al.* (2006)).

As before, we use the notations $R_{1,i}(t)$, $R_{2,i}(t)$, and $S_i(t)$, $Q_i(t)$, and $I_i(t)$ for the approximations of $R_1(x_i, t)$, $R_2(x_i, t)$, $S(x_i, t)$, $Q(x_i, t)$, and $I(x_i, t)$, respectively.

We consider $\Omega = [-a, a]$ to be a bounded domain on $\mathbb{R}$ to represent the habitat of foxes. Let x_i to be a sequence of uniformly spaced points on $[-a, a]$, such that $x_i = -a + ih$, where $h = \frac{2a}{N+1}$ is the spacing stepsize and $i = 0, ..., N+1$. In addition,

126

we define z_k be a sequence of uniformly spaced points on $[-a, a]$, such that $z_k = -a + kh, k = 0, ..., N+1$, and $h = \frac{2a}{N+1}$. We replace x with x_i for $i = 1, ..., N$, and set

$$Q_i(t) = \int_{-a}^{a} [\kappa_1(x_i - z)R_1(z, t) + \kappa_2(x_i - z)R_2(z, t)]dz.$$

From the previous section, we have $Q_i(t) = Q_{1,i}(t) + Q_{2,i}(t)$, where $Q_{1,i}(t)$ and $Q_{2,i}(t)$ are defined in (5.3.3). Therefore, when $i = 1, ..., N$, we obtain the following nonlinear systems of differential equations for the model in (6.2.1)

$$
\begin{aligned}
S_i'(t) =& -\beta S_i(t)Q_i(t), \\
R_{1,i}'(t) =& D\frac{R_{1,i+1}(t) - 2R_{1,i}(t) + R_{1,i-1}(t)}{h^2} + p_1 I_i(t) - \nu_1 R_{1,i}(t), \\
R_{2,i}'(t) =& p_2 I_i(t) - \nu_2 R_{2,i}(t), \\
I_i'(t) =& \theta\beta S_i(t)Q_i(t) - \theta I_i(t).
\end{aligned}
\tag{6.3.1}
$$

We assume that (6.3.1) satisfy the following boundary conditions

$$R_1(-a, t) = w_1(t), \quad R_1(a, t) = w_2(t), \quad t \geq 0,$$

where $w_1(t)$ and $w_2(t)$ are given functions. So, when $i = 1$, the scheme for R_1 shall be

$$R_{1,1}'(t) = D\frac{R_{1,2}(t) - 2R_{1,1}(t)}{h^2} + \frac{D}{h^2}w_1(t) + p_1 I_1(t) - \nu_1 R_{1,1}(t), \tag{6.3.2}$$

and when $i = N$, the scheme for R_1 shall be

$$R_{1,N}'(t) = D\frac{R_{1,N-1}(t) - 2R_{1,N}(t)}{h^2} + \frac{D}{h^2}w_2(t) + p_1 I_N(t) - \nu_1 R_{1,N}(t), \tag{6.3.3}$$

with the following initial conditions,

$$
\begin{aligned}
S_i(0) =& S_0(x_i), \\
R_{1,i}(0) =& R_1^\circ(x_i), \\
R_{2,i}(0) =& R_2^\circ(x_i), \\
I_i(0) =& I_0(x_i),
\end{aligned}
\tag{6.3.4}
$$

for $i = 1, ..., N$.

6.4   Discretization in Time

We introduce the notation

$$S(t) = \begin{bmatrix} S_1(t) \\ \vdots \\ S_N(t) \end{bmatrix}, \quad R_1(t) = \begin{bmatrix} R_{1,1}(t) \\ \vdots \\ R_{1,N}(t) \end{bmatrix}, \quad R_2(t) = \begin{bmatrix} R_{2,1}(t) \\ \vdots \\ R_{2,N}(t) \end{bmatrix},$$

$$I(t) = \begin{bmatrix} I_1(t) \\ \vdots \\ I_N(t) \end{bmatrix}, \quad y(t) = \begin{bmatrix} S(t) \\ R_1(t) \\ R_2(t) \\ I(t) \end{bmatrix}, \quad y_0 = \begin{bmatrix} S(0) \\ R_1(0) \\ R_2(0) \\ I(0) \end{bmatrix}.$$

We define $f(y(t))$ to be the right hand side of the differential equation system in (6.3.1). Therefore, the systems in (6.3.1) with the initial conditions in (6.3.4) can be written as

$$\begin{cases} y'(t) = f\big(y(t)\big), & t \geq 0, \\ y(0) = y_0 \in \mathbb{R}^{4N}, \end{cases} \tag{6.4.1}$$

where $f : \mathbb{R}^{4N} \to \mathbb{R}^{4N}$.

The problems (6.4.1) will be solved by the explicit continuous Runge-Kutta method of fourth order with $s = 6$ stages, and the embedded discrete Runge-Kutta method of third order, which is used for the estimation of local discretization errors of the method of order four. This embedded pair was proposed by Owren and Zennaro (Owren and Zennaro (1991, 1992b,a)), see also (Bellen and Zennaro (2003)). The coefficients of this embedded pair are given by the Butcher table with continuous

$$\begin{array}{c|c}
\mathbf{c} & \mathbf{A} \\
\hline
\mathbf{y}_h & \mathbf{b}(\theta) \\
\hline
\hat{\mathbf{y}}_{n+1} & \hat{\mathbf{b}}
\end{array} \;=\;$$

c	A					
0						
$\frac{1}{6}$	$\frac{1}{6}$					
$\frac{11}{37}$	$\frac{44}{1369}$	$\frac{369}{1369}$				
$\frac{11}{17}$	$\frac{3388}{4913}$	$-\frac{8349}{4913}$	$\frac{8140}{4913}$			
$\frac{13}{15}$	$-\frac{36764}{408375}$	$\frac{767}{1125}$	$-\frac{32708}{136125}$	$\frac{210392}{408375}$		
1	$\frac{1697}{18876}$	0	$\frac{50653}{116160}$	$\frac{299693}{1626240}$	$\frac{3375}{11648}$	
$y_h(t_n+\theta h_n)$	$b_1(\theta)$	$b_2(\theta)$	$b_3(\theta)$	$b_4(\theta)$	$b_5(\theta)$	$b_6(\theta)$
$\hat{y}_{n+1}$	$\frac{101}{363}$	0	$-\frac{1369}{14520}$	$\frac{11849}{14520}$	0	0

,

Table 6.1: The coefficients of the optimal pair of continuous and discrete Runge-Kutta method of order $p = 4$ with $s = 6$ stages.

weights $b_i(\theta)$ given by

$$
\begin{cases}
b_1(\theta) = -\frac{866577}{824252}\theta^4 + \frac{1806901}{618189}\theta^3 - \frac{104217}{37466}\theta^2 + \theta, \\[2mm]
b_2(\theta) = 0, \\[2mm]
b_3(\theta) = \frac{12308679}{5072320}\theta^4 - \frac{2178079}{380424}\theta^3 + \frac{861101}{230560}\theta^2, \\[2mm]
b_4(\theta) = -\frac{7816583}{10144640}\theta^4 + \frac{6244423}{5325936}\theta^3 - \frac{63869}{293440}\theta^2, \\[2mm]
b_5(\theta) = -\frac{624375}{217984}\theta^4 + \frac{982125}{190736}\theta^3 - \frac{1522125}{762944}\theta^2, \\[2mm]
b_6(\theta) = \frac{296}{131}\theta^4 - \frac{461}{131}\theta^3 + \frac{165}{131}\theta^2.
\end{cases}
\tag{6.4.2}
$$

To compute the approximate solution for the ordinary differential equation $y_h(t_n)$, we search for the index q such that $t_n \in (t_q, t_{q+1}]$, then the approximation shall be

$$
\begin{aligned}
y_h(t_n) = {}& b_1(\theta)F_{1,q} + b_2(\theta)F_{2,q} + b_3(\theta)F_{3,q} + b_4(\theta)F_{4,q} + b_5(\theta)F_{5,q} \\
& + b_6(\theta)F_{6,q},
\end{aligned}
\tag{6.4.3}
$$

where $b_i(\theta)$ is in (6.4.2),

$$\theta = \frac{t_n - \tau - t_q}{t_{q+1} - t_q} \in (0, 1],$$ (6.4.4)

and

$$F_{k,q} = f\big(y_h(t_q + c_k h_q)\big),$$ (6.4.5)

for $k = 1, 2, 3, 4, 5, 6$, $h_q = t_{q+1} - t_q$, and $\mathbf{c} = [c_1, c_2, c_3, c_4, c_5, c_6]^T$. The estimation of the local discretization errors are given by

$$\mathrm{EST}(t_{n+1}) = \big\|\hat{y}_{n+1} - y_h(t_{n+1})\big\|_2.$$

and the initial stepsize h_0 is computed by

$$h_0 = \min\left\{0.01\,\tau, \frac{\mathrm{TOL}^{1/5}}{\|f(0, y_0)\|_2}\right\},$$

where TOL is the accuracy tolerance, and it is selected by the user of the code. Then for $n = 0, 1, \ldots$, the stepsize h_n from t_n to $t_{n+1} = t_n + h_n$ is accepted if

$$\mathrm{EST}(t_{n+1}) \leq \mathrm{TOL}.$$

The new stepsize h_{n+1} from t_{n+1} to $t_{n+2} = t_{n+1} + h_{n+1}$ is computed by

$$h_{n+1} = \eta\,h_n \left(\frac{\mathrm{TOL}}{\mathrm{EST}(t_{n+1})}\right)^{1/5},$$

where η is a safety coefficient to avoid too many rejected steps. In our implementation of the code we have chosen $\eta = 0.8$. If

$$\mathrm{EST}(t_{n+1}) > \mathrm{TOL},$$

the stepsize is rejected, and the computations are repeated with a halved stepsize $h_n/2$.

The construction of embedded pairs of continuous and discrete Runge-Kutta methods employed in this section, and their convergence and order properties, are discussed in (Owren and Zennaro (1991, 1992b,a)) and in the monographs (Bellen and Zennaro (2003); Hairer *et al.* (1993)).

6.5   Units Check

From Table 5.3 and Table 5.4, the net units of both sides of the equations in (6.2.1) are consistent, $\left(\frac{fox/km}{day}\right)$.

6.6   Numerical Experiments and Simulations

In this section, we present the results of numerical experiments for (6.2.1) with continuous Runge-Kutta methods of order four implemented in a variable stepsize environment as described in Section 6.4. We compute approximations to these systems for $x \in [-a, a]$, $a = 50$ [km], and $t \in [t_0, t_{end}]$, $t_0 = 0$ [day], $t_{end} = 180$ [day]. We choose $N = 199$ unless otherwise specified.

We assume the Dirichlet boundary conditions at $x = -a$ and $x = a$, of the form

$$R_1(-a, t) = w_1(t) = 0 \,[\text{fox/km}], \quad R_1(a, t) = w_2(t) = 0 \,[\text{fox/km}], \, t \in [0, t_{end}],$$

and initial conditions

$$S_i(0) = S_0(x_i), \; R_{1,i}(0) = R_1^\circ(x_i), \; R_{2,i}(0) = R_2^\circ(x_i), \; I_i(0) = I_0(x_i),$$

$i = 1, 2, \ldots, N$, where the functions $S_0(x)$, $R_1^\circ(x)$, $R_2^\circ(x)$, and $I_0(x)$ are defined by

$$R_1^\circ(x) = \begin{cases} 0.2 \,[\text{fox/km}], & -5 \le x \le 5, \\ 0 \quad [\text{fox/km}], & \text{otherwise,} \end{cases}$$

$$R_2^\circ(x) = 0 \,[\text{fox/km}], \qquad I_0(x) = 0 \,[\text{fox/km}], \quad x \in [-a, a].$$

As in Section 5.6, if we assume

$$\kappa_1(z) = \Gamma_1(z, b) = \frac{1}{\sqrt{4\pi b}} e^{\frac{-z^2}{4b}}, \tag{6.6.1}$$

then

$$\kappa_2(z) = \Gamma_1(z, 2b). \tag{6.6.2}$$

131

We let $\Gamma_2(t,x)$ to be the fundamental solution of $\partial_t - \Delta_x$ in two space dimensions. Then the mean maximum distance of a territorial fox from the center of its home-range (the mean radius of its home-range) is given by

$$r_0 = \int_{\mathbb{R}^2} |z| \Gamma_2(z,b) dz = \int_{\mathbb{R}^2} |z| (4b\pi)^{-1} e^{-|z|^2/(4b)} dz,$$

where $|\cdot|$ being the Euclidean norm in $\mathbb{R}^2$. We translate the integral into polar coordinates $(z_1, z_2) = (r\cos\theta, r\sin\theta)$, where $0 \leq r \leq \infty$ and $\theta \in [0, 2\pi)$, so we shall have

$$r_0 = \frac{1}{4\pi b} \int_0^{2\pi} \int_0^{\infty} r^2 e^{-r^2/(4b)} dr d\theta = \frac{1}{2b} \int_0^{\infty} r^2 e^{-r^2/4b} dr = b^{1/2}\pi^{1/2},$$

(see Section 5.6). So the mean area of the home range is

$$A = \pi r_0^2 = b\pi^2.$$

So $b = A\pi^{-2}$ [km^2]. A is between 2 and 8 [km^2] according to (Toma and Andral (1977)), the average area is taken as 5 [km^2] by (Källén *et al.* (1985)) and (Murray *et al.* (1986)). Then b is $5\pi^{-2}$ [km^2] ≈ 0.506605918 [km^2]. If the latent period has exponentially distributed length with constant exit rate θ, then we have $\theta = 1/\tau$ [1/day]. The numerical values of the parameters $S_0, \beta, D, b, \tau, \nu_1$ and ν_2 are also summarized in Table 4.1.

6.6.1 I. $p_1 = p_2 = 0.5$

We assume the chance for a rabid fox to diffuse or to be territorial is equal, i.e., $p_1 = p_2 = 0.5$. The basic reproduction number of the rabies is

$$\mathcal{R}_0 = \left(\frac{p_1}{\nu_1} + \frac{p_2}{\nu_2}\right)\beta S_0 = 4.6 > 1.$$

The discrete forms of (6.2.1) with the boundary conditions in (6.2.2) give us the numerical results presented on Fig. 6.6.1–6.6.5. Fig. 6.6.1 and Fig. 6.6.2 show

132

the dynamics of susceptible foxes, diffusing rabid foxes, and territorial rabid foxes at specific times. Surface plots of approximations $S_h(x,t)$, $R_{1,h}(x,t)$, $R_{2,h}(x,t)$ and $I_h(x,t)$ to $S(x,t)$, $R_1(x,t)$, $R_2(x,t)$ and $I(x,t)$ are presented on Fig. 6.6.3. Fig. 6.6.4 depicts contour plots of susceptible foxes, diffusing rabid foxes, the territorial rabid foxes. The contour plots in Fig. 6.6.4 demonstrate that rabies spreads with asymptotic speed

$$c^\diamond \approx 81 \, [\text{km/year}].$$

We also present in Fig. 6.6.5 the stepsize pattern for the algorithm described in Section 6.4 for the accuracy tolerances $\text{TOL} = 10^{-3}$, 10^{-6}, 10^{-9}, and 10^{-12}. On these figures the rejected steps are denoted by '$\times$'.
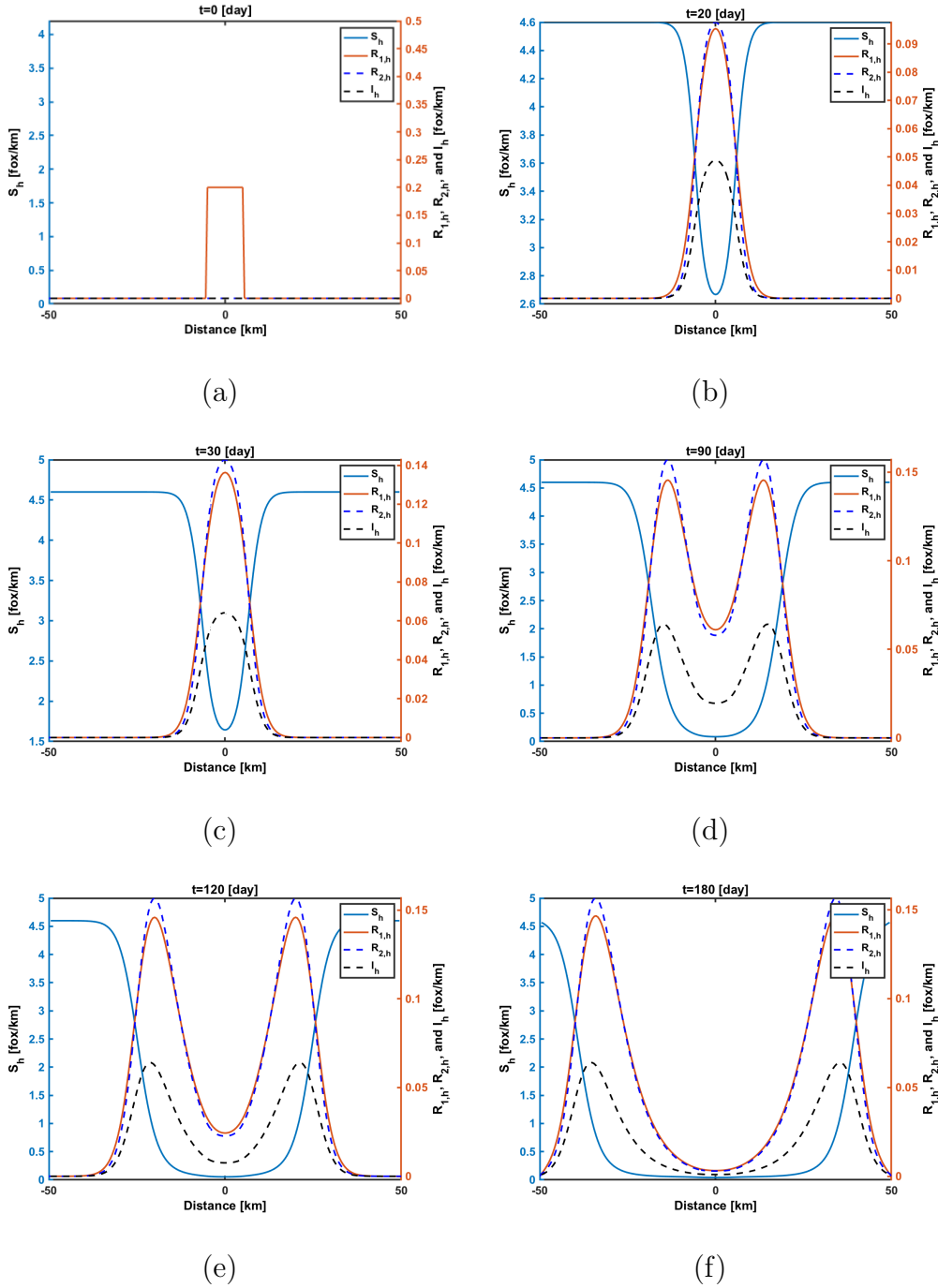
Figure 6.6.1: Approximations $S_h(x,t)$, $R_{1,h}(x,t)$, $R_{2,h}(x,t)$ and $I_h(x,t)$ to $S(x,t)$, $R_1(x,t)$, $R_2(x,t)$ and $I(x,t)$ at t=0, 20, 30, 90, 120, 180 when $p_1 = p_2 = 0.5$.
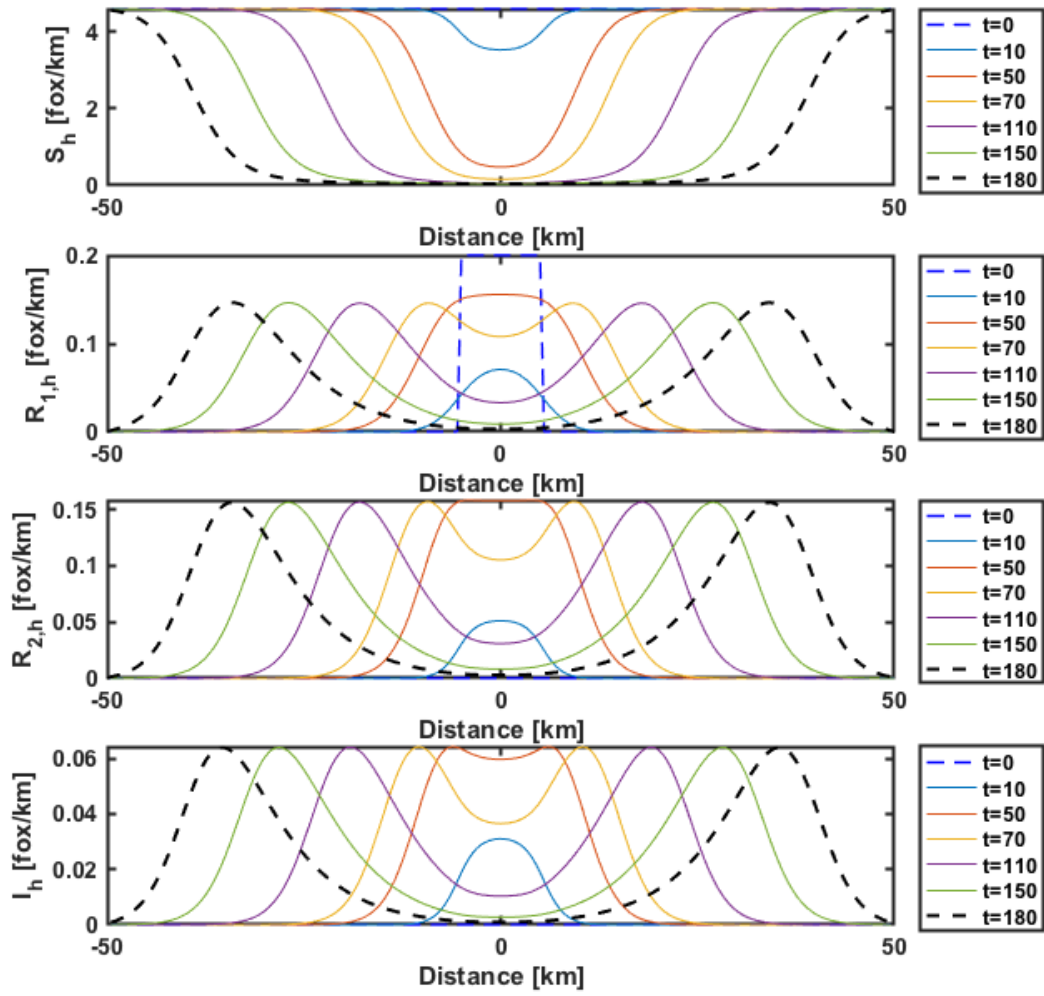
134

Figure 6.6.2: Approximations of fox population densities at different times when $p_1 = p_2 = 0.5$.
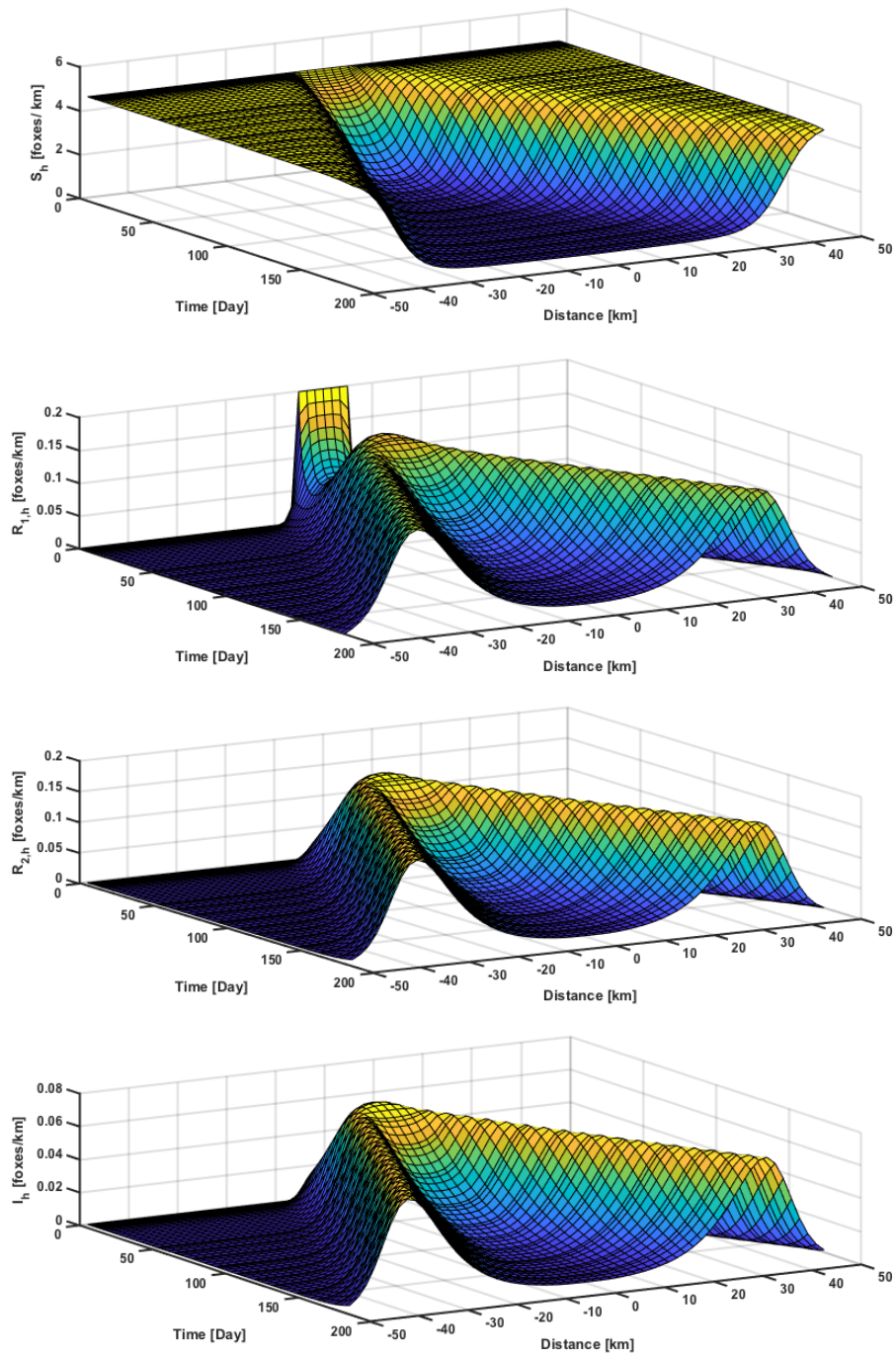
Figure 6.6.3: Surface plots of approximations $S_h(x,t)$, $R_{1,h}(x,t)$, $R_{2,h}(x,t)$ and $I_h(x,t)$ to $S(x,t)$, $R_1(x,t)$, $R_2(x,t)$ and $I(x,t)$ when $p_1 = p_2 = 0.5$ and $N = 59$.

136

Figure 6.6.4: Contour plots of approximations $S_h(x,t)$ (top), $R_{1,h}(x,t)$, $R_{2,h}(x,t)$ and $I_h(x,t)$ (bottom) to $S(x,t)$, $R_1(x,t)$, $R_2(x,t)$ and $I(x,t)$ when $p_1 = p_2 = 0.5$.

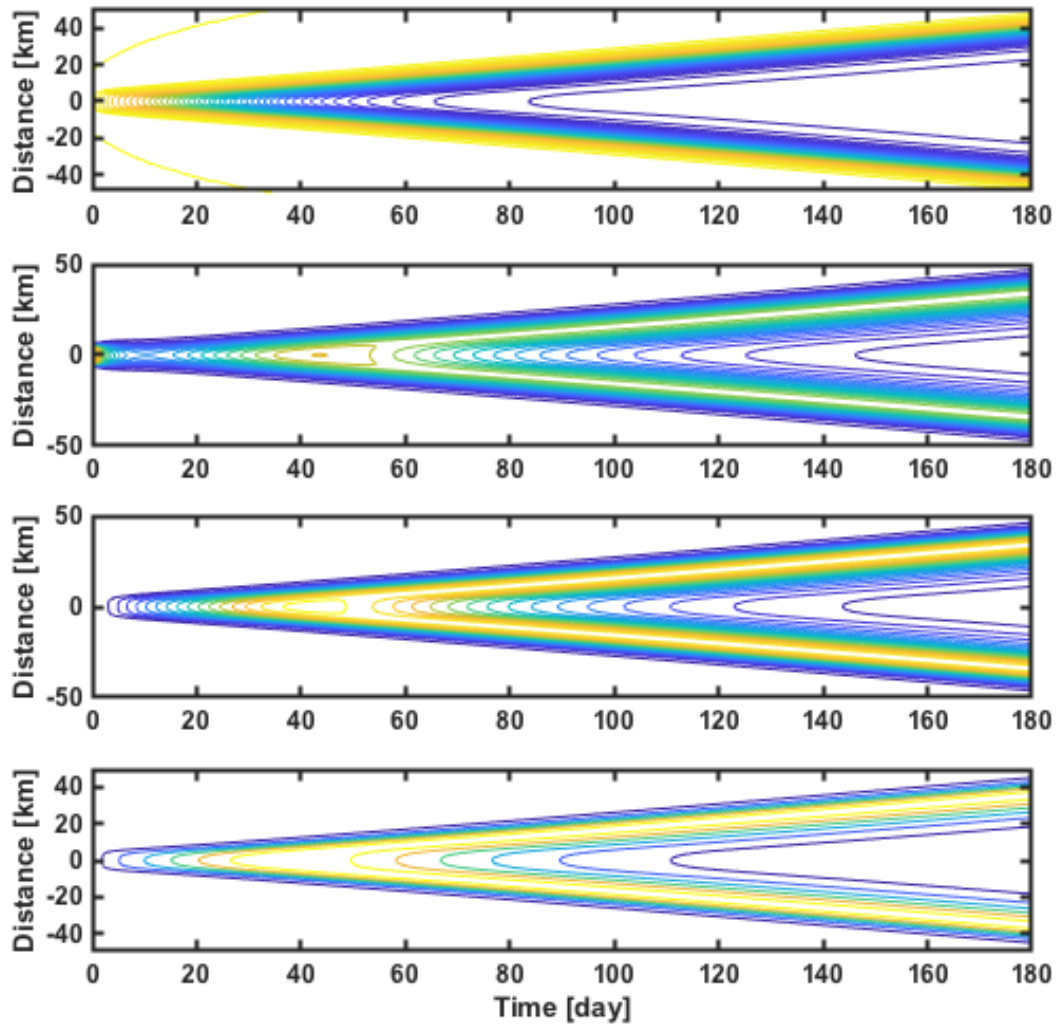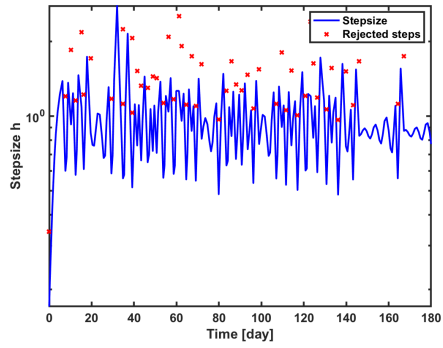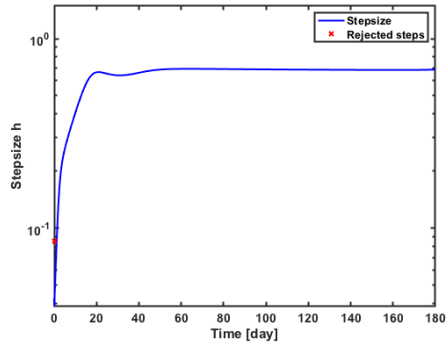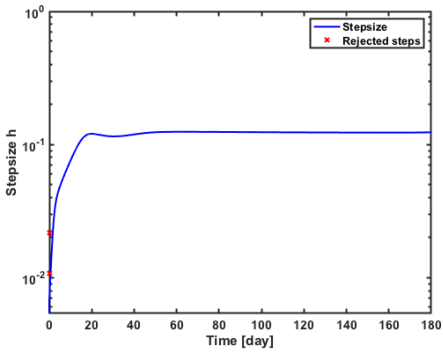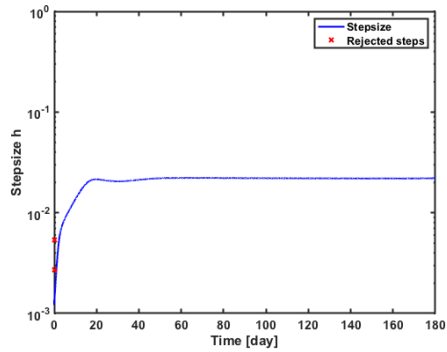Figure 6.6.5: Variable stepsize pattern for the algorithm based on continuous Runge-Kutta method of fourth order with $N = 119$, $p_1 = p_2 = 0.5$, and Tol $= 10^{-3}(a)$, $10^{-6}(b), 10^{-9}(c), 10^{-12}(d)$. Rejected steps are denoted by '$\times$'.

6.6.2 II. $p_1 = 0.3$, $p_2 = 0.7$

Since there are no changes to the density of I as we change p_1 or p_2, we are not going to discuss the density of I in this case and in the coming cases. The basic reproduction number of the rabies

$$\mathcal{R}_0 = \left(\frac{p_1}{\nu_1} + \frac{p_2}{\nu_2}\right)\beta S_0 = 4.6 > 1.$$

The discrete forms of the model in (6.2.1) with the boundary conditions in (6.2.2) give us the numerical results presented on Fig. 6.6.6–6.6.9. Fig. 6.6.6 and Fig. 6.6.7 show the dynamics of susceptible foxes, diffusing rabid foxes, and territorial rabid foxes at specific times. Surface plots of approximations $S_h(x,t)$, $R_{1,h}(x,t)$, and $R_{2,h}(x,t)$ to $S(x,t)$, $R_1(x,t)$, and $R_2(x,t)$ are presented on On Fig. 6.6.8. Fig. 6.6.9 depicts contour plots of susceptible foxes, diffusing rabid foxes, the territorial rabid foxes. The contour plots in Fig. 6.6.9 demonstrate that rabies spreads with asymptotic speed

$$c^{\diamond} \approx 73\,[\text{km/year}].$$

Figure 6.6.6: Approximations $S_h(x,t)$, $R_{1,h}(x,t)$, and $R_{2,h}(x,t)$ to $S(x,t)$, $R_1(x,t)$, and $R_2(x,t)$ at t=0, 20, 30, 90, 120, 180 when $p_1 = 0.3$ and $p_2 = 0.7$.

Figure 6.6.7: Approximations of fox population densities at different times when $p_1 = 0.3$ and $p_2 = 0.7$.
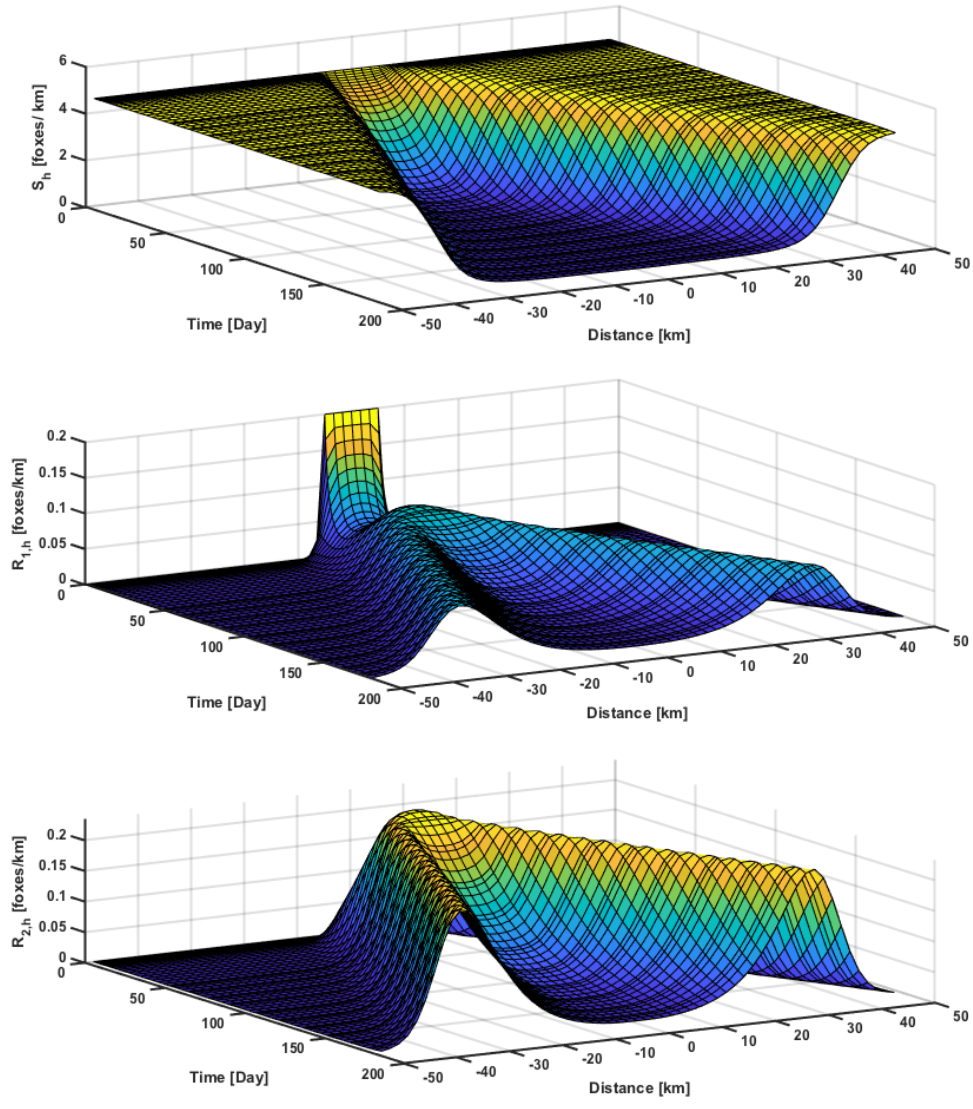
Figure 6.6.8: Surface plots of approximations $S_h(x,t)$, $R_{1,h}(x,t)$, and $R_{2,h}(x,t)$ to $S(x,t)$, $R_1(x,t)$, and $R_2(x,t)$ when $p_1 = 0.3$, $p_2 = 0.7$, and $N = 59$.

Figure 6.6.9: Contour plots of approximations $S_h(x,t)$ (top), $R_{1,h}(x,t)$ (middle), and $R_{2,h}(x,t)$ (bottom) to $S(x,t)$, $R_1(x,t)$, and $R_2(x,t)$ when $p_1 = 0.3$ and $p_2 = 0.7$.

6.6.3 III. $p_1 = 0.7$, $p_2 = 0.3$

The basic reproduction number of the rabies is

$$\mathcal{R}_0 = \left(\frac{p_1}{\nu_1} + \frac{p_2}{\nu_2}\right)\beta S_0 = 4.6 > 1.$$

The discrete forms of the model in (6.2.1) with the boundary conditions in (6.2.2) give us the numerical results presented on Fig. 6.6.10–6.6.13. Fig. 6.6.10 and Fig. 6.6.11 show the dynamics of susceptible foxes, diffusing rabid foxes, and territorial rabid foxes at specific times. Surface plots of approximations $S_h(x,t)$, $R_{1,h}(x,t)$, and $R_{2,h}(x,t)$ to $S(x,t)$, $R_1(x,t)$, and $R_2(x,t)$ are presented on On Fig. 6.6.12. Fig. 6.6.13 depicts contour plots of susceptible foxes, diffusing rabid foxes, the territorial rabid foxes. The contour plots in Fig. 6.6.13 demonstrate that rabies spreads with asymptotic speed

$$c^\diamond \approx 91 \, [\text{km/year}].$$

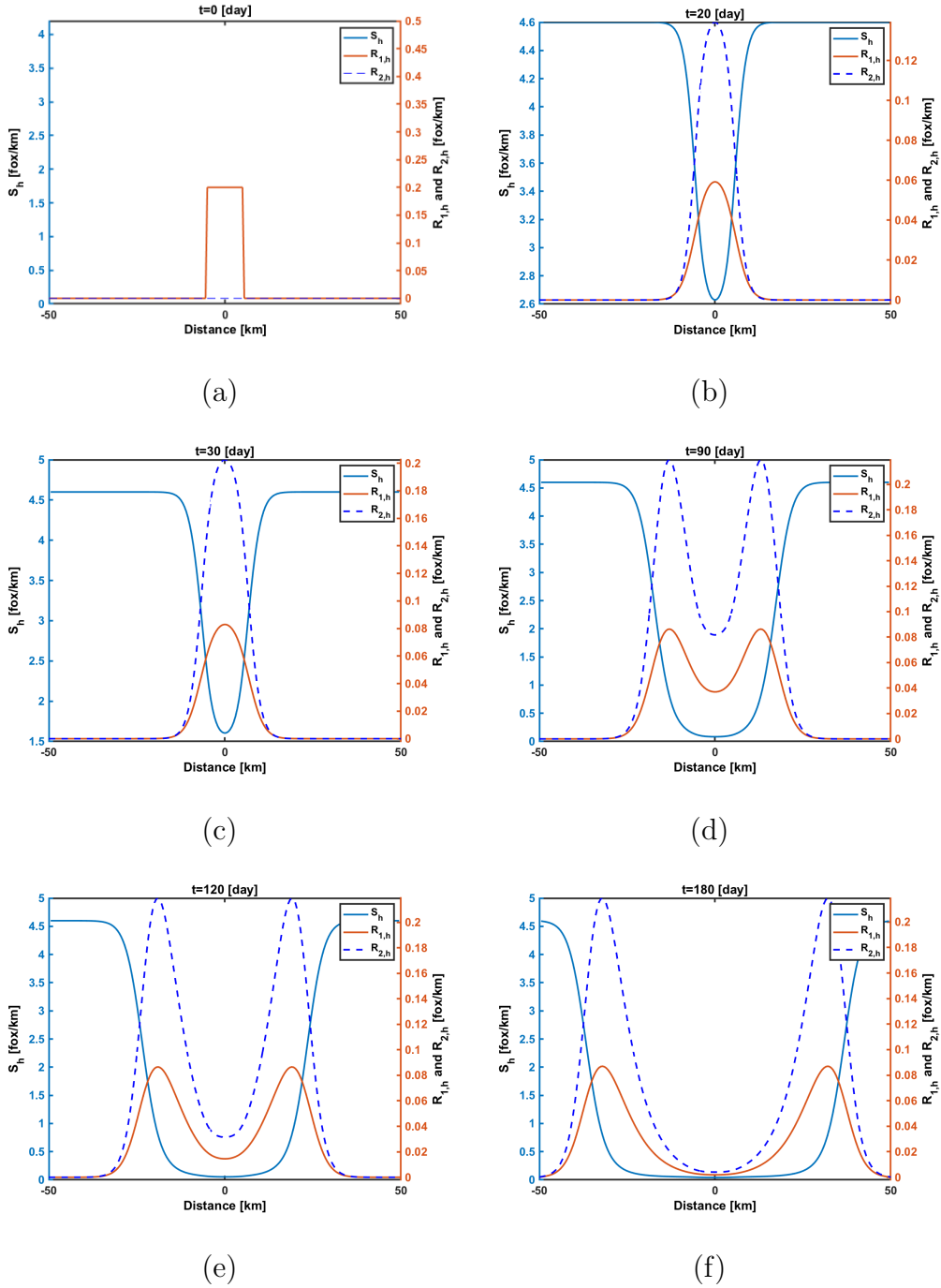Figure 6.6.10: Approximations $S_h(x,t)$, $R_{1,h}(x,t)$, and $R_{2,h}(x,t)$ to $S(x,t)$, $R_1(x,t)$, and $R_2(x,t)$ at t=0, 20, 30, 90, 120, 180 when $p_1 = 0.7$ and $p_2 = 0.3$.

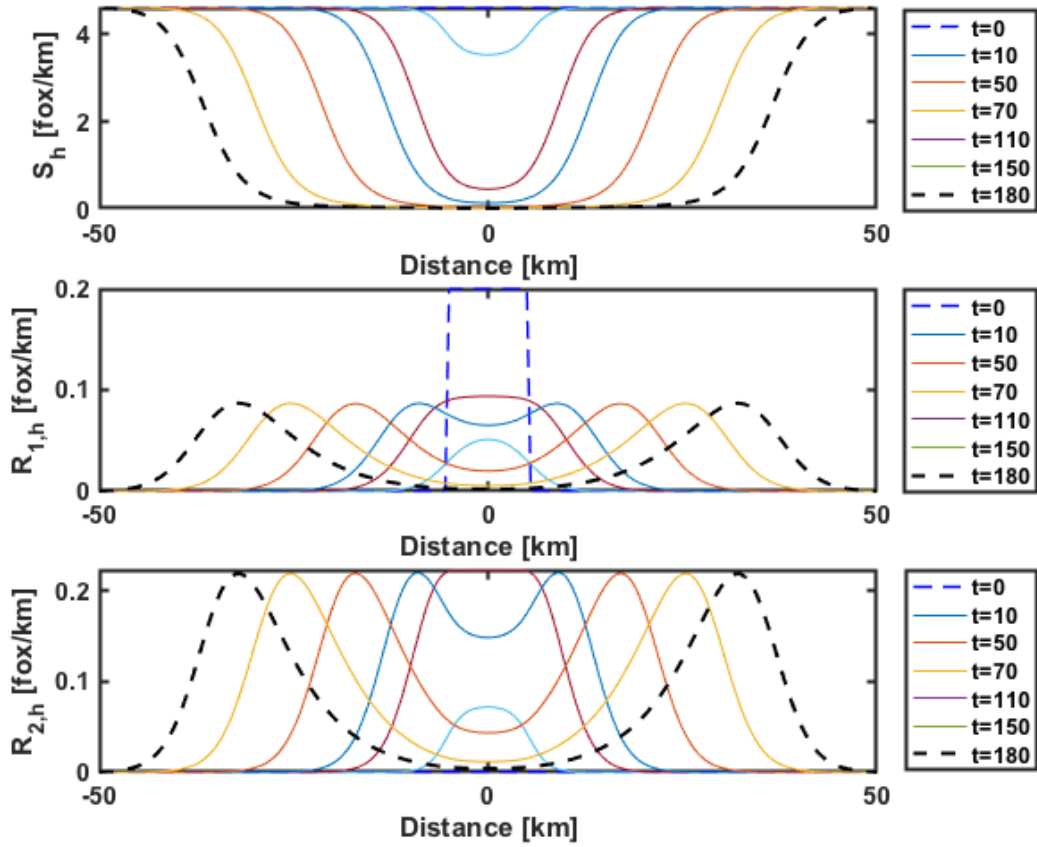Figure 6.6.11: Approximations of fox population densities at different times when $p_1 = 0.7$ and $p_2 = 0.3$.
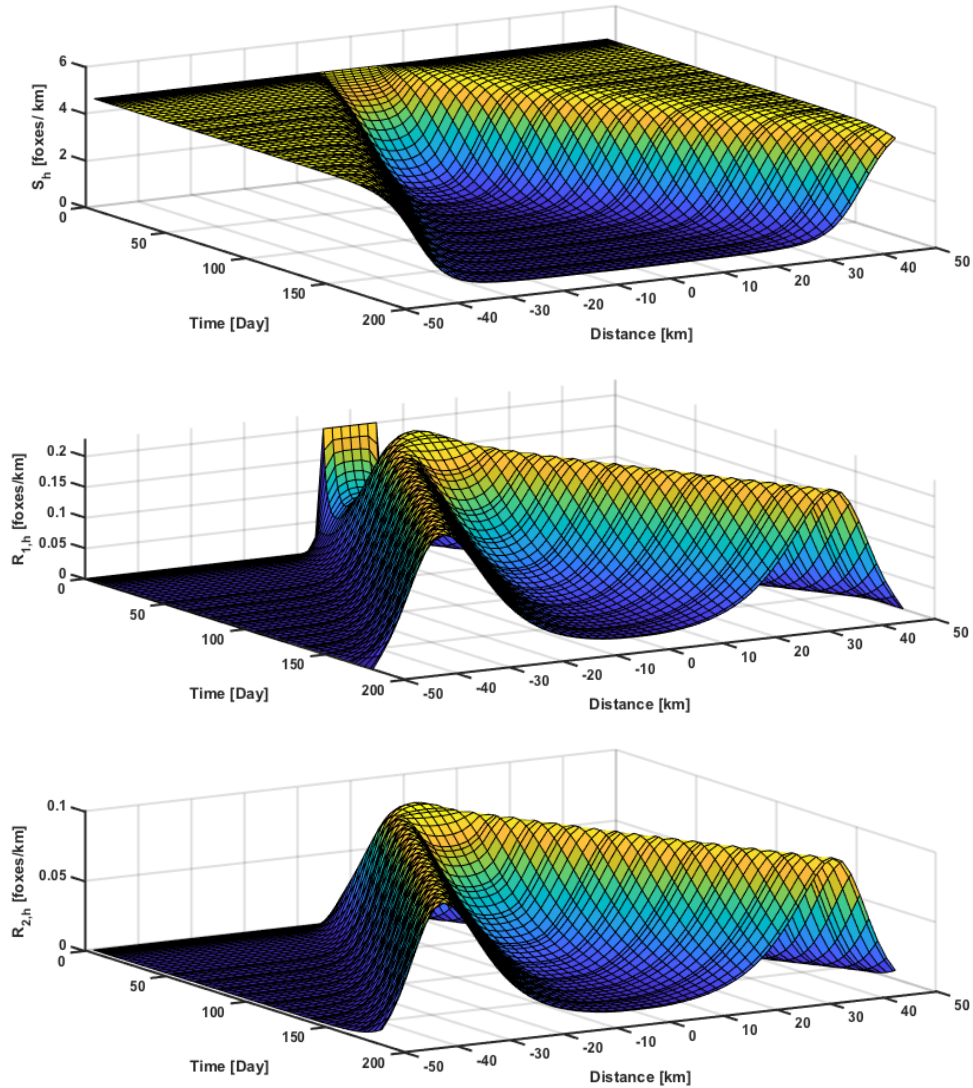
Figure 6.6.12: Surface plots of approximations $S_h(x,t)$, $R_{1,h}(x,t)$, and $R_{2,h}(x,t)$ to $S(x,t)$, $R_1(x,t)$, and $R_2(x,t)$ when $p_1 = 0.7$, $p_2 = 0.3$, and $N = 59$.
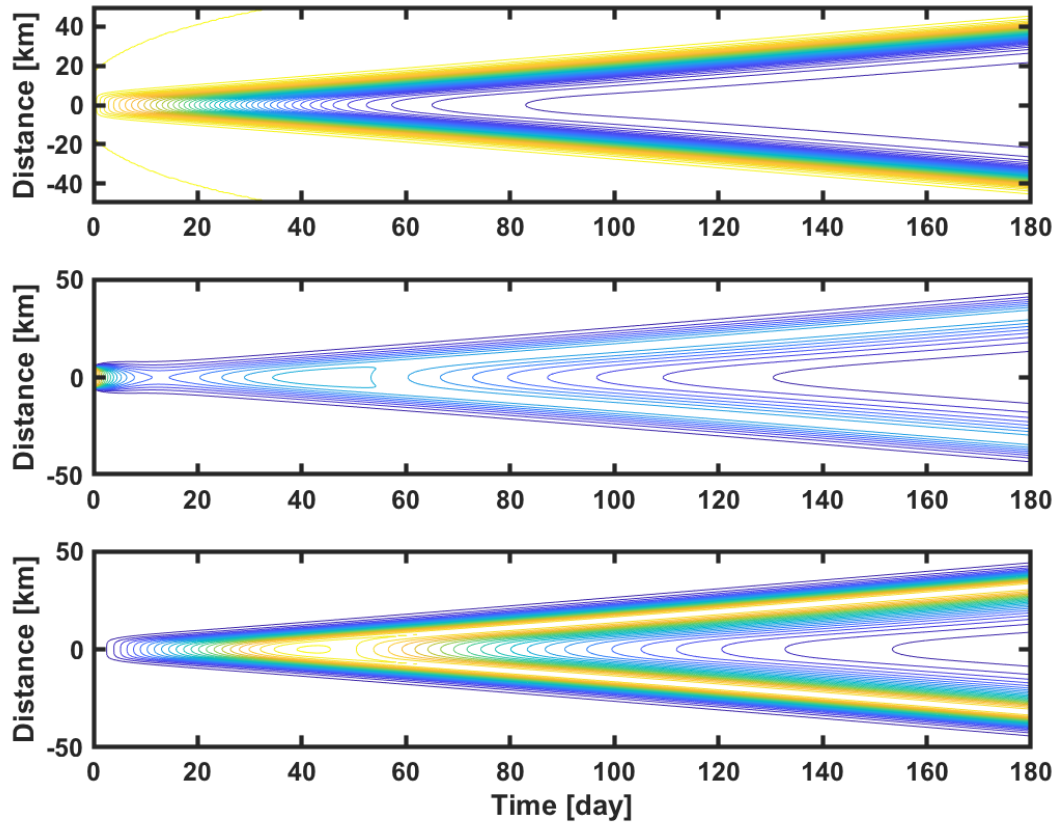
Figure 6.6.13: Contour plots of approximations $S_h(x,t)$ (top), $R_{1,h}(x,t)$ (middle), and $R_{2,h}(x,t)$ (bottom) to $S(x,t)$, $R_1(x,t)$, and $R_2(x,t)$ when $p_1 = 0.7$ and $p_2 = 0.3$.

6.6.4 IV. $p_1 = 1$, $p_2 = 0$

Since $p_1 = 1$, all rabid foxes diffuse. The basic reproduction number of the rabies

$$\mathcal{R}_0 = \left(\frac{p_1}{\nu_1} + \frac{p_2}{\nu_2}\right)\beta S_0 = 4.6 > 1.$$

The discrete forms of the model in (6.2.1) with the boundary conditions in (6.2.2) give us the numerical results presented on Fig. 6.6.14–6.6.17. Fig. 6.6.14 and Fig. 6.6.15 show the dynamics of susceptible foxes, diffusing rabid foxes, and territorial rabid foxes at specific times. Surface plots of approximations $S_h(x,t)$, $R_{1,h}(x,t)$, and $R_{2,h}(x,t)$ to $S(x,t)$, $R_1(x,t)$, and $R_2(x,t)$ are presented on On Fig. 6.6.16. Fig. 6.6.17 depicts contour plots of susceptible foxes, diffusing rabid foxes, the territorial rabid foxes. The contour plots in Fig. 6.6.17 demonstrate that rabies spreads with asymptotic speed

$$c^\diamond \approx 97\,[\text{km/year}].$$

We also calculate $c^\diamond$ using contour plots for different values of S_0 when all rabid foxes diffuse, i.e., $p_1 = 1$. These speeds are given in Table 6.2.

S_0 [fox/km]	$c^\diamond$ [km/year]	c^* [km/year]
1.5	30	33
2.0	45	50
2.5	61	64
3	73	76
4.6	97	105

Table 6.2: Comparison between $c^\diamond$ and c^* for various values of S_0 when the latent period has exponentially distributed length and $p_1 = 1$. Other numerical values of the parameters are in Table 4.1.
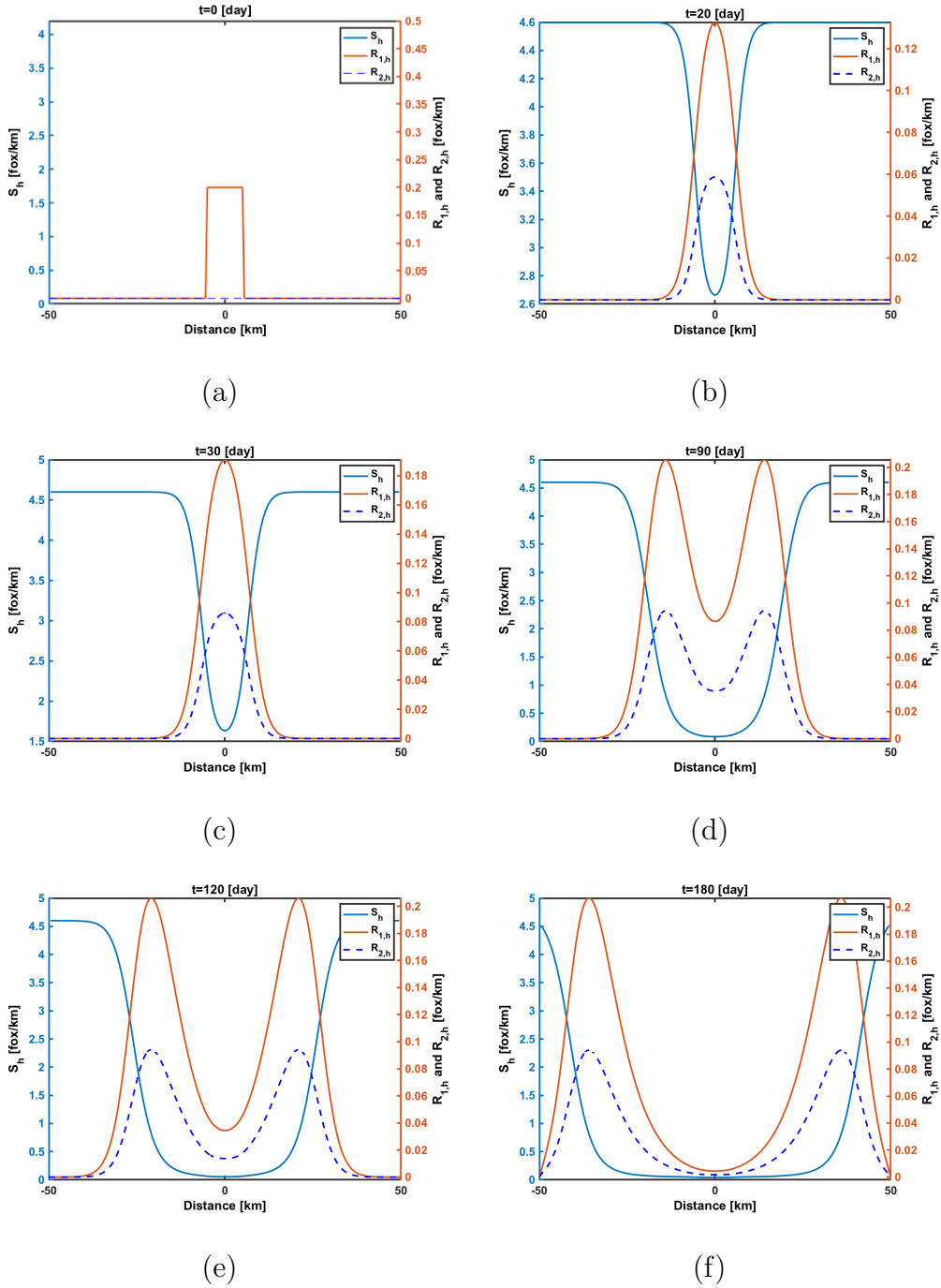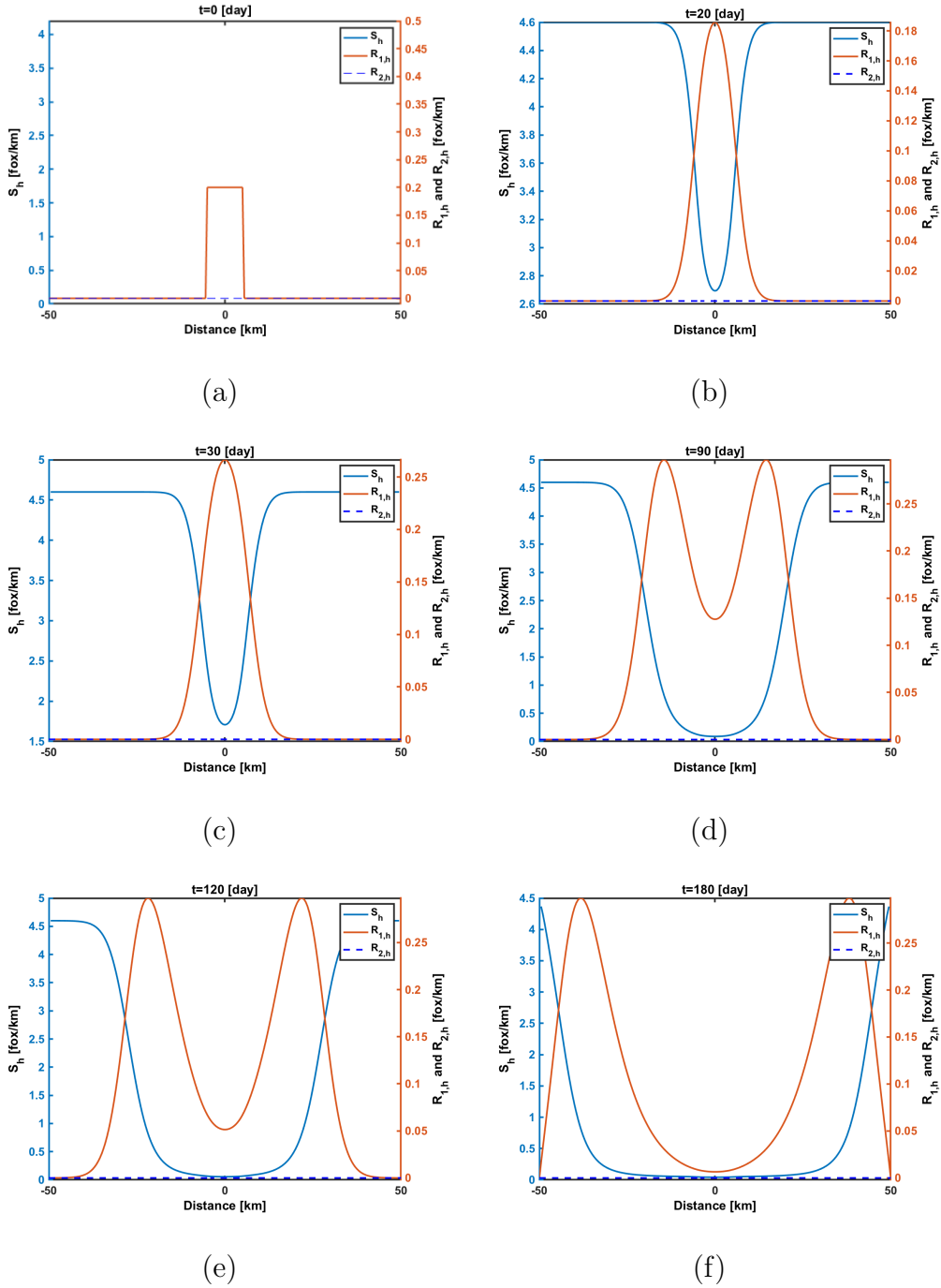
Figure 6.6.14: Approximations $S_h(x, t)$, $R_{1,h}(x, t)$, and $R_{2,h}(x, t)$ to $S(x, t)$, $R_1(x, t)$, and $R_2(x, t)$ at t=0, 20, 30, 90, 120, 180 when $p_1 = 1$ and $p_2 = 0$.
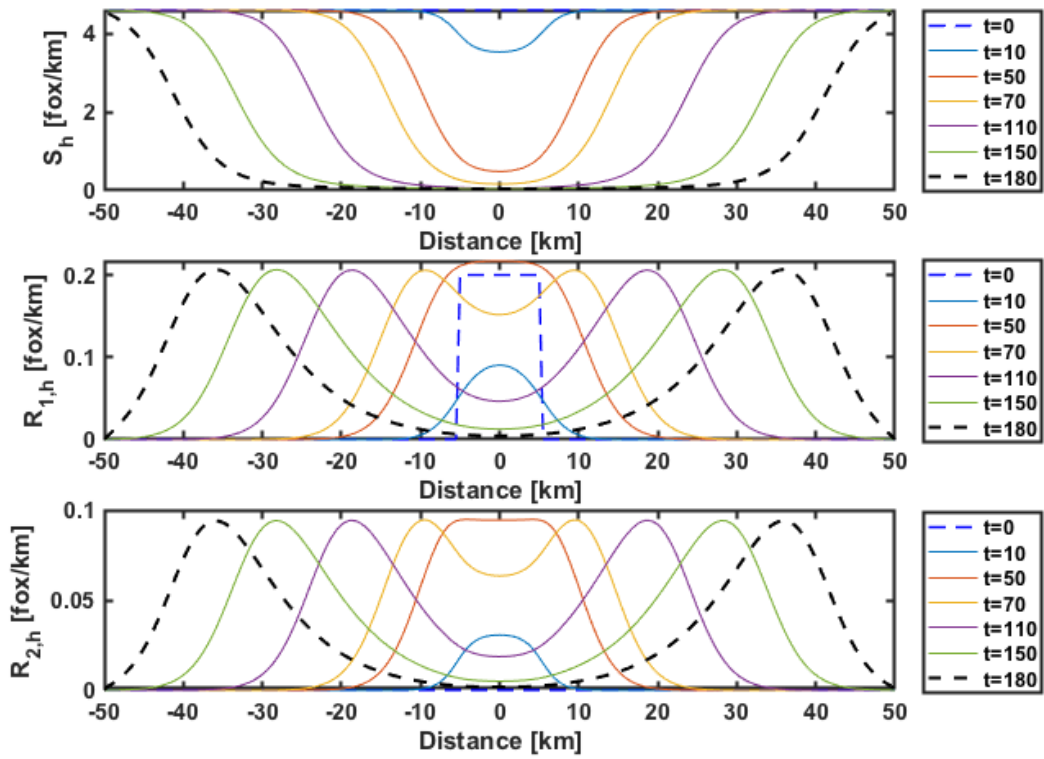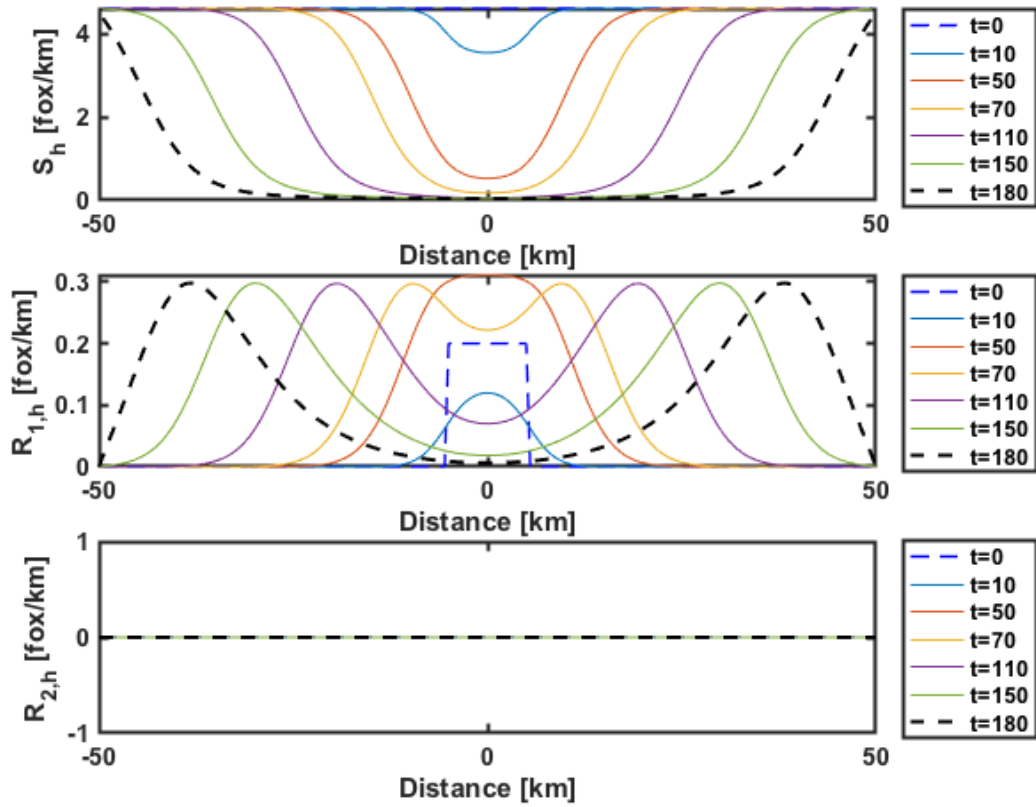
Figure 6.6.15: Approximations of fox population densities at different times when $p_1 = 1$ and $p_2 = 0$.

Figure 6.6.16: Surface plots of approximations $S_h(x,t)$, $R_{1,h}(x,t)$, and $R_{2,h}(x,t)$ to $S(x,t)$, $R_1(x,t)$, and $R_2(x,t)$ when $p_1 = 1$, $p_2 = 0$, and $N = 59$.
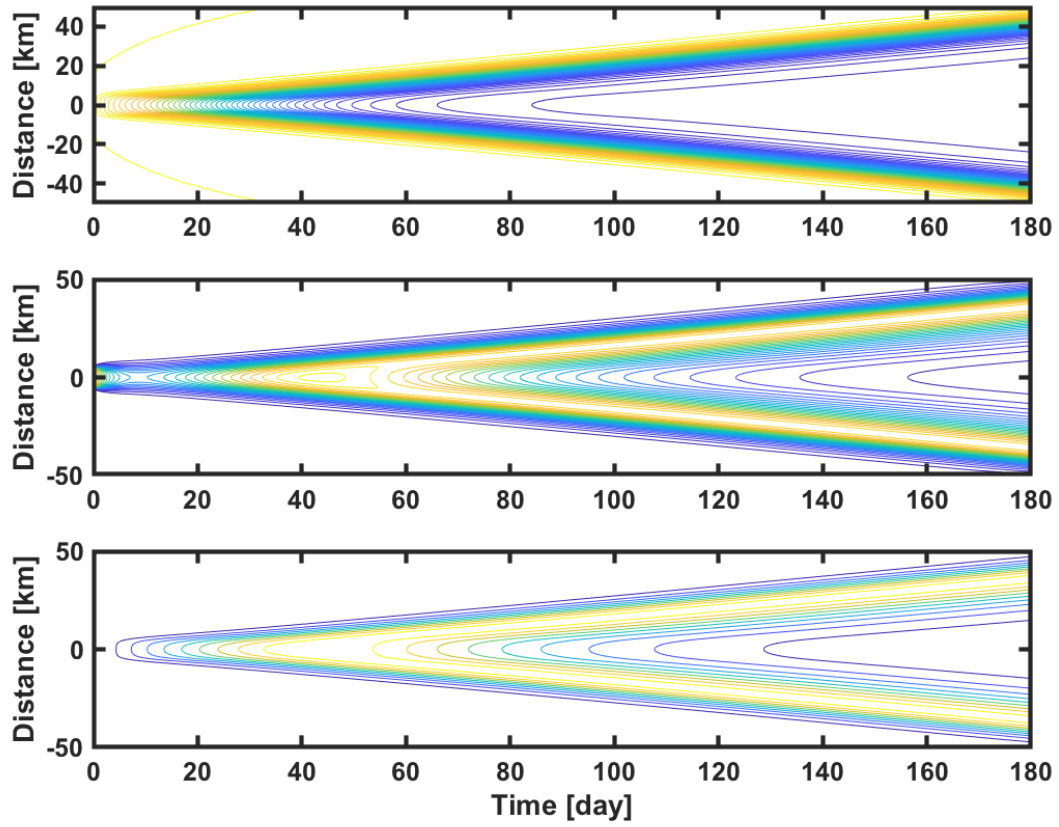
Figure 6.6.17: Contour plots of approximations $S_h(x,t)$ (top) and $R_{1,h}(x,t)$ (bottom) to $S(x,t)$ and $R_1(x,t)$ when $p_1 = 1$ and $p_2 = 0$.

6.6.5 V. $p_1 = 0$, $p_2 = 1$

In the fifth case, we assume all infectious foxes are territorial. The basic reproduction number of the rabies

$$\mathcal{R}_0 = \left(\frac{p_1}{\nu_1} + \frac{p_2}{\nu_2}\right)\beta S_0 = 4.6 > 1.$$

The discrete forms of the model in (6.2.1) with the boundary conditions in (6.2.2) give us the numerical results presented on Fig. 6.6.18–6.6.21. Fig. 6.6.18 and Fig. 6.6.19 show the dynamics of susceptible foxes, diffusing rabid foxes, and territorial rabid foxes at specific times. Surface plots of approximations $S_h(x,t)$, $R_{1,h}(x,t)$, and $R_{2,h}(x,t)$ to $S(x,t)$, $R_1(x,t)$, and $R_2(x,t)$ are presented on On Fig. 6.6.20. Fig. 6.6.21 depicts contour plots of susceptible foxes, diffusing rabid foxes, the territorial rabid foxes. The contour plots in Fig. 6.6.21 demonstrate that rabies spreads with asymptotic speed

$$c^\diamond \approx 61\,[\mathrm{km/year}].$$
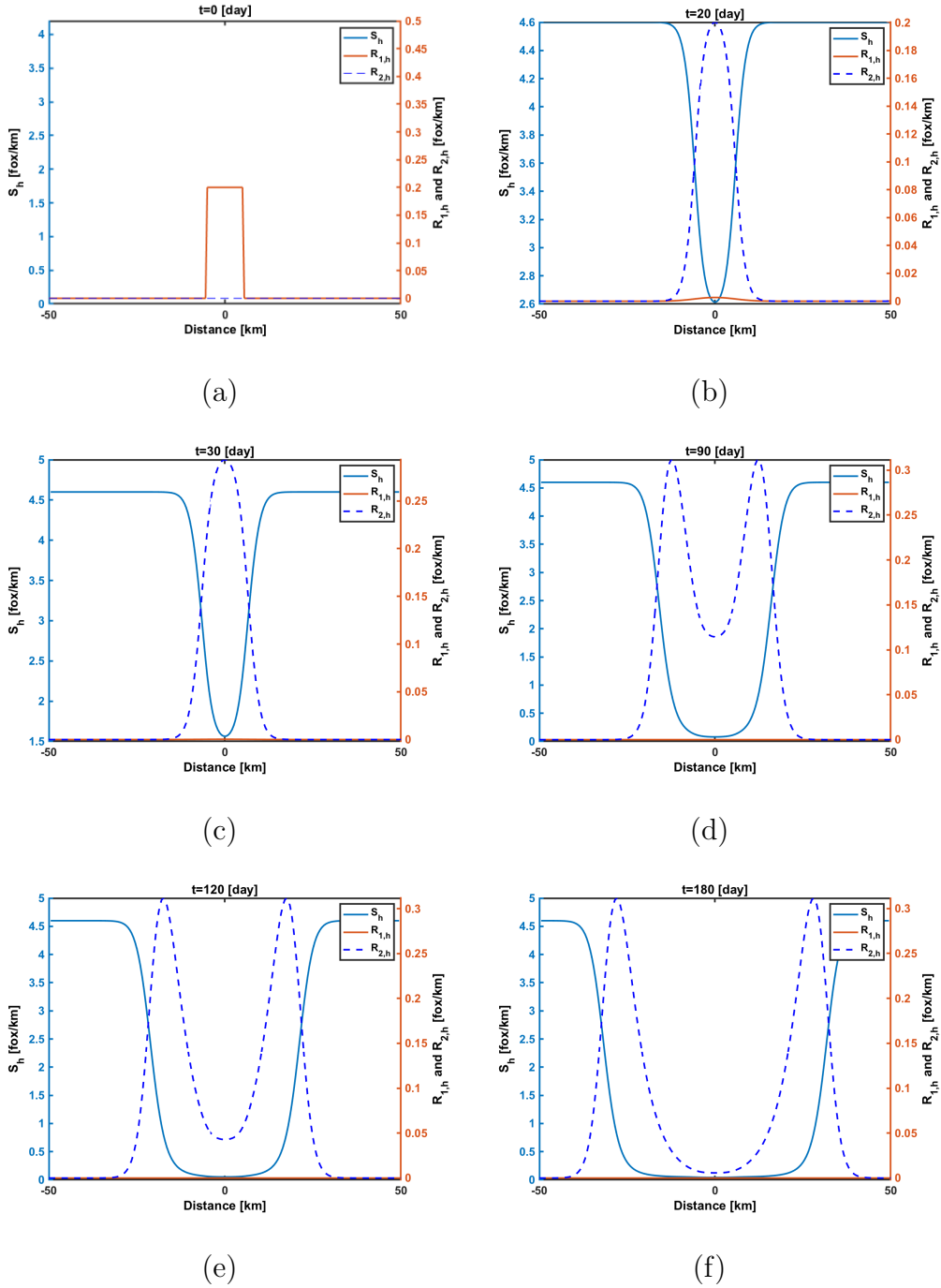
Figure 6.6.18: Approximations $S_h(x,t)$, $R_{1,h}(x,t)$, and $R_{2,h}(x,t)$ to $S(x,t)$, $R_1(x,t)$, and $R_2(x,t)$ at t=0, 20, 30, 90, 120, 180 when $p_1 = 0$ and $p_2 = 1$.

155
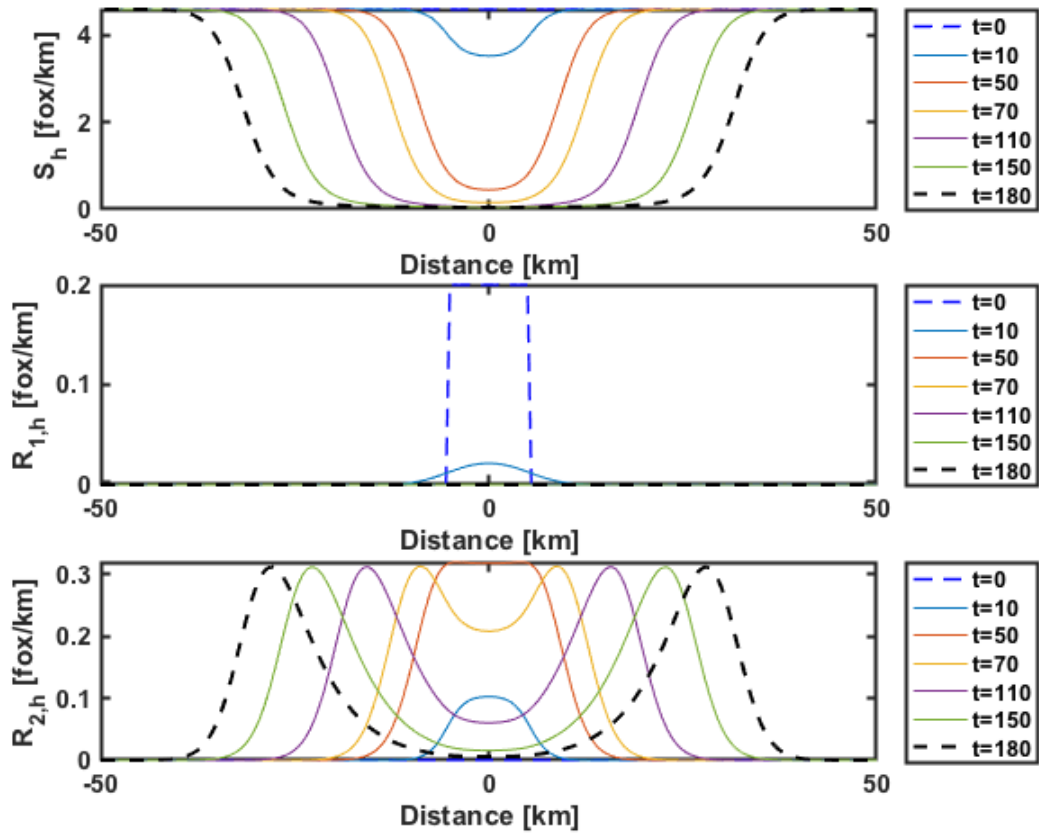
Figure 6.6.19: Approximations of fox population densities at different times when $p_1 = 0$ and $p_2 = 1$.
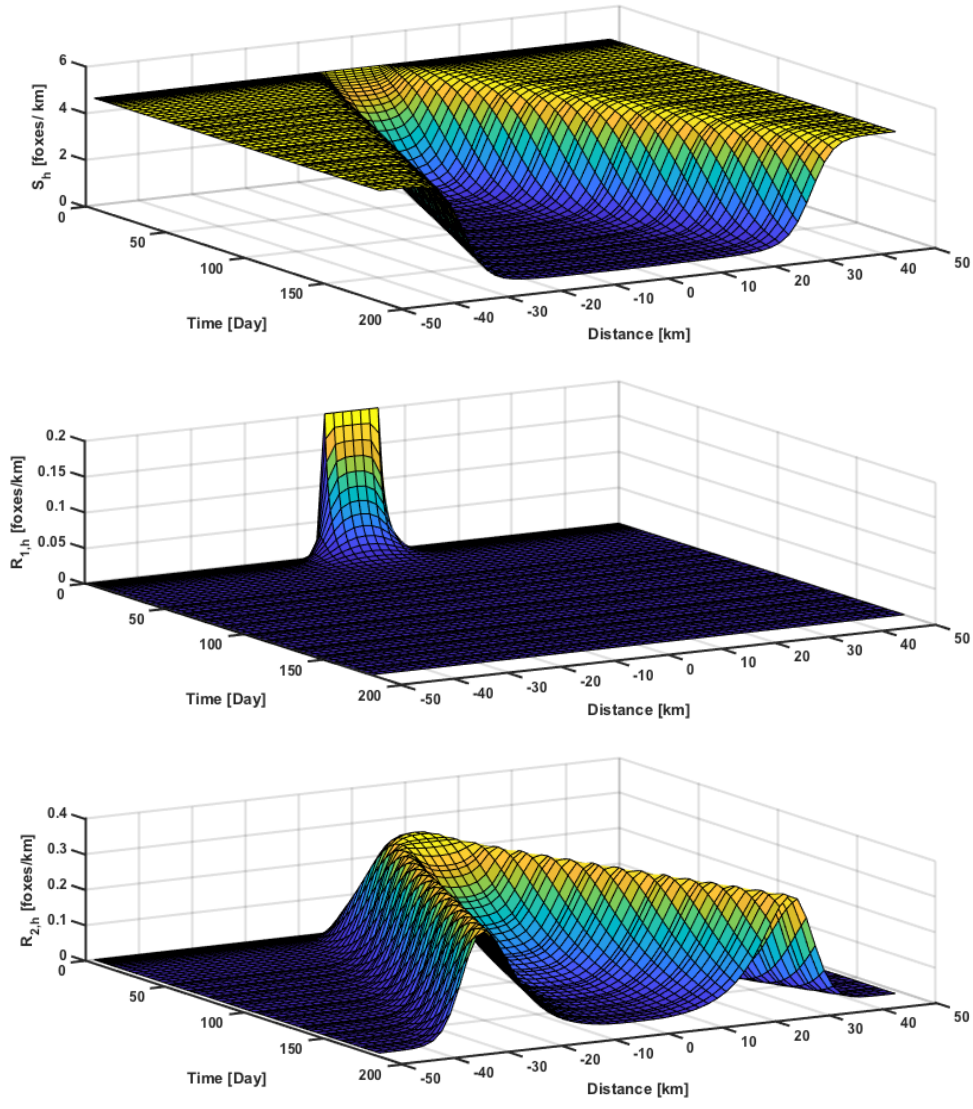
Figure 6.6.20: Surface plots of approximations $S_h(x,t)$, $R_{1,h}(x,t)$, and $R_{2,h}(x,t)$ to $S(x,t)$, $R_1(x,t)$, and $R_2(x,t)$ when $p_1 = 0$, $p_2 = 1$, and $N = 59$.
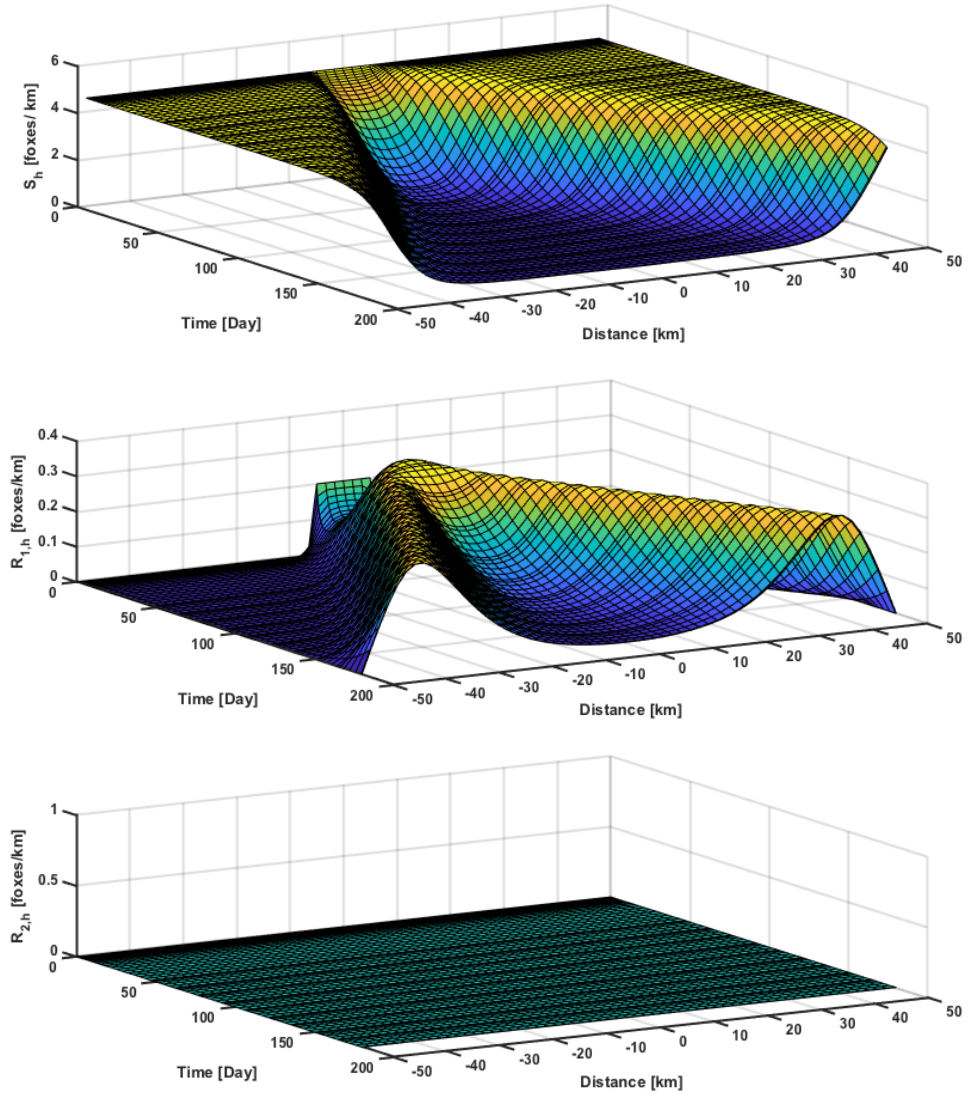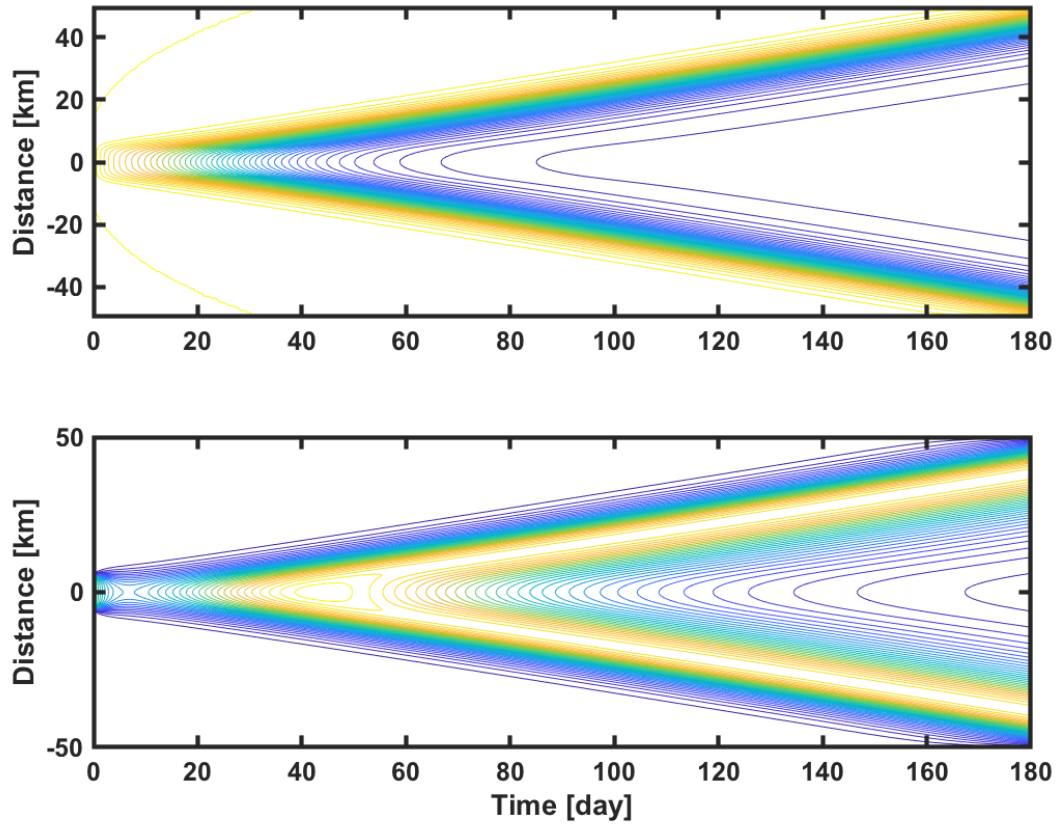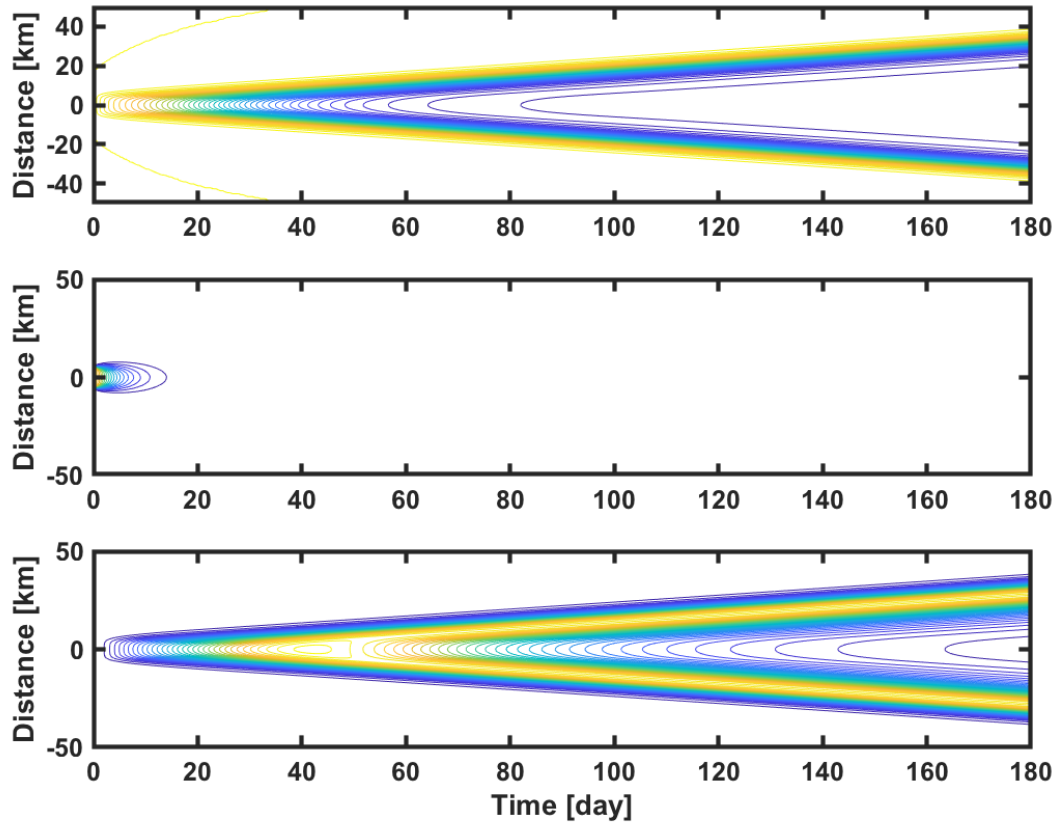
Figure 6.6.21: Contour plots of approximations $S_h(x,t)$ (top), $R_{1,h}(x,t)$ (middle), and $R_{2,h}(x,t)$ (bottom) to $S(x,t)$, $R_1(x,t)$, and $R_2(x,t)$ when $p_1 = 0$ and $p_2 = 1$.

6.7 Discussion and Conclusions

When the latent period is exponentially distributed, the unique solutions of the system (4.5.5) are

$$(c^*, \lambda) \approx (0.182245 \,[\text{km/day}], 0.773071) \approx (66.5195 \,[\text{km/year}], 0.773071)$$

when $p_1 = 0$,

$$(c^*, \lambda) \approx (0.235233 \,[\text{km/day}], 0.550237) \approx (85.86 \,[\text{km/year}], 0.550237)$$

when $p_1 = 0.3$,

$$(c^*, \lambda) \approx (0.253677 \,[\text{km/day}], 0.522531) \approx (92.592 \,[\text{km/year}], 0.522531)$$

when $p_1 = 0.5$,

$$(c^*, \lambda) \approx (0.268893 \,[\text{km/day}], 0.504089) \approx (98.146 \,[\text{km/year}], 0.504089)$$

when $p_1 = 0.7$, and

$$(c^*, \lambda) \approx (0.288236 \,[\text{km/day}], 0.484747) \approx (105.206 \,[\text{km/year}], 0.484747)$$

when $p_1 = 1$. The contour plots in Fig. 6.6.21, Fig. 6.6.9,Fig. 6.6.4,Fig. 6.6.13, and Fig. 6.6.17 demonstrate that

$$c^\diamond \approx 61 \,[\text{km/year}] \quad \text{when} \quad p_1 = 0,$$

$$c^\diamond \approx 73 \,[\text{km/year}] \quad \text{when} \quad p_1 = 0.3,$$

$$c^\diamond \approx 81 \,[\text{km/year}] \quad \text{when} \quad p_1 = 0.5,$$

$$c^\diamond \approx 91 \,[\text{km/year}] \quad \text{when} \quad p_1 = 0.7,$$

and

$$c^\diamond \approx 97 \,[\text{km/year}] \quad \text{when} \quad p_1 = 1.$$

Therefore, the asymptotic speeds c^*, which we get by solving the system (4.5.5), are quite close to asymptotic speeds $c^\diamond$, which we get from the contour plots. In addition, the asymptotic speeds c^* and $c^\diamond$ confirm that the epidemic model on a bounded domain Ω with Dirichlet boundary conditions shows a less severe epidemic outbreak than the epidemic model on $\mathbb{R}^n$, and the spread of the disease modeled on Ω is not as fast as the spread of the disease modeled on $\mathbb{R}^n$, as discussed in Section 3.6. Furthermore, the latent period with fixed length always gives the smallest spreading speeds (see Section 4.4.1).

(Murray *et al.* (1986); Murray and Seward (1992)) assume that all rabid foxes diffuse, foxes reproduce and die from natural causes, and rabid foxes exit the latent period with exponentially distributed length. Hence, we compare the asymptotic speeds in (Murray *et al.* (1986); Murray and Seward (1992)) to the speeds c^* that we have by solving the system (4.5.5) and to the speeds $c^\diamond$ that we have from contour plots when the latent period has exponentially distributed length and $p_1 = 1$. The unique solutions of the system (4.5.5) show that the asymptotic velocity of rabies spread $c^* \approx 105.2\,[\text{km/year}]$ with $S_0 = 4.6\,[\text{fox/km}]$ and $\beta = 73\,[\text{km}^2/\text{year}]$, while the speeds of initial waves are about $103\,[\text{km/year}]$ with carrying capacity of $4.6\,[\text{fox/km}^2]$ and $\beta = 80\,[\text{km}^2/\text{year}]$ in (Murray and Seward, 1992, Table 2) when there are no immune rabid foxes. Another remarkable thing is that the spreading speeds c^* and $c^\diamond$ that are in Table 4.2 with $\beta = 80\,[\text{km}^2/\text{year}]$ and Table 6.2 with $\beta = 73\,[\text{km/year}]$, respectively, compare quite well with the velocity of the epidemic in (Murray *et al.*, 1986, Table 3) and (Murray and Seward, 1992, Table 2) for $\beta = 80\,[\text{km}^2/\text{year}]$ and different values of S_0 and when there are no immune rabid foxes in (Murray and Seward (1992)). This suggests that ignoring the natural turnover of fox population does not have a huge impact on the speed of rabies spread.

The numerical simulations depict that the density of diffusing rabid foxes R_1 decays until some of the infected foxes exit the latent period with mean length θ, as shown in Fig. 6.6.1, Fig. 6.6.2, Fig. 6.6.3, Fig. 6.6.6, Fig. 6.6.7, Fig. 6.6.8, Fig. 6.6.10, Fig. 6.6.11, Fig. 6.6.12, Fig. 6.6.14, Fig. 6.6.15, Fig. 6.6.16, Fig. 6.6.18, Fig. 6.6.19, and Fig. 6.6.20. The decrease in the density of diffusing rabid foxes is because the death from rabies ν_1, which gives the rabid foxes as few as five days on average to live (Anderson *et al.* (1981); Murray *et al.* (1986); Murray (1989); Murray and Seward (1992)).

Since we assume there are no territorial rabid foxes initially at time zero, the density of territorial rabid foxes R_2 is zero, as presented in Fig. 6.6.1(a). When some of the infected foxes leave the latent period, we see R_2 grows again before it loses some of its members with rate ν_2, as demonstrated in Fig. 6.6.1, Fig. 6.6.2, Fig. 6.6.3, Fig. 6.6.6, Fig. 6.6.7, Fig. 6.6.8, Fig. 6.6.10, Fig. 6.6.11, Fig. 6.6.12, Fig. 6.6.14, Fig. 6.6.15, Fig. 6.6.16, Fig. 6.6.18, Fig. 6.6.19, and Fig. 6.6.20.

Since, by assumptions, no foxes are born and infected foxes cannot recover and become susceptible again, the densities of susceptible foxes continue to decrease, as shown in Fig. 6.6.1, Fig. 6.6.2, Fig. 6.6.3, Fig. 6.6.6, Fig. 6.6.7, Fig. 6.6.8, Fig. 6.6.10, Fig. 6.6.11, Fig. 6.6.12, Fig. 6.6.14, Fig. 6.6.15, Fig. 6.6.16, Fig. 6.6.18, Fig. 6.6.19, and Fig. 6.6.20.

The embedded pair of Runge-Kutta methods was implemented in a variable step-size environment with the estimates of the local discretization errors computed according to the formula

$$\text{EST}(t_{n+1}) = \left\| \hat{y}_{n+1} - y_h(t_{n+1}) \right\|_2,$$

161

(see Section 6.4). The stepsize h_n from t_n to $t_{n+1} = t_n + h_n$ for $n = 0, 1, \ldots,$ is accepted if

$$\text{EST}(t_{n+1}) \leq \text{TOL},$$

but if

$$\text{EST}(t_{n+1}) > \text{TOL},$$

the stepsize is rejected, and the computations are repeated with a halved stepsize $h_n/2$. Fig. 6.6.5 show that almost all rejected steps occur for $\text{Tol} = 10^{-3}$.

Chapter 7

DISCUSSION AND CONCLUSIONS

Previous mathematical models have assumed that either all rabid foxes are territorial (van den Bosch *et al.* (1990)) or all rabid foxes diffuse (Källén *et al.* (1985); Liu (2013); Murray *et al.* (1986); Murray (1989); Murray and Seward (1992); Ou and Wu (2006)). Differently from these studies, our model assumes that some of the rabid foxes essentially behave like susceptible and exposed foxes and keep their home-ranges, while the other rabid foxes loose the attachment to their home-range and disperse by diffusion. We call the first ones *territorial rabid* foxes and the second ones *diffusing (wandering (Toma and Andral (1977))) rabid* foxes. The question we are trying to answer is how the partition of rabid foxes into territorial and diffusing rabid foxes influences the spreading speed of fox rabies. To tackle this question analytically, we reduced (2.2.2) to a single nonlinear integral equation

$$u(x,t) = u_0(x,t) + \int_0^t \int_{\mathbb{R}^n} \xi(r, |x - z|) F(u(z, t - s)) dz dr.$$

u is the cumulative rate of rabid foxes meet the susceptible foxes. The integral kernel ξ essentially consists of convolutions of the movements of territorial foxes about the center of their home-range κ_1 and of the fundamental solution of the partial differential operator $\partial_t - D\Delta_x$ and of Υ, and $F(u) = 1 - e^{-u}$. u_0 combines the various initial conditions, and it is given in (2.3.37). Biologically, ξ is the contribution of diffusing and territorial rabid foxes to the infection rate.

For special form of (2.2.2) with arbitrary distributed length of the latent state, we show that space-time Laplace transform is given by

$$\Xi(c, \lambda) = \left(-\frac{p_1 \hat{\kappa}_1(\lambda)}{\nu_1 + \lambda c - \lambda^2 D} - \frac{p_2 (\hat{\kappa}_1(\lambda))^2}{\nu_2 + \lambda c} \right) \beta S_0 \int_0^\infty e^{-\lambda c r} d\Upsilon(r)$$

if $\nu_1 + \lambda c - \lambda^2 D > 0$, otherwise $\Xi(c, \lambda) = \infty$, where

$$\hat{\kappa}_1(\lambda) = \int_{\mathbb{R}^n} e^{-\lambda z_1} \kappa_1(z) dz.$$

For the numerical computation of c^*, we assume that the movements of territorial foxes about the center of their home-range are normally distributed, i.e.,

$$\kappa_1(z) = \Gamma_n(z, b) = (4\pi b)^{-n/2} e^{-|z|^2/(4b)}, \qquad z \in \mathbb{R}^n, \tag{7.0.1}$$

where $|\cdot|$ is the Euclidean norm on $\mathbb{R}^n$, $b > 0$, and Γ_n is the fundamental solutions associated with the differential operator $\partial_t - \Delta_x$ for n space dimensions. Then $\hat{\kappa}_1(\lambda) = e^{b\lambda^2}$ (see, Proposition 2.5.1), and

$$\Xi(c, \lambda) = -\left(\frac{p_1 e^{b\lambda^2}}{\nu_1 + \lambda c - \lambda^2 D} + \frac{p_2 e^{2b\lambda^2}}{\nu_2 + \lambda c}\right) \beta S_0 \int_0^\infty e^{-\lambda c r} d\Upsilon(r).$$

The *basic reproduction number of rabies* is given by

$$\mathcal{R}_0 = \Xi(0, 0) = \left(\frac{p_1}{\nu_1} + \frac{p_2}{\nu_2}\right) \beta S_0.$$

If $\mathcal{R}_0 > 1$, the asymptotic spreading speed $c^* > 0$ is uniquely determined as the solution of the system

$$\Xi(c^*, \lambda) = 1, \quad \frac{d}{d\lambda} \Xi(c^*, \lambda) = 0. \tag{7.0.2}$$

Otherwise, if $\mathcal{R}_0 \leq 1$, we define $c^* := 0$.

(Sartwell (1950, 1966)) concludes that the log-normal distribution perfectly fits the incubation periods of various infectious diseases. (Farrell (2017); Farrell *et al.* (2018)) discuss the distribution of the time between infection and disease induced death for data from infection experiments involving tiger salamander larvae and ranavirus. They find that log-normal distribution fits these data better than Gamma and Weibull distributions (Farrell (2017); Farrell *et al.* (2018)). The length of the latent period has been also described by a distribution of fixed length or by Gamma distribution

in many works (see, e.g., Beretta and Kuang (2001); Jones *et al.* (2012, 2013, 2016)).

When we assume the length of the latent period is log-normally distributed, we obtain

$$\Xi(c, \lambda) = \left(\frac{p_1 e^{\lambda^2 b}}{\nu_1 + \lambda c - \lambda^2 D} + \frac{p_2 e^{2\lambda^2 b}}{\nu_2 + \lambda c} \right) \beta S_0$$

$$\left(\frac{1}{\sqrt{2\pi}} \int_0^\infty \exp\left(\frac{-1}{2} t^2 \right) \left(e^{-\lambda cme^{-\sigma t}} + e^{-\lambda cme^{\sigma t}} \right) dt \right). \tag{7.0.3}$$

Therefore, as $\sigma \to 0$, we have

$$\Xi(c, \lambda) \to \left(\frac{p_1 e^{\lambda^2 b}}{\nu_1 + \lambda c - \lambda^2 D} + \frac{p_2 e^{2\lambda^2 b}}{\nu_2 + \lambda c} \right) \beta S_0 e^{-\lambda cm}.$$

So, as $\sigma \to 0$ in (7.0.3), the length of the latent period converges to a distribution of fixed length m. On the other hand, when we assume that the latent periods is Gamma distribution, we obtain

$$\Xi(c, \lambda) = \left(\frac{p_1 \beta S_0 e^{b\lambda^2}}{\nu_1 + \lambda c - \lambda^2 D} + \frac{p_2 \beta S_0 e^{2b\lambda^2}}{\nu_2 + \lambda c} \right) \left(\frac{h}{h + \tau \lambda c} \right)^h. \tag{7.0.4}$$

If $h = 1$, the length of the latent period is exponentially distributed. In addition, $\left(\frac{h}{h+\tau\lambda c} \right)^h \to e^{-\lambda c\tau}$ as $h \to \infty$. Therefore, as $h \to \infty$ in (7.0.4), the length of the latent period converges to a distribution of fixed length τ.

Rabies moves with speed ranging from 30 to 60 [km/year] according to (van den Bosch *et al.* (1990); Toma and Andral (1977)) and from 20 to 60 [km/year] according to (Lloyd (1980)). A study performed in three areas in the state of Baden-Württemberg (Germany) from January 1963 to March 31, 1971, found that the center of the frontwave moved at about 27 [km/year] (Bögel *et al.* (1976)) while the mean distance of new cases ahead of the frontline within a month was approximately 4.8 [km] (Bögel *et al.* (1976); Moegle *et al.* (1974)). We calculated c^* numerically for latent periods of fixed length and Gamma distributed length by solving (7.0.2).

When we assume the latent periods is Gamma distribution with $h = 1$, the length of the latent period is exponentially distributed, and c^* will be

$$(c^*, \lambda) \approx (0.182245 \, [\text{km/day}], 0.773071) \approx (66.5195 \, [\text{km/year}], 0.773071)$$

when $p_1 = 0$,

$$(c^*, \lambda) \approx (0.235233 \, [\text{km/day}], 0.550237) \approx (85.86 \, [\text{km/year}], 0.550237)$$

when $p_1 = 0.3$,

$$(c^*, \lambda) \approx (0.253677 \, [\text{km/day}], 0.522531) \approx (92.592 \, [\text{km/year}], 0.522531)$$

when $p_1 = 0.5$,

$$(c^*, \lambda) \approx (0.268893 \, [\text{km/day}], 0.504089) \approx (98.146 \, [\text{km/year}], 0.504089)$$

when $p_1 = 0.7$, and

$$(c^*, \lambda) \approx (0.288236 \, [\text{km/day}], 0.484747) \approx (105.206 \, [\text{km/year}], 0.484747)$$

when $p_1 = 1$. A plot of c^* versus p_1 when the length of the latent period is exponentially distributed is given in Fig. 4.10.1. Also, when the length of the latent period is exponentially distributed, the asymptotic speeds $c^\diamond$ that we get from the contour plots in Chapter 6 demonstrate that

$$c^\diamond \approx 61 \, [\text{km/year}] \quad \text{when} \quad p_1 = 0,$$

$$c^\diamond \approx 73 \, [\text{km/year}] \quad \text{when} \quad p_1 = 0.3,$$

$$c^\diamond \approx 81 \, [\text{km/year}] \quad \text{when} \quad p_1 = 0.5,$$

$$c^\diamond \approx 91 \, [\text{km/year}] \quad \text{when} \quad p_1 = 0.7,$$

and

$$c^\diamond \approx 97\,[\text{km/year}] \quad \text{when} \quad p_1 = 1.$$

For $h = 5$, we obtain

$$(c^*, \lambda) \approx (0.0958041\,[\text{km/day}], 1.01582) \approx (34.9685\,[\text{km/year}], 1.015829)$$

when $p_1 = 0$,

$$(c^*, \lambda) \approx (0.140481\,[\text{km/day}], 0.558589) \approx (51.2754\,[\text{km/year}], 0.558589)$$

when $p_1 = 0.3$,

$$(c^*, \lambda) \approx (0.151185\,[\text{km/day}], 0.537392) \approx (55.1824\,[\text{km/year}], 0.537392)$$

when $p_1 = 0.5$,

$$(c^*, \lambda) \approx (0.159787\,[\text{km/day}], 0.523766) \approx (58.3222\,[\text{km/year}], 0.523766)$$

when $p_1 = 0.7$, and

$$(c^*, \lambda) \approx (0.170476\,[\text{km/day}], 0.510225) \approx (62.2238\,[\text{km/year}], 0.510225)$$

when $p_1 = 1$.

When the latent period has a fixed length, we have following speeds

$$(c^*, \lambda) \approx (0.0774794\,[\text{km/day}], 1.20104) \approx (28.28\,[\text{km/year}], 1.20104)$$

when $p_1 = 0$,

$$(c^*, \lambda) \approx (0.121047\,[\text{km/day}], 0.566099) \approx (44.1821\,[\text{km/year}], 0.566099)$$

when $p_1 = 0.3$,

$$(c^*, \lambda) \approx (0.129782\,[\text{km/day}], 0.548928) \approx (47.3705\,[\text{km/year}], 0.548928)$$

when $p_1 = 0.5$,

$$(c^*, \lambda) \approx (0.136702 \,[\text{km/day}], 0.538601) \approx (49.8961 \,[\text{km/year}], 0.538601)$$

when $p_1 = 0.7$, and

$$(c^*, \lambda) \approx (0.145169 \,[\text{km/day}], 0.529397) \approx (52.9868 \,[\text{km/year}], 0.529397)$$

when $p_1 = 1$. A plot of c^* versus p_1 when the latent period has a fixed length is presented on Fig. 4.10.1. On the other hand, the numerical simulations for this case show that

$$c^\diamond \approx 26 \,[\text{km/year}] \quad \text{when} \quad p_1 = 0,$$

$$c^\diamond \approx 37 \,[\text{km/year}] \quad \text{when} \quad p_1 = 0.3,$$

$$c^\diamond \approx 43 \,[\text{km/year}] \quad \text{when} \quad p_1 = 0.5,$$

$$c^\diamond \approx 45 \,[\text{km/year}] \quad \text{when} \quad p_1 = 0.7,$$

and

$$c^\diamond \approx 47 \,[\text{km/year}] \quad \text{when} \quad p_1 = 1.$$

It seems that as $h \to \infty$, the more realistic speeds we have. Also, we conclude that the asymptotic speeds c^*, which we get by solving the system (7.0.2), are quite close to asymptotic speeds $c^\diamond$, which we get from the contour plots. In addition, the asymptotic speeds c^* and $c^\diamond$ confirm that the epidemic model on a bounded domain Ω with Dirichlet boundary conditions shows a less severe epidemic outbreak than the epidemic model on $\mathbb{R}^n$, and the spread of the disease modeled on Ω is not as fast as the spread of the disease modeled on $\mathbb{R}^n$, as discussed in Section 3.6. The reason for choosing Dirichlet boundary conditions has also discussed in Section 3.6. Another important observation is that the numerical results confirm for the spreading speeds c^* and $c^\diamond$ that the latent period with fixed length gives the smallest spreading

speeds, as discussed in Section 4.4.1. In addition, the numerical simulations confirm that Theorem 2.6.5 in Section 2.6.3 holds.

Our results show that the spreading speed is a decreasing function of the mean length of the latent period τ, and the spreading speed is an increasing function of β, S_0, D and the durations $1/\nu_i$ of the infectious periods for diffusing and territorial rabid foxes and also of b if κ_1 is given by (7.0.1). b is a measure of how far territorial foxes move away from the center of their home-ranges if this distance is normally distributed ($2b$ is the variance of the normal distribution in each direction), and S_0 is the initial value of the density of susceptible foxes. A study in three areas in the state of Baden-Württemberg of Germany finds that the mean distance of new rabies cases ahead of the monthly determined rabies frontline very slightly decreases if the hunting indicator of the fox density (foxes shot per km^2 per year) increases (Bögel *et al.*, 1976, Table 3). The likely explanation is that the home-range size is not independent of fox density but depends on it in a decreasing fashion as observed in (Sargeant (1972)) and assumed in (van den Bosch *et al.*, 1990, Sec.7.2) where b is assumed to be proportional to $1/S_0$ (van den Bosch *et al.*, 1990, (7.6)). Differently from (Bögel *et al.* (1976); van den Bosch *et al.* (1990)), we assume b and S_0 to be independent.

Also, c^* increases as we increase the proportion of wandering rabid foxes p_1 when the latent period has fixed length, exponentially distributed length, and Gamma distributed length, as demonstrated by the numerical simulations shown in Fig. 4.10.1. The last happens for what we believe is a realistic choice of parameters b and D. In general, the monotone behavior of c^* as a function of p_1 depends on the relation between b and D, as depicted in Fig. 4.8.1. In addition, the numerical results in Fig. 4.8.1 suggest that $\mathcal{R}_0$ may not need to be very close to 1 for the results in Theorem 4.8.1 to hold.

169

Hence, to impede the spread of the disease when latent periods have arbitrary distributed length, we need to decrease the values of β, S_0, b, and D and increase the rates of Υ, ν_1, and ν_2 based on the theorems discussed in Section 2.6.3 and Fig. 4.10.1.

When $p_1 = 0$, all rabid foxes are territorial, and the asymptotic speeds of spread c^* that we obtain by solving the system (4.4.7) for a latent period of fixed length can be compared with the asymptotic speeds in (van den Bosch et $al.$ (1990)). There are differences in some assumptions and in the determination of parameters, though; for instance, it is assumed in (van den Bosch et $al.$ (1990)) that the sizes of the home-ranges decrease with fox density while we assume them to be independent. For a fox population density S_0 of 4.6 [fox/km], we obtain an asymptotic speed of rabies spread $c^* \approx 28.3$ [km/year], while (van den Bosch et $al.$, 1990, Fig.7) shows an asymptotic speed of about 33 [km/year] when $S_0 = 4.6$ [fox/km^2]. Furthermore, for this case, the asymptotic speed of rabies spread c^* compares quite well with the observed speeds about 27 [km/year] in (Bögel et $al.$ (1976)) and from 20 to 60 [km/year] according to (Lloyd (1980)).

The rabies model in (Murray, 1989, Sec.20.4) (Murray et $al.$ (1986); Murray and Seward (1992)) incorporates the turnover of the fox population into an epidemic model with diffusing rabid foxes and exponentially distributed length of the latent period. Newborn foxes enter the population at a fixed per capita rate and all foxes are subject to a natural density-dependent per capita death rate. We have not included this turnover in order to be able to analyze a model that includes territorial rabid foxes. In reality, fox reproduction is seasonal. In Britain, e.g., most cubs are born between mid-March and mid-April (Lloyd, 1980, p.115) as it seems to be the case in continental Europe (Toma and Andral, 1977, III.A.2). In order to have an educated guess about the impact of population turnover, we look at the special case of our model with the same assumptions, including that susceptible and incubating foxes stay at

the center of their home-ranges all the time. In Table 4.2, we compare spreading speeds that have been determined by numerically solving system (4.5.5) with the minimum wave speeds calculated in (Murray, 1989, Sec.20.4) (Murray *et al.* (1986); Murray and Seward (1992)). The results agree qualitatively and are not too different quantitatively. For instance, the unique solutions of the system (4.5.5) show that the asymptotic velocity of rabies spread $c^* \approx 112$ [km/year] with $S_0 = 4.6$ [fox/km] as in Table 4.2, while the speeds of initial waves are about 103 [km/year] with carrying capacity of 4.6 [fox/km^2] as in (Murray and Seward, 1992, Table 2) when there are no immune rabid foxes. A non-spatial endemic model with non-seasonal births is compared to one with birth pulses in (Roberts and Kao (1998)), and though there are differences in the solution behavior they are not too pronounced. This gives us encouraging results that the qualitative behavior of the spreading speed is not affected by the omission of population turnover and that the quantitative results contain useful information as long as they are seen as approximations in Table 4.2.

REFERENCES

Alanazi, K. M., Z. Jackiewicz and H. R. Thieme, "Numerical simulations of spread of rabies in a spatially distributed fox population", Mathematics and Computers in Simulation (to appear) (2018a).

Alanazi, K. M., Z. Jackiewicz and H. R. Thieme, "Spreading speeds of rabies with territorial and diffusing rabid foxes", (preprint) (2018b).

Alanazi, K. M., Z. Jackiewicz and H. R. Thieme, "Numerical simulations of the spread of rabies in two-dimensional space", Applied Numerical Mathematics **135**, 87–98 (2019).

Anderson, R. M., H. C. Jackson, R. M. May and A. M. Smith, "Population dynamics of fox rabies in Europe", Nature **289**, 765–771 (1981).

Andral, L., M. Artois, M. F. A. Aubert and J. Blancou, "Radio-pistage de renards enrages", Comparative Immunology, Microbiology and Infectious Diseases **5**, 285–291 (1982).

Arizona Department of Health Services, AZ Rabies Control and Bite Management Manual, URL https://www.azdhs.gov/preparedness/epidemiology-disease-control/rabies/ (Accessed: Aug. 2018).

Arizona Department of Health Services, Rabies in AZ, URL https://www.azdhs.gov/preparedness/epidemiology-disease-control/rabies/ (Accessed: Aug. 2018).

Aronson, D. G., *Nonlinear Diffusion*, vol. 14, chap. The asymptotic speed of propagation of a simple epidemic, pp. 1–23 (Pitman London, 1977).

Aronson, D. G. and H. F. Weinberger, *Partial Differential Equations and Related Topics*, vol. 446, chap. Nonlinear diffusion in population genetics, combustion, and nerve pulse propagation, pp. 5–49 (Springer, 1975).

Aronson, D. G. and H. F. Weinberger, "Multidimensional nonlinear diffusion arising in population dynamics", Adv. in Math. **30**, 33–76 (1978).

Artois, M., M. Aubert, J. Blancou, J. Barrat, M. L. Poulle and P. Stahl, "écologie des comportements de transmission de la rage", Annales de recherches vétérinaires **22**, 163–172 (1991).

Bartoszewski, Z. and Z. Jackiewicz, "Stability analysis of two-step Runge-Kutta methods for delay differential equations", Computers and Mathematics with Applications **44**, 83–93 (2002).

Bartoszewski, Z. and Z. Jackiewicz, "Derivation of continuous explicit two-step Runge-Kutta methods of order three", Journal of computational and applied mathematics **205**, 764–776 (2007).

Bartoszewski, Z. and Z. Jackiewicz, "Construction of highly stable parallel two-step Runge–Kutta methods for delay differential equations", Journal of computational and applied mathematics **220**, 257–270 (2008).

Bartoszewski, Z., Z. Jackiewicz and Y. Kuang, "Numerical solution of threshold problems in epidemics and population dynamics", Journal of Computational and Applied Mathematics **279**, 40–56 (2015).

Beaumont, C., J.-B. Burie, A. Ducrot and P. Zongo, "Propagation of salmonella within an industrial hens house", SIAM Journal on Applied Mathematics **72**, 1113–1148 (2012).

Bellen, A. and M. Zennaro, *Numerical Methods for Delay Differential Equations* (Oxford Science Publications, Clarendon Press, Oxford, 2003).

Beretta, E. and Y. Kuang, "Modeling and analysis of a marine bacteriophage infection with latency", Nonlinear Analysis RWA , 35–74 (2001).

Beyer, H. L., K. Hampson, T. Lembo, S. Cleaveland, M. Kaare and D. Haydon, "Metapopulation dynamics of rabies and the efficacy of vaccination", Proceedings of the Royal Society B **278**, 2182–2190 (2011).

Bhattacharya, P. K. and P. Burman, *Theory and Methods of Statistics* (Academic Press, 2016).

Bögel, K., H. Moegle, F. Knorpp, A. Arata, K. Dietz and P. Diethelm, "Characteristics of the spread of a wildlife rabies epidemic in Europe", Bull. World Health. Organ. **54**, 433–447 (1976).

Borchering, R. K., H. Liu, M. C. Steinhaus, C. L. Gardner and Y. Kuang, "A simple spatiotemporal rabies model for skunk and bat interaction in northeast texas", Journal of Theoretical Biology **314**, 16–22 (2012).

Bouin, E., J. Garnier, C. Henderson and F. Patout, "Thin front limit of an integro-differential fisher-kpp equation with fat-tailed kernels", SIAM Journal on Mathematical Analysis **50**, 3, 3365–3394 (2018).

Bourhy, H., B. Kissi, L. Audry, M. Smreczak, M. Sadkowska-Todys, K. Kulonen, N. Tordo, J. F. Zmudzinski and E. C. Holmes, "Ecology and evolution of rabies virus in Europe", Journal of General Virology **80**, 2545–2557 (1999).

Centers for Disease Control and Prevention (CDC), Rabies, URL https://www.cdc.gov/rabies/ (Accessed: Jul. 2015).

Childs, J. E. and L. A. Real, *Rabies*, chap. Epidemiology-4, pp. 123–199 (Academic Press, 2007), 2nd edn.

D'Ambrosio, R. and Z. Jackiewicz, "Continuous two-step Runge-Kutta methods for ordinary differential equations", Numerical Algorithms **54**, 169–193 (2010).

D'Ambrosio, R. and Z. Jackiewicz, "Construction and implementation of highly stable two-step continuous methods for stiff differential systems", Math. Comput. Simulation **81**, 1707–1728 (2011).

David, J. M., L. Andral and M. Artois, "Computer simulation model of the epizootic disease of vulpine rabies", Ecological Modelling **15**, 107–125 (1982).

Diekmann, O., "Thresholds and travelling waves for the geographical spread of infection", J. Math. Biol. **6**, 109–130 (1978).

Diekmann, O., "Run for your life. a note on the asymptotic speed of propagation of an epidemic", J. Diff. Eqns **33**, 58–73 (1979).

Ducrot, A. and P. Magal, "Travelling wave solutions for an infection-age structured model with diffusion", Proceedings of the Royal Society of Edinburgh Section A: Mathematics **139**, 3, 459–482 (2009).

Fang, J., X. Yu and X. Q. Zhao, "Traveling waves and spreading speeds for time-space periodic monotone systems", J. Funct. Anal. **272**, 4222–4262 (2017).

Farrell, A., *Prey-predator-parasite: An ecosystem model with fragile persistence*, Ph.D. thesis, Arizona State University (2017).

Farrell, A. P., J. P. Collins, A. L. Greer and H. R. Thieme, "Times from infection to disease-induced death and their influence on final population sizes after epidemic outbreaks", Bull. Math. Biol. **80**, 1937–1961 (2018).

Florida Department of Health, Rabies, URL http://www.floridahealth.gov/diseases-and-conditions/rabies/ (Accessed: Aug. 2018).

Garnier, J., "Accelerating solutions in integro-differential equations", SIAM Journal on Mathematical Analysis **43**, 4, 1955–1974 (2011).

Garnier, J. and M. A. Lewis, "Expansion under climate change: the genetic consequences", Bulletin of mathematical biology **78**, 11, 2165–2185 (2016).

Garroni, M. G. and J. L. Menaldi, *Green Functions for Second Order Parabolic Integro-Differential Problems* (Longman Scientific & Technical, Essex, 1992).

Gladwell, I., L. F. Shampine and R. W. Brankin, "Automatic selection of the initial step size for an ode solver", J. Comput. Appl. Math. **18**, 175–192 (1987).

Gourley, S. A. and Y. Kuang, "A delay reaction-diffusion model of the spread of bacteriophage infection", SIAM Journal on Applied Mathematics **65**, 550–566 (2004).

Hairer, E., S. P. Norsett and G. Wanner, *Solving Ordinary Differential Equations I: Nonstiff Problems* (Springer-Verlag, New York, 1993).

Hass, C. C. and J. W. Dragoo, "Rabies in hooded and striped skunks in Arizona", Journal of Wildlife Diseases **42**, 825–829 (2005).

Holmala, K. and K. Kauhala, "Ecology of wildlife rabies in Europe", Mammal Review **36**, 17–36 (2006).

Jackiewicz, Z., H. Liu, B. Li and Y. Kuang, "Numerical simulations of traveling wave solutions in a drift paradox inspired diffusive delay population model", Math. Comput. Simulation **96**, 95–103 (2014).

Jackiewicz, Z., M. Rahman and B. D. Welfert, "Numerical solution of a fredholm integro-differential equation modelling neural networks", Applied Numerical Mathematics **56**, 423–432 (2006).

Jackiewicz, Z. and M. Zennaro, "Variable-step explicit two-step Runge-Kutta methods", Mathematics of computation **59**, 421–438 (1992).

Jackiewicz, Z. and B. Zubik-Kowal, "Spectral collocation and waveform relaxation methods for nonlinear delay partial differential equations", Applied Numerical Mathematics **56**, 433–443 (2006).

Jackiewicz, Z. and B. Zubik-Kowal, "Discrete variable methods for delay-differential equations with threshold-type delays", Journal of Computational and Applied Mathematics **228**, 514–523 (2009).

Jones, D. A., G. Röst, H. L. Smith and H. R. Thieme, "On spread of phage infection of bacteria in a petri dish", SIAM J. Applied Math. **72**, 670–688 (2012).

Jones, D. A., H. L. Smith and H. R. Thieme, "Spread of viral infection of immobilized bacteria", Networks and Heterogeneous Media **8**, 327–342 (2013).

Jones, D. A., H. L. Smith and H. R. Thieme, "Spread of phage infection of bacteria in a petri dish", Discrete Contin. Dyn. Syst. Ser. B **21**, 471–496 (2016).

Källén, A., P. Arcuri and J. D. Murray, "A simple model for the spatial spread and control of rabies", J. Theoret. Biol. **116**, 377–393 (1985).

Kot, M., *Elements of mathematical ecology* (Cambridge University Press, 2001).

Leslie, M. J., S. Messenger, R. E. Rhohde, J. Smith, R. Cheshier, C. Cathleen and C. E. Rupprecht, "Bat-associated rabies virus in skunks", Emerging Infectious Diseases **12**, 1274–1277 (2006).

Liang, X. and X. Q. Zhao, "Asymptotic speeds of spread and traveling waves for monotone semiflows with applications", Comm. Pure Appl. Math. **60**, 1–40 (2007).

Liu, H., *Spatial spread of rabies in wildlife*, Ph.D. thesis, Arizona State University (2013).

Lloyd, H. G., *The Red Fox* (Batsford LTD, London, 1980).

Macdonald, D. W., *Rabies and wildlife: A biologist's perspective* (Oxford University Press, New York, 1980).

Metz, A. J. J., D. Mollison and F. van den Bosch, *The geometry of ecological interactions: simplifying spatial complexity*, chap. The dynamics of invasion waves (Cambridge University Press, 2000).

Moegle, H., F. Knorpp, K. Bögel, A. Arata, D. K and P. Diethelm, "Zur epidemiologie der wildtiertollwut", Zbl. Vet. Med. B **21**, 647–659 (1974).

Murray, J. D., *Mathematical Biology* (Springer, Berlin Heidelberg, 1989).

Murray, J. D., S. E. A and D. L. Brown, "On the spatial spread of rabies among foxes", Proceedings of the Royal Society of London. Series B, Biological Sciences **229**, 111–150 (1986).

Murray, J. D. and W. L. Seward, "On the spatial spread of rabies among foxes with immunity", Journal of Theoretical Biology **156**, 327–348 (1992).

Ou, C. and J. Wu, "Spatial spread of rabies revisited: influence of age-dependent diffusion on nonlinear dynamics", SIAM J. Appl. Math. **67**, 138–163 (2006).

Owren, B. and M. Zennaro, "Order barriers for continuous explicit Runge-Kutta methods", Mathematics of Computation **56**, 645–661 (1991).

Owren, B. and M. Zennaro, "Continuous explicit Runge-Kutta methods", in "Institute of mathematics and its applications conference", vol. 39, pp. 97–105 (Oxford University Press, New York, 1992a).

Owren, B. and M. Zennaro, "Derivation of efficient, continuous, explicit Runge-Kutta methods", SIAM Journal on Scientific and Statistical Computing **13**, 1488–1501 (1992b).

Rass, L. and J. Radcliffe, *Spatial Deterministic Epidemics, American Mathematical Society* (Providence, 2003).

Recktenwald, G. W., *Numerical Methods with MATLAB : Implementations and Applications* (Prentice Hall, New Jersey, 2000).

Rees, E., B. Pond, R. Tinline and D. Bélanger, *Advances in Virus Research*, vol. 79, chap. Understanding effects of barriers on the spread and control of rabies, pp. 421–447 (Elsevier, 2011).

Roberts, M. G. and R. R. Kao, "The dynamics of an infectious disease in a population with birth pulses", Mathematical biosciences **149**, 1, 23–36 (1998).

Ruan, S., *Mathematics for Life Science and Medicine*, chap. Spatial-temporal dynamics in nonlocal epidemic models, pp. 97–122 (Springer, 2007), 2nd edn.

Ruan, S., "Modeling the transmission dynamics and control of rabies in China", Math. Biosci. **286**, 65–93 (2017).

Rudin, W., *Real and complex analysis* (Tata McGraw-Hill Education, 1966).

Sargeant, A. B., "Red fox spatial characteristics in relation to waterfowl predation", The Journal of Wildlife Management pp. 225–236 (1972).

Sartwell, P. E., "The distribution of incubation periods of infectious diseases", American Journal of Hygiene **51**, 310–318 (1950).

Sartwell, P. E., "The incubation period and the dynamics of infectious disease", American Journal of Epidemiology **83**, 204–318 (1966).

Schiesser, W. E., *Partial differential equation analysis in biomedical engineering: case studies with MATLAB* (Cambridge University Press, Cambridge, 2013).

Schiesser, W. E. and G. W. Griffiths, *A Compendium of Partial Differential Equation Models Method of Lines Analysis with Matlab* (Cambridge University Press, Cambridge, 2009).

Shampine, L. F., I. Gladwell and S. Thompson, *Solving ODEs with matlab* (Cambridge University Press, Cambridge, 2003).

Shampine, L. F. and M. K. Gordon, *Computer Solution of Ordinary Differential Equations: The Initial Value Problem* (W. H. Freeman, San Francisco, 1975).

Shigesada, N., K. Kawasaki and H. F. Weinberger, "Spreading speeds of invasive species in a periodic patchy environment: effects of dispersal based on local information and gradient-based taxis", Japan J. Indust. Appl. Math. **32**, 675–705 (2015).

Shu, H., X. Pan, X.-S. Wang and J. Wu, "Traveling waves in epidemic models: Non-monotone diffusive systems with non-monotone incidence rates", Journal of Dynamics and Differential Equations pp. 1–19 (2018).

Smith, G. C. and D. Wilkinson, "Modeling control of rabies outbreaks in red fox populations to evaluate culling, vaccination, and vaccination combined with fertility control", Journal of wildlife diseases **39**, 278–286 (2003).

Smith, H. L. and H. R. Thieme, "Strongly order preserving semiflows generated by functional differential", J. Differential Equations **93**, 332—363 (1991).

Smith, H. L. and H. R. Thieme, *Dynamical Systems and Population Persistence* (American Mathematical Society, 2011).

Smith, H. L. and H. R. Thieme, "Persistence of bacteria and phages in a chemostat", Journal of mathematical biology **64**, 951–979 (2012).

Sparkes, J., S. McLeod, G. Ballard, P. J. S. Fleming, G. Körtner and W. Y. Brown, "Rabies disease dynamics in naïve dog populations in australia", Preventive Veterinary Medicine **131**, 127–136 (2016).

Stanoyevitch, A., *Introduction to Numerical Ordinary and Partial Differential Equations Using MATLAB* (John Wily and Sons, Inc., Hoboken, New Jersey, 2005).

Thieme, H. R., "A model for the spatial spread of an epidemic", J. Math. Biology **4**, 337–351 (1977).

Thieme, H. R., "Asymptotic estimates of the solutions of nonlinear integral equations and asymptotic speeds for the spread of populations", J. Reine Angew. Math. **306**, 94–121 (1979a).

Thieme, H. R., "On a class of hammerstein integral equations", Manuscripta mathematica **1**, 49–84 (1979b).

Thieme, H. R., "Some mathematical considerations of how to stop the spatial spread of a rabies epidemic", in "Biological Growth and Spread", pp. 310–319 (Lecture Notes in Biomathematics 38. Springer, 1980).

Thieme, H. R., *Mathematics in Population Biology* (Princeton University Press, Princeton, 2003).

Thieme, H. R., "Book report on Rass and Radcliffe (2003)", Math. Biosci. **202**, 218–225 (2006).

Thieme, H. R. and X. Q. Zhao, "A nonlocal delayed and diffusive predator–prey model", Nonlinear Anal.: Real World Appl. **2**, 145–160 (2001).

Thieme, H. R. and X. Q. Zhao, "Asymptotic speeds of spread and traveling waves for integral equations and delayed reaction-diffusion models", Journal of Differential Equations **195**, 430–470 (2003).

Tian, B. and R. Yuan, "Traveling waves for a diffusive seir epidemic model with standard incidences", Science China Mathematics **60**, 5, 813–832 (2017).

Toma, B. and L. Andral, "Epidemiology of fox rabies", in "Advances in virus research", vol. 21, pp. 1–36 (1977).

van den Bosch, F., J. A. J. Metz and O. Diekmann, "The velocity of spatial population expansion", J. Math. Biol. **28**, 529–565 (1990).

Vial, F., S. Cleaveland, D. Rasmussen and D. T. Haydon, "Development of vaccination strategies for the management of rabies in African wild dogs", Biological Conservation **131**, 180–192 (2006).

Wang, H., "Spreading speeds and traveling waves for non-cooperative reaction diffusion systems", Journal of Nonlinear Science **21**, 747–783 (2011).

Wang, Z.-C. and J. Wu, "Travelling waves of a diffusive kermack–mckendrick epidemic model with non-local delayed transmission", Proceedings of the Royal Society of London A: Mathematical, Physical and Engineering Sciences **466**, 2113, 237–261 (2010).

Weinberger, H. F., M. A. Lewis and B. Li, "Anomalous spreading speeds of cooperative recursion systems", Journal of mathematical biology **55**, 2, 207–222 (2007).

White, P. C. L., S. Harris and G. C. Smith, "Fox contact behaviour and rabies spread: a model for the estimation of contact probabilities between urban foxes at different population densities and its implications for rabies control in britain", Journal of Applied Ecology **32**, 693–706 (1995).

World Health Organization (WHO), Rabies, URL http://www.who.int/newsroom/fact-sheets/detail/rabies (Accessed: Jul. 2015).

World Health Organization (WHO), What is rabies, URL http://www.who.int/rabies/about/en/ (Accessed: Jul. 2015).

Wu, R. and X. Q. Zhao, "Propagation dynamics for a spatially periodic integrodifference competition model", J. Differential Equations **264**, 6507–6534 (2018).

Xu, Z., "Traveling waves in an seir epidemic model with the variable total population", Discrete & Continuous Dynamical Systems-B **21**, 10, 3723–3742 (2016).

Zhang, J., Z. Jin, G. Sun, X. Sun and S. Ruan, "Spatial spread of rabies in China", J. Appl. Anal. Comput. **2**, 111–126 (2012).

Zhao, X.-Q. and D. Xiao, "The asymptotic speed of spread and traveling waves for a vector disease model", Journal of Dynamics and Differential Equations **18**, 4, 1001–1019 (2006).

APPENDIX A

CO-AUTHOR PERMISSIONS

I certify that my co-authors, Dr. Zdzislaw Jackiewicz and Dr. Horst R. Thieme have given me permission, in writing, to include all material in my PhD thesis for Chapters 2 - 6.

APPENDIX B

COMPUTER CODES FOR CHAPTER 4

B.1 Latent Period of Fixed Length

Here is a Mathematica code that solves numerically the system of equations (4.4.7) when the latent period has a fixed length. $\Xi(c^*, \lambda)$ is given in (4.4.4).

```
(* Define the parameters of the model *)
tau=28;
beta=0.2;
d=200/365;
p1=0.5;
p2=1- p1;
nu1=0.2;
nu2=0.2;
b= 0.506605918;
(* Define the initial function S_0 *)
S0=4.6;
(* Define the system of nonlinear equations for c and lb *)
eq1=(p1*beta*S0/(nu1+lb*c-lb^2*d))*Exp[lb^2*b-lb*c*tau]+
    (p2*beta*S0/(nu2+lb*c))*Exp[2*lb^2*b-lb*c*tau];
eq2=D[eq1,lb];
sol=FindRoot[{eq1==1,eq2==0},{lb,1/2},{c,1/5}];
lb=lb/.sol;
c=c/.sol;
c1= c*365
```

B.2 Latent Period of Exponentially Distributed Length

The following is a Mathematica code that solves numerically (4.5.5), where $\Xi(c^*, \lambda)$ is given by (4.5.4).

```
(* Define the parameters of the model *)
theta=1/28;
beta=0.2;
d=200/365;
p1=0.5;
p2=1-p1;
nu1=0.2;
nu2=0.2;
b= 0.506605918;
(* Define the initial function S_0 *)
S0=4.6;
(* Define the system of nonlinear equations for c and lb *)
eq1=(p1*beta*S0/(nu1+lb*c-lb^2*d))*(theta/(theta+lb*c))*Exp[lb^2*b]+
    (p2*beta*S0/(nu2+lb*c))*(theta/(theta+lb*c))*Exp[2*lb^2*b];
eq2=D[eq1,lb];
sol=FindRoot[{eq1==1,eq2==0},{lb,1/3},{c,1/3}];
lb=lb/.sol;
c=c/.sol;
c1= c*365
```

B.3 Latent Period of Gamma Distributed Length

The following is a Mathematica code that solves numerically (4.6.5), where $\Xi(c^*, \lambda)$ is given by (4.6.4).

```mathematica
(* Define the parameters of the model *)
tau=28;
beta=0.2;
h=2;
d=200/365;
p1=0.5;
p2=1- p1;
nu1=0.2;
nu2=0.2;
b= 0.506605918;
(* Define the initial function S_0 *)
S0=4.6;
(* Define the system of nonlinear equations for c and lb *)
eq1=(p1*beta*S0/(nu1+lb*c-lb^2*d))*Exp[lb^2*b]* (h/(h+tau*lb*c))^h+
    (p2*beta*S0/(nu2+lb*c))*Exp[2*lb^2*b]*(h/(h+tau*lb*c))^h;
eq2=D[eq1,lb];
sol=FindRoot[{eq1==1,eq2==0},{lb,1/2},{c,1/5}];
lb=lb/.sol;
c=c/.sol;
c1= c*365
```

APPENDIX C

COMPUTER CODES FOR CHAPTER 5

Here are Matlab codes for the systems of ordinary differential equations (5.3.5) and delay differential equations (5.3.6) when the latent period has a fixed length.

```matlab
% Define system of ordinary differential equations by discretization in
% space variables of the model for the spread of rabies in a spatially
% distributed fox population for 0<=t<=tau (work with Z. Jackiewicz and
    H. Thieme)
%
function yp=fg(t,y)
N=length(y)/3;
% Define parameters of the model
tau=28;
beta=0.2;
D=200/365;
p1=0.5;
p2=1-p1;
nu1=0.2;
nu2=0.2;
% Define grids in space variables
a=50;
delx=2*a/(N+1);
xh0=-a;
xhNp1=a;
xh=linspace(-a+delx,a-delx,N);
zh0=-a;
zhNp1=a;
zh=linspace(-a+delx,a-delx,N);
% Define vectors S, R1, and R2
S=y(1:N);
R1=y(N+1:2*N);
R2=y(2*N+1:3*N);
% Define Sp
Sp=zeros(N,1); % Reserve storage
for i=1:N
Th=(delx/2)*(kappa1(xh(i)-zh0)*w1(t)+kappa2(xh(i)-zh0)*R2(1));
for k=1:N
    Th=Th+delx*(kappa1(xh(i)-zh(k))*R1(k)+kappa2(xh(i)-zh(k))*R2(k));
end
Th=Th+(delx/2)*(kappa1(xh(i)-zhNp1)*w2(t)+kappa2(xh(i)-zhNp1)*R2(N));
Sp(i)=-beta*S(i)*Th;
end
% if (t>=0 & t<=tau)
% Define R1p
R1p=zeros(N,1); % Reserve storage
R1p(1)=(D/delx^2)*(-2*R1(1)+R1(2))+(D/delx^2)*w1(t)-nu1*R1(1);
for i=2:N-1
    R1p(i)=(D/delx^2)*(R1(i-1)-2*R1(i)+R1(i+1))-nu1*R1(i);
end
R1p(N)=(D/delx^2)*(R1(N-1)-2*R1(N))+(D/delx^2)*w2(t)-nu1*R1(N);
% Define R2p
R2p=zeros(N,1); % Reserve storage
for i=1:N
    R2p(i)=-nu2*R2(i);
end
% end
yp=[Sp;R1p;R2p];
```

```matlab
% Define system of delay differential equations by discretization in
% space variables of the model for the spread of rabies in a spatially
% distributed fox population (work with Z. Jackiewicz and H. Thieme)
%
function yp=f(t,y,z)
N=length(y)/3;
% Define parameters of the model
tau=28;
beta=0.2;
D=200/365;
p1=0.5;
p2=1-p1;
nu1=0.2;
nu2=0.2;
% Define grids in space variables
a=50;
delx=2*a/(N+1);
xh0=-a;
xhNp1=a;
xh=linspace(-a+delx,a-delx,N);
zh0=-a;
zhNp1=a;
zh=linspace(-a+delx,a-delx,N);
% Define vectors S, Stau, R1, R1tau, R2 and R2tau
S=y(1:N);
Stau=z(1:N);
R1=y(N+1:2*N);
R1tau=z(N+1:2*N);
R2=y(2*N+1:3*N);
R2tau=z(2*N+1:3*N);
% Define Sp
Sp=zeros(N,1); % Reserve storage
for i=1:N
Th=(delx/2)*(kappa1(xh(i)-zh0)*w1(t)+kappa2(xh(i)-zh0)*R2(1));
for k=1:N
    Th=Th+delx*(kappa1(xh(i)-zh(k))*R1(k)+kappa2(xh(i)-zh(k))*R2(k));
end
Th=Th+(delx/2)*(kappa1(xh(i)-zhNp1)*w2(t)+kappa2(xh(i)-zhNp1)*R2(N));
Sp(i)=-beta*S(i)*Th;
end
% Define R1p and R2p
R1p=zeros(N,1); % Reserve storage
R2p=zeros(N,1); % Reserve storage
Thtau=(delx/2)*(kappa1(xh(1)-zh0)*w1(t-tau)+kappa2(xh(1)-zh0)*R2tau(1));
for k=1:N
    Thtau=Thtau+delx*(kappa1(xh(1)-zh(k))*R1tau(k)+kappa2(xh(1)-zh(k))*
    R2tau(k));
end
Thtau=Thtau+(delx/2)*(kappa1(xh(1)-zhNp1)*w2(t-tau)+kappa2(xh(1)-zhNp1)*
    R2tau(N));
R1p(1)=(D/delx^2)*(-2*R1(1)+R1(2))+(D/delx^2)*w1(t)+p1*beta*Stau(1)*
    Thtau-nu1*R1(1);
R2p(1)=p2*beta*Stau(1)*Thtau-nu2*R2(1);
for i=2:N-1
    Thtau=(delx/2)*(kappa1(xh(i)-zh0)*w1(t-tau)+kappa2(xh(i)-zh0)*R2tau
    (1));
for k=1:N
```

```
54        Thtau=Thtau+delx*(kappa1(xh(i)-zh(k))*R1tau(k)+kappa2(xh(i)-zh(k))*
          R2tau(k));
55 end
56 Thtau=Thtau+(delx/2)*(kappa1(xh(i)-zhNp1)*w2(t-tau)+kappa2(xh(i)-zhNp1)*
          R2tau(N));
57 R1p(i)=(D/delx^2)*(R1(i-1)-2*R1(i)+R1(i+1))+p1*beta*Stau(i)*Thtau-nu1*R1
          (i);
58 R2p(i)=p2*beta*Stau(i)*Thtau-nu2*R2(i);
59 end
60 Thtau=(delx/2)*(kappa1(xh(N)-zh0)*w1(t-tau)+kappa2(xh(N)-zh0)*R2tau(1));
61 for  k=1:N
62        Thtau=Thtau+delx*(kappa1(xh(N)-zh(k))*R1tau(k)+kappa2(xh(N)-zh(k))*
          R2tau(k));
63 end
64 Thtau=Thtau+(delx/2)*(kappa1(xh(N)-zhNp1)*w2(t-tau)+kappa2(xh(N)-zhNp1)*
          R2tau(N));
65 R1p(N)=(D/delx^2)*(R1(N-1)-2*R1(N))+(D/delx^2)*w2(t)+p1*beta*Stau(N)*
          Thtau-nu1*R1(N);
66 R2p(N)=p2*beta*Stau(N)*Thtau-nu2*R2(N);
67 yp=[Sp;R1p;R2p];
```

APPENDIX D

COMPUTER CODES FOR CHAPTER 6

Here is a Matlab code for the system of ordinary differential equations (6.3.1) when the latent period has exponentially distributed length.

```matlab
% Define system of ordinary differential equations by discretization in
% space variables of the model for the spread of rabies in a spatially
% distributed fox population (work with Z. Jackiewicz and H. Thieme)
%
function yp=f(t,y)
N=length(y)/4;
% Define parameters of the model
theta=1/28;
beta=0.2;
D=200/365;
p1=0.5;
p2=1-p1;
nu1=0.2;
nu2=0.2;
% Define grids in space variables
a=50;
delx=2*a/(N+1);
xh0=-a;
xhNp1=a;
xh=linspace(-a+delx,a-delx,N);
zh0=-a;
zhNp1=a;
zh=linspace(-a+delx,a-delx,N);
% Define vectors S, R1, R2, and I
S=y(1:N);
R1=y(N+1:2*N);
R2=y(2*N+1:3*N);
I=y(3*N+1:4*N);
% Define Sp and Ip
Sp=zeros(N,1);  % Reserve storage
Ip=zeros(N,1); % Reserve storage
for i=1:N
Th=(delx/2)*(kappa1(xh(i)-zh0)*w1(t)+kappa2(xh(i)-zh0)*R2(1));
for k=1:N
    Th=Th+delx*(kappa1(xh(i)-zh(k))*R1(k)+kappa2(xh(i)-zh(k))*R2(k));
end
Th=Th+(delx/2)*(kappa1(xh(i)-zhNp1)*w2(t)+kappa2(xh(i)-zhNp1)*R2(N));
Sp(i)=-beta*S(i)*Th;
Ip(i)=theta*beta*S(i)*Th-theta*I(i);
end
% Define R1p
R1p=zeros(N,1); % Reserve storage
R1p(1)=(D/delx^2)*(-2*R1(1)+R1(2))+(D/delx^2)*w1(t)+ ...
        p1*I(1)-nu1*R1(1);
for i=2:N-1
    R1p(i)=(D/delx^2)*(R1(i-1)-2*R1(i)+R1(i+1))+ ...
            p1*I(i)-nu1*R1(i);
end
R1p(N)=(D/delx^2)*(R1(N-1)-2*R1(N))+(D/delx^2)*w2(t)+ ...
        p1*I(N)-nu1*R1(N);
% Define R2p
R2p=zeros(N,1); % Reserve storage
for i=1:N
    R2p(i)=p2*I(i)-nu2*R2(i);
```

```matlab
55 end
56 yp=[Sp;R1p;R2p;Ip];
```